

X-631-65-13

NASA TMX-55185

FACILITY FORM 602

N65-21655  
120  
(PAGES)  
JMX-55185  
(NASA CR OR TMX OR AD NUMBER)

(THRU)  
(CODE)  
30  
(CATEGORY)

# ATTITUDE DETERMINATION OF SPIN STABILIZED SPACECRAFT USING A DIGITAL ASPECT SENSOR

GPO PRICE \$ \_\_\_\_\_

OTS PRICE(S) \$ \_\_\_\_\_

Hard copy (HC) \$4.00

Microfiche (MF) .75

MARCH 1965

NASA

GODDARD SPACE FLIGHT CENTER

GREENBELT, MARYLAND

X-631-65-13

ATTITUDE DETERMINATION  
OF SPIN STABILIZED SPACECRAFT  
USING A DIGITAL ASPECT SENSOR

March 1965

Goddard Space Flight Center  
Greenbelt, Maryland

## LIST OF ILLUSTRATIONS

<u>Figure</u>		<u>Page</u>
1	Euler rotation angles . . . . .	2
2	Relationship of energy to precession half angle for constant momentum . . . . .	6
3	Celestial sphere representation of a precessing satellite using a digital aspect sensor . . . . .	7
4	Quantized field of view of a digital aspect sensor . . . . .	7
5	Typical plots of sun sightings from digital aspect sensors..	9
6	Plot of 1/2 cycle of the curve defined by equation 28 . . . .	10
7	Digital fan crossing sun in the precession case . . . . .	15
8	Definition of variables needed to solve the horizon sensor problem . . . . .	18
9	Relationship between $\Delta t_c$ and $\delta$ . . . . .	22
10	Position of the momentum vector relative to the sun and the zenith vector . . . . .	22
11	Position of a sensor $S_i$ relative to the aspect sensor in a spacecraft coordinate system . . . . .	26
12	Relative positions of a sensor axis, the spacecraft $z$ -axis, and the momentum vector . . . . .	26
13	Relationships of sensor axis $S_i$ with respect to the spacecraft $z$ -axis and the momentum vector . . . . .	27
14	Relationships of a sensor axis with respect to an external vector . . . . .	30

## CONTENTS

	<u>Page</u>
ENERGY AND MOMENTUM CONSIDERATIONS .....	1
MEASUREMENTS USING THE DIGITAL ASPECT SENSOR .....	7
Calculation of $\beta$ and $\theta$ .....	8
Calculation of $\dot{\phi}$ and $\dot{\psi}$ .....	12
Calculation of $\phi_0$ and $\psi_0$ .....	14
MEASUREMENTS USING A HORIZON DETECTOR .....	17
SPACECRAFT ATTITUDE DETERMINATION .....	24
Error Calculations .....	25
Sensor Position as a Function of Time .....	26
APPENDIX A .....	00
APPENDIX B .....	00
APPENDIX C .....	00
APPENDIX D .....	00
APPENDIX E .....	00
APPENDIX F .....	00

List of Illustrations (Continued)

<u>Figure</u>		<u>Page</u>
15	Relationships necessary for finding times of maximum and minimum angles between a sensor and an external vector . . . . .	30
A	Sun sightings defined within a quantized time base . . . . .	00
AA	Relationship of spacecraft to sunlit earth . . . . .	

## ATTITUDE DETERMINATION OF SPIN STABILIZED SPACECRAFT USING A DIGITAL ASPECT SENSOR

### ENERGY AND MOMENTUM CONSIDERATIONS

The problem of the force free motion of a rigid body has been extensively treated by a number of people and a great many methods for solutions have been formulated. The most common and most useful for our discussion was formulated by Euler. The Euler angles are shown in Figure 1. They are defined as three successive rotations performed in specific sequence. The sequence is as follows: (1) Rotate the initial system of axes counter-clockwise about the Z axis by an angle  $\phi$ , which produces a set of intermediate axes ( $x'$ ,  $y'$ ,  $z'$ ). (2) Next rotate the intermediate set of axes ( $x'$ ,  $y'$ ,  $z'$ ) counterclockwise through an angle  $\theta$ , about the  $x'$  axis forming the line of nodes. This produces a second set of intermediate axes ( $x''$ ,  $y''$ ,  $z''$ ). (3) Finally, rotate this set of axes counterclockwise through an angle  $\psi$  about the  $z''$  axis, forming the ( $x$ ,  $y$ ,  $z$ ) axes.

The three angles  $\theta$ ,  $\phi$ , and  $\psi$  then completely describe the orientation of the  $x$ ,  $y$ ,  $z$  coordinate system with respect to the  $X$ ,  $Y$ ,  $Z$  coordinate system.

Now let the  $X$ ,  $Y$ ,  $Z$  coordinate system define an inertial space. Assume a rotating satellite situated in this inertial space where the momentum vector, ( $L$ ), of the rotating satellite is orientated along the  $Z$  axis of the inertial space.  $x$ ,  $y$ , and  $z$  may now represent a coordinate system fixed in the rotating satellite. The axes  $x$ ,  $y$ ,  $z$  are aligned with the three principle moments of inertia of the satellites  $I_1$ ,  $I_2$ , and  $I_3$ . The instantaneous values of momentum about the  $x$ ,  $y$ , and  $z$  axes become  $p_x$ ,  $p_y$ , and  $p_z$  respectively.

$$p_x = I_1 \omega_x \quad (1)$$

$$p_y = I_2 \omega_y \quad (2)$$

$$p_z = I_3 \omega_z \quad (3)$$

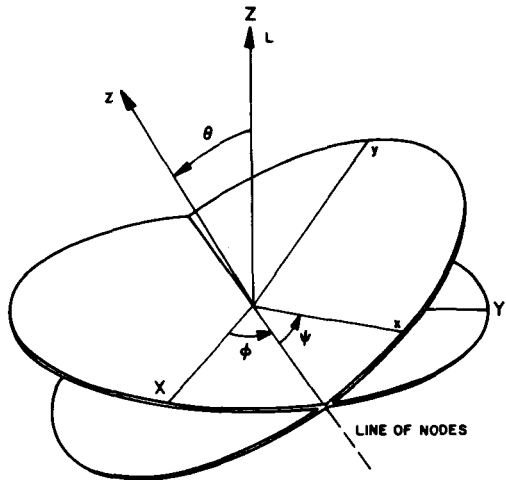


Figure 1—Euler rotation angles

Where  $\omega_x$ ,  $\omega_y$ , and  $\omega_z$  are the instantaneous values of angular velocity about x, y, and z.

From examination of Figure 1 it can be seen that the components of L are:

$$p_x = L \sin \theta \sin \psi \quad (4)$$

$$p_y = L \sin \theta \cos \psi \quad (5)$$

$$p_z = L \cos \theta \quad (6)$$

By the process of infinitesimal rotations<sup>1</sup> a relationship is established between the angular velocities  $\omega_x$ ,  $\omega_y$ , and  $\omega_z$ , and the rate of change of the Euler angles  $\dot{\phi}$ ,  $\dot{\psi}$ , and  $\dot{\theta}$ . These relations are stated in equations (7), (8), and (9).

$$\omega_x = \dot{\phi} \sin \theta \sin \psi + \dot{\theta} \cos \psi \quad (7)$$

$$\omega_y = \dot{\phi} \sin \theta \cos \psi - \dot{\theta} \sin \psi \quad (8)$$

$$\omega_z = \dot{\phi} \cos \theta + \dot{\psi} \quad (9)$$

Substituting 7, 8, and 9 in 1, 2 and 3 gives

$$p_x = I_1 (\dot{\phi} \sin \theta \sin \psi + \dot{\theta} \cos \psi) \quad (10)$$

$$p_y = I_2 (\dot{\phi} \sin \theta \cos \psi - \dot{\theta} \sin \psi) \quad (11)$$

$$p_z = I_3 (\dot{\phi} \cos \theta + \dot{\psi}) \quad (12)$$

<sup>1</sup>Pg. 134, Goldstein, H. — Classical Mechanics, Addison-Wesley Publishing Co., Reading, Mass. 1957.

Multiplying (4) by  $\sin \psi$  and (5) by  $\cos \psi$  gives,

$$p_x \sin \psi = L \sin \theta \sin^2 \psi \quad (13)$$

$$p_y \cos \psi = L \sin \theta \cos^2 \psi \quad (14)$$

Now add expressions (13) and (14) to get

$$L \sin \theta = p_x \sin \psi + p_y \cos \psi \quad (15)$$

Assume for simplicity that the satellite is balanced in such a way as to make  $I_1 = I_2$ .

Making this assumption, and substituting (10), and (11) in (15) gives

$$L \sin \theta = I_1 \dot{\phi} \sin \theta \quad (16)$$

or

$$L = I_1 \dot{\phi} \quad (17)$$

Again, multiplying (4) by  $\cos \psi$  and (5) by  $\sin \psi$  and subtracting gives the following expressions.

$$p_x \cos \psi - p_y \sin \psi = L \sin \theta \sin \psi \cos \psi - L \sin \theta \sin \psi \cos \psi \quad (18)$$

$$p_x \cos \psi - p_y \sin \psi = 0 \quad (19)$$

Substituting expressions (10), and (11) into expression (19) gives

$$I_1 \dot{\theta} = 0 \quad (20)$$

or  $\theta$  is time independent.

Substituting expression (17), into expression (6), and then (6) into (12),

$$I_1 \dot{\phi} \cos \theta = I_2 (\dot{\phi} \cos \theta + \dot{\psi}) \quad (21)$$

or,

$$\text{a) } \dot{\psi} = \frac{I_1 - I_3}{I_3} \dot{\phi} \cos \theta \quad \text{b) } \dot{\phi} = \frac{I_3 \dot{\psi}}{(I_1 - I_3) \cos \theta} \quad (22)$$

$\dot{\psi}$  is the angular velocity of the satellite about the satellite z-axis. This will be called spin rate. This is to be distinguished from the apparent rotation rate of the satellite with respect to a fixed external point. This apparent rotation rate has an average value of  $(\dot{\phi} + \dot{\psi})$ .

$\dot{\phi}$  is the angular velocity of the satellite z-axis about the momentum vector (or more precisely, the angular velocity of the line of nodes). This will be called the precession rate.\*

$\dot{\theta}$  is the rate of change of the precession half-cone angle. Such a motion is called nutation.\* A satellite with appreciable nutation presents an extremely difficult, if not insoluable, motion determination problem. Nutation is the result of  $I_1 \neq I_2$  and  $\theta \neq 0$ .

As previously mentioned, if  $I_1$  is made equal to  $I_2$ ,  $\dot{\theta} = 0$  and there is no nutation.

$\theta$  is the precession cone half angle.

A freely rotating satellite which has both spin and precession motions experiences time dependent accelerations at various points in its structure. Since most satellites are not absolutely rigid bodies, some flexing of the structure occurs and energy is thus dissipated through frictional losses. Momentum is,

---

\*NOTE: The use of the terms precession and nutation are defined in a force free field according to the astronomers' convention, i.e.: Precession rate is the rate of rotation of the lines of nodes and nutation is the short term fluctuation in the precession cone half angle. This convention is quite different from that used in the theory of gyroscopic motion. Gyroscopic precession is the motion of the gyroscopic spin axis as a result of an external torque applied perpendicular to the spin axis. Gyroscopic nutation is the wobble of the gyro axis about the momentum vector. Nutation in the gyro sense is similar to precession in the astronomical sense.

of course, conserved as long as no external forces act on the satellite. The effect of such energy losses can be seen by examining the following equations:

The Lagrangian is written

$$L = T - V = 1/2 (I_1 \omega_x^2 + I_2 \omega_y^2 + I_3 \omega_z^2) - V(\theta, \phi, \psi) \quad (23)$$

Since we are considering force free motion,  $V(\theta, \phi, \psi) = 0$ .

Substituting (7), (8), (9), in (23) gives

$$T = 1/2 [I_1 (\dot{\phi} \sin \theta \sin \psi + \dot{\theta} \cos \psi)^2 + I_2 (\dot{\phi} \sin \theta \cos \psi - \dot{\theta} \sin \psi)^2$$

$$+ I_3 (\dot{\phi} \cos \theta + \dot{\psi})^2] \quad (24)$$

Assuming again that the satellite is balanced so that  $I_1 = I_2$ , expression (24) reduces to

$$T = 1/2 I_1 (\dot{\phi}^2 \sin^2 \theta + \dot{\theta}^2) + 1/2 I_3 (\dot{\phi} \cos \theta + \dot{\psi})^2 \quad (25)$$

Since  $\theta$  is a constant (equation 19),  $\dot{\theta} = 0$ . Now substituting equation (22a) in (25) gives

$$T = 1/2 I_1 \dot{\phi}^2 \left( \sin^2 \theta + \frac{I_1}{I_3} \cos^2 \theta \right) \quad (26)$$

Substituting  $L = I_1 \dot{\phi}$  from (17) gives

$$T = \frac{L^2}{2I_1} \left( \sin^2 \theta + \frac{I_1}{I_3} \cos^2 \theta \right) \quad (27)$$

In the absence of any external forces  $L$  is a constant. If precession motion causes energy to be dissipated internally through battery liquids sloshing, non-rigid members flexing, etc.,  $T$  becomes smaller. Since  $L$  is not affected by internal dissipation of energy, the value of  $\theta$  then must change; as shown in Figure 2, the value of  $\theta$  will tend toward  $0^\circ$ , or  $90^\circ$ , or remain constant depending on the value of the ratio  $I_1/I_3$ .

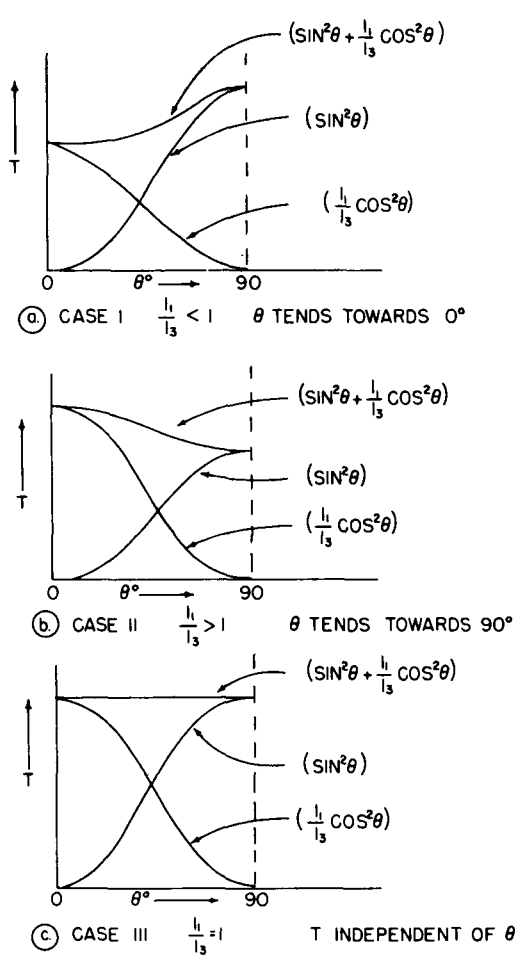


Figure 2—Relationship of energy to precession half angle for constant momentum.

Case I — If  $I_1/I_3 < 1$ ,  $\theta$  tends toward  $0^\circ$ . In this case the precession-coning will damp out in time. Since it is usually desirable for the satellite to rotate about the  $z$ -axis, most spin stabilized satellites are balanced so that the  $z$ -axis coincides with the largest inertia moment, that is so that  $I_1/I_3 < 1$ .

It should not be assumed that damping of the precession cone implies that  $\dot{\phi}$  goes to zero. Equation 22 states that when  $\theta = 0^\circ$ ,  $\dot{\phi} = I_3 \dot{\psi}/I_3 - I_3$ . It can be seen from Figure 1 that the apparent rotation velocity of the satellite for  $\theta = 0^\circ$  is  $(\dot{\phi} + \dot{\psi})$ .

Case II — On the other hand if  $I_1/I_3 > 1$ ,  $\theta$  tends toward  $90^\circ$ . In this case the precession cone opens up until the satellite begins to spin like a propeller. In this mode  $\dot{\psi}$  goes to zero (Equation 22).

Case III — The third possibility is that  $I_1/I_3 = 1$ . In this case the satellite is perfectly symmetrical about all axes and there is no way of distinguishing the  $z$ -axis dynamically. In this case  $I_1 = I_3$  and from equation 22 again  $\dot{\psi} = 0$ .

The final result of any of these three cases is to cause the satellite to rotate with no wobbling motion about the axis of the largest moment of inertia.

It should be noted that Case III is difficult to achieve in reality.  $I_1$  is seldom made exactly equal to  $I_3$  and in fact, our symmetry assumption that  $I_1 = I_2$  is seldom precisely true either. Thus, it may happen that if the three moments

are very nearly equal, the condition where  $I_1 > I_3 > I_2$ , or  $I_1 < I_3 < I_2$  may inadvertently occur. This possibility raises a fundamental problem associated with asymmetrical rotating bodies.\* That is, if a body is shaped so that either  $I_1 > I_3 > I_2$ , or  $I_1 < I_3 < I_2$ , and the body is set rotating about  $I_3$ , its motion is unstable. This instability is such that any slight perturbation will send the body into wild, unpredictable, and quite violent gyrations. The change in spin axis caused by this type of instability occurs in a time interval on the order of one revolution period and requires no energy dissipation. Thus, this instability is quite different from Case II where the change in spin axis occurs over many spin periods and depends entirely on the dissipation of energy.

### MEASUREMENTS USING THE DIGITAL ASPECT SENSOR

To make the measurements necessary to determine the motion of a spinning satellite, assume that a photo detector is mounted behind a slit situated on the side of the rotating satellite. Let the axis of this detector be along the satellite  $x$ -axis with the slit positioned parallel to the satellite  $z$ -axis. Then the field of view of this detector will be a fan which will sweep across the sky, which is the celestial sphere, as the satellite rotates. This is shown in Figure 3. Now further assume that this fan field of view is quantized into a number of segments as shown in Figure 4. This may be done if instead of a simple slit and photo

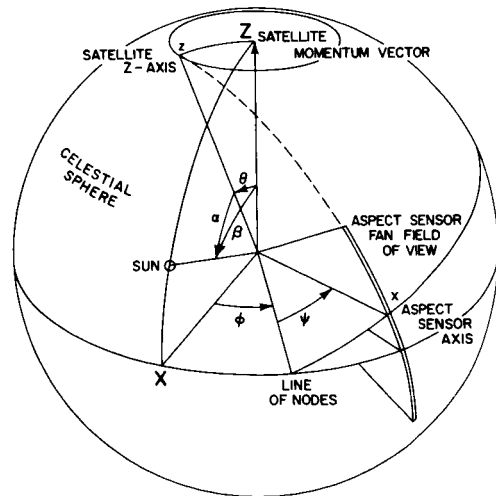


Figure 3—Celestial sphere representation of a precessing satellite using a digital aspect sensor.

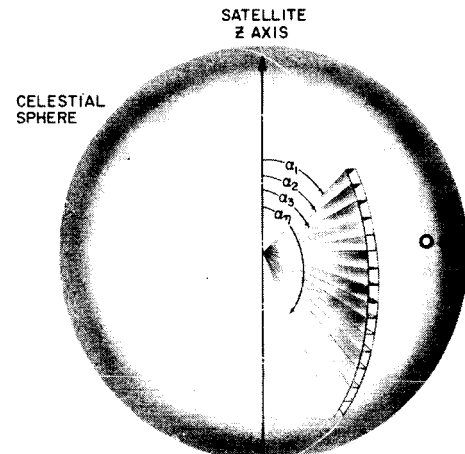


Figure 4—Quantized field of view of a digital aspect sensor

---

NOTE: For a rigorous treatment of the stability of asymmetrical rotating rigid bodies see page 116 of "Mechanics" by Landau, L. D. and Lifshitz, E.M., Addison-Wesley Publishing Co., 1960.

detector, a digital aspect sensor<sup>2,3</sup> is used to provide the fan shaped field of view. Each of the fan segments has a unique identifying number. As the satellite rotates, if a bright object such as the sun should be in a portion of the sky swept out by one of these quantized fan segments, the number corresponding to that particular segment would be transmitted to the ground. This number then defines the angle between the satellite  $z$ -axis and the sun vector. This angle must lie between the upper and lower edges of the particular quantized fan segment. The angles between the edges of these quantized segments and the  $z$ -axis are listed in a calibration table and are designated  $\alpha_1, \alpha_2, \alpha_3, \dots, \alpha_n$ . If there is no precession coning, the same segment number will be repeatedly transmitted upon each revolution of the satellite.

Most of the discussion in the rest of this section deals with problems caused by precession coning. For the zero precession case the spin rate  $\dot{\psi}$  and precession rate  $\dot{\phi}$  can be found from equations (38) and (39). The reader may then skip to equations (51) and (52) where the initial phase angles  $\psi_0$  and  $\phi_0$  can be set equal to zero at time  $t_0$ . Much of the following discussion of precession motion determination will reduce to a degenerate case for zero precession.

#### Calculation of $\beta$ and $\theta$

In the event of precession coning the motion of the fan across the celestial sphere is quite complicated. The first quantities to be calculated from the data are the angles  $\beta$  and  $\theta$ .

If the satellite is balanced so that  $I_1 = I_2$ , the angle  $\alpha$  between the  $z$ -axis of the satellite and the sun vector will be a function of time given by (28)

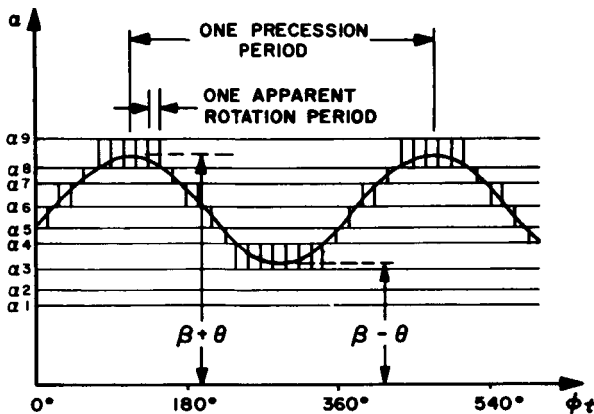
$$\cos \alpha = \cos \beta \cos \theta + \sin \theta \sin \beta \sin \dot{\phi} \quad (28)$$

Where  $\beta$  is the angle between the momentum vector and the sun vector. Figure 5 is a graph of (28) showing sun sightings for the two cases where  $I_1 > I_3$ , and  $I_1 < I_3$ . If  $I_1 > I_3$ , the fan "sees" the sun many times for one cycle of  $\dot{\phi}$ . If  $I_1 < I_3$ ,  $\dot{\phi}$  completes more than one cycle per sun sighting. Often the best

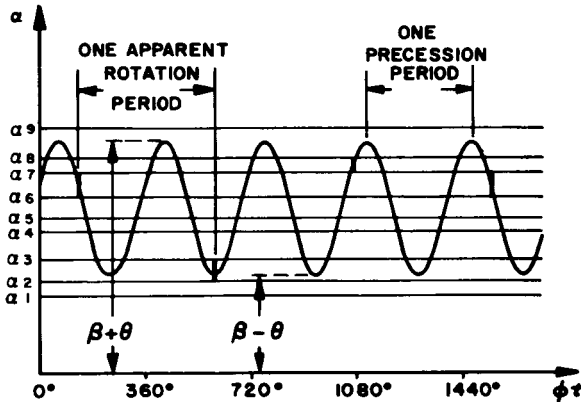
---

<sup>2</sup>Albus, James S., "A Digital Solar Aspect Sensor," *Astronautics*, January 1962 also NASA TN D-1062.

<sup>3</sup>Albus, James S. and Schaefer, David H., "Satellite Attitude Determination: Digital Sensing and On-Board Processing," *IEEE Transactions on Space Electronics and Telemetry*, Vol. SET-9, pp. 71-77, September 1963.



(a)  $I_1 > I_3$



(b)  $I_1 < I_3$

Figure 5—Typical plots of sun sightings from a digital aspect sensor

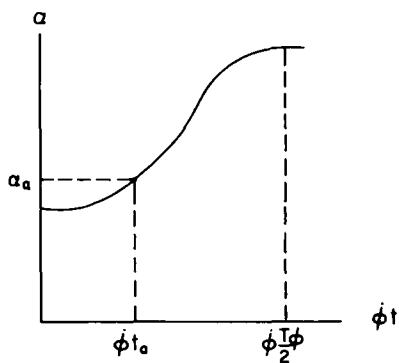
method of calculating  $\beta$  and  $\theta$  is to plot the  $\alpha$  limits for the sun sightings and fit a curve. It is possible to apply a statistical approach to the calculation of  $\beta$  and  $\theta$  over a period which is long compared with any beat frequency set up between  $\phi$  and  $\psi$ . However, this is sometimes in practice a prohibitively long period of time.

To calculate the values of  $\beta$  and  $\theta$ , take some time interval  $T_1 - T_0$  such that at  $T_1$  and  $T_0$   $(\phi - \pi/2) < \xi_1$  and  $(\psi + \pi/2) < \xi_2$ , where  $\xi_1$  and  $\xi_2$  are arbitrarily small angles. From Figure 3 it can be seen that these restrictions make  $\alpha$  a minimum at  $T_0$  and  $T_1$ . Between  $T_0$  and  $T_1$  the sun appears at semi-regular

intervals which are not integrally related with  $\dot{\phi}$ . Therefore, over a period which is long compared to any beat frequency which might appear between  $\dot{\phi}$  and  $\dot{\psi}$ , all values of  $(\dot{\phi}t)$  between 0 and  $2\pi$  become equally probable.

Now the probability of a sun appearance in the segment nearest the spin axis is equal to  $N_a/N$  (where  $N_a$  is the number of appearances of the sun in the nearest segment, and  $N$  is the total number of times the sensor fan crosses the sun during  $T_1 - T_0$ ). Thus, the probability at any instant of  $\alpha > \alpha_a$  is  $N_a/N$ .

A half cycle of the curve (28) is plotted in Figure 6.



If an arbitrary point along the  $\dot{\phi}t$  axis is chosen, the probability that the corresponding value of  $\alpha$  is less than  $\alpha_a$  is  $2t_a/T_\phi$ . The relationship between  $\alpha_a$  and  $t_a$  is given by substituting in (28)

$$\begin{aligned}\cos \alpha_a &= \cos \beta \cos \theta + \sin \beta \\ \sin \theta \cos (\dot{\phi}t_a) &\end{aligned}\tag{29a}$$

Figure 6—Plot of 1/2 cycle of the curve defined by Equation 28.

which can be expressed as

$$\cos \alpha_a = \cos \beta \cos \theta + \sin \beta \sin \theta \cos \left( \pi \frac{2t_a}{T_\phi} \right) \tag{29b}$$

We have already shown that the probability of a solar appearance during the interval  $T_1 - T_0$  in the nearest fan segment is  $N_a/N$ . If  $\alpha_a$  is set equal to the value of the most distant edge of the nearest quantized segment, then  $N_a/N$  may be substituted for  $2t_a/T$  in (29b) to give (30).

$$\cos \alpha_a = \cos \beta \cos \theta + \sin \beta \sin \theta \cos \left( \frac{\pi N_a}{N} \right) \tag{30}$$

Similarly,

$$\cos \alpha_b = \cos \beta \cos \theta + \sin \beta \sin \theta \cos \left( \frac{\pi N_b}{N} \right) \tag{31}$$

where  $\alpha_a$  is the most distant edge of the nearest quantized fan segment to the spin axis, and  $N_a$  is the number of sun appearances in the nearest segment.  $\alpha_b$  is the nearest edge of the most distant quantized fan segment.  $N_b$  is the number of sun appearances in all segments except the most distant.  $N$  is the total number of all sun appearances during the interval  $T_1 - T_0$ .

The restrictions on  $T_0$  and  $T_1$  may now be disregarded by making  $N$  sufficiently large.

Writing (30) and (31) in more convenient form for solution gives

$$\left. \begin{aligned} \cos(\beta + \theta) &= \frac{ad - bc + a - c}{d - b} = \frac{a(d+1) - c(b+1)}{d - b} \\ \cos(\beta - \theta) &= \frac{ad - bc - a + c}{d - b} = \frac{a(d-1) - c(b-1)}{d - b} \end{aligned} \right\} \quad (32)$$

where

$$a = \cos \alpha_a$$

$$b = \cos(\pi N_a / N)$$

$$c = \cos \alpha_b$$

$$d = \cos(\pi N_b / N)$$

Note that equation (32) is ambiguous as to the quadrant of  $(\beta + \theta)$  and  $(\beta - \theta)$ . Thus the digital sun sensor does not indicate directly whether the sun is inside or outside of the precession cone. Ignorance of this ambiguity can lead to considerable confusion if the sun happens to lie inside the cone. Resolution of the ambiguity is not straightforward unless the approximate size of the precession cone can be independently measured.

If the rotation rate can be determined by an independent means such as a magnetometer or a telemetry AGC record use of equations (36) and (37) will provide an indication of whether the sun is inside or outside the precession cone. However, if the magnetic field vector or the ground receiving station is inside the precession cone this method itself is subject to the same type of ambiguity. Another method is to reconstruct a time history of a precession cycle on the celestial sphere. The phase of the  $\phi$  and  $\psi$  angles will usually provide an indication of whether  $(\beta - \theta)$  is plus or minus.

Where the sun only appears in two quantitized segments, there are not enough known quantities to solve for both  $\beta$  and  $\theta$ . In this case, unless  $\theta$  can be estimated from previous data, assume  $\theta$  equal to width of smallest segment in which the sun appears. Then solve (33) for  $\beta$ .

$$\cos \beta = \frac{ab \pm c \sqrt{(b^2 + c^2) - a^2}}{(b^2 + c^2)} \quad (33)$$

$$0 \leq \beta < 180^\circ$$

where

$$a = \cos \alpha_a$$

$$b = \cos \theta$$

$$c = \sin \theta \cos (\pi N_a / N)$$

In this case, if  $\theta$  is constant over a period of days, an accurate measure of  $\theta$  can sometimes be made by noticing how long the sun's appearances oscillate from one segment to the other. The velocity of the sun's yearly motion, multiplied by the crossover oscillation time, give  $2\theta$ .  $\beta$  at the midpoint of the crossover time is exactly the value of the calibrated angle  $\alpha_n$ . Other factors besides the sun's apparent motion can of course cause  $\beta$  to slowly vary over a period of days. These factors are external torques caused by magnetic fields, radiation pressure, aerodynamic drag, plasma winds, gravitational gradients, etc.

### Calculation of $\dot{\phi}$ and $\dot{\psi}$

Having now calculated  $\theta$  and  $\beta$  we proceed to determine the spin rate  $\dot{\psi}$ , and the precession rate  $\dot{\phi}$ . In the general case where precession motion is present, the apparent rotation period, which is the time between successive crossings of the sun by the fan field of view, will not be uniform. This is due to the fact that sometimes the fan is tilted forward when it crosses the sun, and sometimes backward. However, the average value of the apparent rotation period is constant. In fact,  $\dot{\phi}$  and  $\dot{\psi}$  may be determined from the average apparent rotation period by the following method:

Choose X in Figure 3 so that the sun lies in the XOZ plane. This may be done with no loss in generality. Choose a time that the fan crosses the sun such that  $(\phi - \pi/2) < \xi_1$  and  $(\psi + \pi/2) < \xi_2$  where  $\xi_1$  and  $\xi_2$  are arbitrarily small angles. Call this time  $T_0$ . This condition can always be satisfied at some time since  $\dot{\phi}$  and  $\dot{\psi}$  are not integral multiples of each other. Now wait for another time when the fan crosses the sun such that these same restrictions can be applied to  $\phi$  and  $\psi$ . Call this time  $T_1$ . Count the number of times the fan crossed the sun between  $T_0$  and  $T_1$ . Call this  $N_r$ .

Then the average period

$$T_{av} = \frac{T_1 - T_0}{N_r}$$

Now from  $T_0$  til  $T_1$ ,  $\psi$  has made  $N_\psi$  revolutions (within an arbitrarily small number of degrees). Therefore,

$$2\pi N_\psi = \dot{\psi} (T_1 - T_0); \quad (34)$$

and during that same time  $\phi$  made  $N_\phi$  revolutions. Therefore,

$$2\pi N_\phi = \dot{\phi} (T_1 - T_0). \quad (35)$$

Now if  $I_1 > I_3$  the value of  $N_\phi$  can be immediately determined by inspection of a plot similar to Figure 5. In fact in the case where  $I_3 > I_1$ , if one has a rough knowledge of  $I_1/I_3$ ,  $N_\phi$  can usually be found by inspection. However, if there is any doubt about  $N_\phi$ , or if the sun lies inside of the precession cone a more rigorous approach is more reliable.

Assume for our discussion a fan field of view  $180^\circ$  in length and negligibly thin. In Figure 4 this would mean that  $\alpha_1 = 0$  and  $\alpha_n = 180^\circ$ . From Figure 3 we can write

$$N_r = N_\psi + N_\phi \quad \text{if } \beta > \theta \quad (36)$$

and

$$N_r \geq N_\psi \quad \text{if } \beta \leq \theta \quad (37)$$

The case where  $N_r > N_\psi$  in equation (37) arises when the sun lies inside certain regions within the precession cone. These regions are quite complicated and will not be discussed here.

For the case where the fan is not  $180^\circ$  in length (i.e.  $\alpha_1 > 0$  and/or  $\alpha_n < 180^\circ$ ) equation (36) holds where  $(\theta + \alpha_1) < \beta < (\alpha_n - \theta)$  and equation (37) holds where  $(\theta - \alpha_1) > \beta > [360^\circ - (\alpha_n + \theta)]$ . If these conditions are not satisfied, a value for  $N_r$  can sometimes be determined by inspection of a plot similar to Figure 5.

If the conditions for equation (36) hold, it can be combined with equations (22), (34), and (35) to give equations (38) and (39).

$$\dot{\phi} = \frac{2\pi N_r}{(T_1 - T_0) \left( 1 + \frac{I_1 - I_3}{I_3} \cos \theta \right)} \quad (38)$$

and

$$\dot{\psi} = \frac{2\pi N_r}{(T_1 - T_0) \left( 1 + \frac{I_3}{(I_1 - I_3)} \cos \theta \right)} \quad (39)$$

Now if the restrictions on choosing the times  $T_0$  and  $T_1$  are discarded, the uncertainty in  $(\dot{\phi} + \dot{\psi})$  will be less than  $\pm (50\% / N_r)$ . Therefore, if  $T_0$  and  $T_1$  are merely chosen a large number of revolutions apart so that  $N_r > 50$  (38) and (39) give quite accurate answers.

The accuracy of  $\dot{\phi}$  and  $\dot{\psi}$  from equations (38) and (39) depends, of course, on the accuracy of  $I_1/I_3$  and  $\theta$ . If  $\dot{\phi}$  and  $\dot{\psi}$  can be roughly determined from equations (38) and (39), and then the knowledge of  $\dot{\phi}$  and  $\dot{\psi}$  used to find  $N_\phi$  by inspection, equations (38) and (39) can then be solved again with  $\dot{\phi}$  and  $\dot{\psi}$  as known and  $I_1/I_3$  unknown. This kind of iteration can be used to refine the value of  $I_1/I_3$  and even under certain conditions to determine  $\theta$ .

#### Calculation of $\phi_0$ and $\psi_0$

The integrals of motion  $\dot{\phi}, \dot{\psi}, \theta$  having now been calculated, it is necessary to establish initial conditions in order to define the instantaneous position of the

satellite in inertial space at a particular time. A particular passage of the slit across the sun may now be chosen as occurring at  $t_0$ .

In Figure 7 the digital fan is shown crossing the sun.  $\alpha_a$  and  $\alpha_b$  correspond to the angles between the spin axis and the upper and lower edges of the quantized fan segment containing the sun. From this figure the following equations may be written

$$\cos \alpha = \cos \beta \cos \theta + \sin \beta \sin \theta \cos (90^\circ - \phi) \quad (40)$$

or in the case of  $\alpha_a$  and  $\alpha_b$

$$\cos \alpha_a = \cos \beta \cos \theta + \sin \beta \sin \theta \cos (90^\circ - \phi_A) \quad (41)$$

$$\cos \alpha_b = \cos \beta \cos \theta + \sin \beta \sin \theta \cos (90^\circ - \phi_B) \quad (42)$$

Substitute the relation

$$\dot{\phi} = \phi(t - t_0) + \phi_0. \quad (43)$$

$$\cos \alpha_a = \cos \beta \cos \theta + \sin \beta \sin \theta \sin (\dot{\phi}(t - t_0) + \phi_{OA}) \quad (44)$$

$$\cos \alpha_b = \cos \beta \cos \theta + \sin \beta \sin \theta \sin (\dot{\phi}(t - t_0) + \phi_{OB}) \quad (45)$$

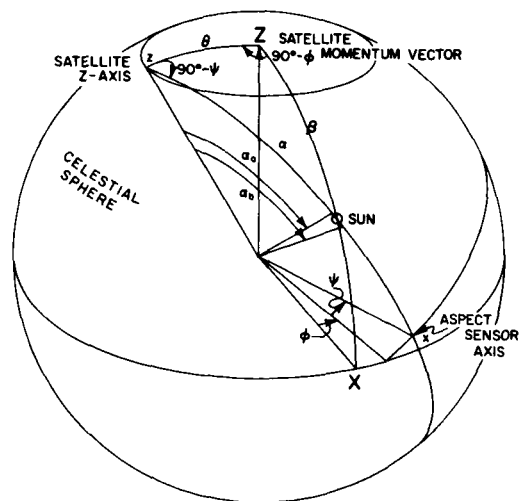


Figure 7—Digital fan crossing sun in the precession case

At  $t = t_0$  (44) and (45) can be solved for  $\phi_{OA}$  and  $\phi_{OB}$ .  $\phi_0$  must lie somewhere between  $\phi_{OA}$  and  $\phi_{OB}$ . However, the solution of (44) and (45) is ambiguous regarding the quadrant of  $\phi_{OA}$  and  $\phi_{OB}$ . This ambiguity may be resolved by choosing a value of  $t$  at a sun sighting approximately an odd number of quarter periods of  $\phi$  away from  $t_0$ . Solve (44) and (45) again for  $\cos \alpha_a$ , and  $\cos \alpha_b$ . This time try first one possible quadrant value for  $\phi_{OA}$  and  $\phi_{OB}$  and then the other. Compare the two values of  $\cos \alpha_a$  and  $\cos \alpha_b$  obtained with the cosine of the actual value of  $\alpha_a$  and  $\alpha_b$  measured at time  $t$ . The closest value should indicate the proper quadrant for  $\phi_{OA}$  and  $\phi_{OB}$ .

Having now determined unique values for  $\phi_{OA}$  and  $\phi_{OB}$ , it is possible to narrow the limits on the value of  $\phi_0$ . The precession rate  $\phi$  is accurately known, and the time of each sun sighting is also well known. Therefore, equations (44) and (45) can be repeatedly solved for  $\phi_{OA}$  and  $\phi_{OB}$  by inserting  $\alpha_a$ ,  $\alpha_b$ , and  $t$  for each sun sighting after  $t_0$ . Since  $\phi_0$  must always lie between  $\phi_{OA}$  and  $\phi_{OB}$ ,  $\phi_0$  must lie between the maximum of the smaller values and the minimum of the larger values of the pair  $\phi_{OA}$  and  $\phi_{OB}$ . This is somewhat tricky when put into practice since whether  $\phi_{OA}$  or  $\phi_{OB}$  is the larger of the pair depends on the quadrant of the argument  $[\phi(t - t_0) + \phi_0]$ . If  $\cos [\phi(t - t_0) + \phi_0]$  is positive,  $\phi_{OA} > \phi_{OB}$ , but if  $\cos [\phi(t - t_0) + \phi_0]$  is negative,  $\phi_{OA} < \phi_{OB}$ .

Once  $\phi_0$  is determined accurately enough, solve (47) for  $\cos \alpha_0$ .

$$\cos \alpha_0 = \cos \beta \cos \theta + \sin \beta \sin \theta \cos (90^\circ - \phi_0) \quad (47)$$

where

$$0 \leq \alpha_0 < 180^\circ \quad (48)$$

Now from the same spherical triangle in Figure 3

$$\cos \psi_0 = \frac{\sin \beta \cos \phi_0}{\sin \alpha_0} \quad (49)$$

$$\sin \psi_0 = \frac{\cos \beta - \cos \theta \cos \alpha_0}{\sin \theta \sin \alpha_0} \quad (50)$$

Solve (49) and (50) for  $\psi_0$ .

The instantaneous value of  $\psi$  and  $\phi$  can now be determined by

$$\dot{\psi} = \psi(t - t_0) + \psi_0 \quad (51)$$

$$\dot{\phi} = \phi(t - t_0) + \phi_0 \quad (52)$$

These equations will hold for some length of time  $t - t_0$ . When errors begin to accumulate, a new  $t_0$  should be chosen and a new set of initial conditions computed.

If the time base in the spacecraft is quantized, there is a quantizing uncertainty in the value of  $t_0$ . Equations for removing quantizing uncertainties in the value of  $t_0$  under the conditions of  $\theta = 0$  are contained in Appendix E.

#### MEASUREMENTS USING A HORIZON DETECTOR

Thus far all the measurements have been made on the sun. Since the sun is considered a point source at infinity, there is an axis of symmetry from the center of gravity of the satellite to the sun. Another inertial reference point is necessary in order to eliminate the ambiguity caused by this symmetry. In general what is needed is another known vector which is not colinear with the sun vector, and an angle  $\delta$  which is measured from this second vector to the spin axis. This second vector may correspond to the magnetic field, to the subsatellite zenith vector, or any other desirable vector.

In the following discussion the use of horizon sensors to measure an angle  $\delta$  between the spin axis and the subsatellite zenith is considered. However, the equations in Section IV apply as well to a  $\delta$  angle measured by any other type of sensor from any other type of second vector.

Infra-red horizon sensors which detect the temperature discontinuity caused by the warm earth against the cold background of outer space can provide horizon sensor data on the dark side of the earth as well as on the sunlit side. Visible light horizon detectors can be used when data is needed only on the sunlit side. Conditions when visible light detectors can be used are in Appendix F. Either type detector usually has a pencil beam field of view arranged so as to provide a pulse upon crossing either into or out of the earth's disc. Sometimes it is

necessary to transmit the knowledge of whether a pulse represents an "in" or "out" crossing, but for satellite applications the difference can usually be determined by relative pulse spacings or prior knowledge about the approximate spin axis orientation.

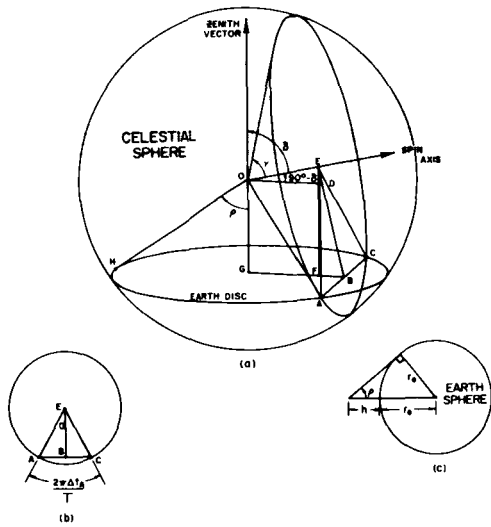


Figure 8—Definition of variables needed to solve the horizon sensor problem

Information is contained in the repetition rate of the pulse pairs, in their spacing, and in their position relative to the sun appearances in the quantized fan. The repetition rate of the pulse pairs can provide a measure of the rotation rate. The information contained in the pulse spacing provides a measure of  $\delta$ , which in this discussion is the angle between the spin axis and the subsatellite zenith vector. The subsatellite zenith vector is a vector from the center of the earth through the center of gravity of the satellite.

If the earth is considered to be a disc inside the celestial sphere, where the center of gravity of the satellite is the center of the sphere, an expression can be derived relating the pulse spacings to  $\delta$ .

Figure 8 represents a satellite rotating with no precession so that  $\theta = 0$ . An earth horizon pipper is mounted at an angle from the satellite Z - axis so as to sweep out a cone which cuts the earth horizons at A and C. From Figure 8b it can be seen that

$$\frac{\overline{EB}}{\overline{EA}} = \cos \left( \frac{\pi \Delta t_A}{T} \right) \quad (53)$$

where  $\Delta t_A$  is the time between horizon pulses and T is the rotation period. From the figure, various other relationships can be derived:

$$\overline{EB} = \overline{ED} + \overline{DB} \quad (54)$$

$$\overline{ED} = \overline{OE} \tan (90^\circ - \delta) \quad \text{where} \quad \overline{OE} = \overline{OH} \cos \gamma \quad (55)$$

$$DB = \overline{OG} \cos (90^\circ - \delta) \quad \text{where} \quad \overline{OG} = \overline{OH} \cos \rho \quad (56)$$

$$\overline{EA} = \overline{OH} \sin \gamma \quad (57)$$

Substituting all these values in expression (53), gives

$$\overline{OH} \cos \gamma \cot \delta + \frac{\overline{OH} \cos \rho}{\sin \delta} = \overline{OH} \sin \gamma \cos \left( \frac{\pi \Delta t_A}{T} \right) \quad (58)$$

which reduces to

$$\cos \rho + \cos \gamma \cos \delta = \sin \gamma \sin \delta \cos \left( \frac{\pi \Delta t_A}{T} \right) \quad (59)$$

where

$$\sin \rho = \frac{r_E}{r_E + h} \quad (60)$$

where

$r_E$  = mean radius of earth

$h$  = apparent altitude of satellite

Rewriting so as to solve explicitly for  $\delta$

$$\cos \delta = \frac{-de \pm f \sqrt{(e^2 + f^2) - d^2}}{(e^2 + f^2)} \quad (61)$$

$$0 \leq \delta < 180^\circ$$

where

$$d = \cos \rho$$

$$e = \cos \gamma$$

$$f = \sin \gamma \cos (\pi \Delta t_A / T)$$

Expression (61) is plotted in Appendix A. It double valued for most of the important cases. In order to minimize this ambiguity it is usually best to make  $\gamma = \rho$  or  $180^\circ - \rho$ . In order to remove the ambiguity altogether a second horizon sensor mounted with a different  $\gamma$  angle can be used. If two sensors are used it is usually best to mount one at an angle  $\gamma_a = \rho$  and the second at an angle  $\gamma_b = 180^\circ - \rho$ . With a system using two such sensors, the absence of a signal from one or the other of the sensors usually will eliminate the ambiguous solution from (61). When both sensors scan the horizon the solution for  $\delta$  becomes single valued, and in addition the satellite apparent altitude can be calculated.

$$\cos \rho + \cos \gamma_a \cos \delta = \sin \gamma_a \sin \delta \cos \frac{\pi \Delta t_a}{T} \quad (62a)$$

$$\cos \rho + \cos \gamma_b \cos \delta = \sin \gamma_b \sin \delta \cos \frac{\pi \Delta t_b}{T} \quad (62b)$$

where  $\Delta t_a$  is the pulse spacing from sensor A and  $\Delta t_b$  is the pulse spacing from sensor B. Subtracting (62b) from (62a) and reducing gives

$$\tan \delta = \frac{p - q}{1 - m} \quad (63)$$

$$0 \leq \delta < 180^\circ$$

where

$$p = \cos \gamma_a$$

$$q = \cos \gamma_b$$

$$l = \sin \gamma_a \cos (\pi \Delta t_a / T)$$

$$m = \sin \gamma_b \cos (\pi \Delta t_b / T)$$

Solution of equation (63) is plotted in Appendix B.

Substituting the values of  $\delta$  just calculated back into equation (62a) and solving for  $\rho$  gives

$$\cos \rho = \sin \gamma_a \sin \delta \cos \left( \frac{\pi \Delta t_a}{T} \right) - \cos \gamma_a \cos \delta \quad (64)$$

$$0 \leq \rho < \frac{\pi}{2}$$

Rewriting equation (60) gives the apparent satellite altitude

$$h = \left( \frac{r_e}{\sin \rho} \right) - r_e \quad (65)$$

This apparent altitude may differ from the true altitude by the thickness of the atmosphere.

Information determining the value of  $\delta$  is also contained in the relative position of the horizon pulses to the quantized fan crossing of the sun. If the satellite is spinning so that  $\theta = 0^\circ$ , horizon pulses will be symmetrical about the time at which the quantized fan plane crosses the center of the earth. Figure 10 illustrates the case where the horizon sensors are mounted so that their fields of view lie in the plane of the quantized fan. The center of the earth is located on the celestial sphere at  $(RA_z + 180^\circ)$  and  $(-D_z)$ , where  $RA_z$  is the right ascension and  $D_z$  the declination of the subsatellite-point zenith vector.  $(180^\circ - \eta)$  is the great circle arc from the sun to the earth's center on the celestial sphere, where  $\eta$  is the great circle arc from the sun to the subsatellite zenith vector.  $\Delta t_c$  is the time midway between horizon pulses minus the time the quantized fan crosses the sun. The relationship between  $\delta$  and  $\Delta t_c$  can now be written from the spherical triangles in Figure 9.

$$\cos (180^\circ - \eta) = \cos \beta \cos (180^\circ - \delta) + \sin \beta \sin (180^\circ - \delta) \quad (66)$$

$$\cos [(\dot{\phi} + \dot{\psi}) \Delta t_c]$$

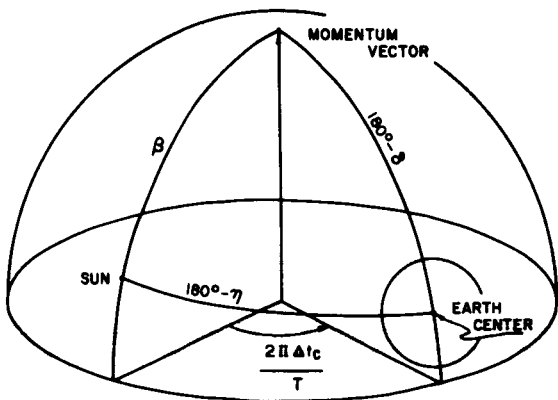


Figure 9—Relationship between  $\Delta t_c$  and  $\delta$

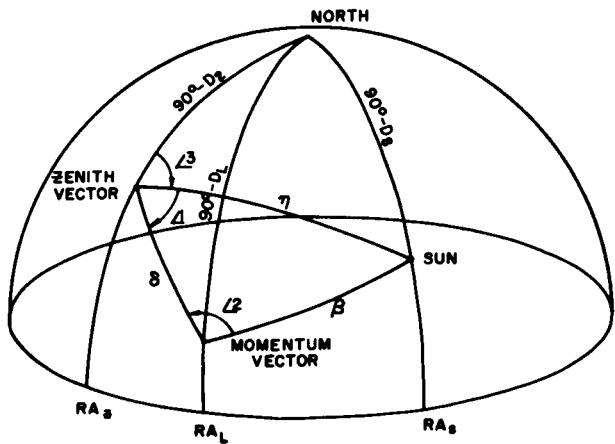


Figure 10—Position of the momentum vector relative to the sun and the zenith vector

or

$$\cos \eta = \cos \beta \cos \delta - \sin \beta \sin \delta \cos [(\dot{\phi} + \dot{\psi}) \Delta t_c] \quad (67)$$

Solving for  $\delta$  gives

$$\cos \delta = \frac{rs \pm u \sqrt{(s^2 + u^2) - r^2}}{(s^2 + u^2)} \quad (68)$$

where  $r = \cos \eta$

$s = \cos \beta$

$$u = -\sin \beta \cos (2\pi \Delta t_c / T)$$

$$0^\circ \leq \delta < 180^\circ$$

and where

$$\cos \eta = \sin D_z \sin D_s + \cos D_z \cos D_s \cos (RA_s - RA_z) \quad (69)$$

where

$D_z$  = declination of subsatellite zenith

$D_s$  = declination of sun

$RA_z$  = right ascension of subsatellite zenith

$RA_s$  = right ascension of sun

$$0 \leq \eta < 180^\circ$$

Calculation of  $\delta$  by (68) should result in 2 solutions. This twofold ambiguity may be resolved by choosing the solution of (68) which most closely corresponds to values of  $\delta$  obtained from (61) or (63).

Calculation of  $\delta$  is often in practice a difficult task owing to the nature of the horizon. Pulse pairs do not always indicate the true horizon. In addition the apparent altitude of the satellite must be measured not from the earth's surface, but from some vaguely defined part of the atmosphere which is often dependent on weather conditions. Finally the earth is not a perfect sphere.

Calculation of  $\delta$  using equation (63) eliminates consideration of the apparent altitude of the satellite, and has proven in practice to usually provide the most reliable method of calculating. Use of equation (68) also eliminates consideration of apparent altitude.

Perturbation analysis of the solution for  $\delta$  indicates that under certain conditions one type of solution for  $\delta$  is less sensitive to measurement errors than another. This type of perturbation analysis is perhaps most understandable when done graphically. Appendix A, B, and C contain plots of the solutions of equations (61), (63), and (68) under various conditions. Sensitivity of  $\delta$  to perturbations in various other parameters can be examined on these plots.

If there is some precession motion present so that  $\theta \neq 0$ , some sort of averaging procedure is needed to obtain an average  $\delta$ . This average  $\delta$  then will be the angle between the second known vector and the satellite momentum vector.

Sufficient information has now been obtained to calculate the instantaneous orientation of the satellite for any moment of time. Thus, knowing the mounting arrangements of any sensor on the satellite, it is possible to calculate the sensor orientation for any time.

## SPACECRAFT ATTITUDE DETERMINATION

The spacecraft momentum vector position can now be calculated. From Figure 10 we may write equations for the values of the auxiliary angles  $\angle 1$  and  $\angle 3$ .

$$\cos \angle 1 = \frac{\cos \beta - \cos \eta \cos \delta}{\sin \eta \sin \delta} \quad (70)$$

$$\sin \angle 1 = \frac{\sin \beta \sin \angle 2}{\sin \eta} \quad (71)$$

where

$$\angle 2 = (\dot{\phi} + \dot{\psi}) \Delta t_c \pm 180^\circ$$

$$\cos \angle 3 = \frac{\sin D_s - \cos \eta \sin D_z}{\sin \eta \cos D_z} \quad (72)$$

$$\sin \angle 3 = \frac{\sin (RA_s - RA_z) \cos D_s}{\sin \eta} \quad (73)$$

Now using the values of  $\angle 1$  and  $\angle 3$  from (70-73) we may find  $RA_L$  and  $D_L$  the right ascension and declination of the momentum vector.

$$\sin D_L = \sin D_z \cos \delta + \cos D_z \sin \delta \cos (\angle 3 + \angle 1) \quad (74)$$

$$-\frac{\pi}{2} < D_L \leq \frac{\pi}{2}$$

$$\cos (RA_L - RA_z) = \frac{\cos \delta - \sin D_z \sin D_L}{\cos D_z \cos D_L} \quad (75)$$

$$\sin (RA_L - RA_z) = \frac{\sin (\angle 3 + \angle 1) \sin}{\cos D_L} \quad (76)$$

$$RA_L = RA_z + (RA_L - RA_z) \quad (77)$$

This solution is unique. If the quadrant of  $(\phi + \psi) \Delta t_c$  is unknown,  $\angle 1$  must be found from equation (70) and two solutions result.

### Error Calculations

It is well to question at this point the accuracy of the position of the momentum vector determined by these methods. Tables of values of the error in the position of the momentum vector caused by a one degree error in  $\delta$  is contained in Appendix D. From these tables certain facts become obvious.

The error is large whenever  $\eta \approx 0$ , or  $\eta \approx 180^\circ$ . The error is also large whenever  $\eta \approx \beta + \delta$ ,  $\delta \approx \eta + \beta$ ,  $\beta \approx \delta + \eta$ , or  $\eta + \beta + \delta \approx 360^\circ$ .

Also contained in Appendix A, B, and C are a series of plots of  $\delta$  vs.  $\Delta t_a$ ,  $\Delta t_b$ , and  $\Delta t_c$  under various conditions. From these plots then it is possible to estimate the error in momentum vector position caused by an error in the measurement of  $\Delta t_a$ ,  $\Delta t_b$ , or  $\Delta t_c$ . From the plots find the slope of the curve under the conditions in question, multiply it by the uncertainty in  $\Delta t_a$ ,  $\Delta t_b$ ,  $\Delta t_c$ . This gives the uncertainty in  $\delta$ . Then go to table and look up the error in momentum vector position corresponding to the error in  $\delta$ .

The table in Appendix D is symmetrical and therefore the error in momentum vector position caused by an uncertainty in  $\beta$  can also be obtained by interchanging the values of  $\beta$  and  $\delta$  and assuming that  $\delta$  is the uncertain quantity. Thus the uncertainties from  $\beta$  can then be combined with those from  $\delta$  to give the total uncertainty.

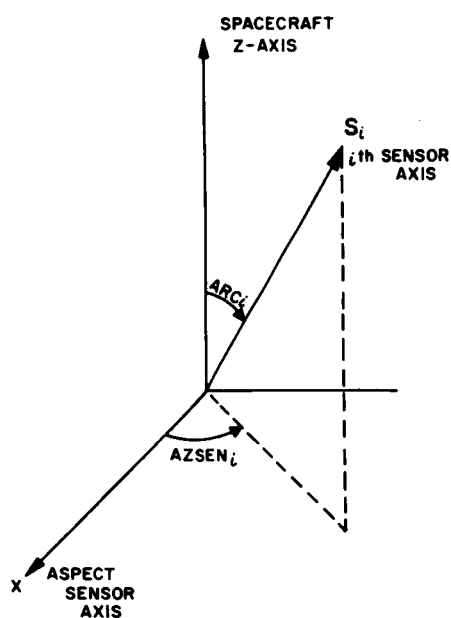


Figure 11—Position of a sensor  $S_i$  relative to the aspect sensor in a spacecraft coordinate system

#### Sensor Position as a Function of Time

The momentum vector having been determined, the constants of motion calculated, and the initial conditions at time  $t_0$  measured, it is now possible to reconstruct the motion history of the spacecraft both forward and backward in time from  $t_0$  over an interval as long as the uncertainties in the above quantities will permit. The look direction of any sensing device on the spacecraft can then be found at any time if the sensor position relative to the aspect sensor is known.

Assume a sensor  $S_i$  mounted on the spacecraft so that its axis makes an angle  $ARC_i$  with the  $I_3$  inertia axis, which is the satellite z-axis, and so that the sensor axis lies at angle  $AZSEN_i$  from the aspect sensor axis measured east along the satellite equator. See Figure 11.

The following solution for the instantaneous position of the individual sensors does not use the conventional coordinate transformations by matrix multiplication. The matrix method is perhaps more elegant, but in general the number of computer operations for the matrix method is considerably in excess of that needed for the method described below.

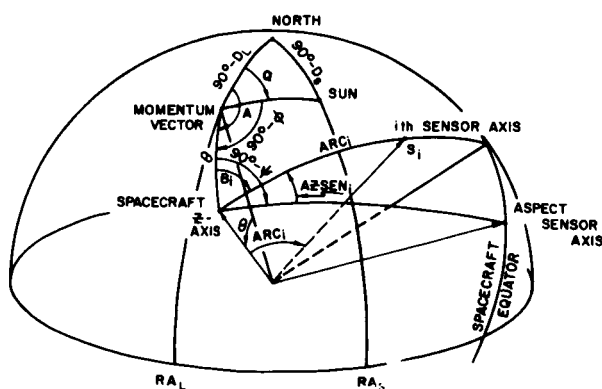


Figure 12—Relative positions of a sensor axis, the spacecraft z-axis, and the momentum vector

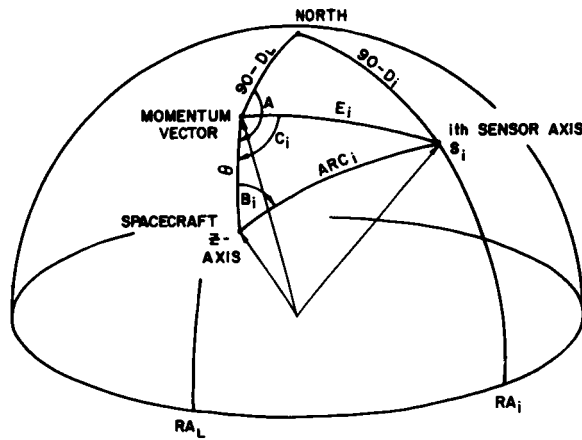


Figure 13—Relationships of sensor axis  $S_i$  with respect to the spacecraft z-axis and the momentum vector

Define an angle A as shown in Figure 12.

$$A = Q + \frac{\pi}{2} - \phi \quad (78)$$

where  $\phi = \dot{\phi}(t - t_0) + \phi_0$  as defined in equation (52) and where

$$\sin Q = \frac{\sin(RA_s - RA_L) \cos D_s}{\sin \beta} \quad (79)$$

$$\cos Q = \frac{\sin D_s - \cos \beta \sin D_L}{\sin \beta \cos D_L} \quad (80)$$

Also from Figure 12

$$B_i = \left( \frac{\pi}{2} - \psi \right) - AZSEN_i \quad (81)$$

where  $\psi = \dot{\psi}(t - t_0) + \psi_0$  as defined in equation (51)

Now solve for the auxiliary angles  $E_i$  and  $C_i$  from Figure 13.

If  $\theta = 0$

$$E_i = \text{ARC}_i \quad \text{and} \quad C_i = \pi - B_i \quad (82)$$

However, if  $\theta > 0$

$$\cos E_i = \cos \theta \cos \text{ARC}_i + \sin \theta \sin \text{ARC}_i \cos B_i \quad (83)$$

$$0 \leq E_i < \pi$$

$$\sin C_i = \frac{\sin B_i}{\sin E_i} \sin \text{ARC}_i \quad (84a)$$

$$\cos C_i = \frac{\cos \text{ARC}_i - \cos \theta \cos E_i}{\sin \theta \sin E_i} \quad (84b)$$

Finally the right ascension  $\text{RA}_i$  and declination  $D_i$  of the sensor  $S_i$  can be found by

$$\sin D_i = \cos E_i \sin D_L + \sin E_i \cos D_L \cos (A - C_i) \quad (85)$$

$$-\frac{\pi}{2} < D_i \leq \frac{\pi}{2}$$

where  $D_L$  is the declination of the momentum vector from equation (74), and

$$\cos (\text{RA}_i - \text{RA}_L) = \frac{\cos E_i - \sin D_L \sin D_i}{\cos D_L \cos D_i} \quad (86)$$

$$\sin (\text{RA}_i - \text{RA}_L) = \frac{\sin (A - C_i) \sin E_i}{\cos D_i} \quad (87)$$

$$RA_i = (RA_i - RA_L) + RA_L \quad (88)$$

where  $RA_L$  is the right ascension of the momentum vector from equation (77)

Thus the aspect problem is uniquely solved for any instant of time. It is now possible to obtain the angle between the sensor  $S_i$  and an external vector such as the magnetic field vector or velocity vector. The coordinates of the  $S_i$  vector need only be substituted into equation (89) along with the coordinates of the external vector to obtain

$$\cos \Omega_i = \sin D_i \sin D_x + \cos D_i \cos D_x \cos (RA_i - RA_x) \quad (89)$$

$$0 \leq \Omega_i < \pi$$

where  $\Omega_i$  = the angle between the external vector and  $S_i$  at an instant of time.

$D_x$  = declination of the external vector

$RA_x$  = right ascension of the external vector

Of course a great deal can be known about the behavior of a particular sensor with respect to an external vector without the complete solution. For instance if the momentum vector is known, the minimum angle a sensor ever makes with an external vector can be found. From Figure 14 the minimum angle  $S_i$  makes with an external vector is given by

$$\Omega_{i \min} = |\Omega_L - ARC_i| - \theta \quad \text{if} \quad (|\Omega_L - ARC_i| - \theta \geq 0) \quad (90)$$

$$\Omega_{i \ min} = 0 \quad \text{if} \quad (|\Omega_L - ARC_i| - \theta < 0) \quad (91)$$

where  $\Omega_L$  is the angle between the momentum vector and the external vector, and  $\theta$  is the half angle of any precession which may be present.

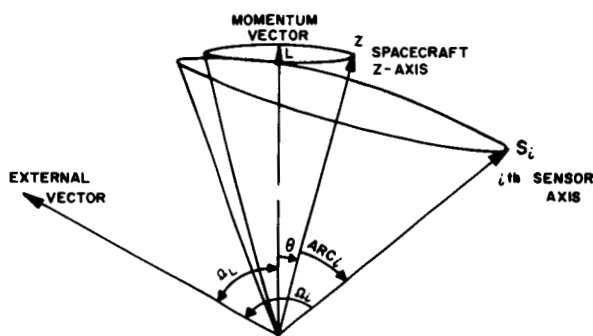
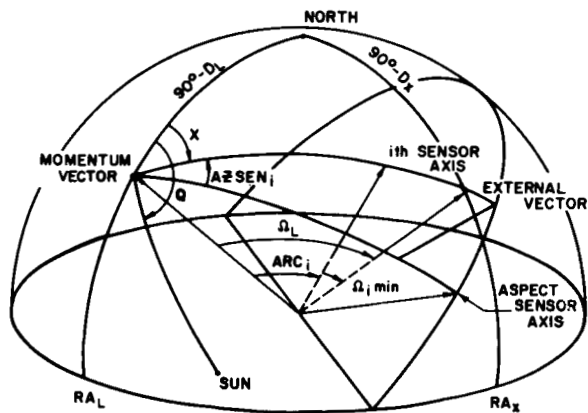


Figure 14—Relationships of a sensor axis with respect to an external vector

Figure 15—Relationships necessary for finding times of maximum and minimum angles between a sensor and an external vector



In like manner, the maximum angle a sensor makes with an external vector is given by

$$\Omega_i \max = \Omega_L + \text{ARC}_i + \theta \quad \text{if } (\Omega_L + \text{ARC}_i + \theta) \leq \pi \quad (92)$$

$$\Omega_i \max = 2\pi - (\Omega_i + \text{ARC}_i) + \theta \quad \left\{ \begin{array}{l} \text{if } (\Omega_L + \text{ARC}_i + \theta) > \pi \\ \text{and } (\Omega_L + \text{ARC}_i - \theta) > \pi \end{array} \right. \quad (93a)$$

$$\Omega_i \max = \pi \quad \left\{ \begin{array}{l} \text{if } (\Omega_L + \text{ARC}_i + \theta) > \pi \\ \text{and } (\Omega_L + \text{ARC}_i - \theta) < \pi \end{array} \right. \quad (93b)$$

The time at which  $\Omega_{i \text{ min}}$  and  $\Omega_{i \text{ max}}$  occur can also be found rather easily in the case where  $\theta = 0$ . From Figure 15 find

$$\cos X = \frac{\sin D_x - \cos \Omega_L \sin D_L}{\sin \Omega_L \cos D_L} \quad (94)$$

$$\sin X = \frac{\cos D_x \sin (RA_x - RA_L)}{\sin \Omega_L} \quad (95)$$

The time at which a sensor makes a minimum angle with the external vector is then

$$t_{\Omega_{i \text{ min}}} = t_s + \frac{(Q - X) - AZSEN_i}{(\dot{\phi} + \dot{\psi})} \quad (96)$$

where  $t_s$  is the time at which the aspect sensor crosses the sun, and  $Q$  is the solution to equations (79) and (80).

The time at which a sensor makes a maximum angle with the external vector is

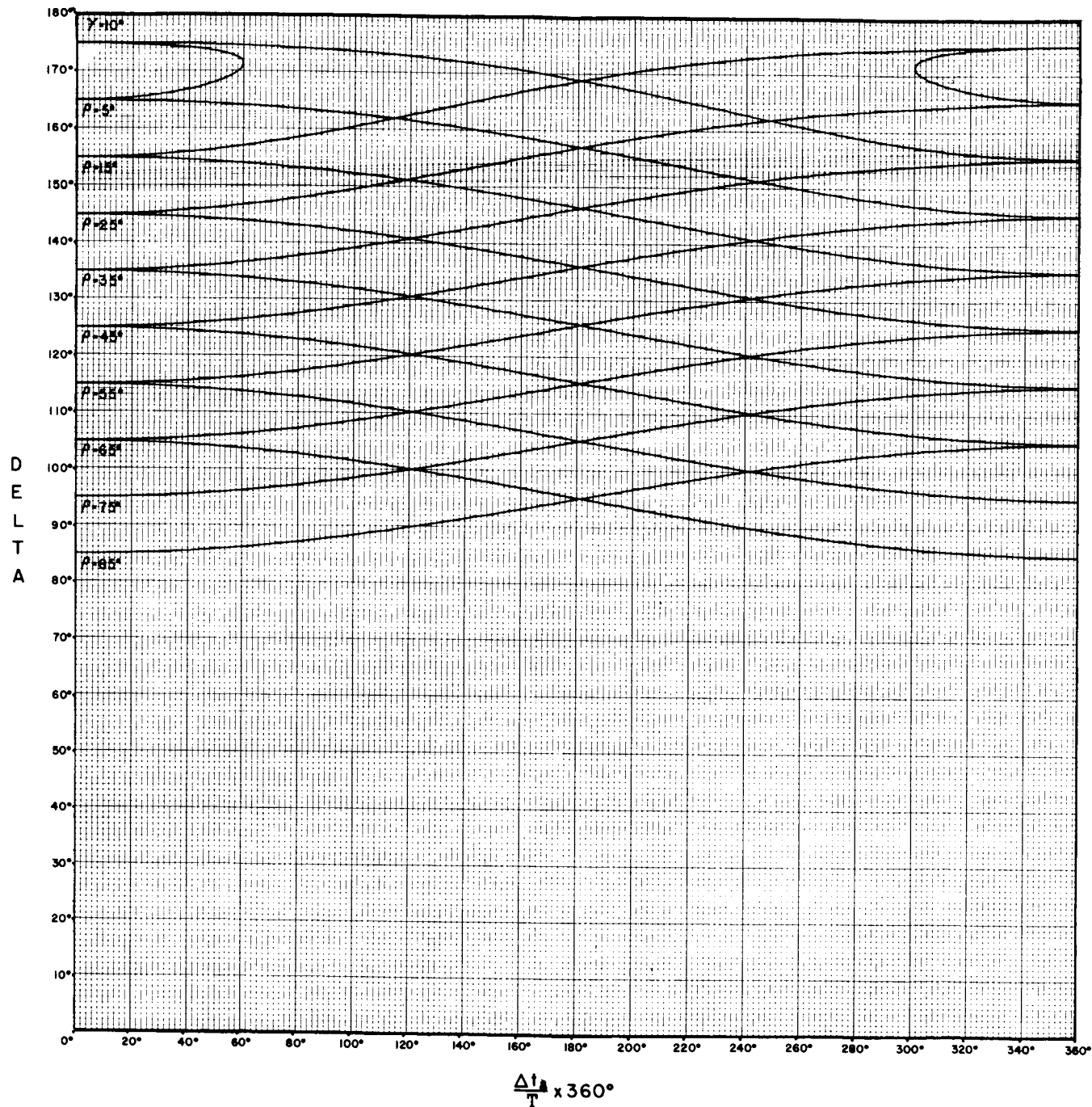
$$t_{\Omega_{i \text{ max}}} = t_{\Omega_{i \text{ min}}} + \frac{\pi}{(\dot{\phi} + \dot{\psi})} \quad (97)$$

If  $\theta \neq 0$ , the general method of solving for  $\Omega_i$  must be used a number of times in a roll period and the minimum value of  $\Omega_i$  set equal to  $\Omega_{i \text{ min}}$ . Similarly for  $\Omega_{i \text{ max}}$ .

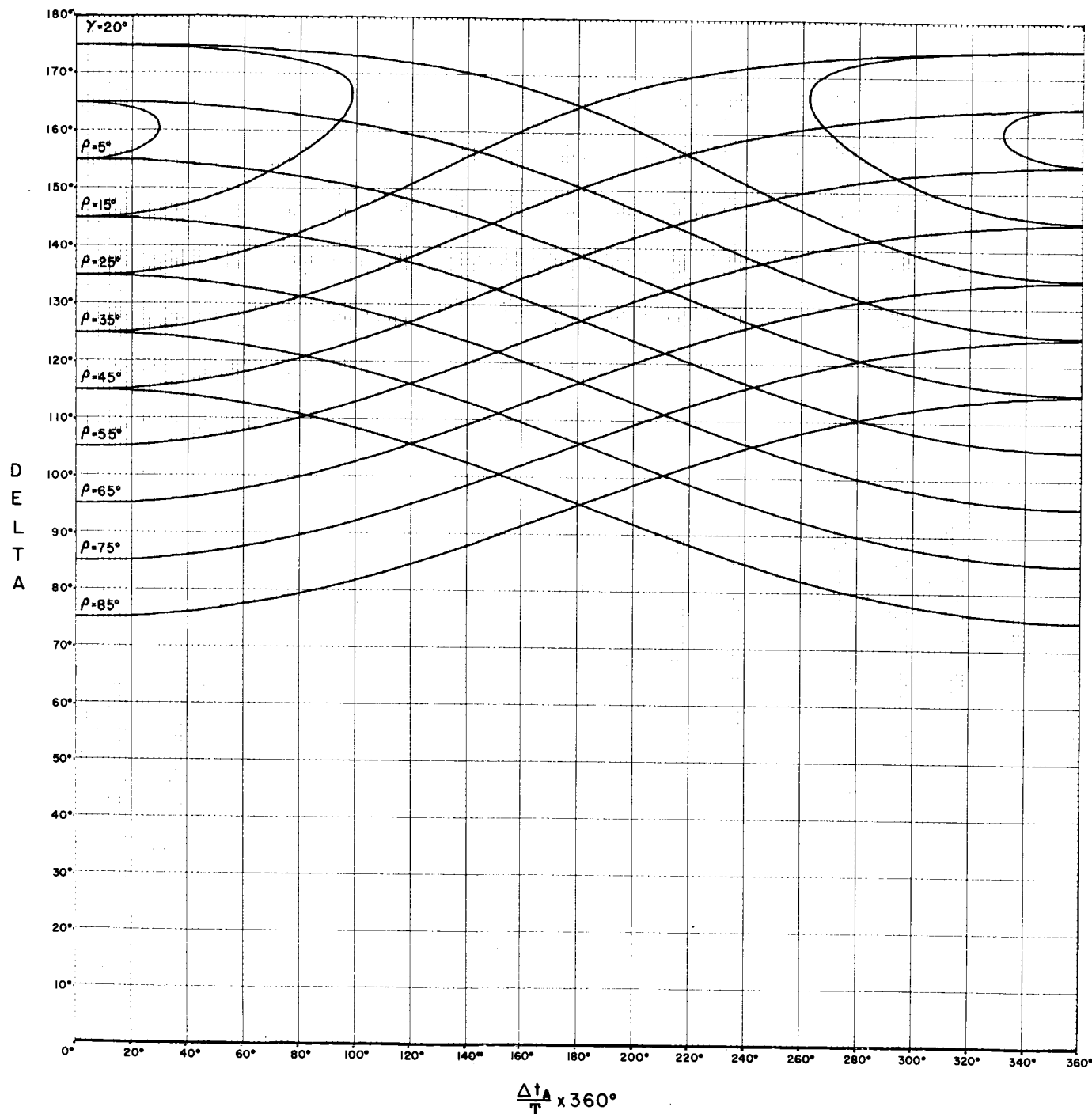
## APPENDIX A

Plots of  $\Delta t_A$  and  $h$   
Solutions of Equation (61)

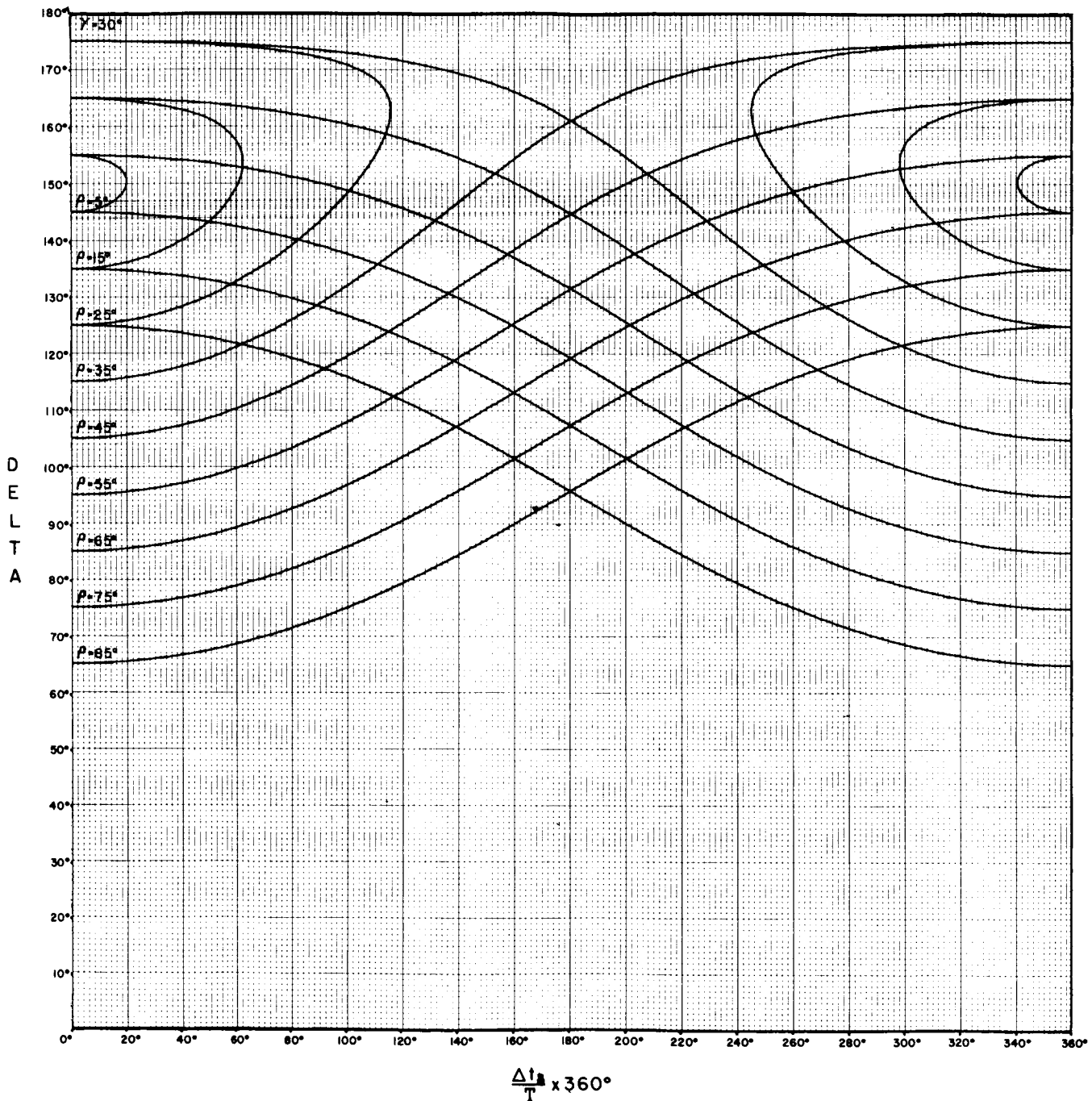
## DELTA V.S. SUN EARTH PULSE SPACING



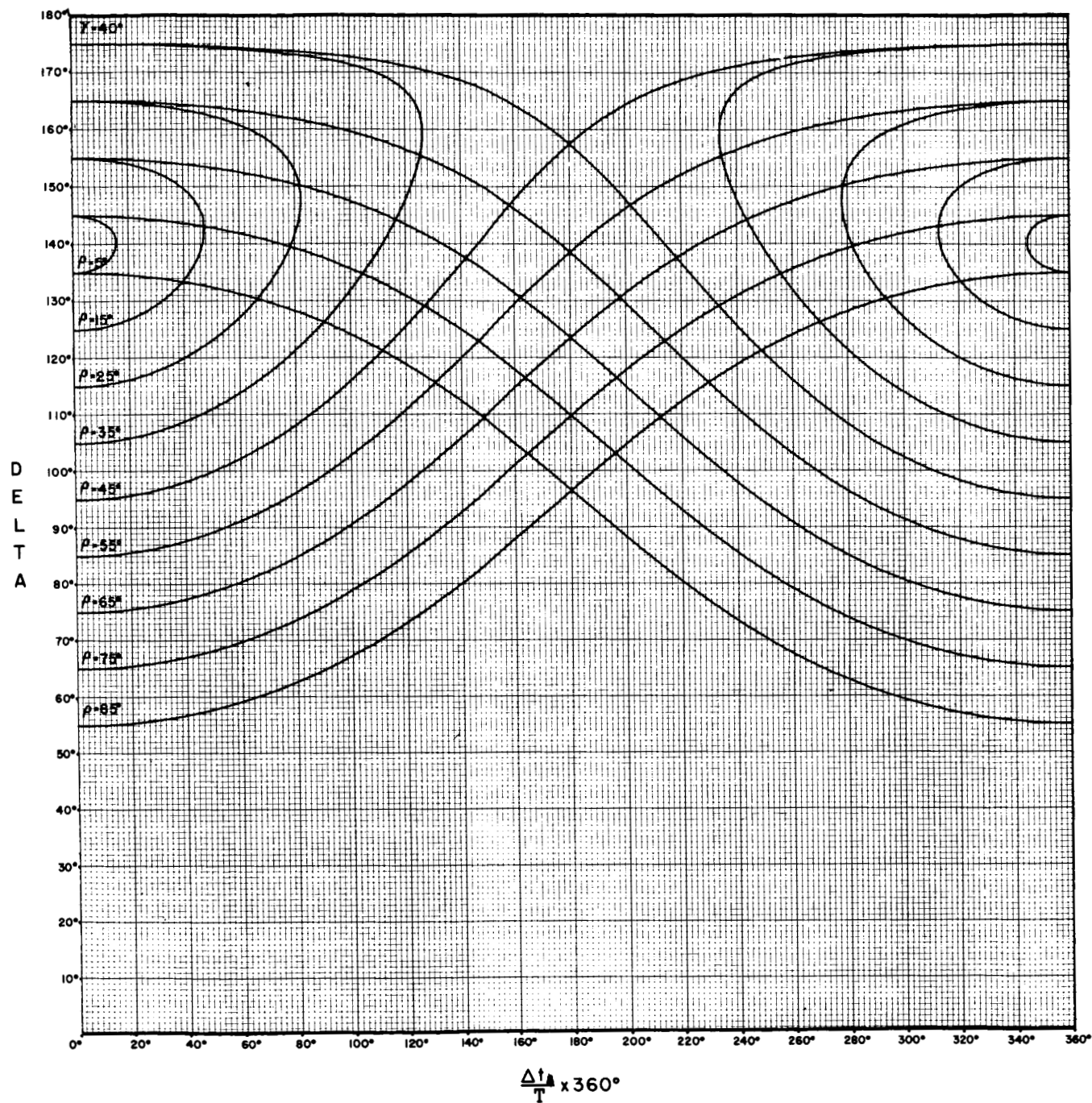
## DELTA V.S. SUN EARTH PULSE SPACING



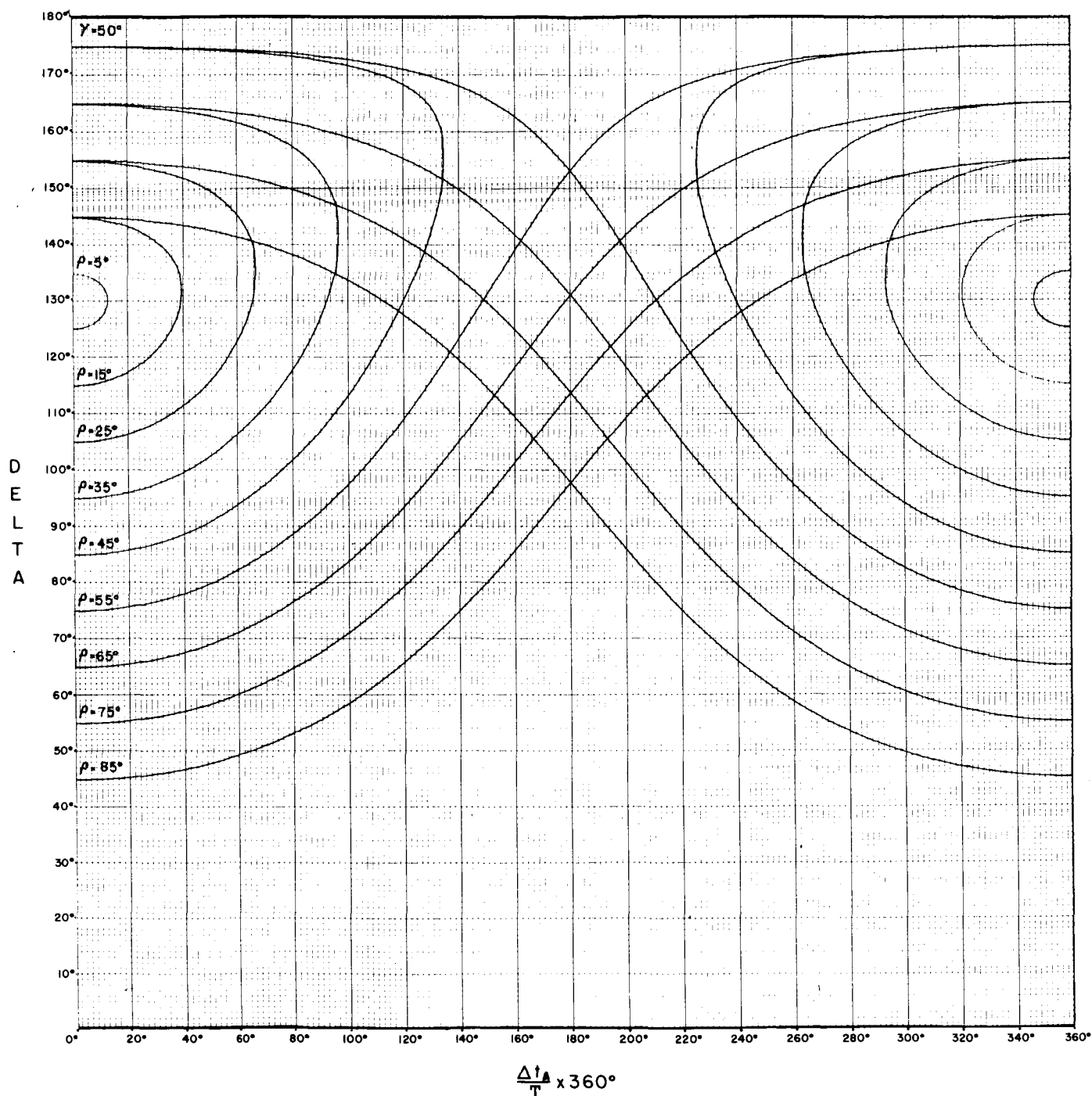
## DELTA V.S. SUN EARTH PULSE SPACING



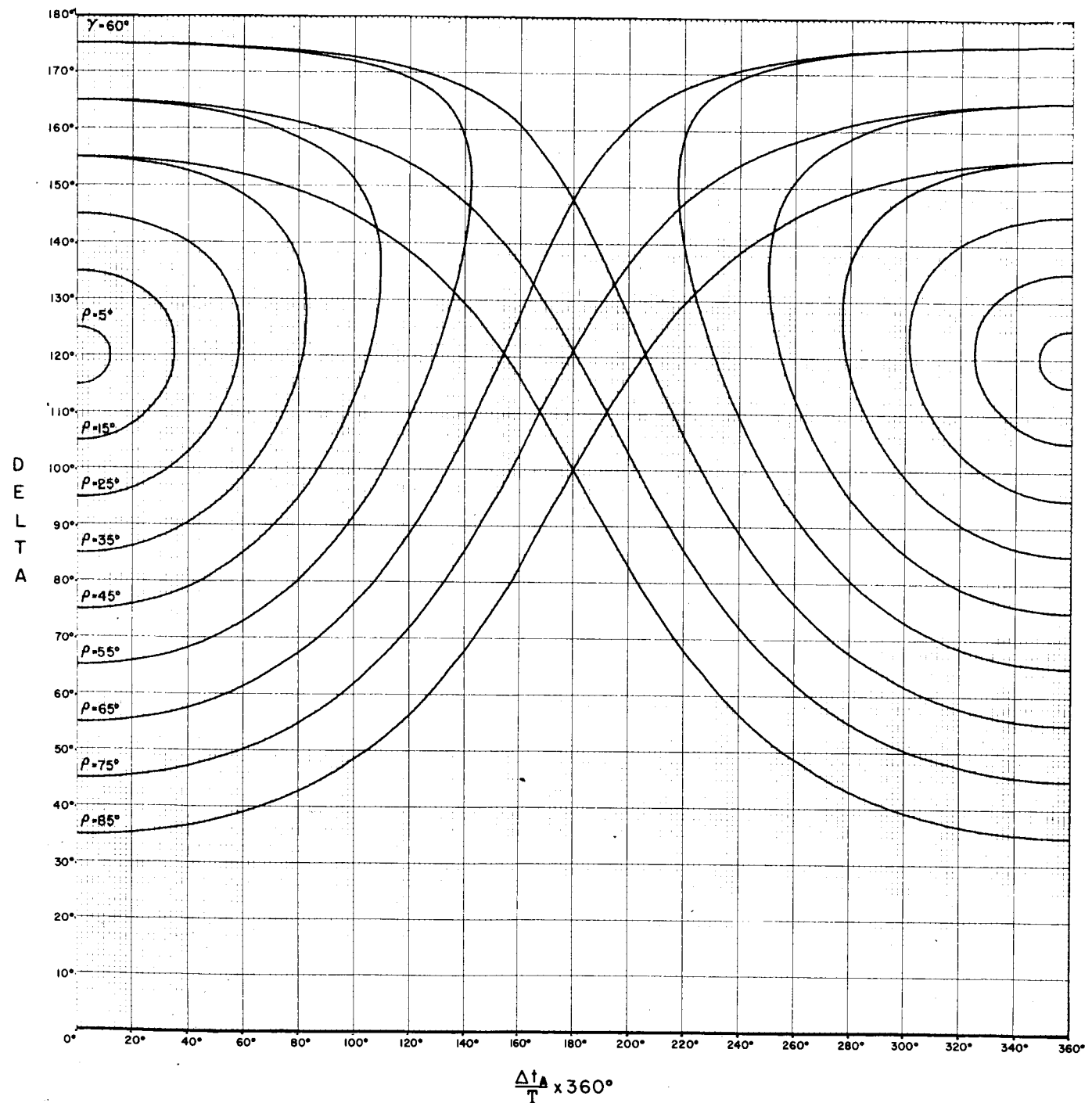
## DELTA V.S. SUN EARTH PULSE SPACING



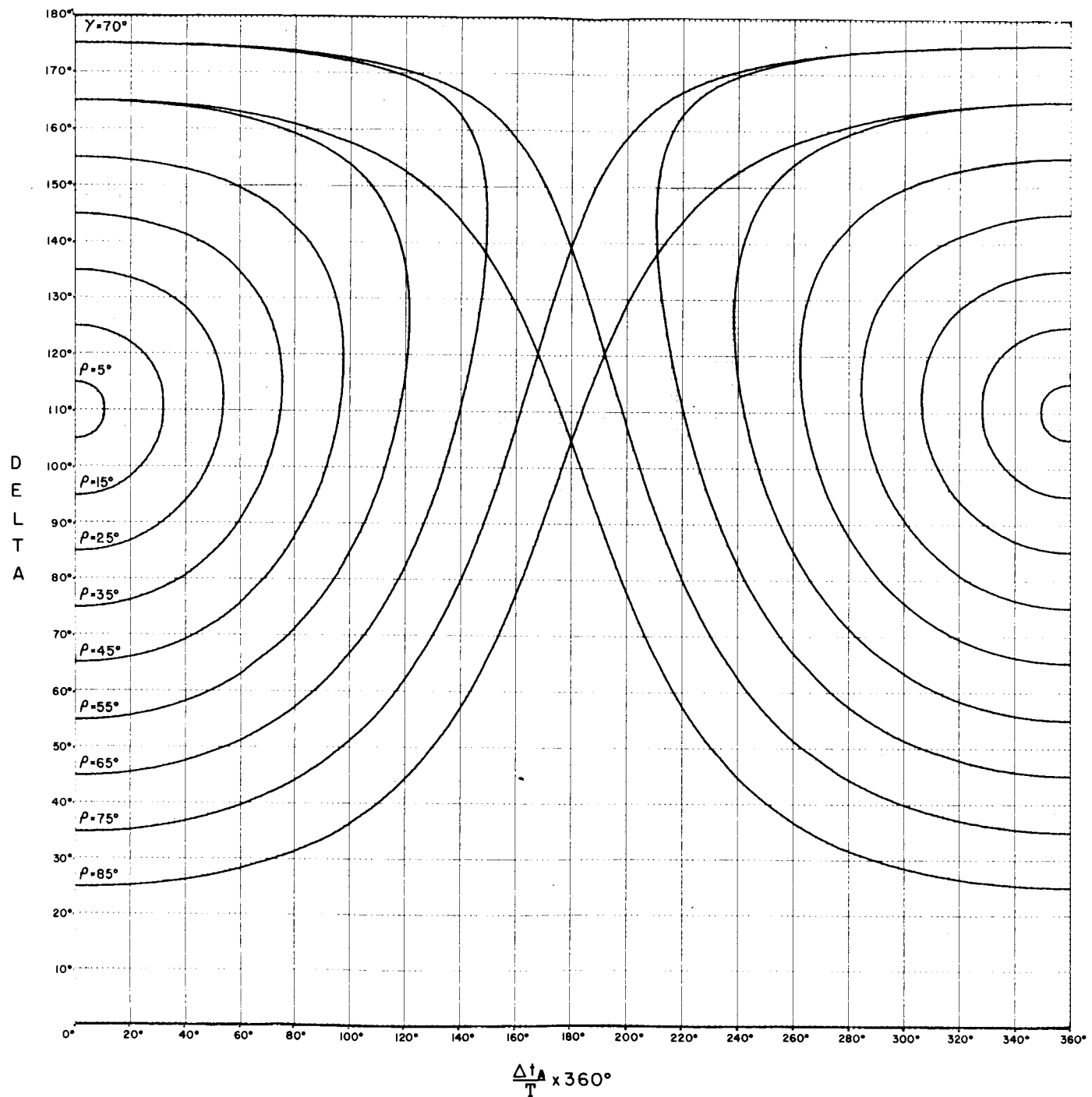
## DELTA V.S. SUN EARTH PULSE SPACING



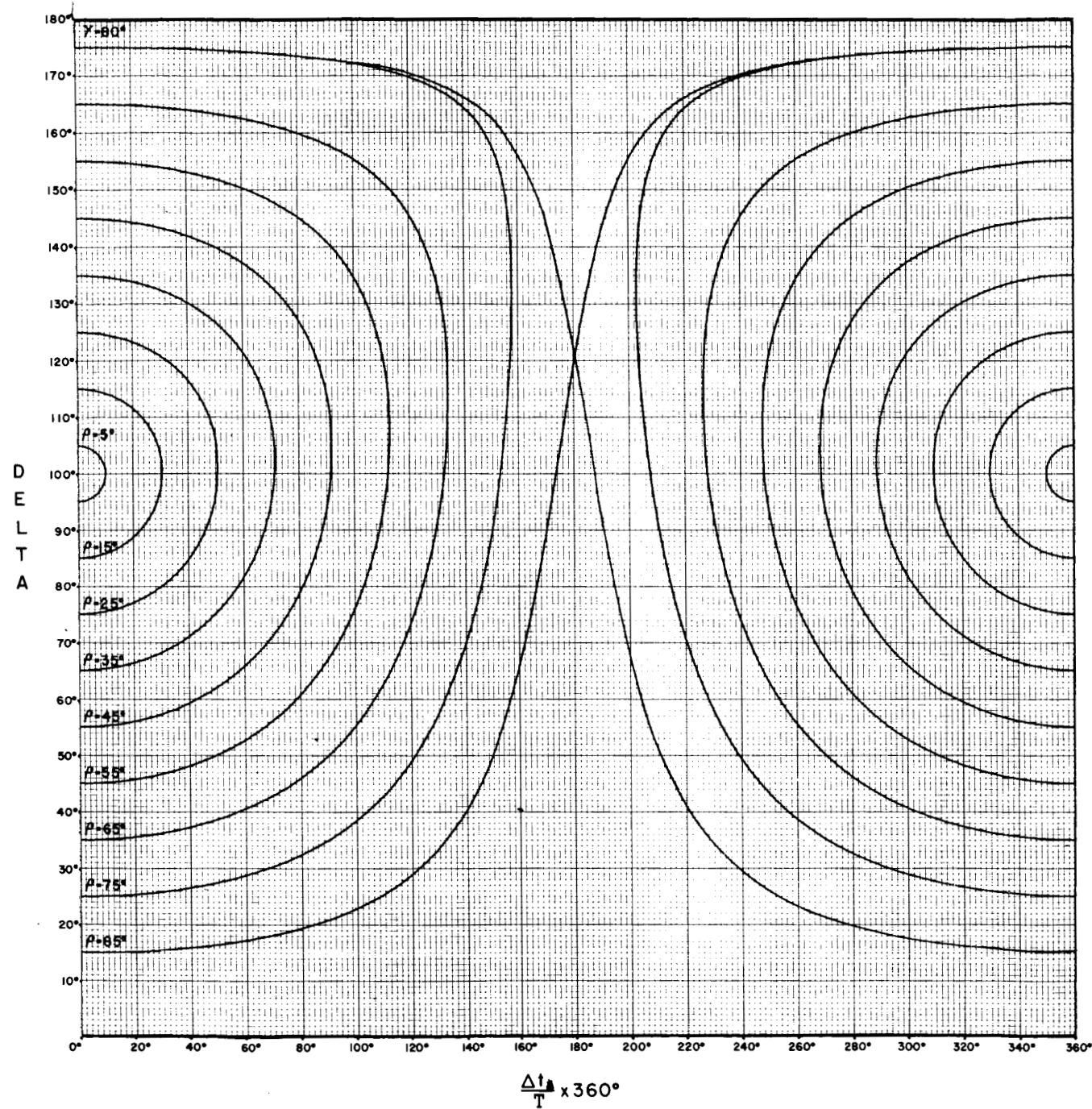
## DELTA V.S. SUN EARTH PULSE SPACING



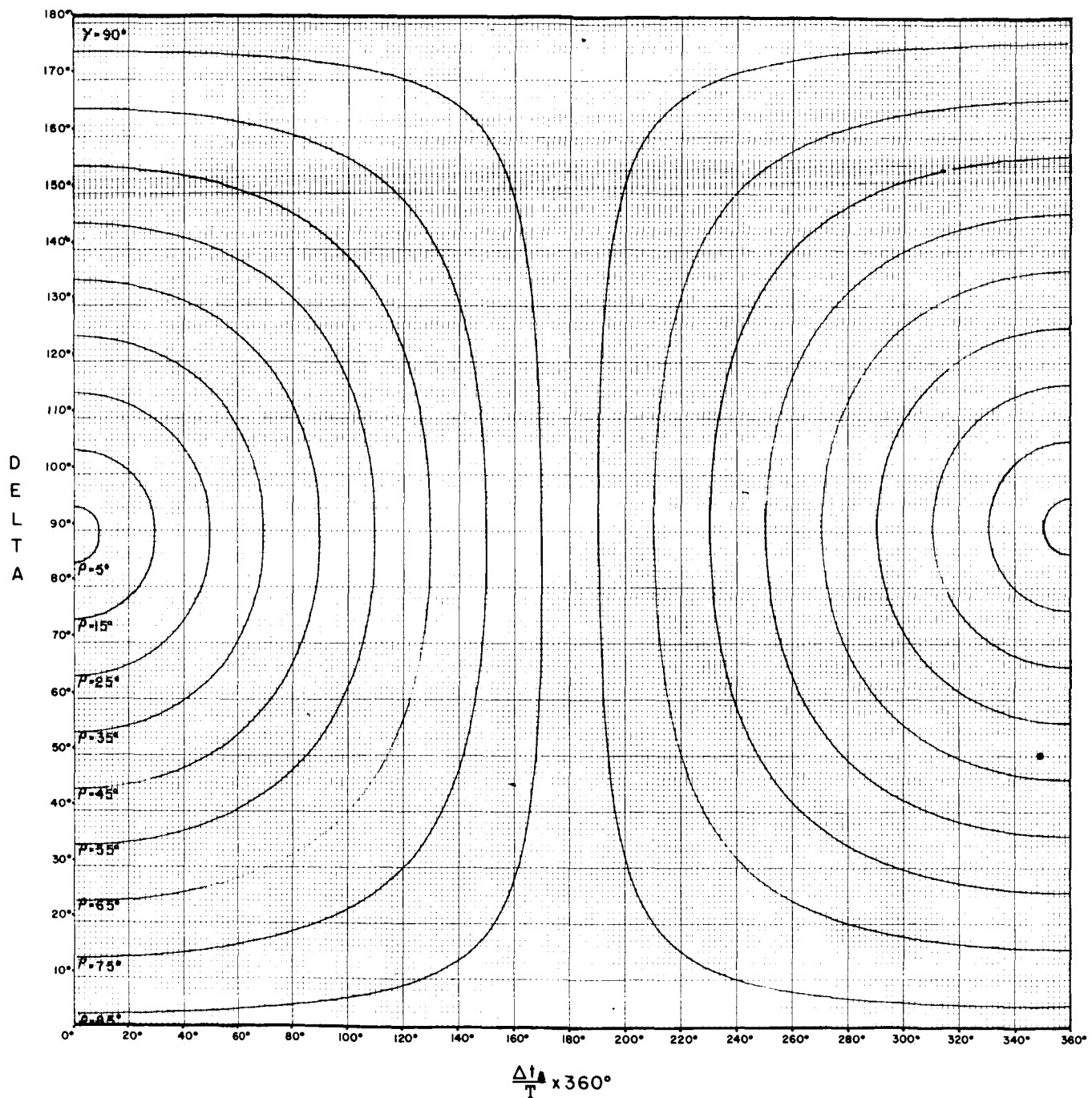
## DELTA V.S. SUN EARTH PULSE SPACING



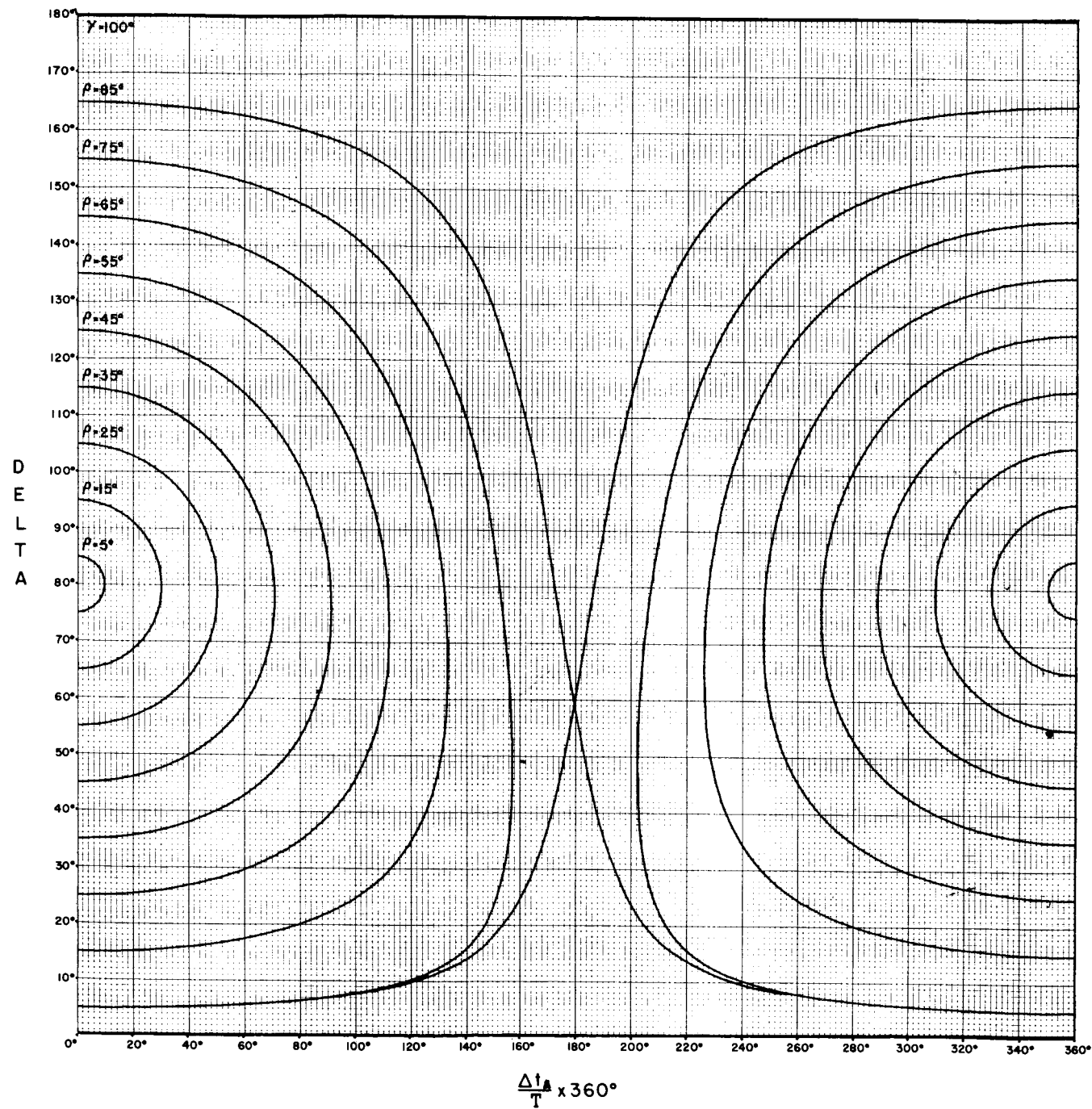
## DELTA V.S. SUN EARTH PULSE SPACING



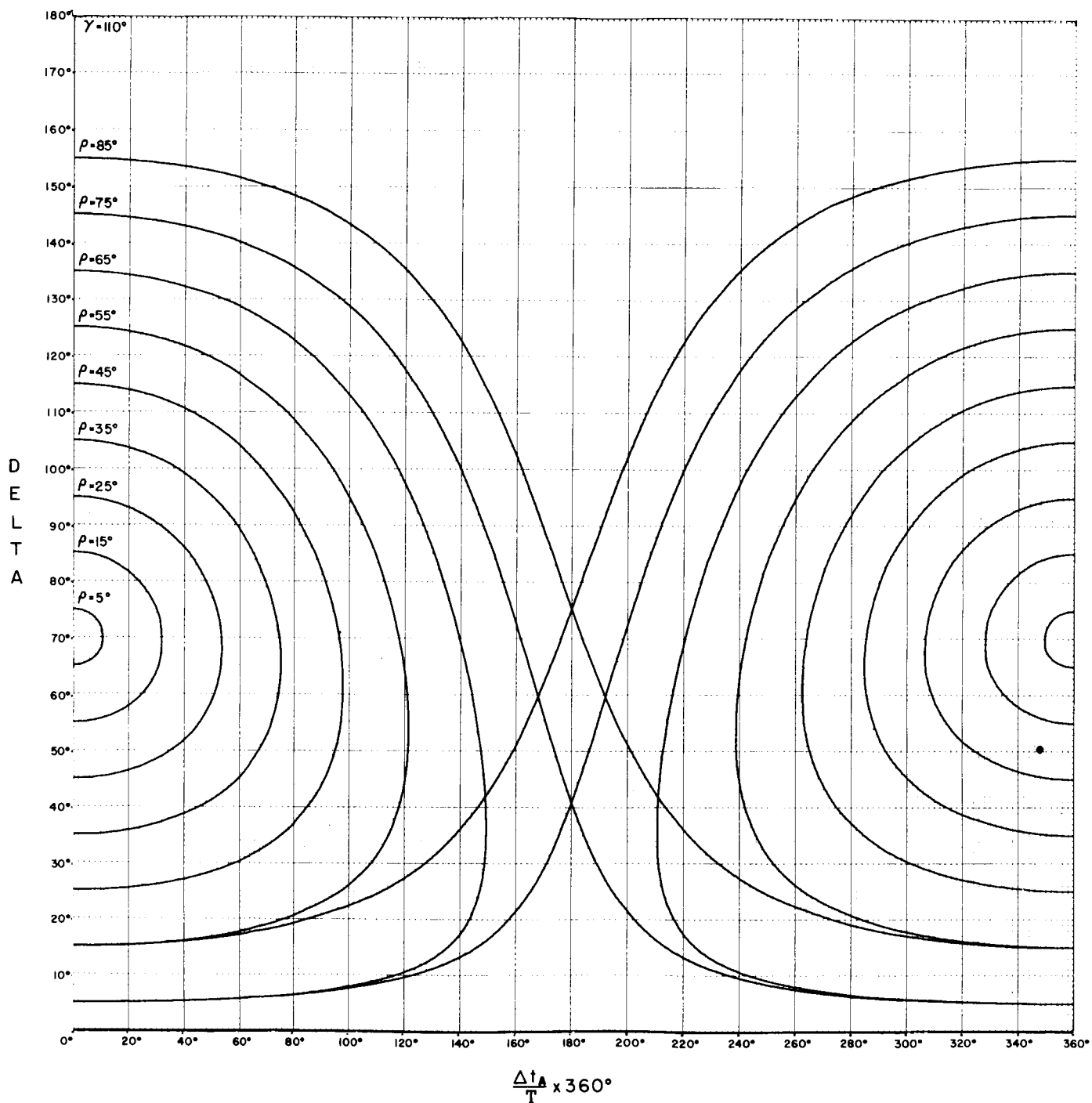
## DELTA V.S. SUN EARTH PULSE SPACING



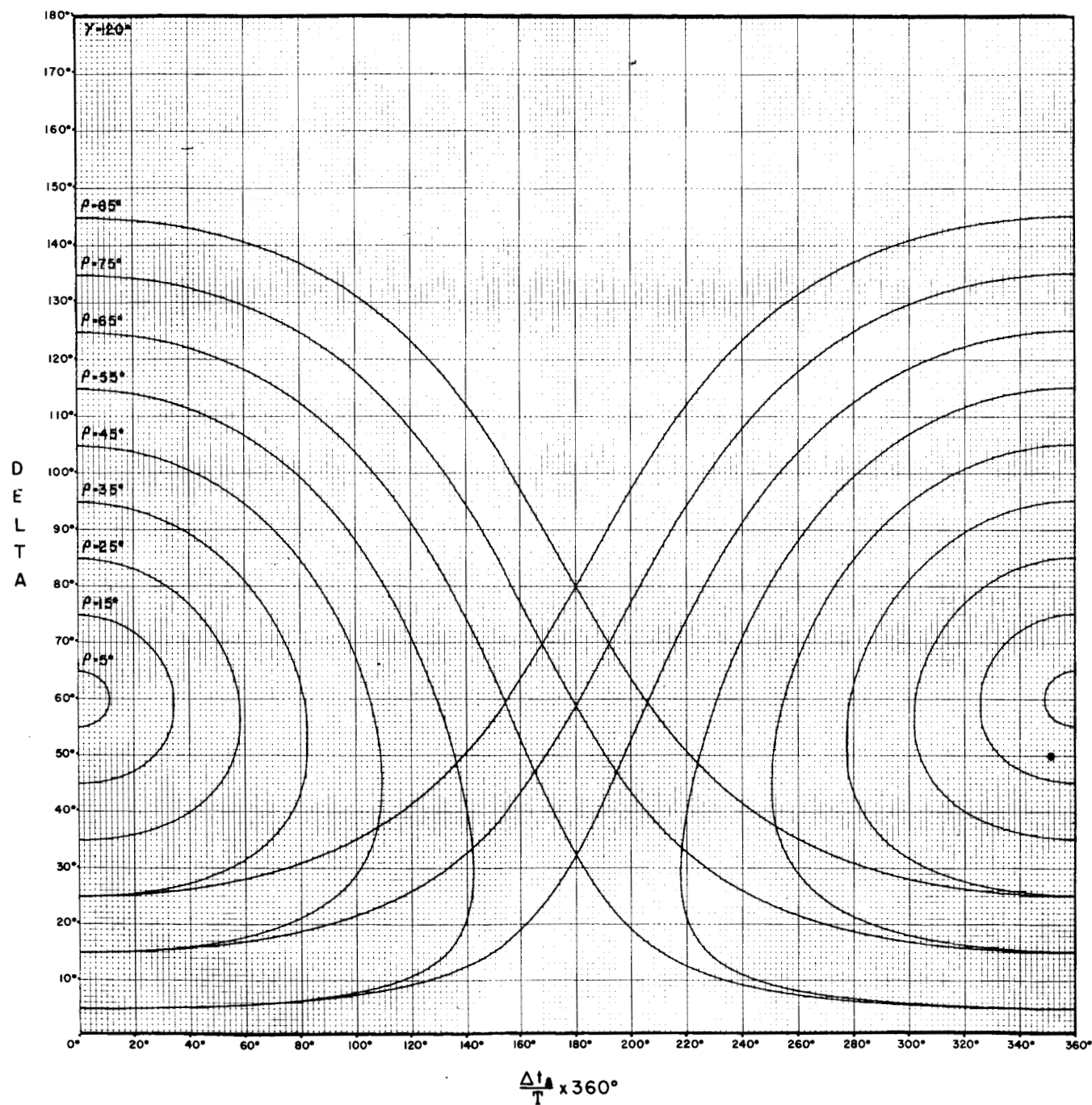
## DELTA V.S. SUN EARTH PULSE SPACING



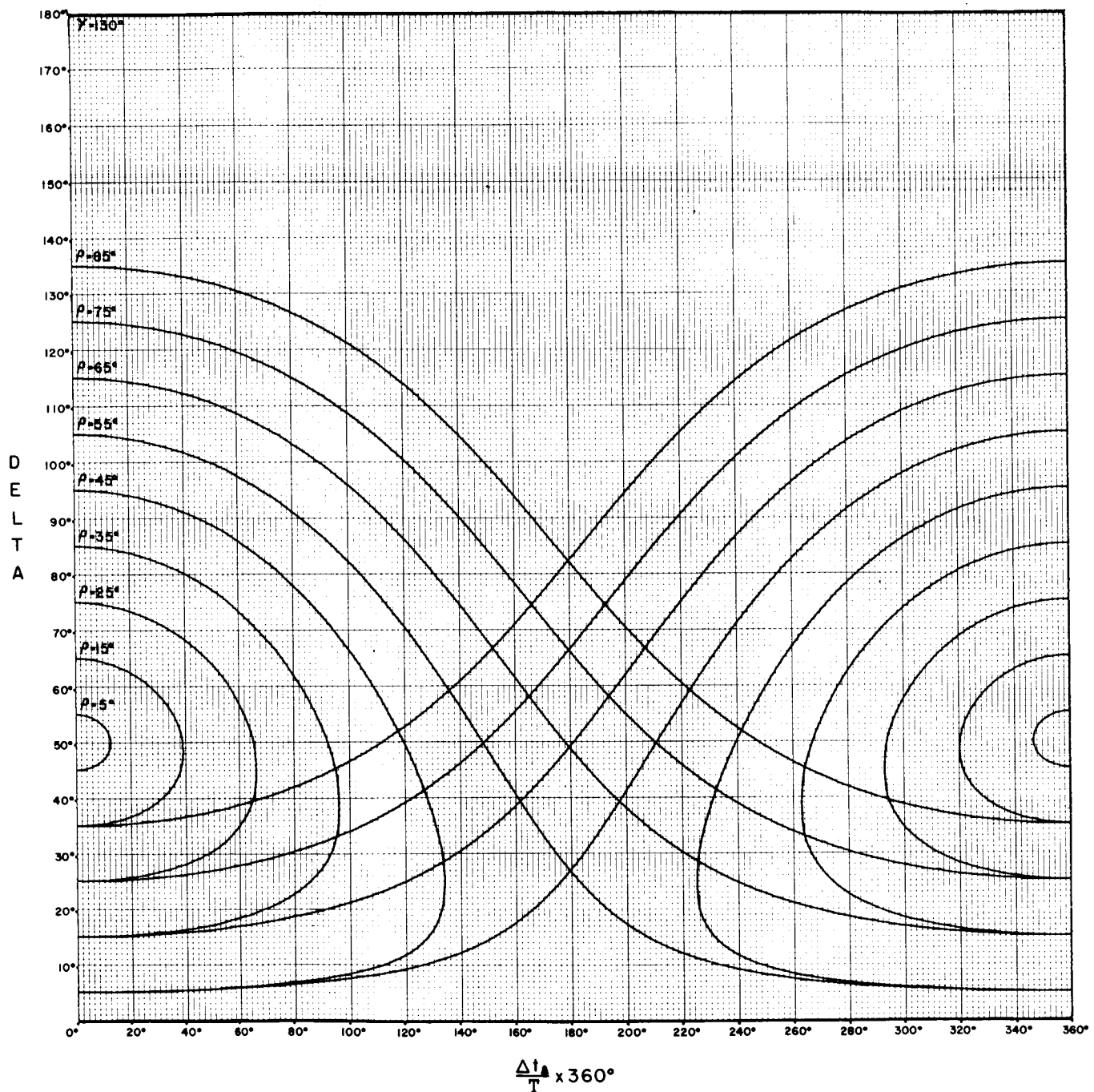
## DELTA V.S. SUN EARTH PULSE SPACING



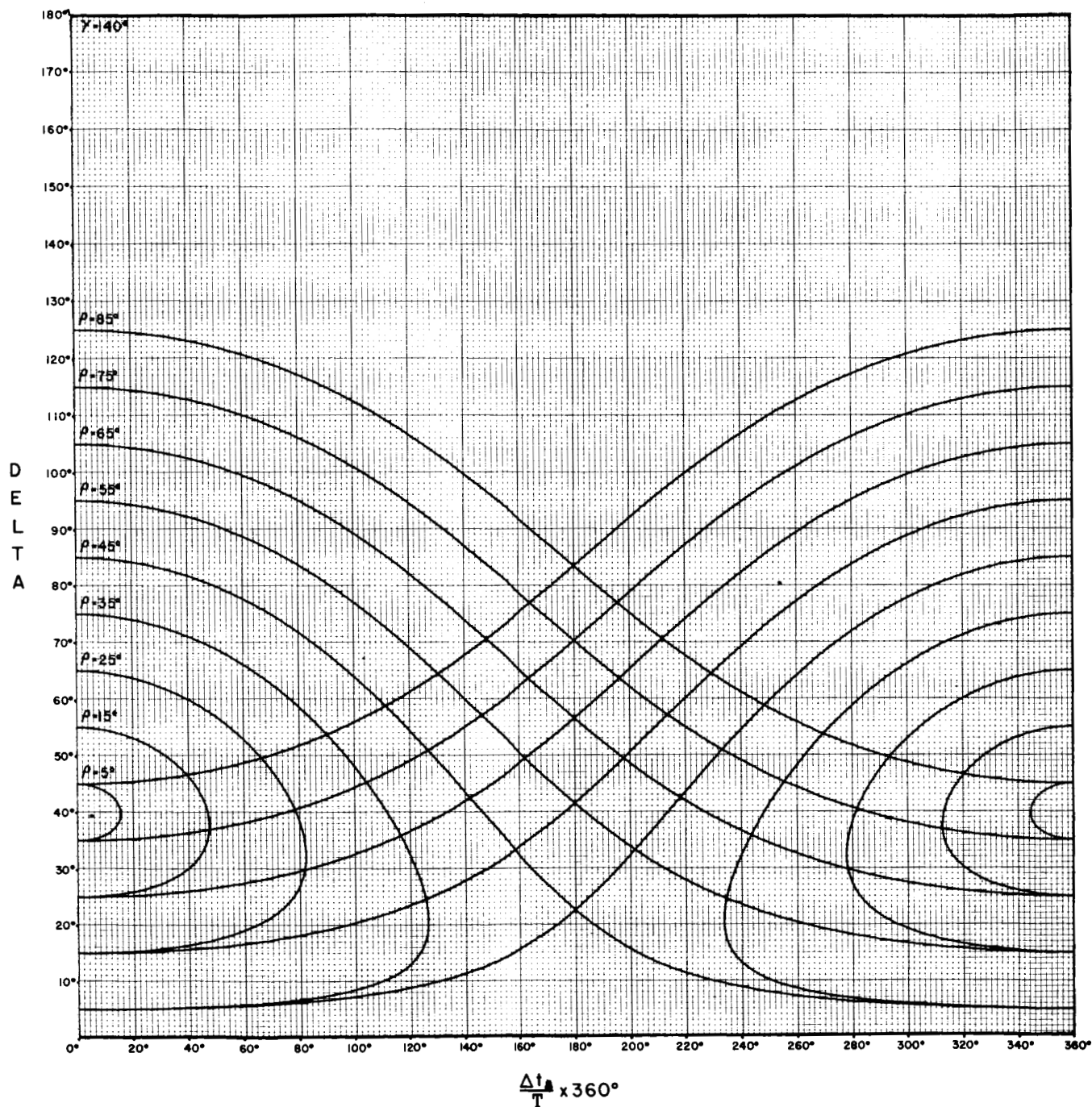
## DELTA V.S. SUN EARTH PULSE SPACING



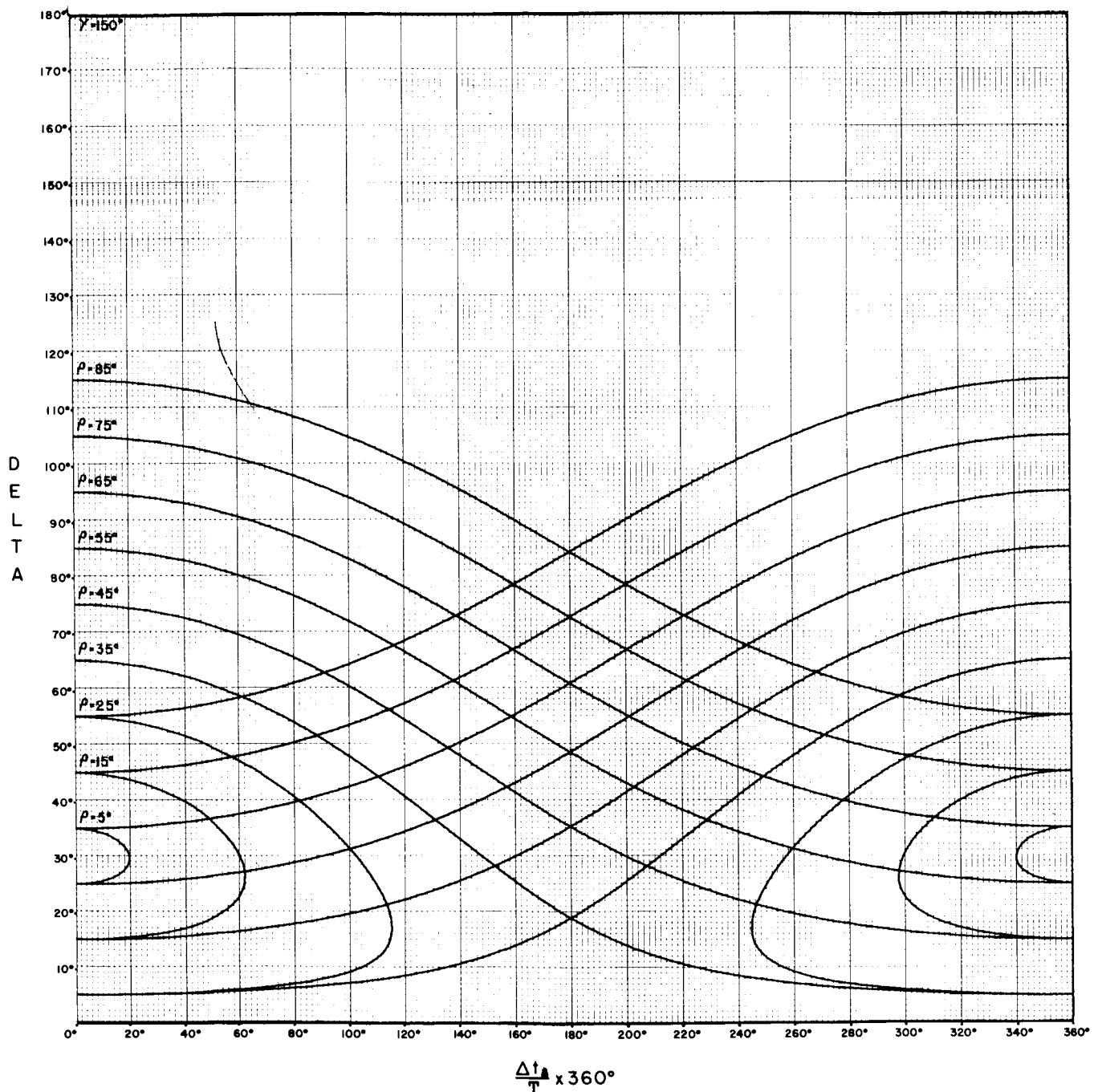
## DELTA V.S. SUN EARTH PULSE SPACING



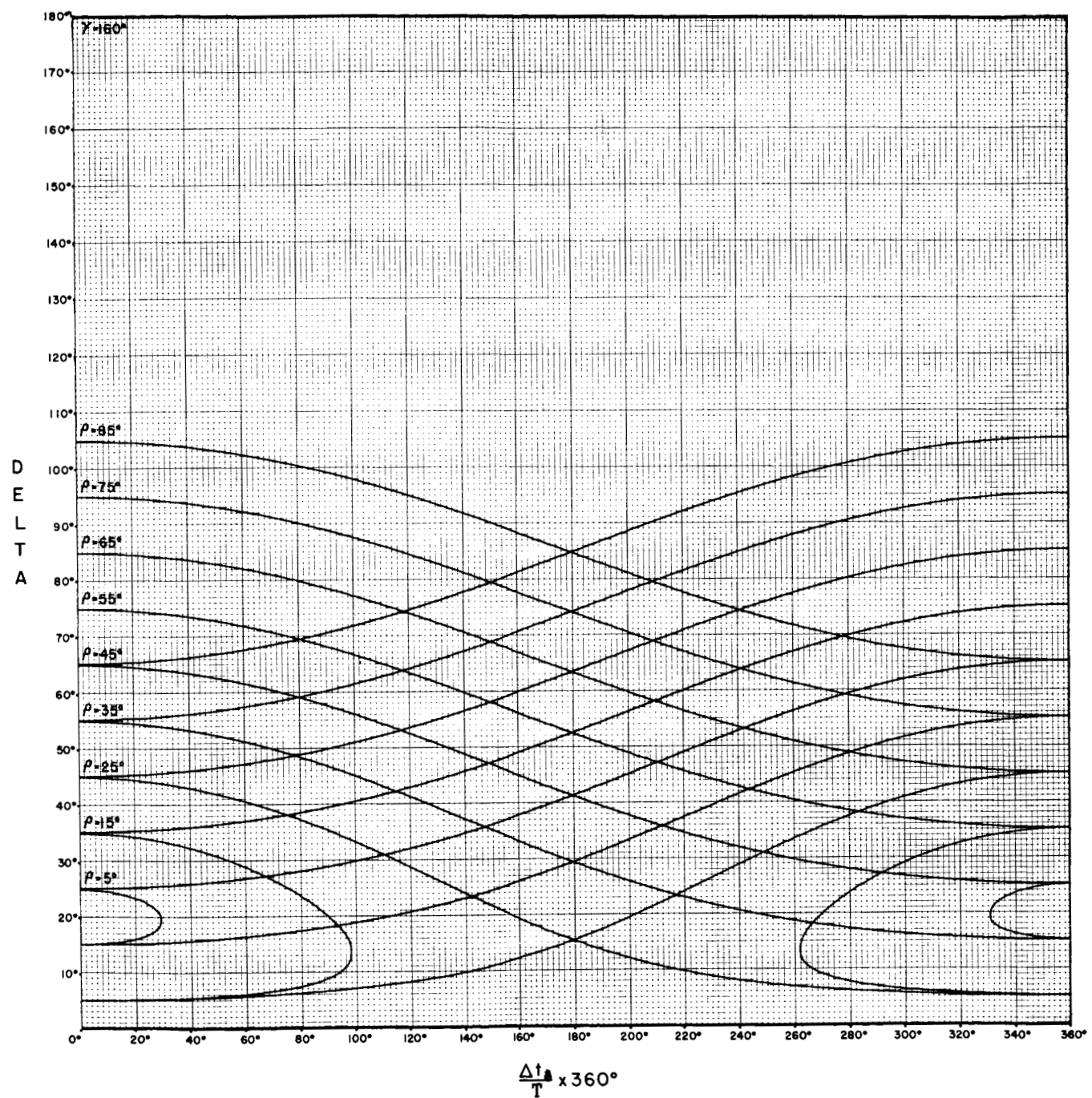
## DELTA V.S. SUN EARTH PULSE SPACING



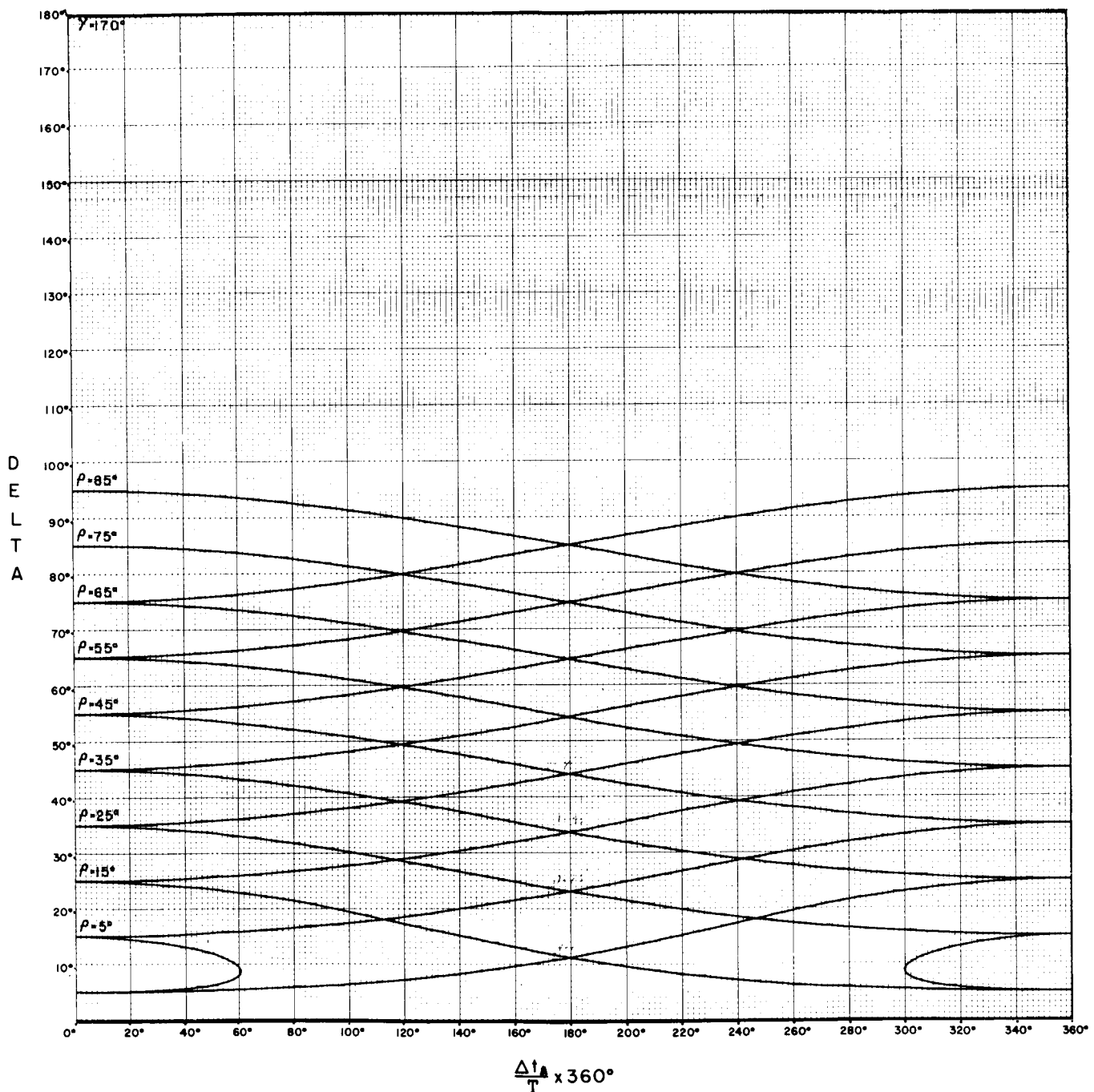
## DELTA V.S. SUN EARTH PULSE SPACING



## DELTA V.S. SUN EARTH PULSE SPACING



## DELTA V.S. SUN EARTH PULSE SPACING

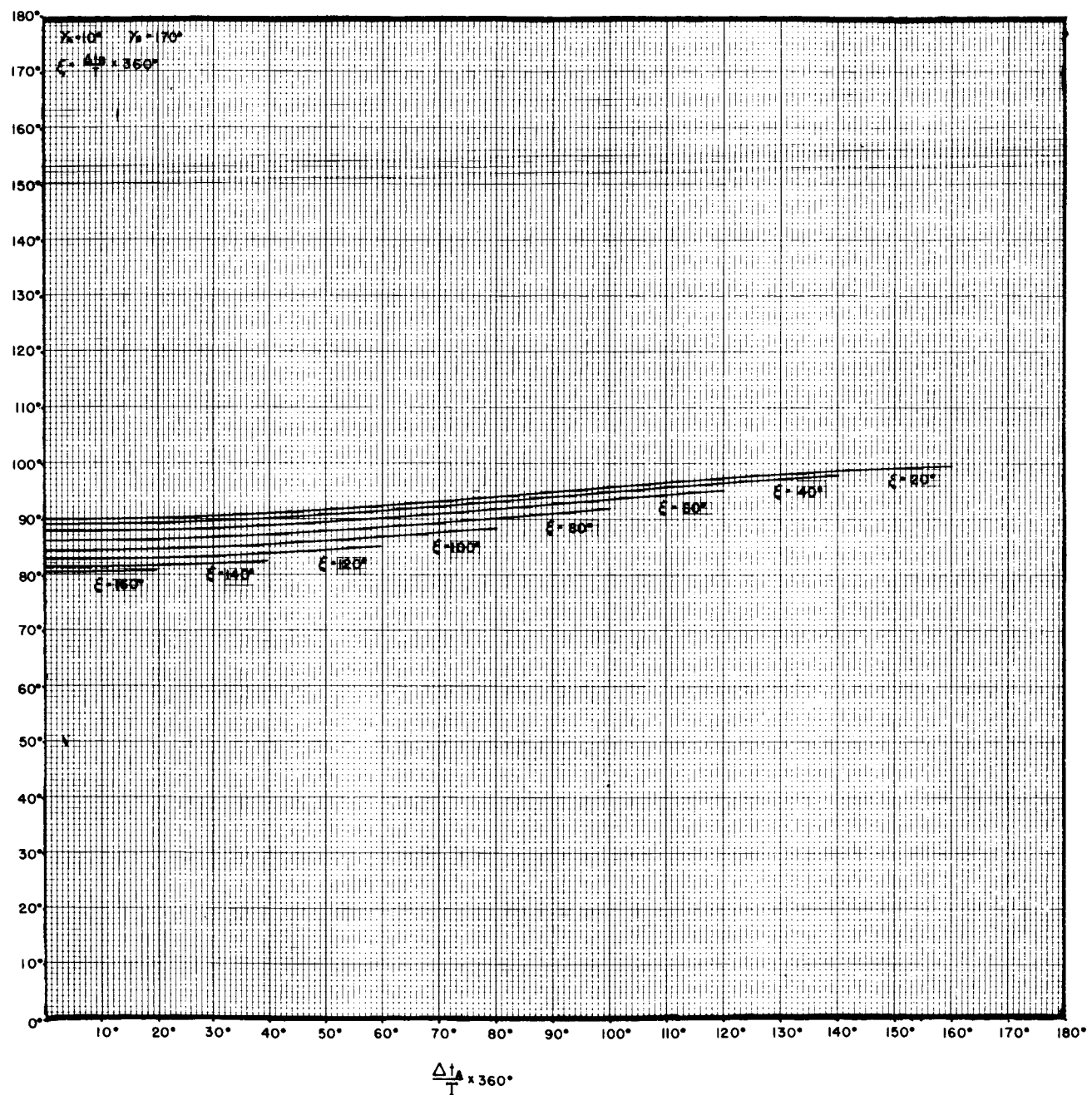


## APPENDIX B

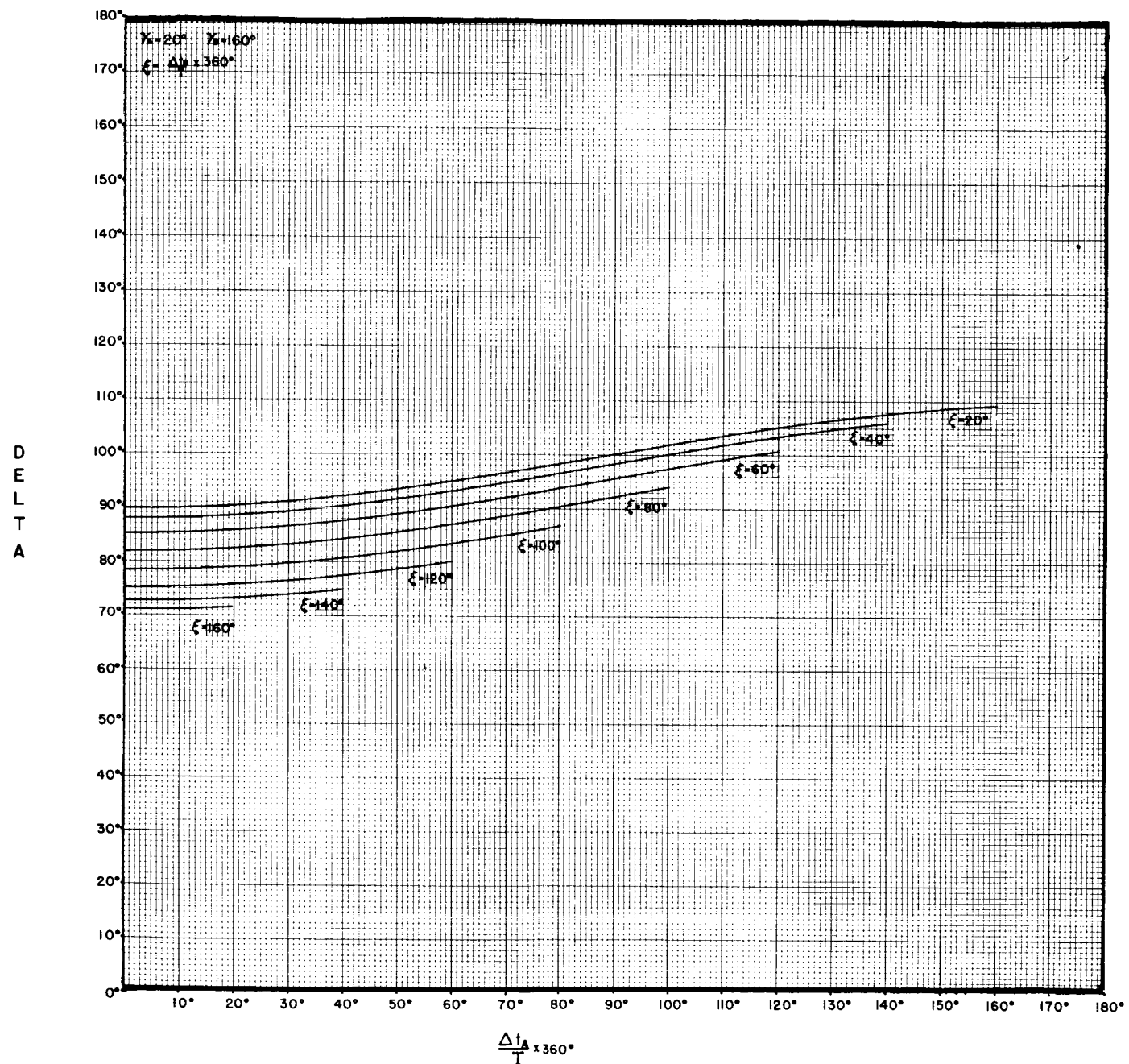
Plots of  $\Delta t_A$  and  $\Delta t_B$   
Solutions of Equation (63)

DELTA FROM A PAIR OF EARTH SENSORS

DELT A

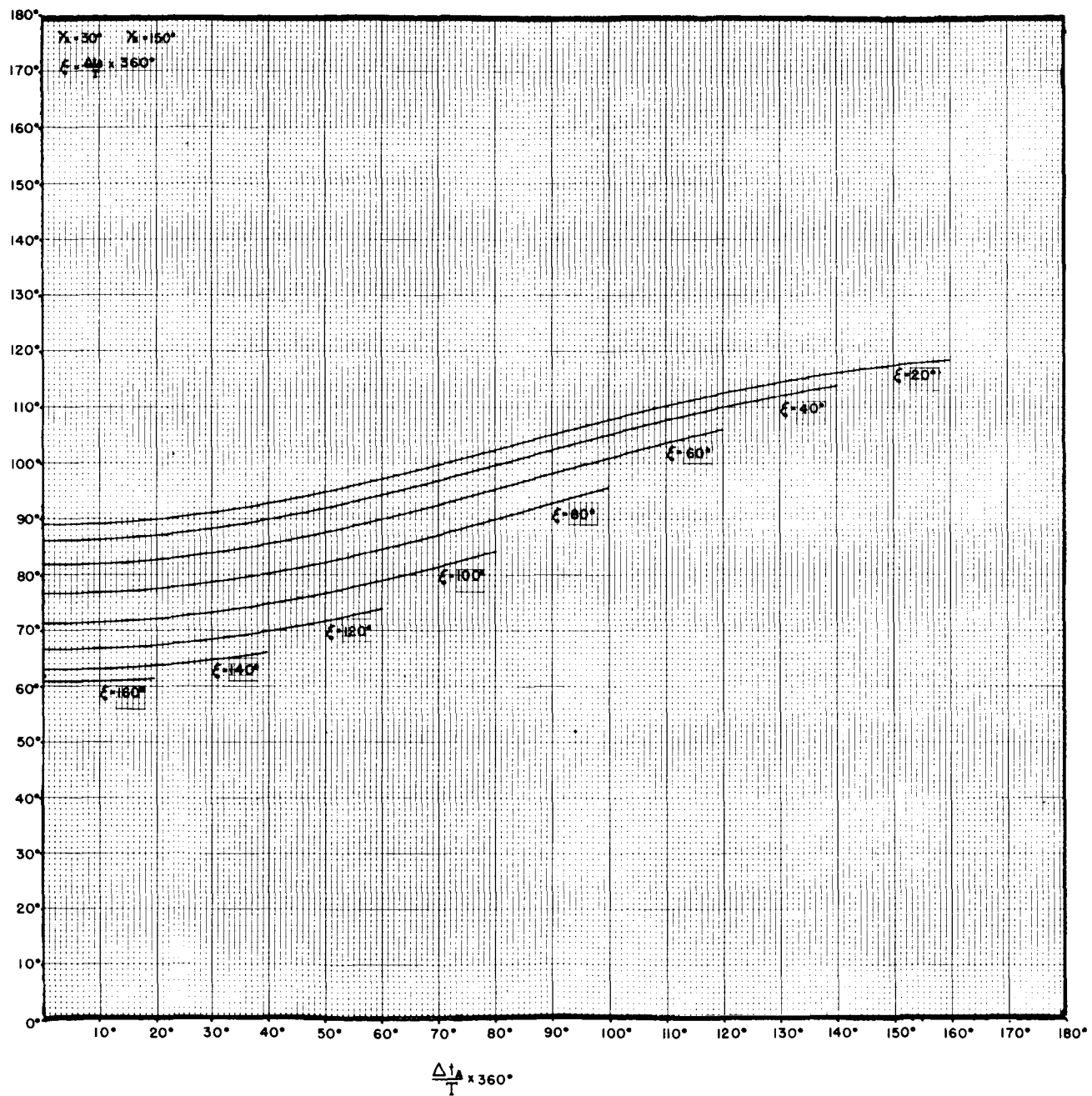


DELTA FROM A PAIR OF EARTH SENSORS

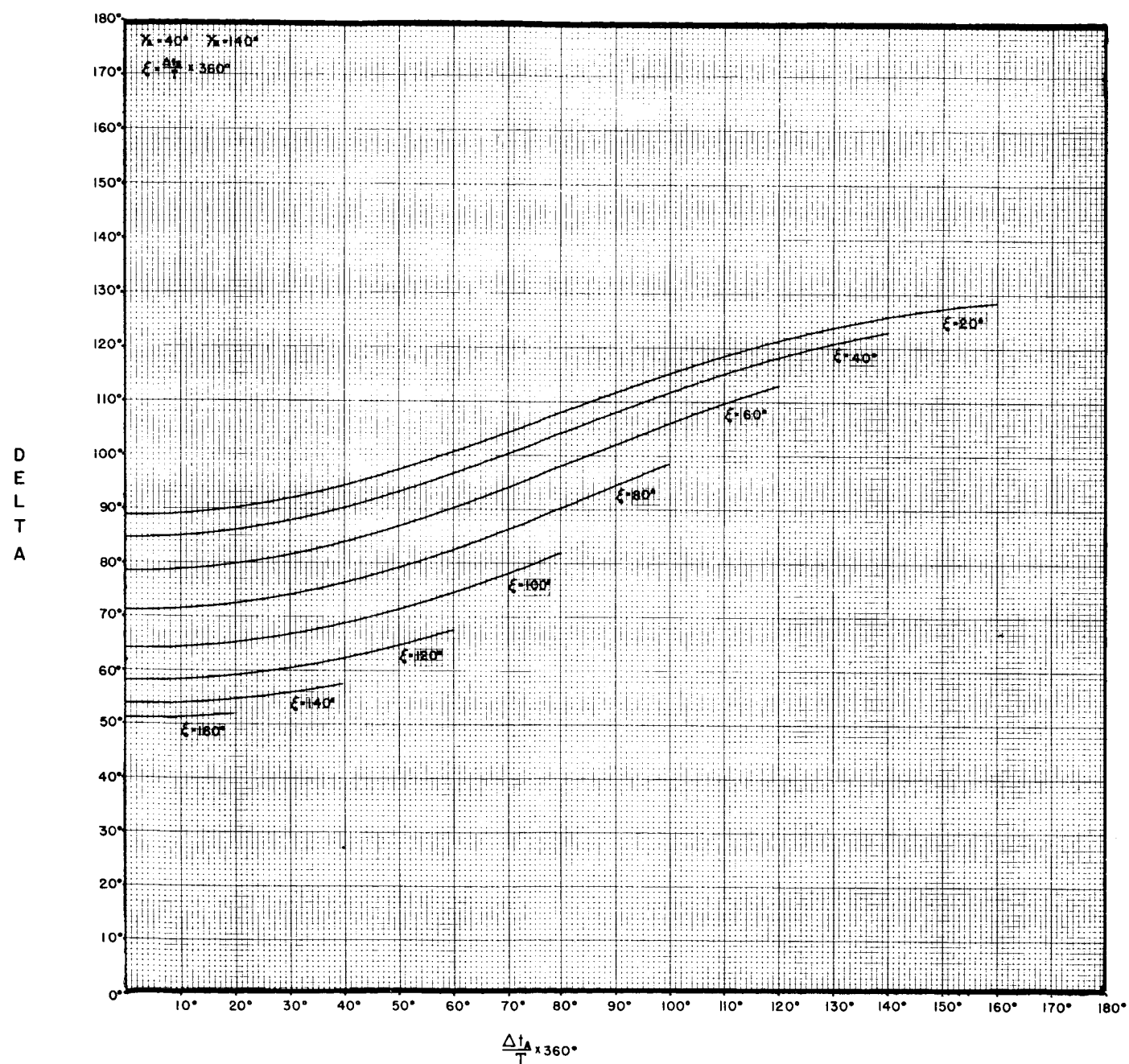


DELTA FROM A PAIR OF EARTH SENSORS

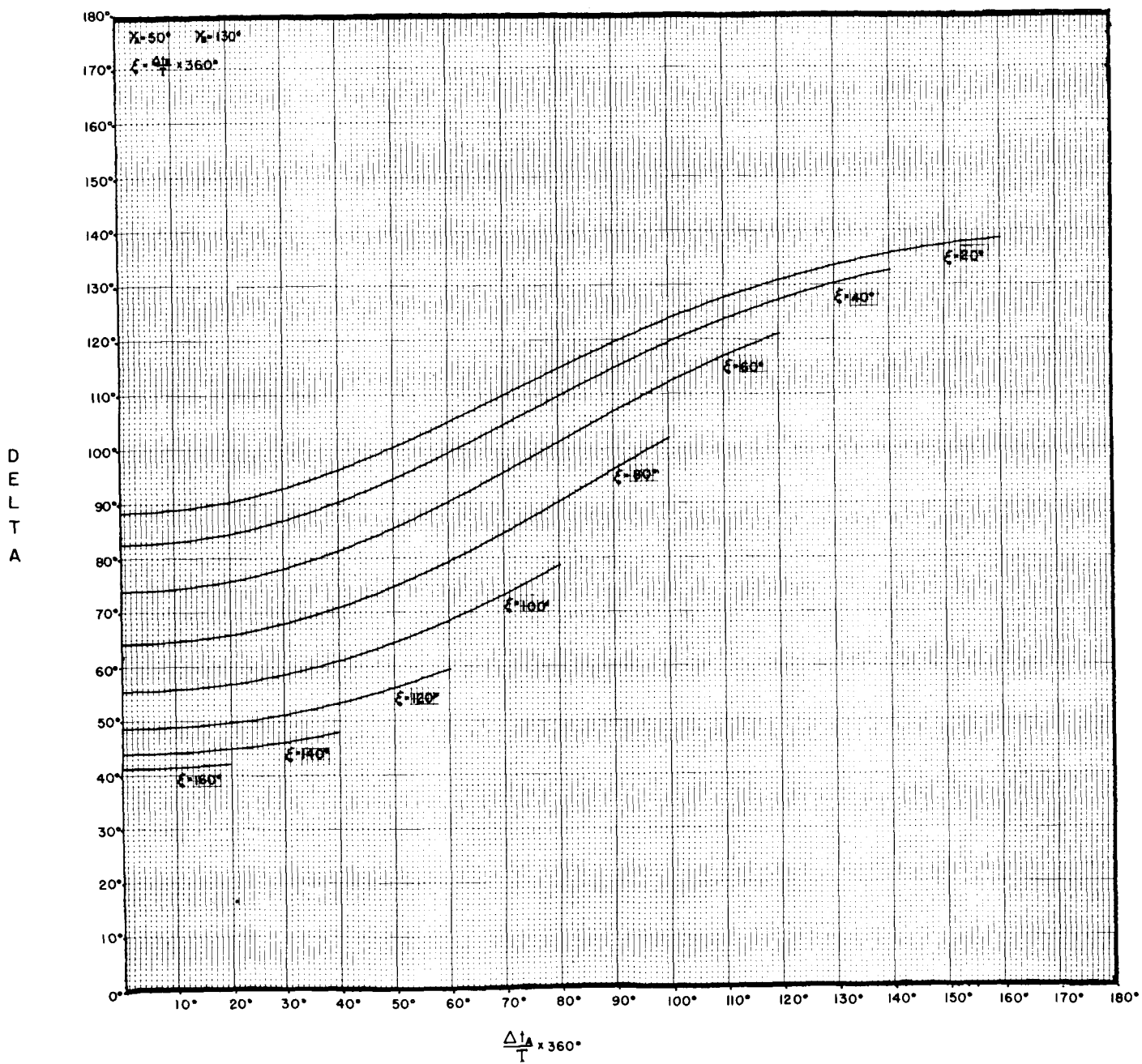
D  
E  
L  
T  
A



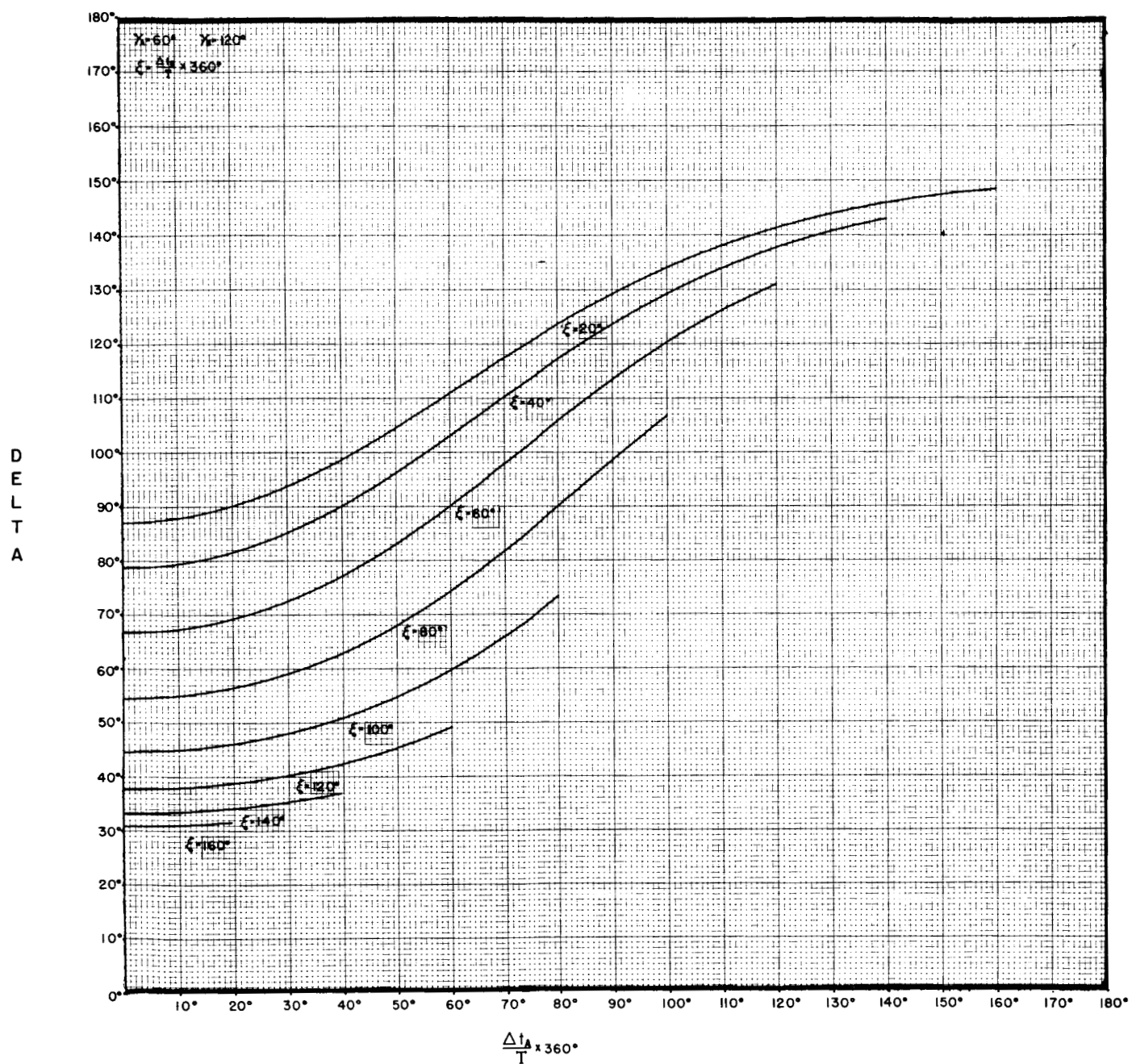
DELTA FROM A PAIR OF EARTH SENSORS



DELTA FROM A PAIR OF EARTH SENSORS

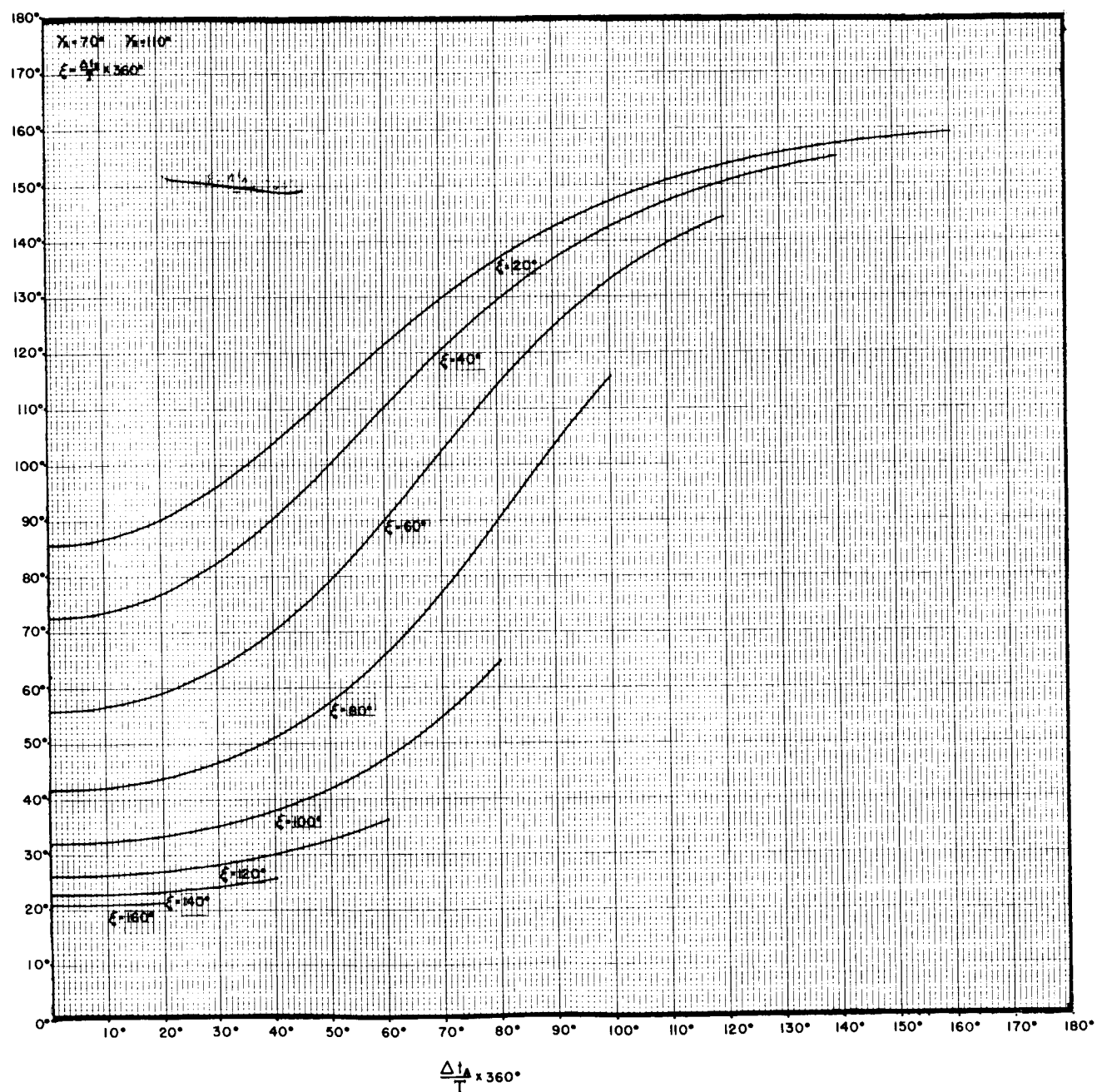


DELTA FROM A PAIR OF EARTH SENSORS

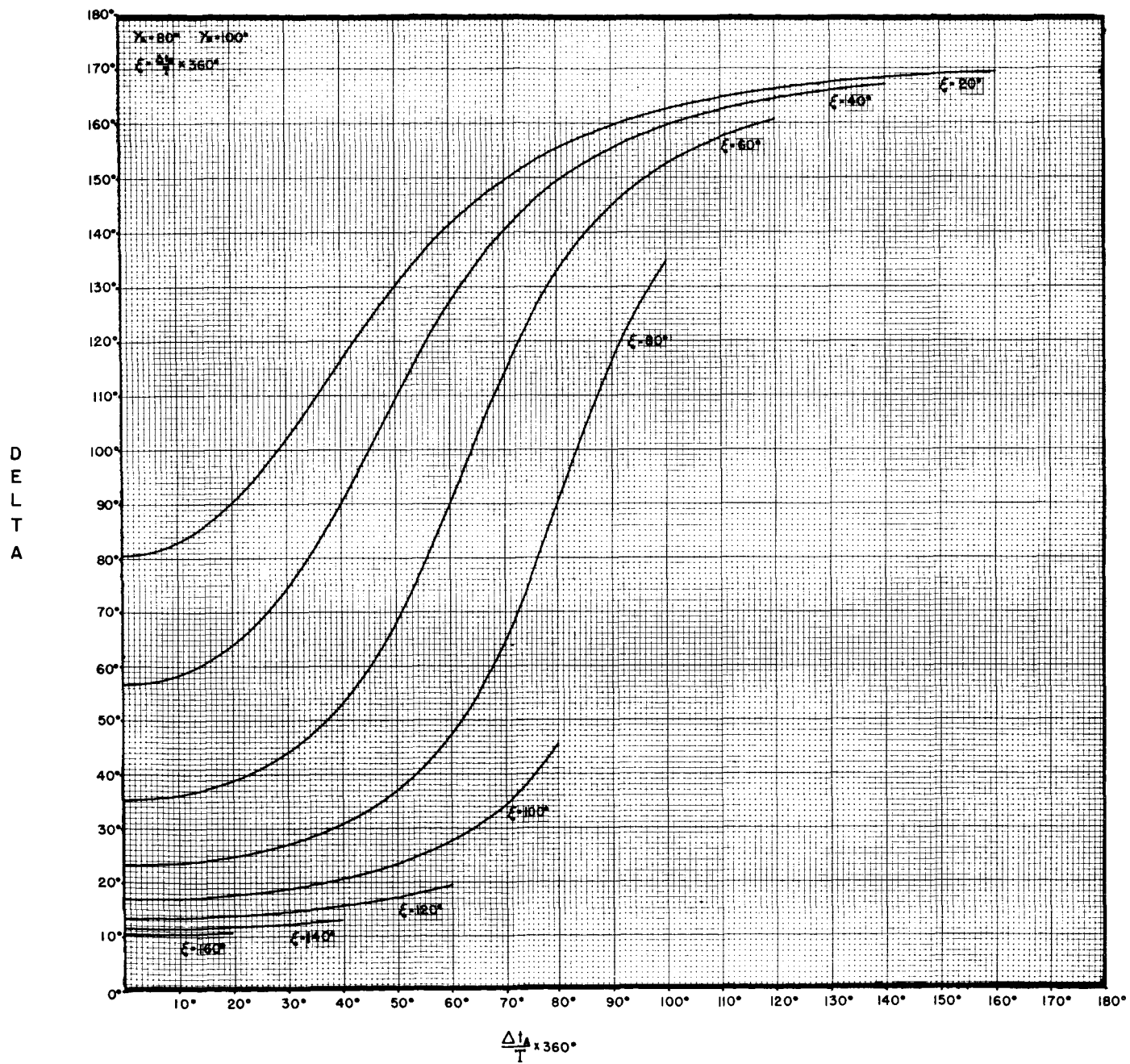


DELTA FROM A PAIR OF EARTH SENSORS

DELT A



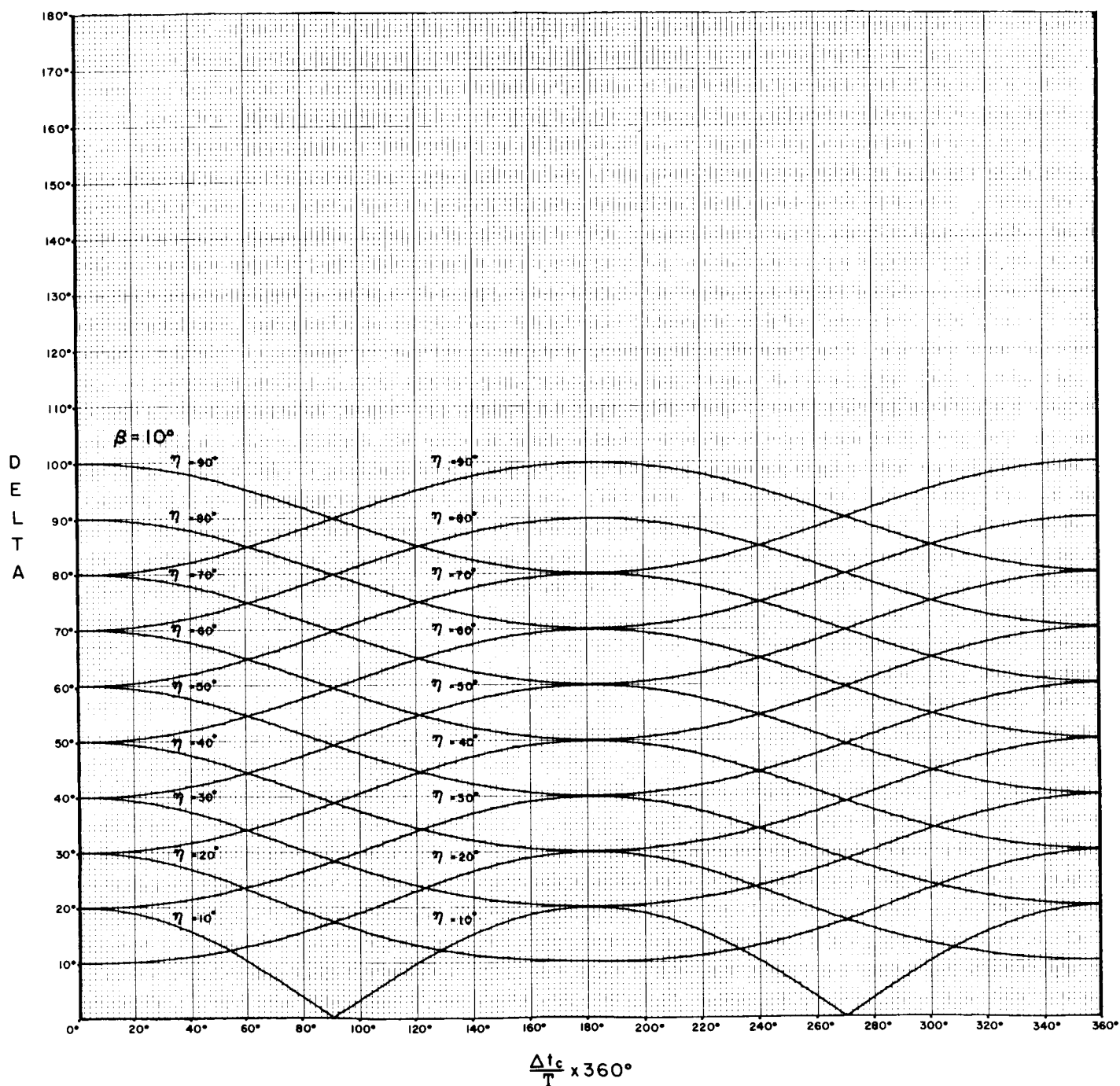
DELTA FROM A PAIR OF EARTH SENSORS



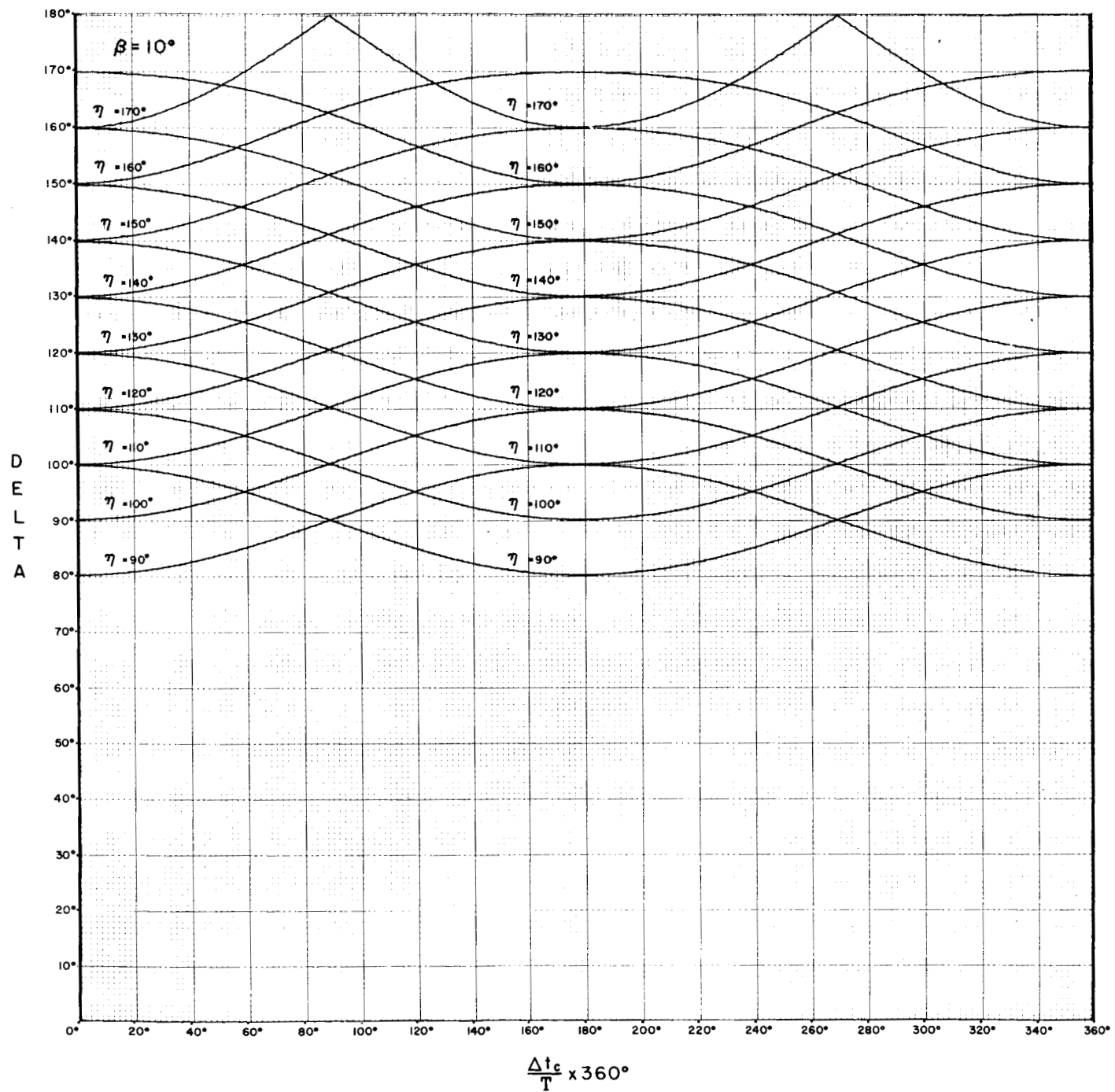
## APPENDIX C

Plots of  $\Delta t_c$  and  $\beta$   
Solution of Equation (68)

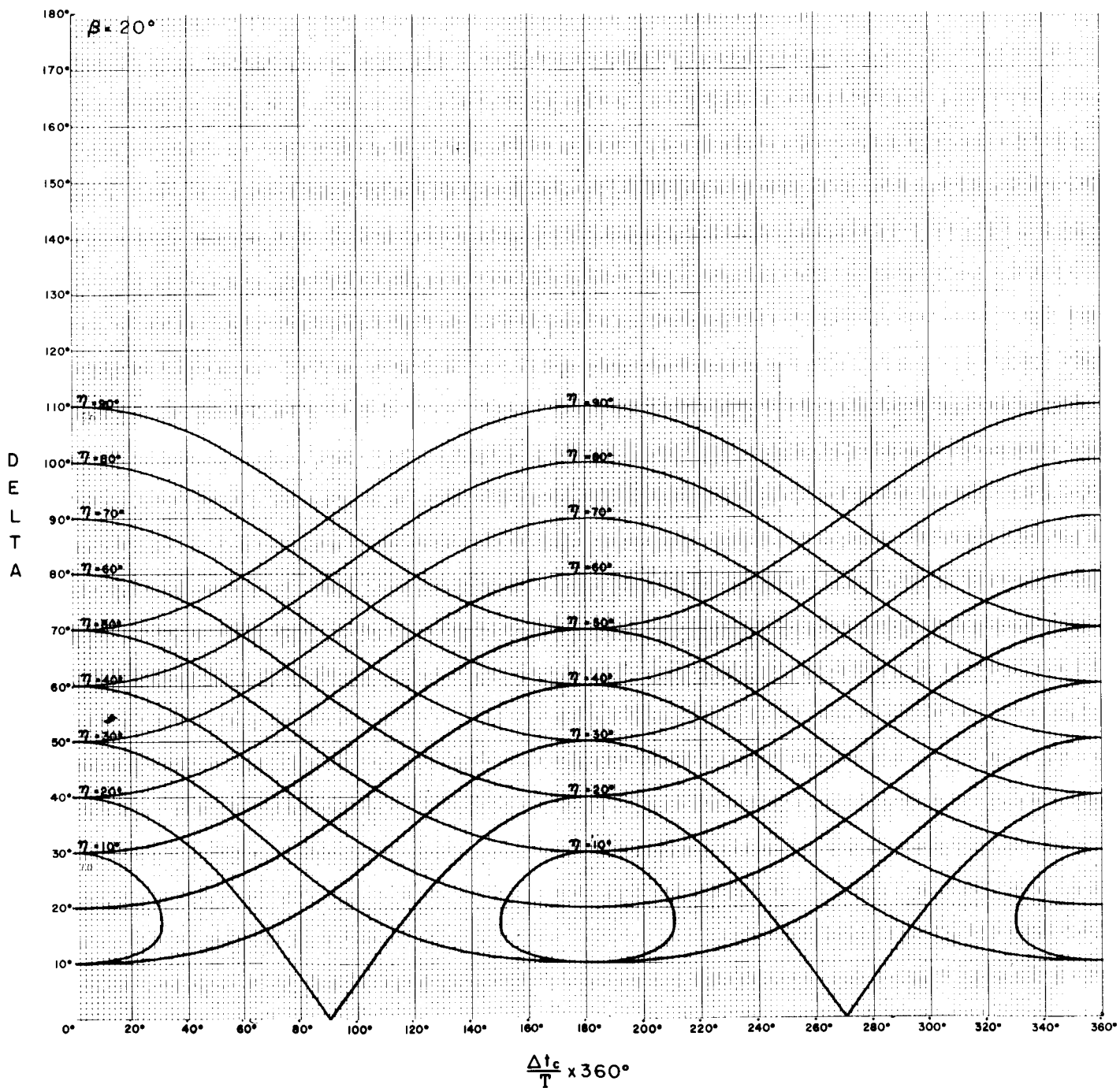
## DELTA V.S. SUN EARTH PULSE SPACING



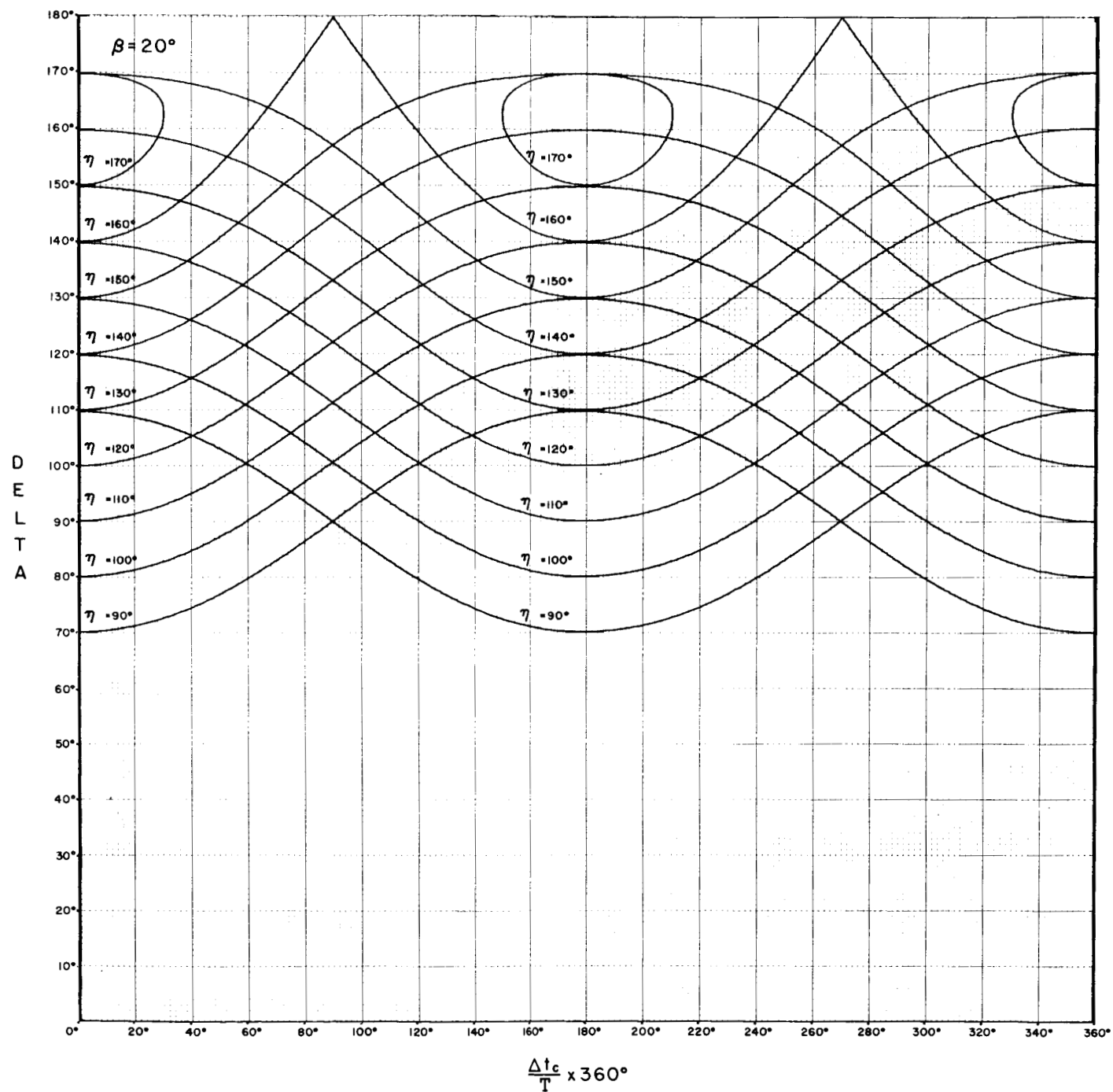
## DELTA V.S. SUN EARTH PULSE SPACING



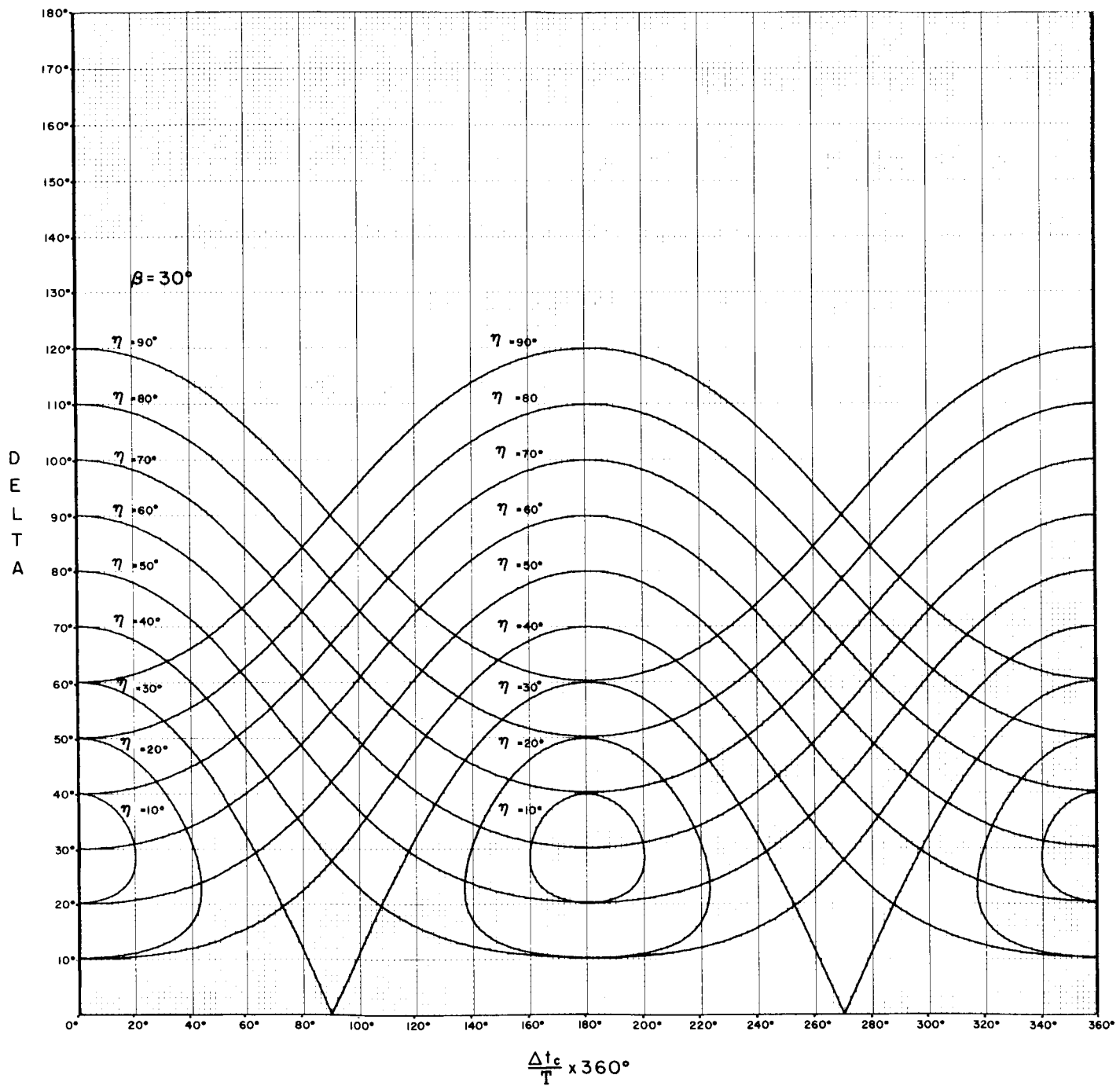
## DELTA V.S. SUN EARTH PULSE SPACING



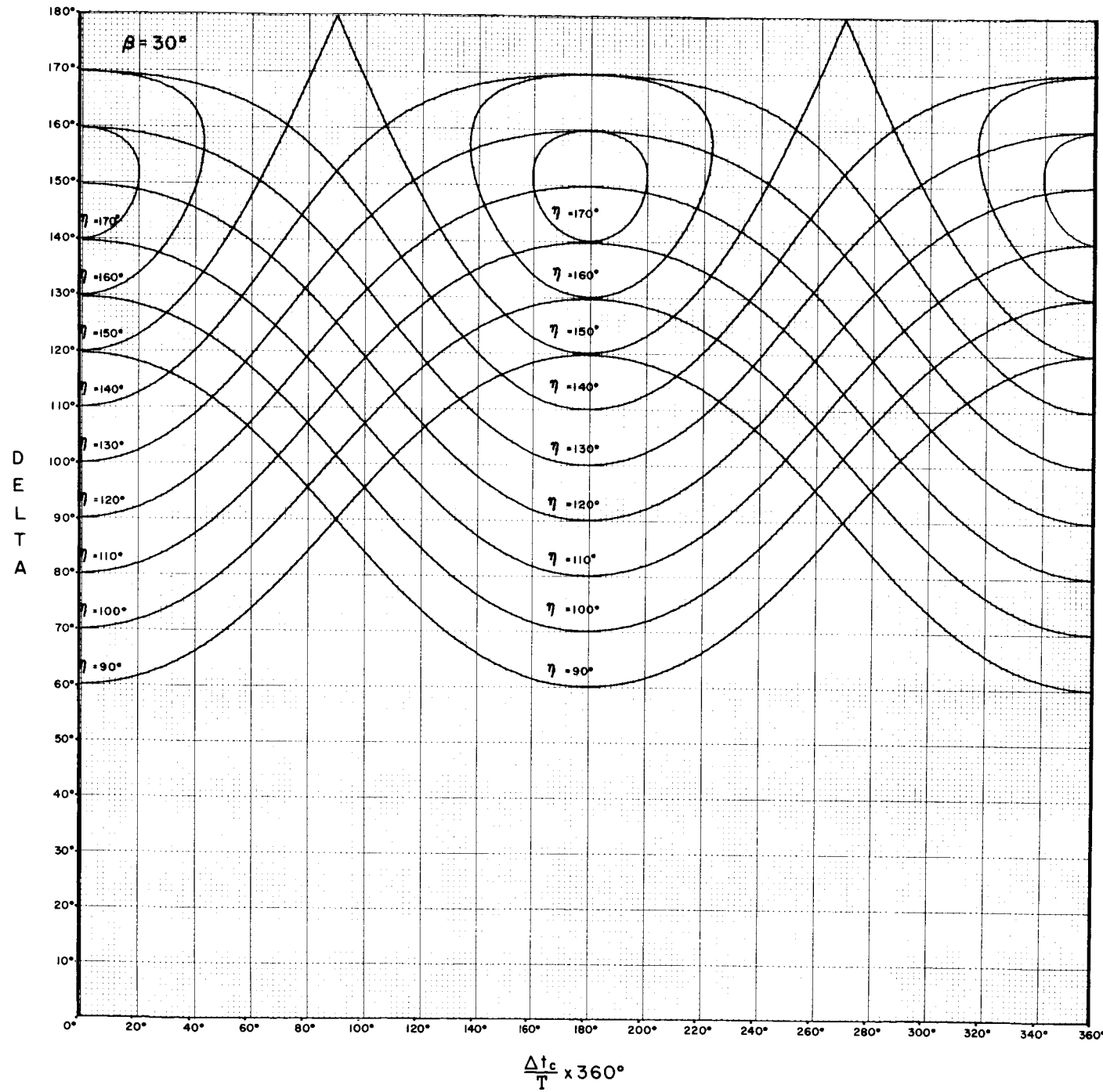
## DELTA V.S. SUN EARTH PULSE SPACING



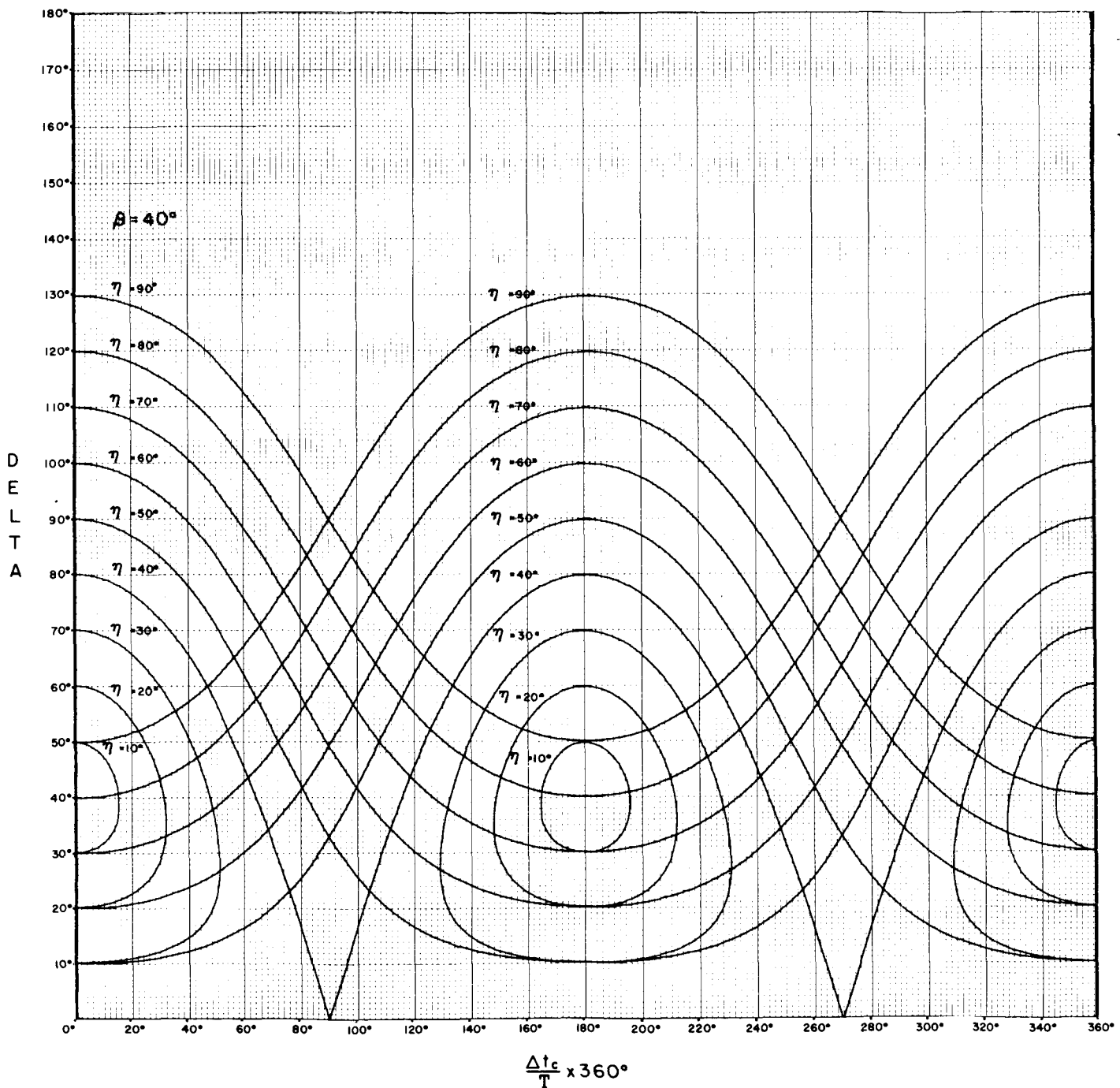
## DELTA V.S. SUN EARTH PULSE SPACING



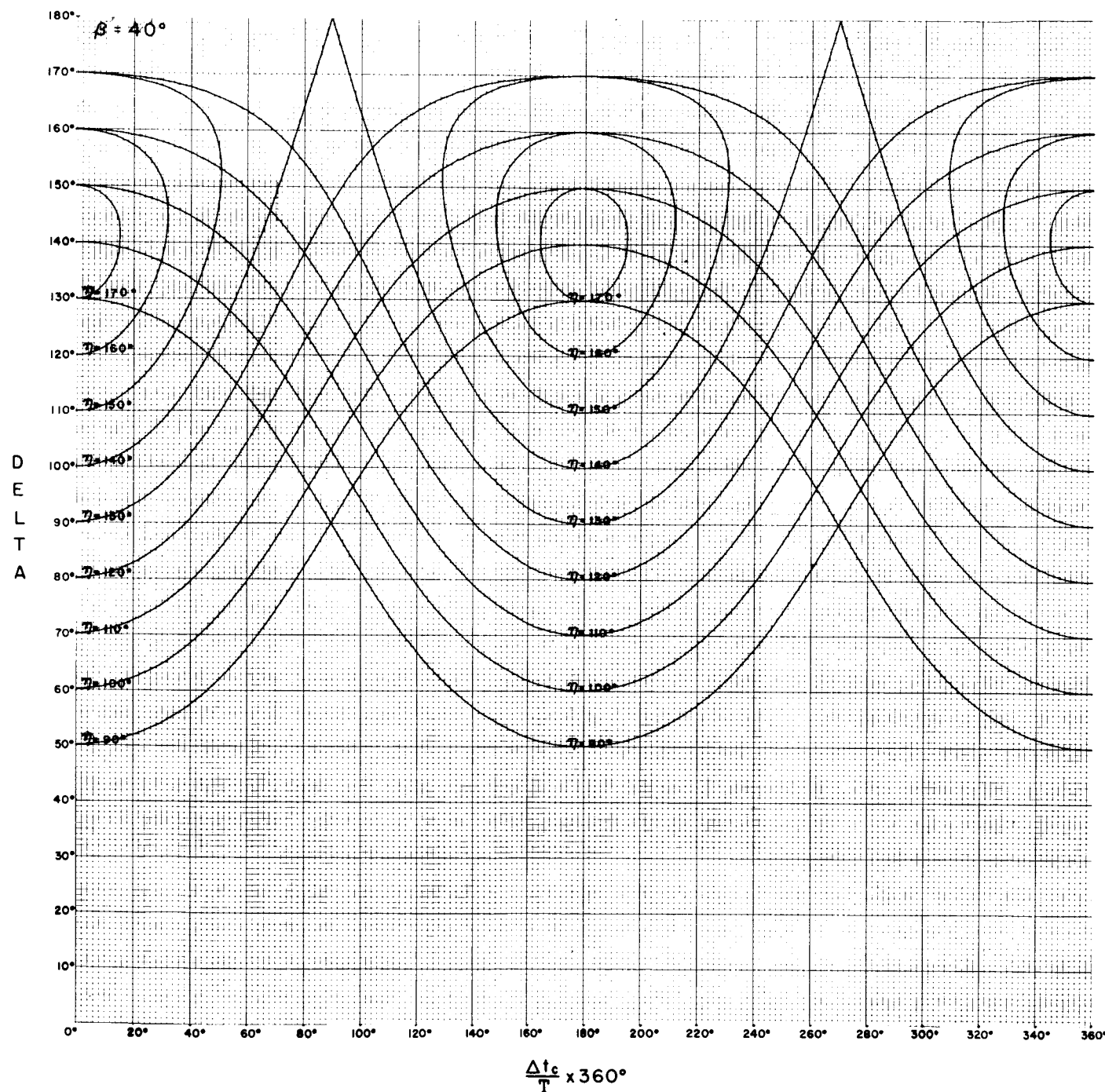
## DELTA V.S. SUN EARTH PULSE SPACING



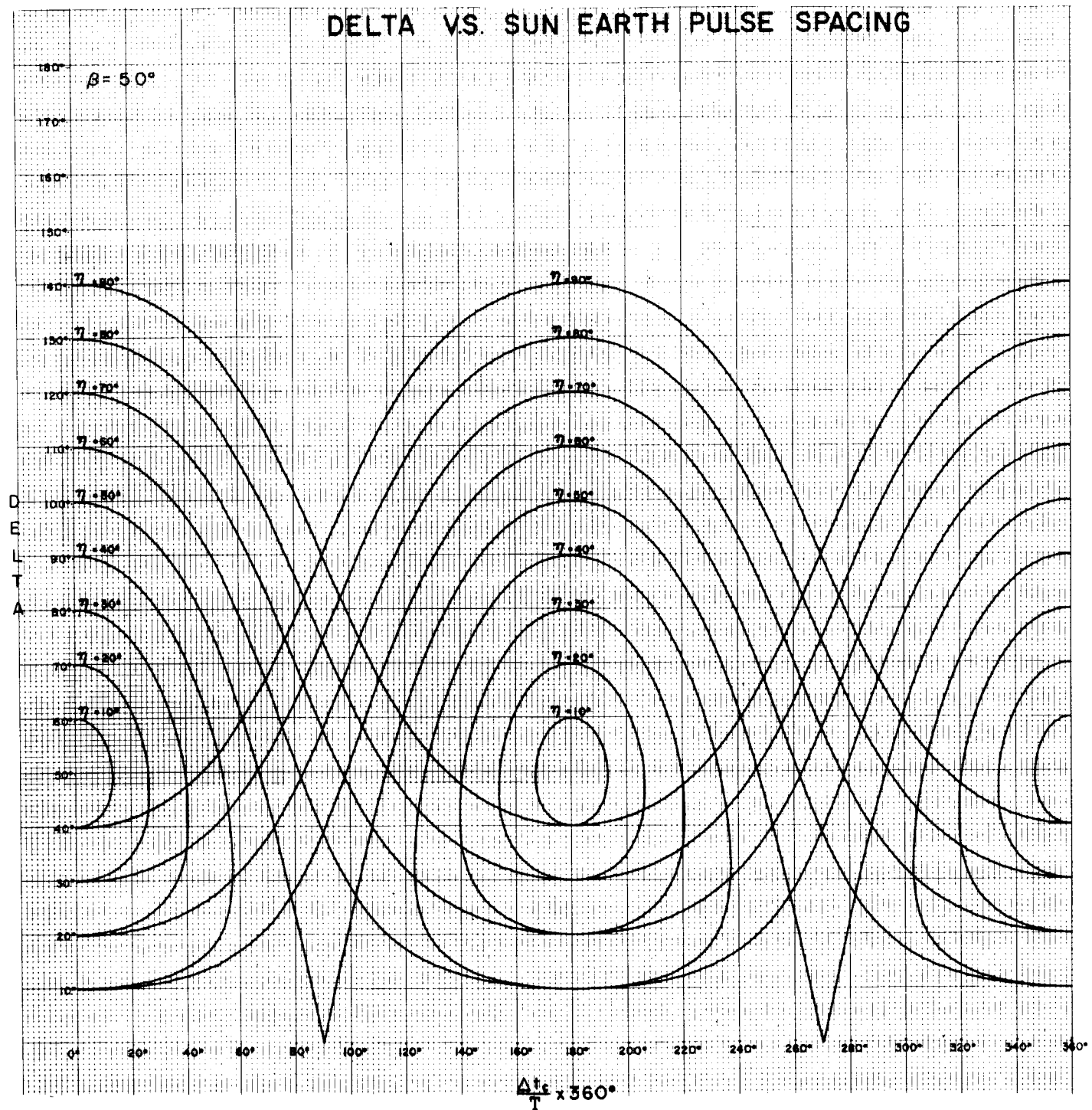
## DELTA V.S. SUN EARTH PULSE SPACING



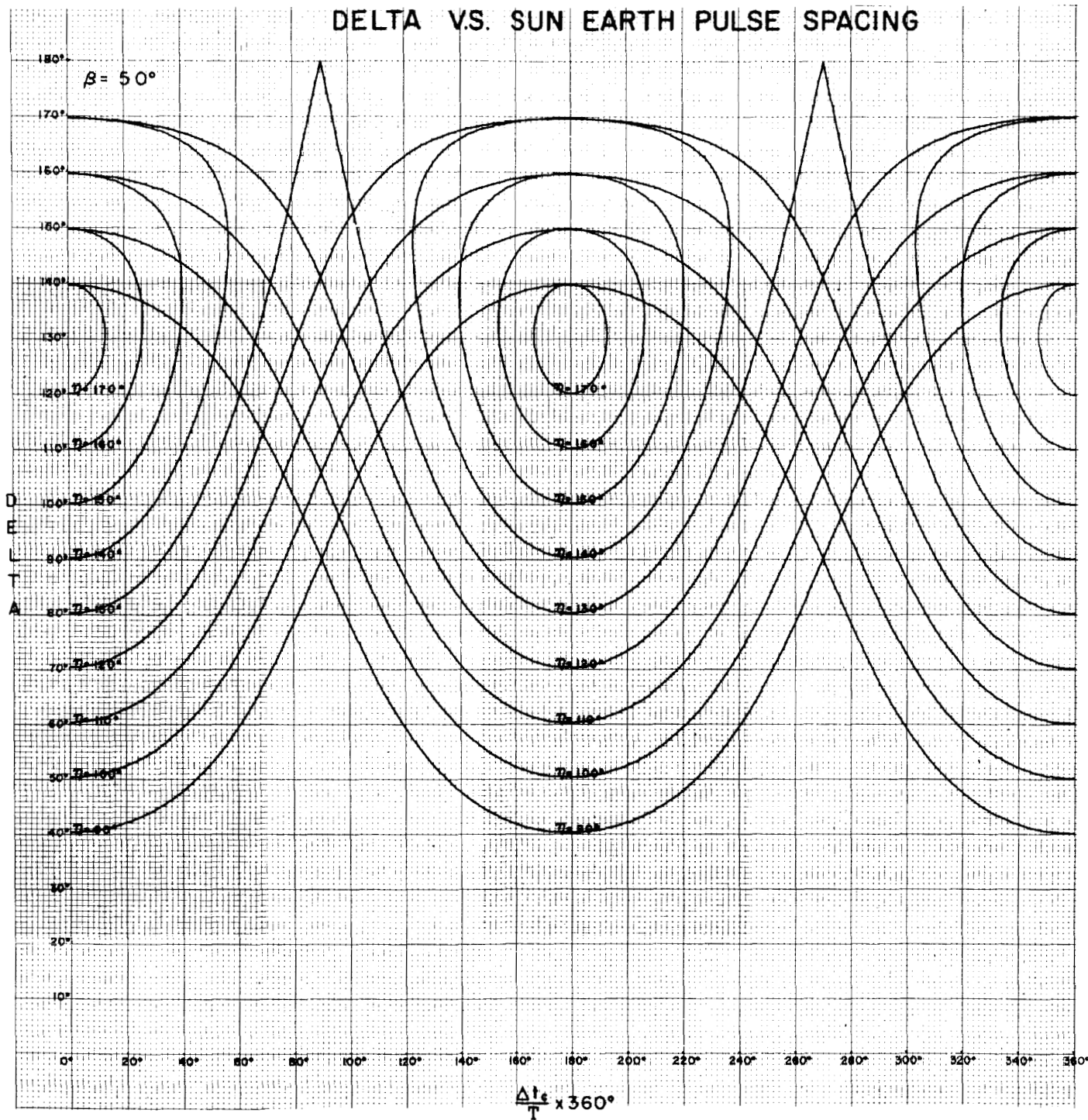
## DELTA V.S. SUN EARTH PULSE SPACING



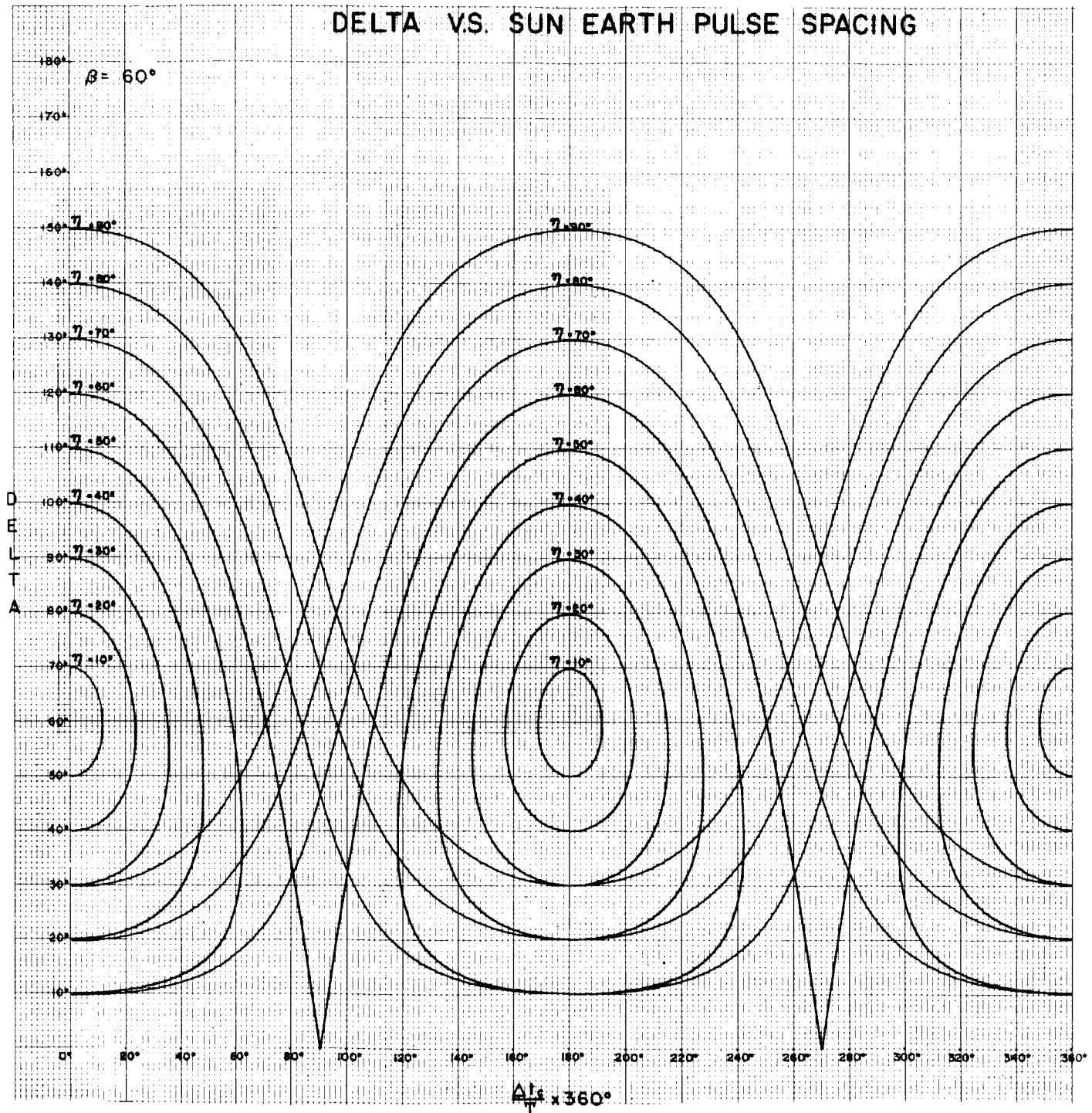
## DELTA V.S. SUN EARTH PULSE SPACING

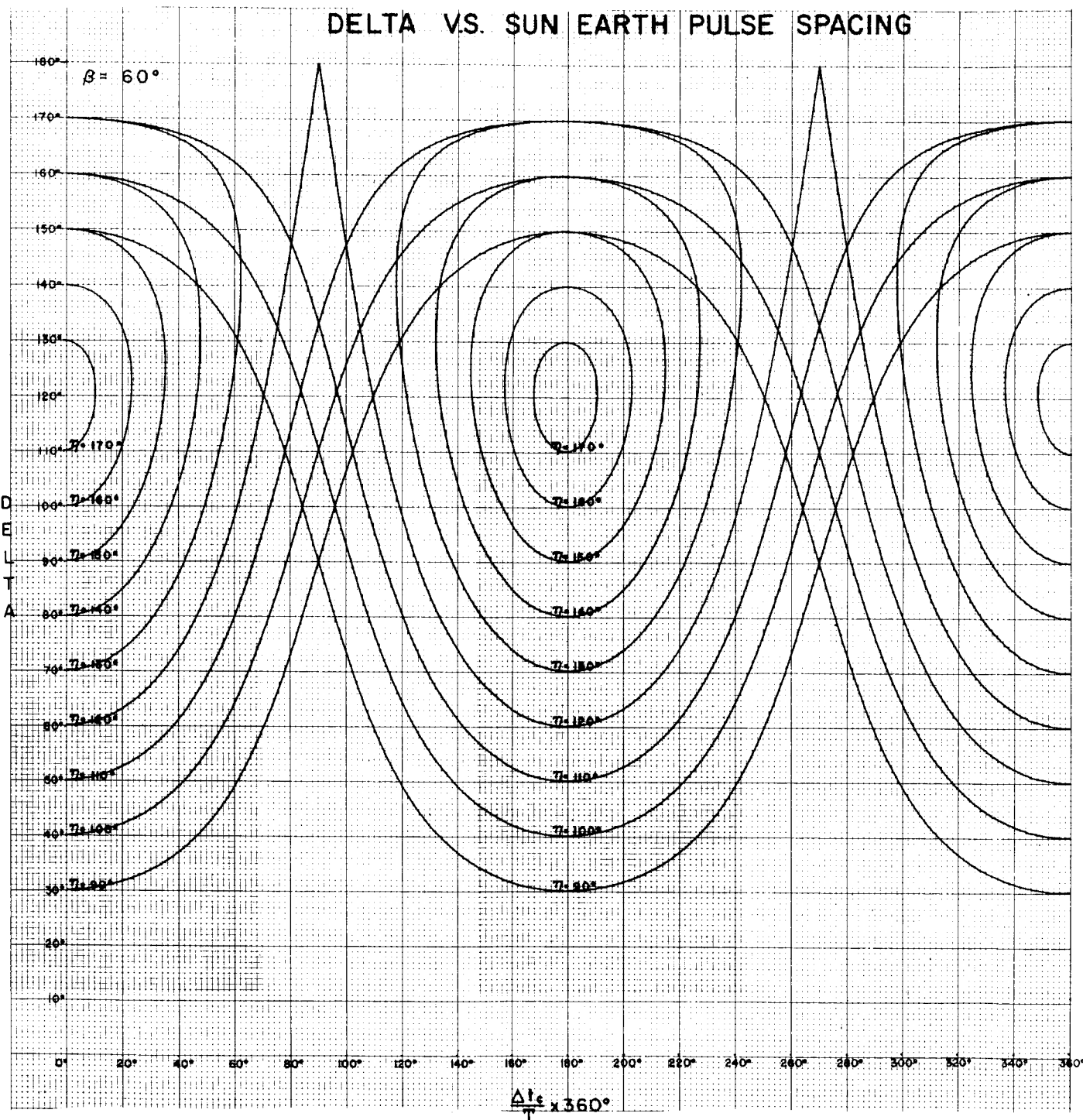


## DELTA V.S. SUN EARTH PULSE SPACING

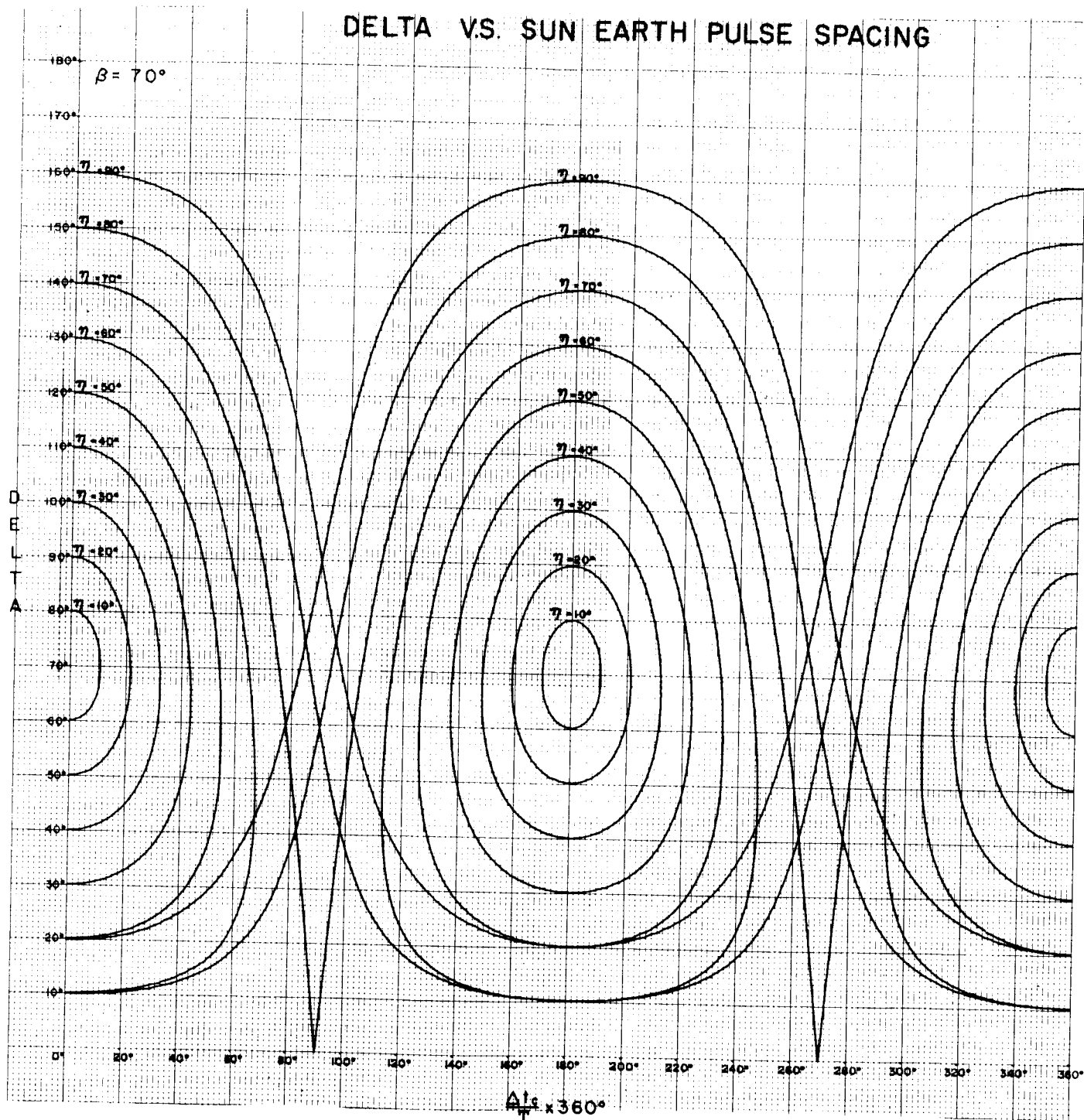


# DELTA V.S. SUN EARTH PULSE SPACING

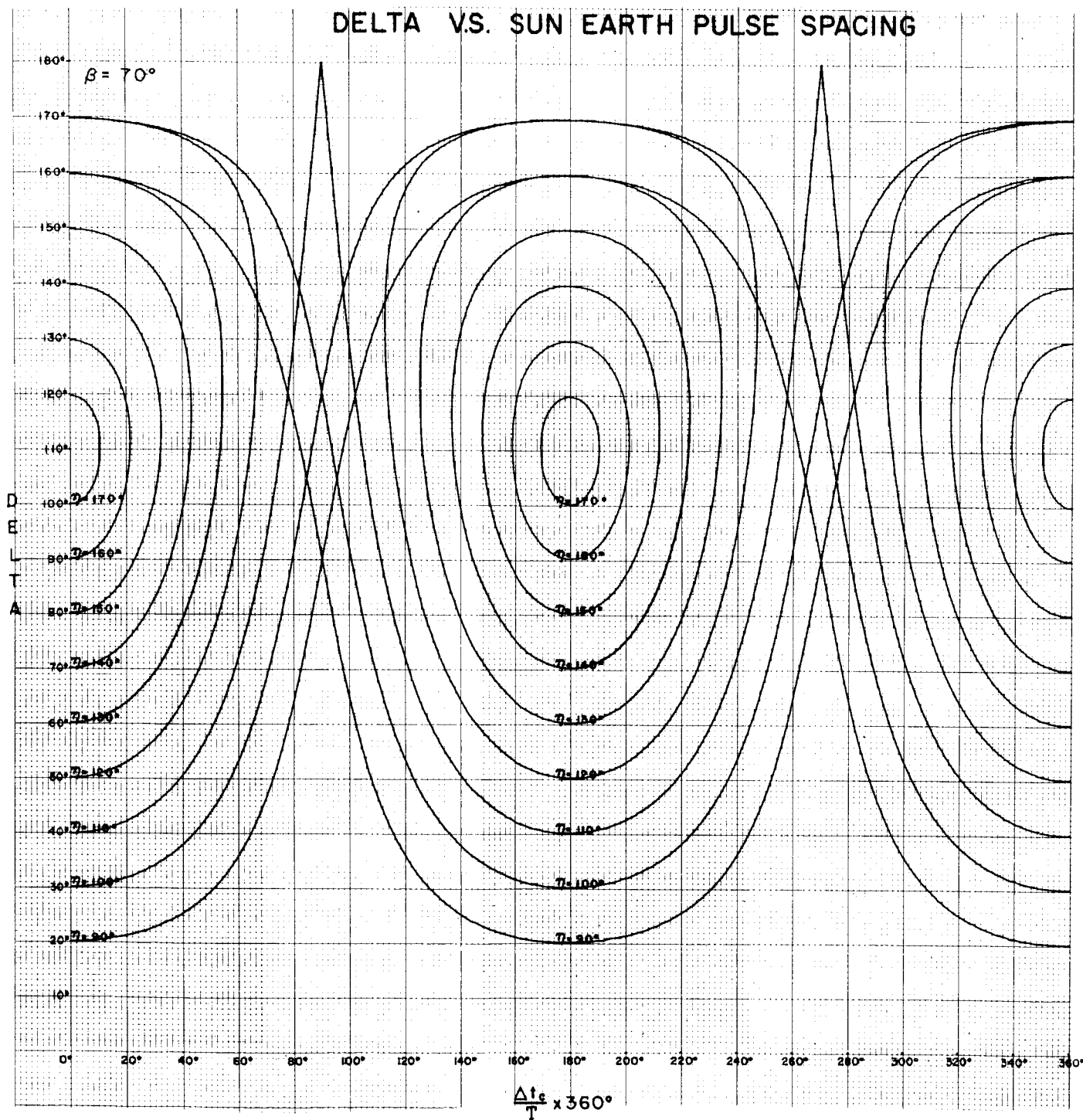




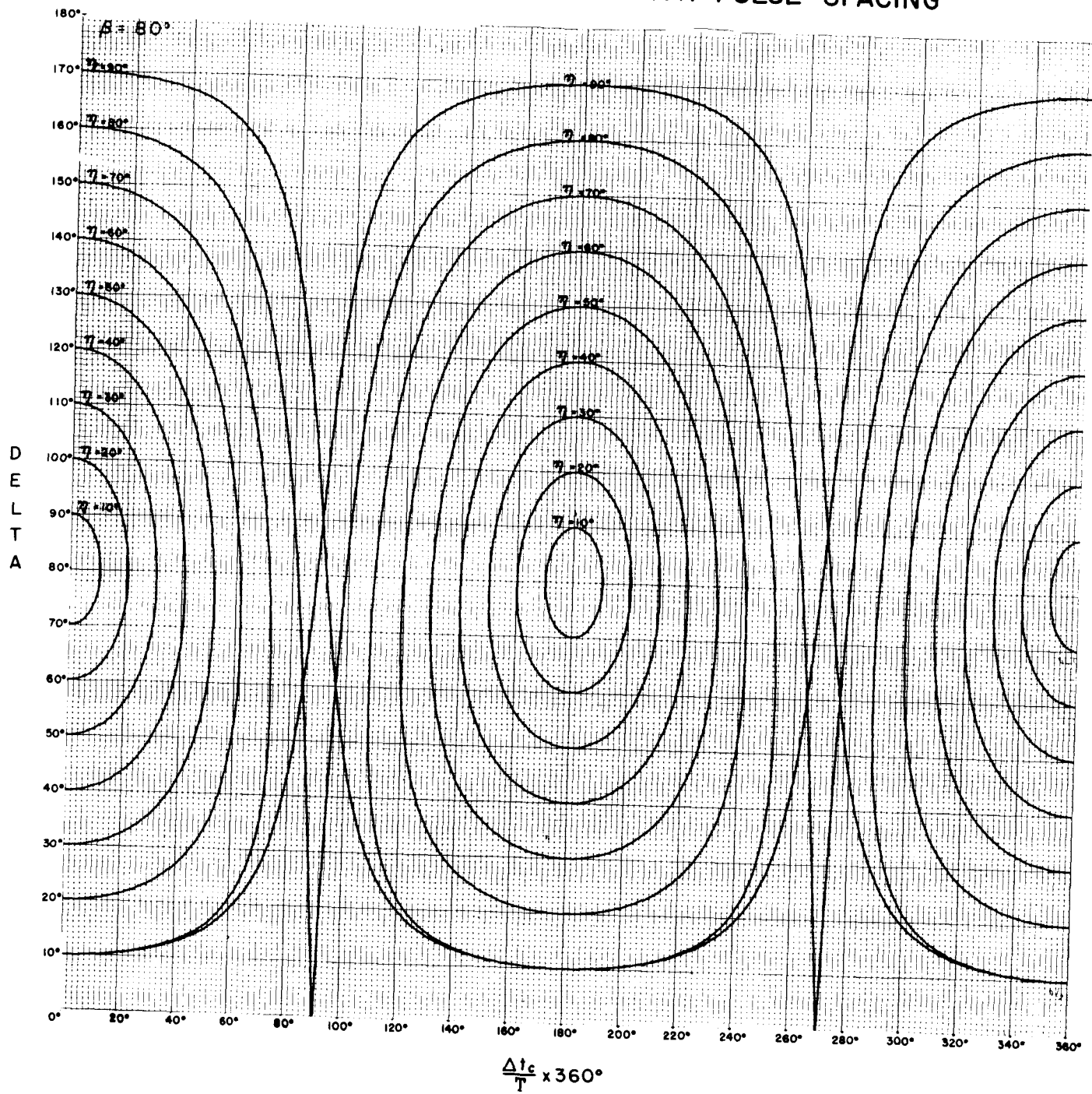
# DELTA V.S. SUN EARTH PULSE SPACING

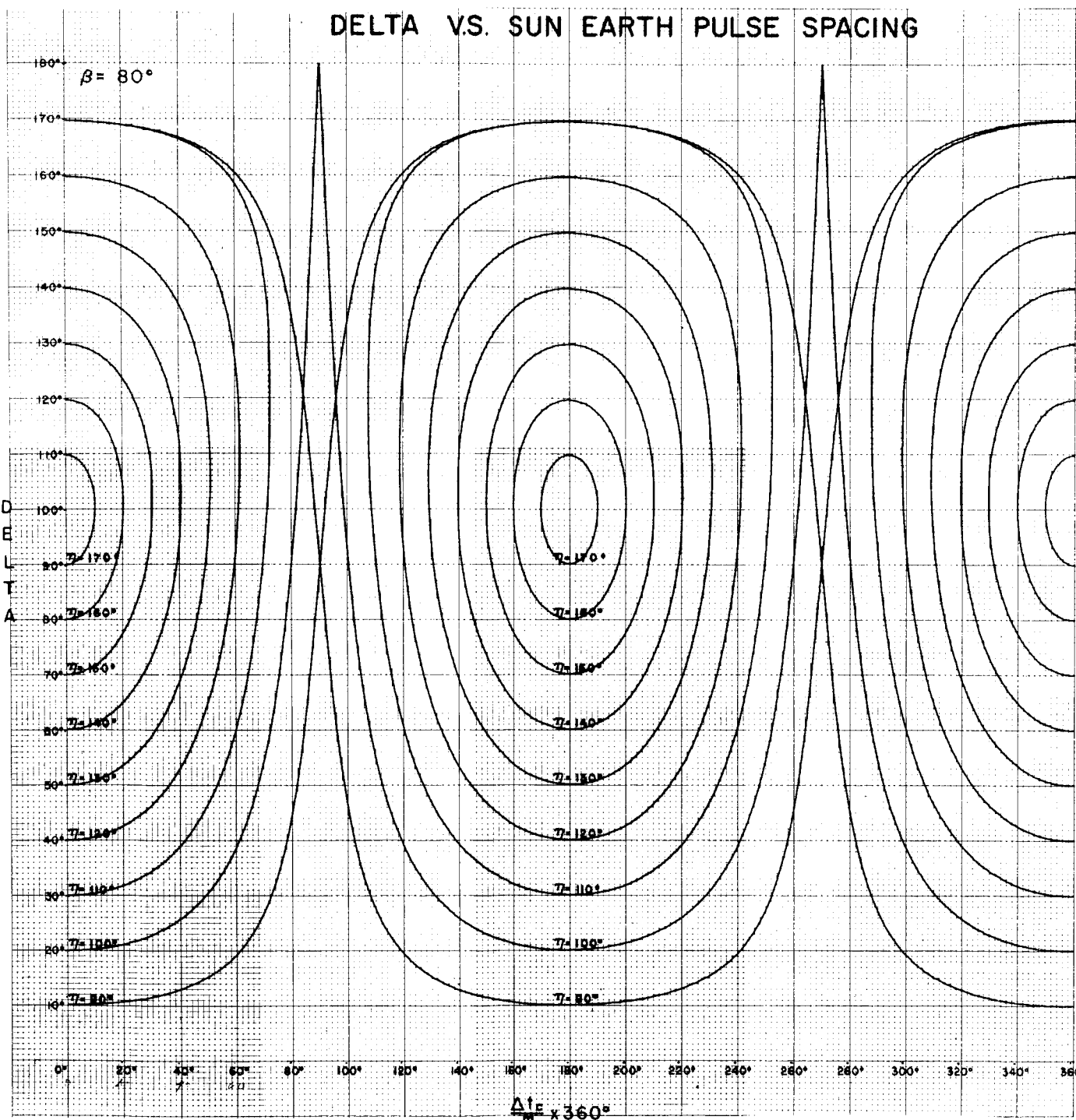


## DELTA V.S. SUN EARTH PULSE SPACING

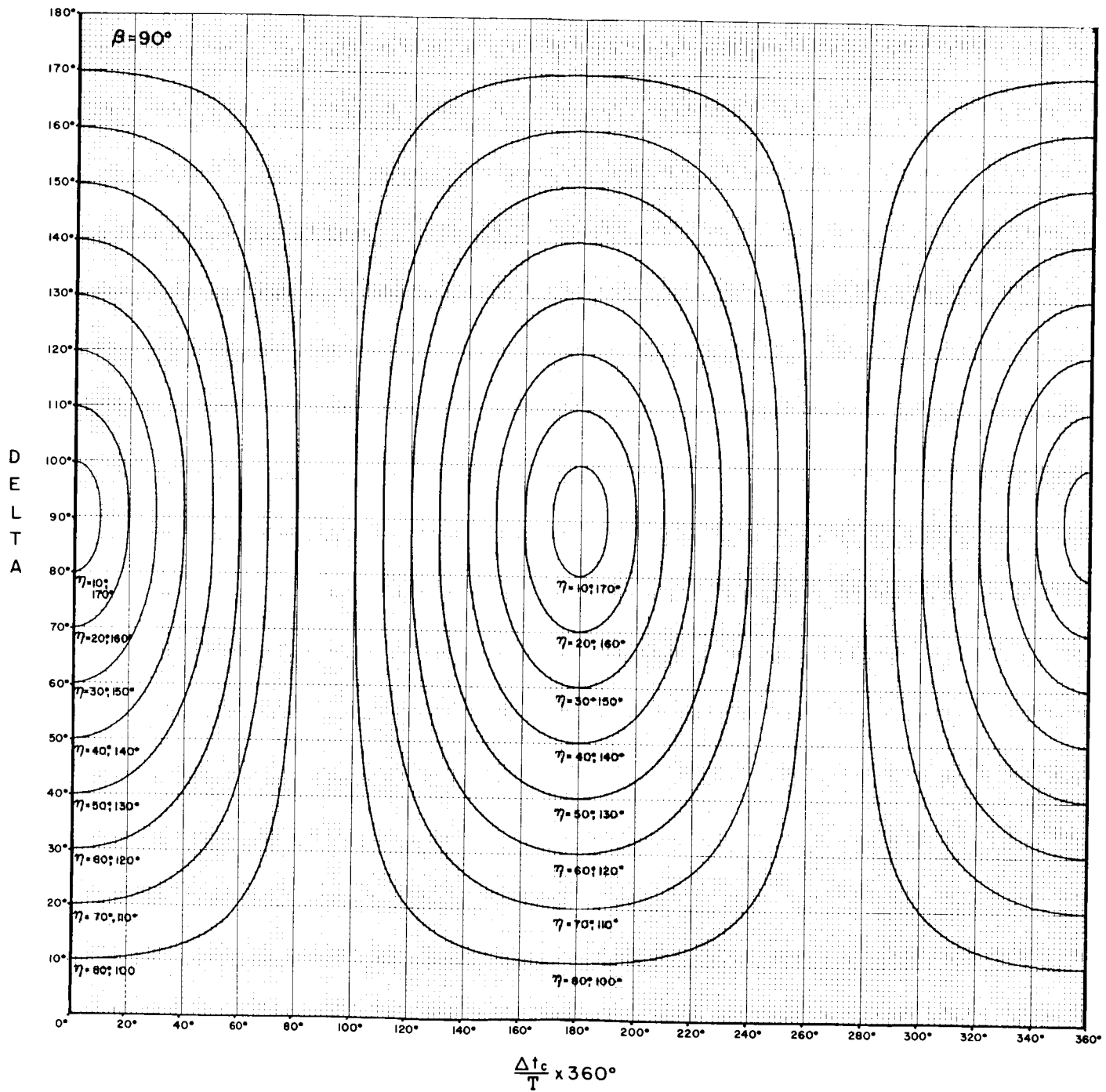


# DELTA V.S. SUN EARTH PULSE SPACING

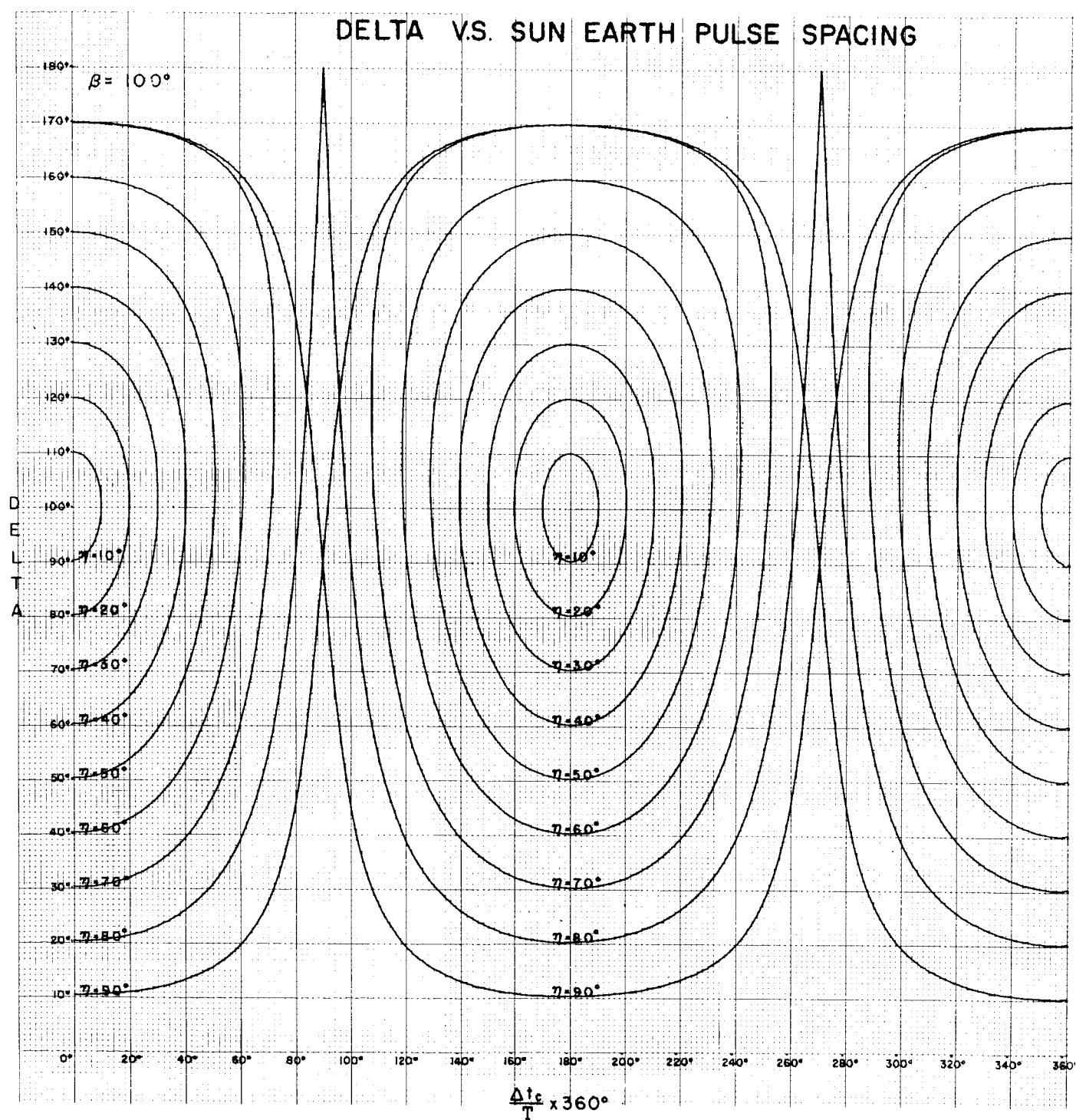




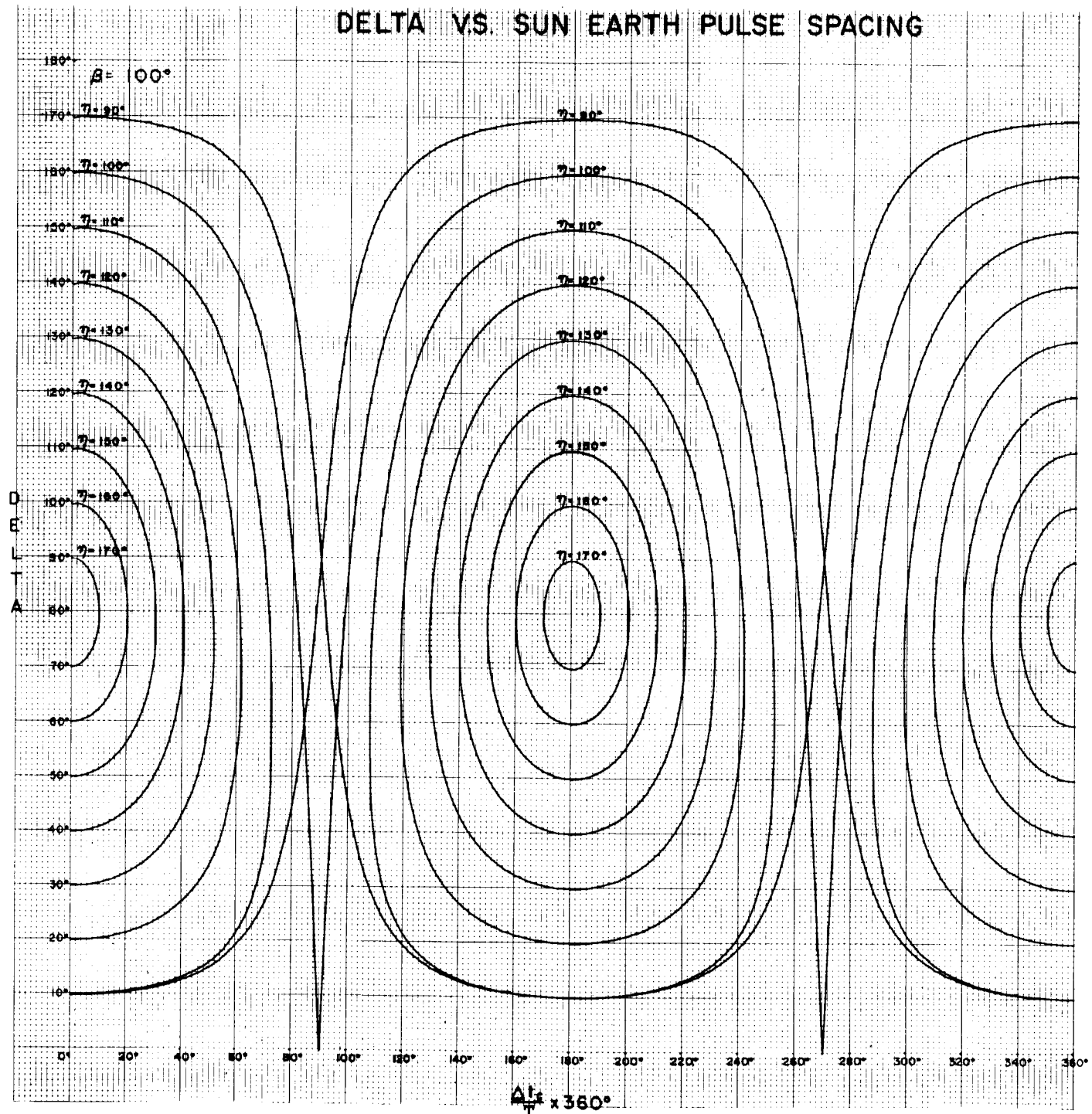
## DELTA V.S. SUN EARTH PULSE SPACING



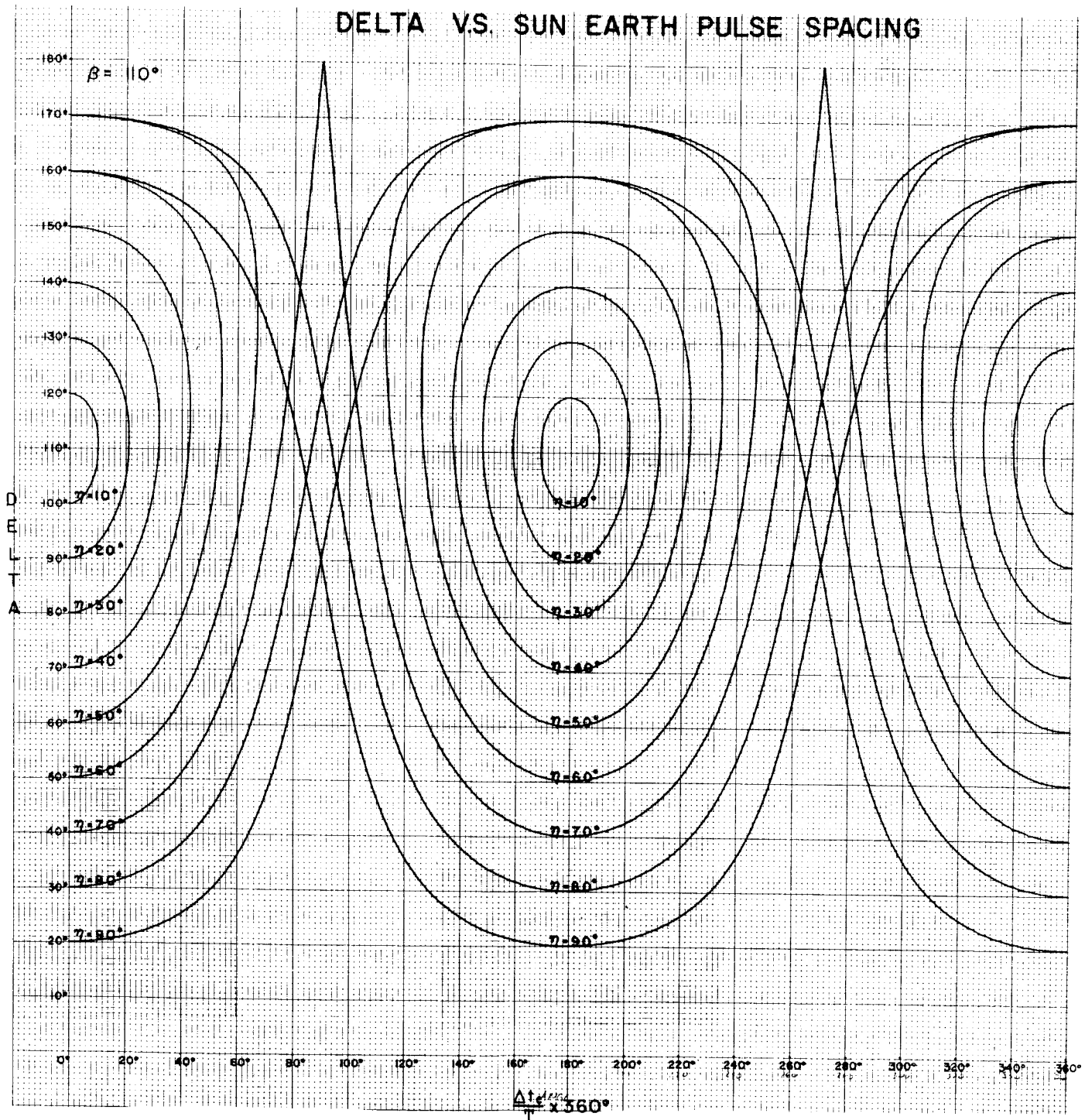
# DELTA V.S. SUN EARTH PULSE SPACING



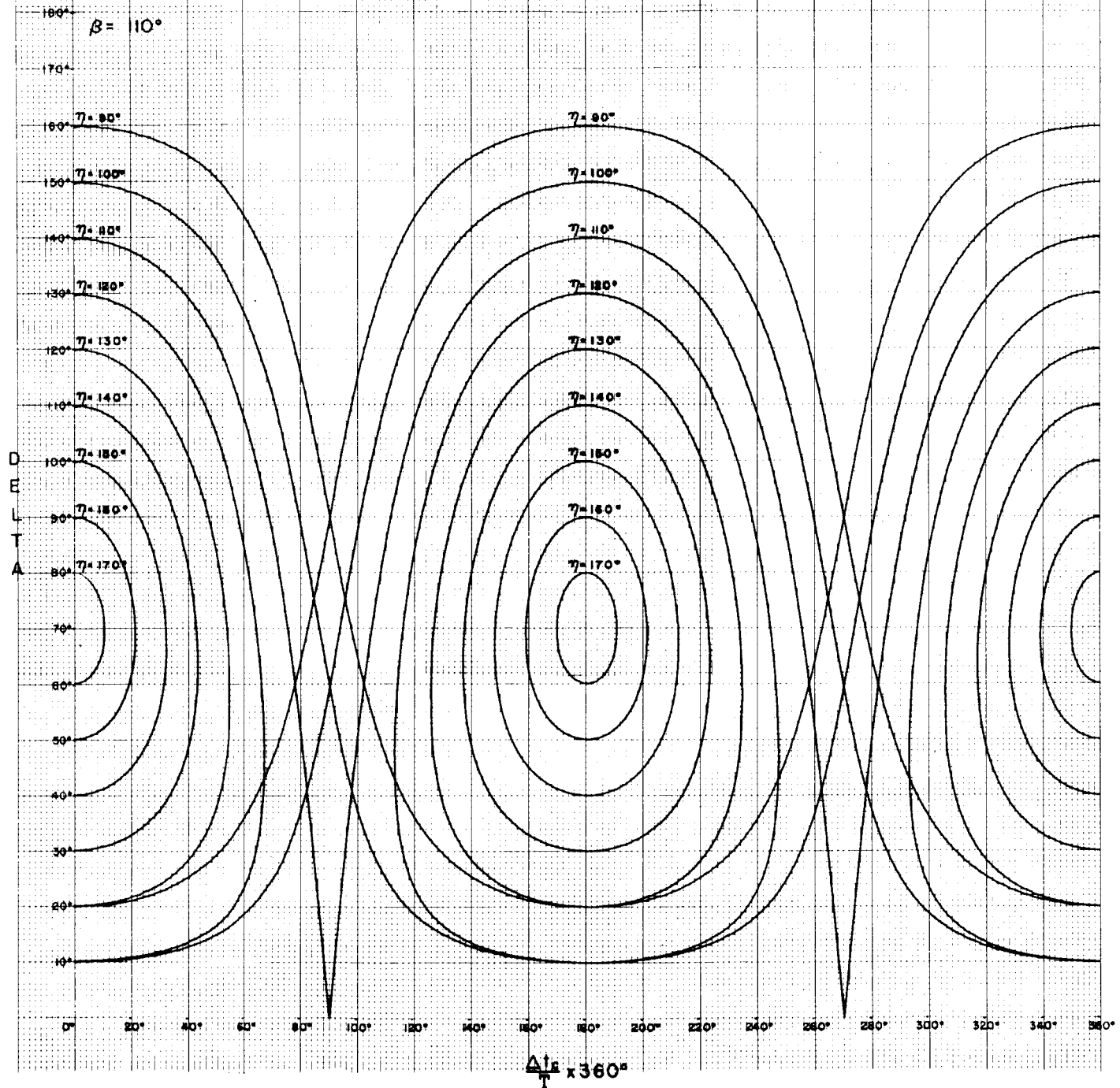
## DELTA VS. SUN EARTH PULSE SPACING

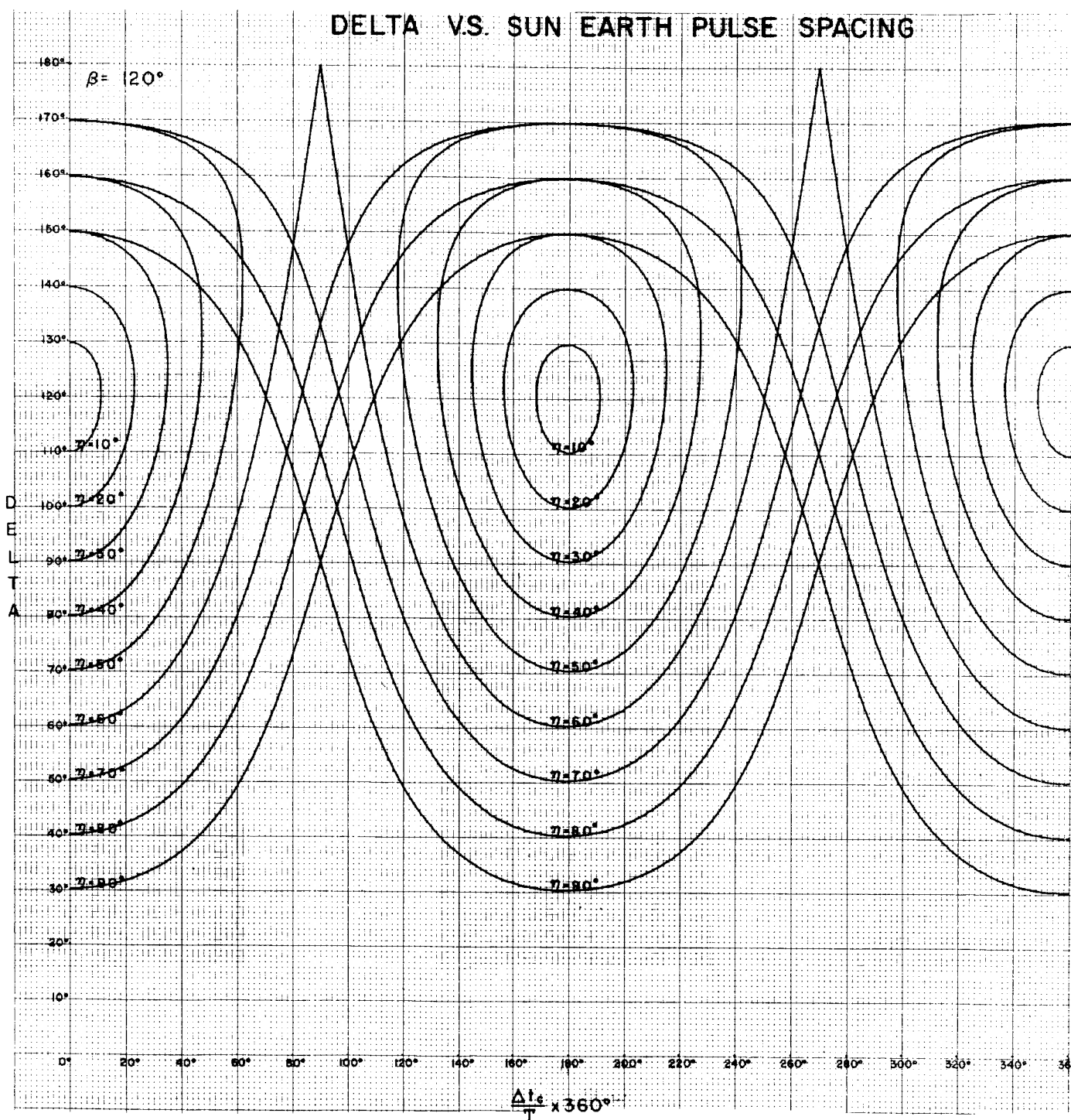


## DELTA V.S. SUN EARTH PULSE SPACING

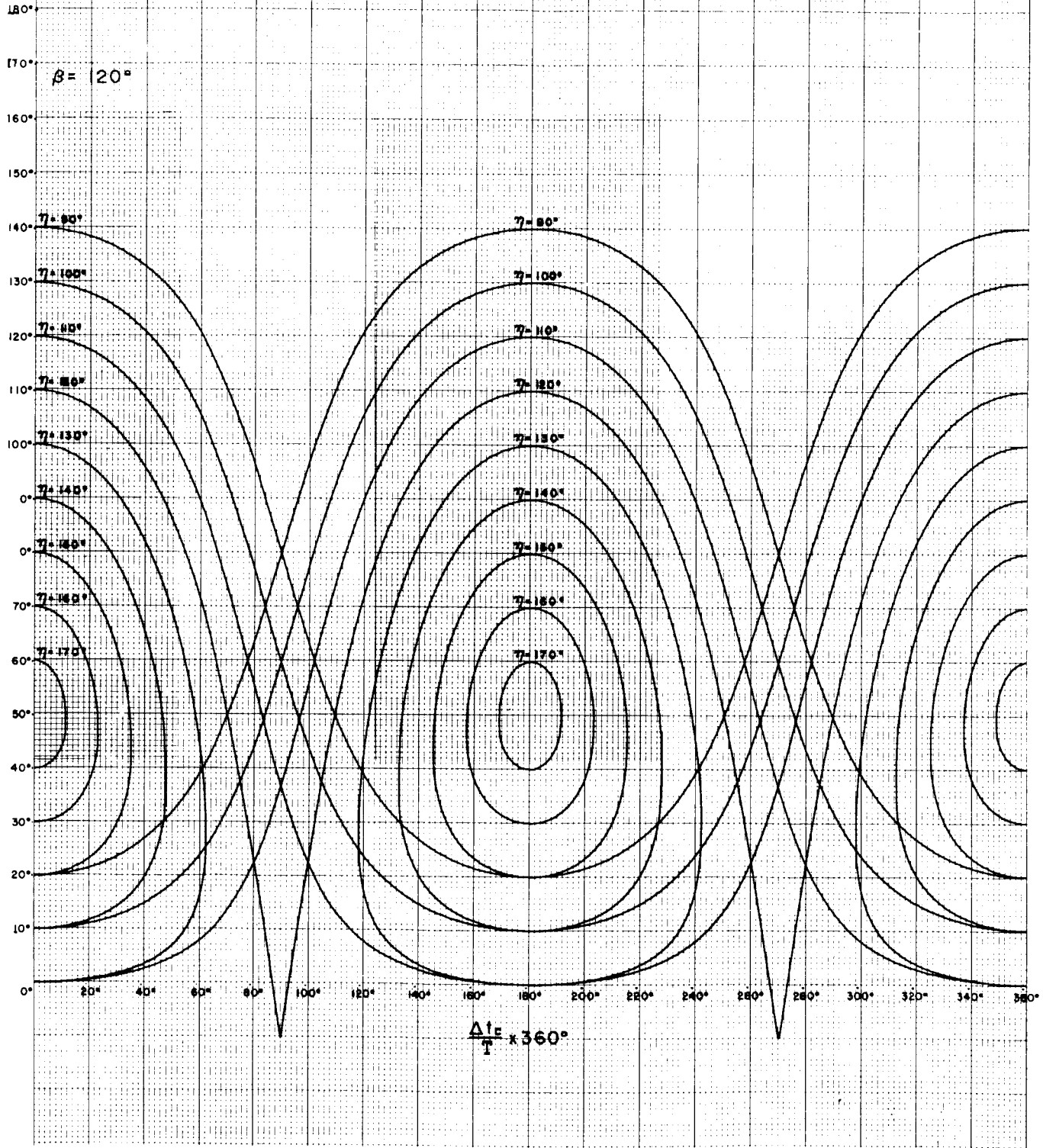


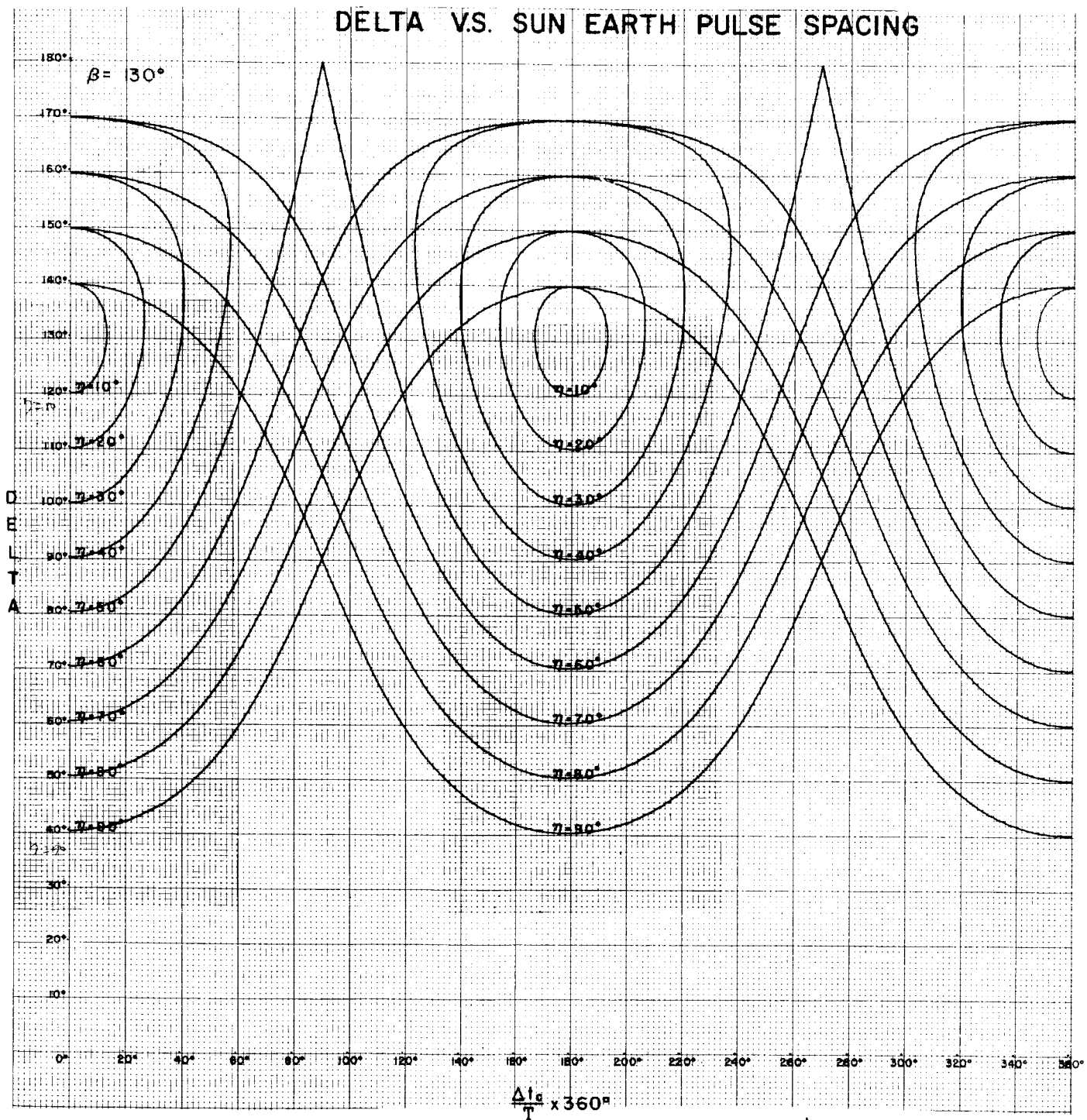
# DELTA V.S. SUN EARTH PULSE SPACING



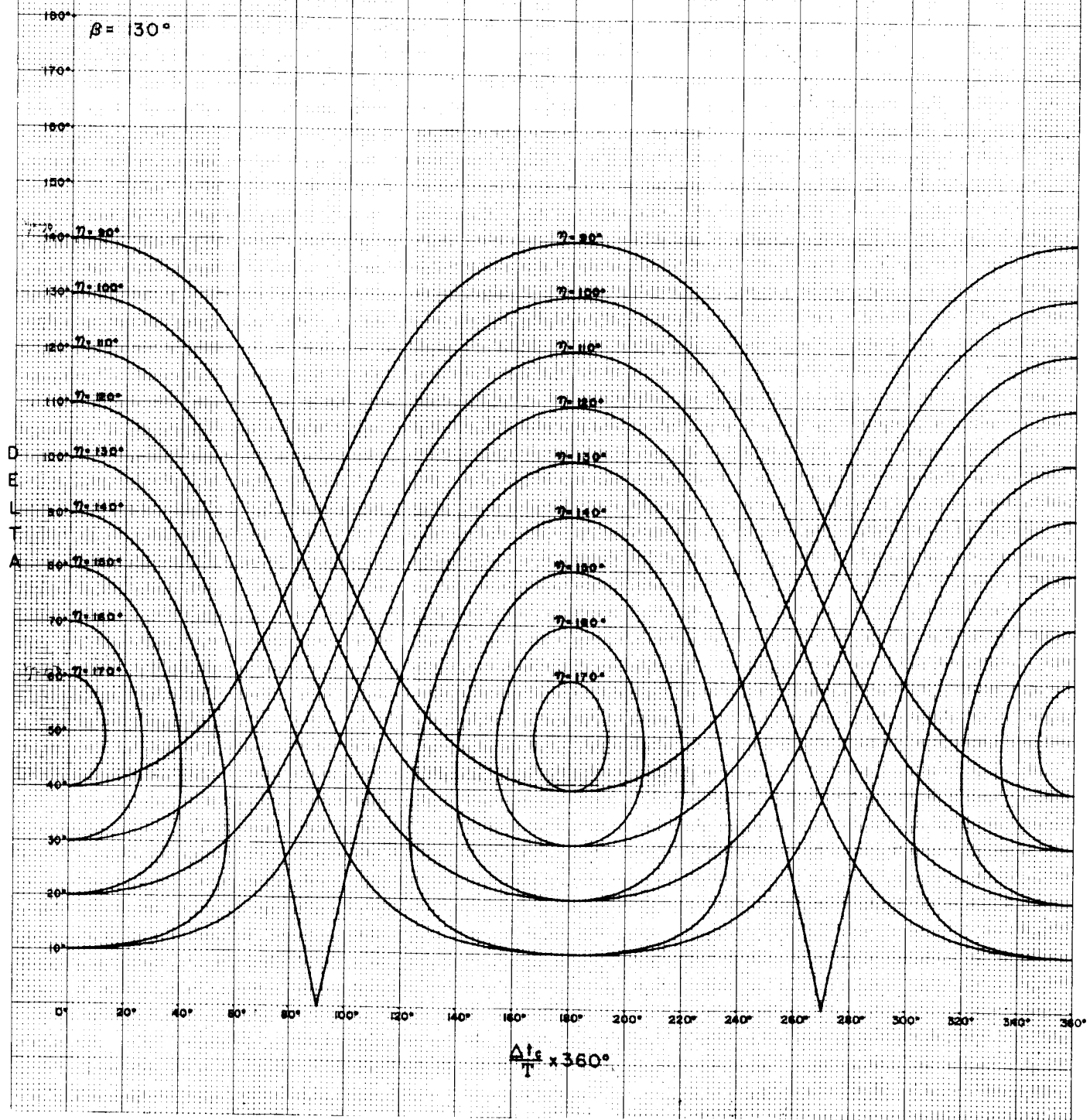


# DELTA V.S. SUN EARTH PULSE SPACING

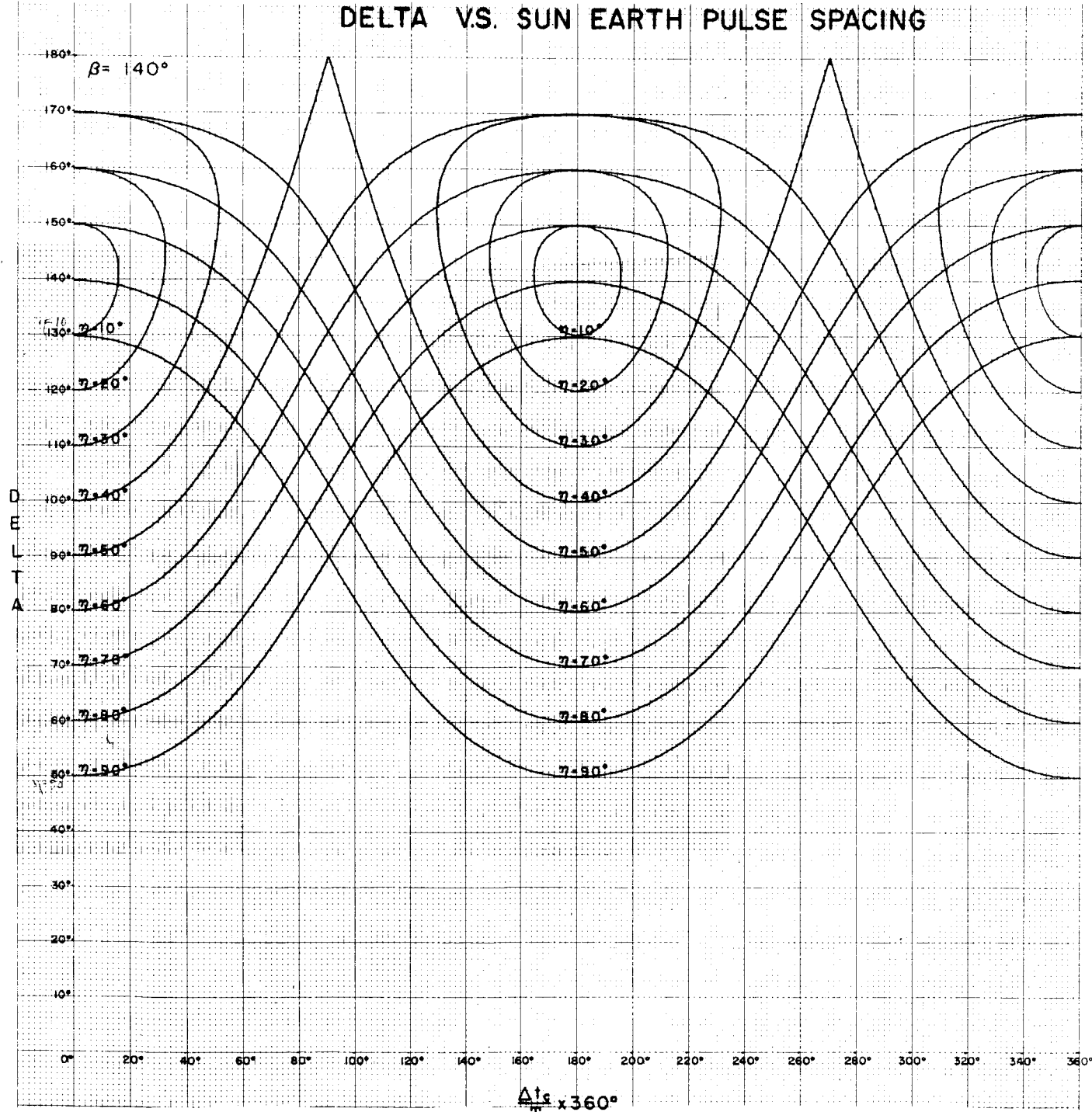




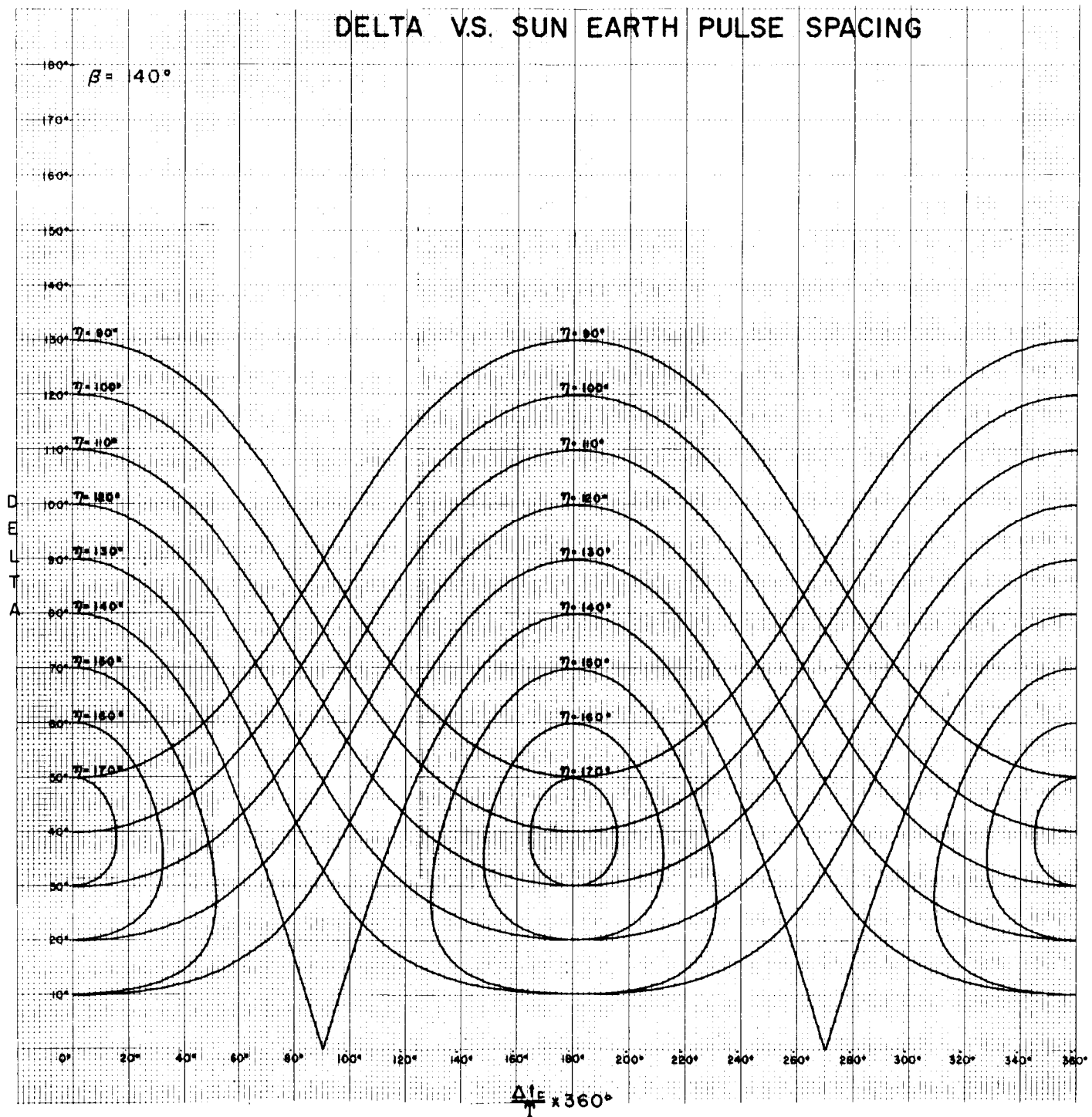
# DELTA V.S. SUN EARTH PULSE SPACING



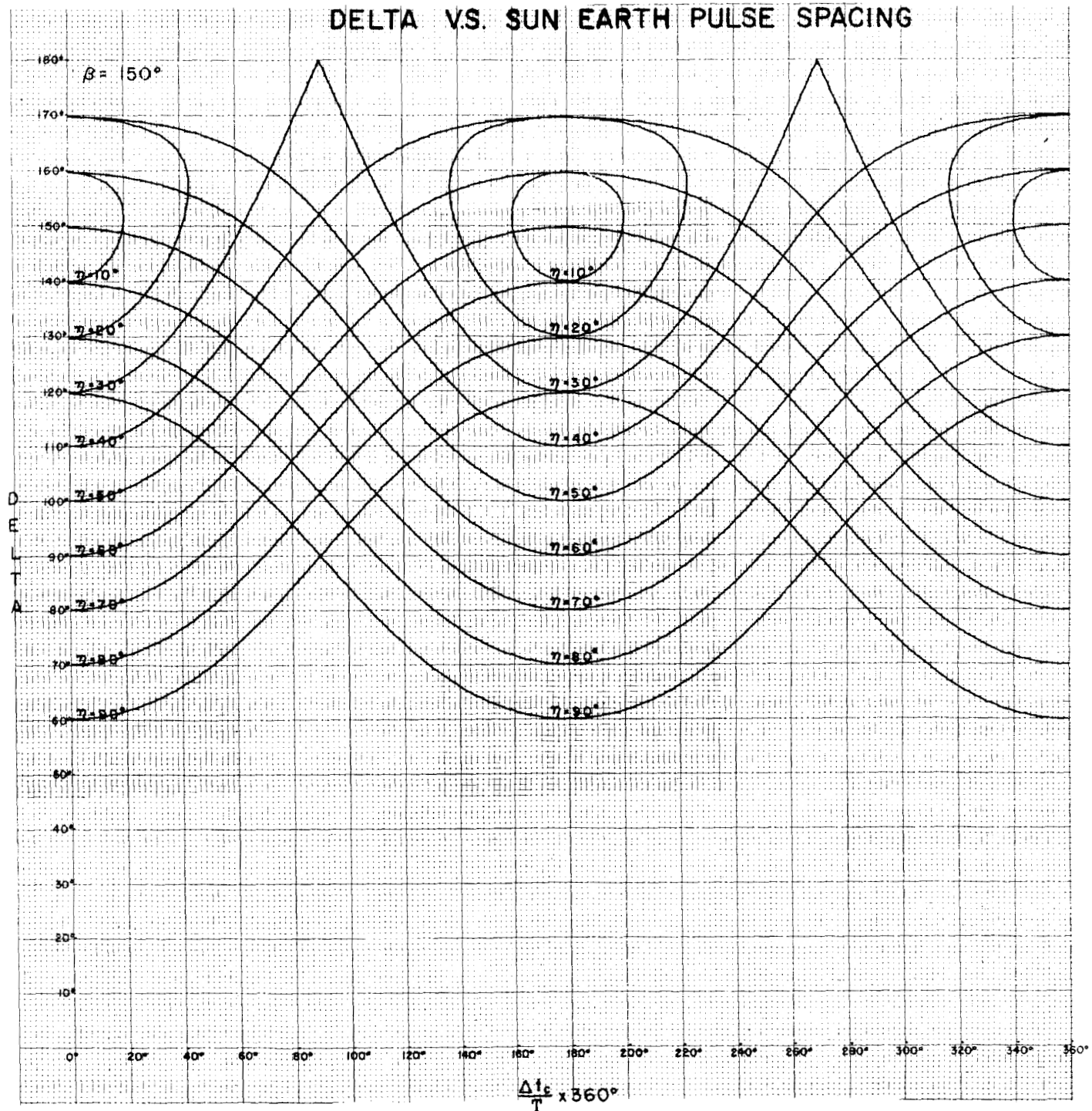
## DELTA V.S. SUN EARTH PULSE SPACING



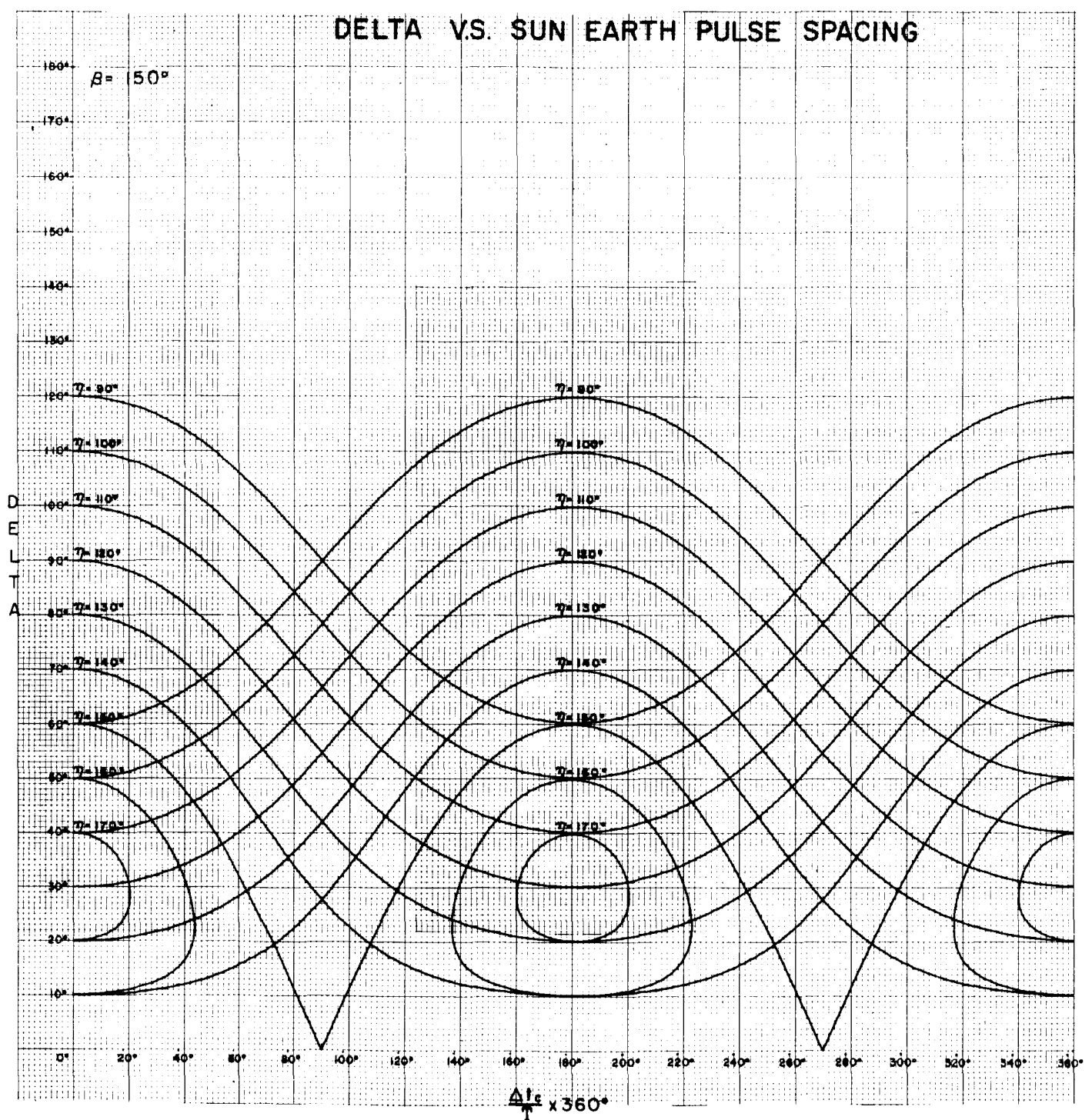
# DELTA V.S. SUN EARTH PULSE SPACING

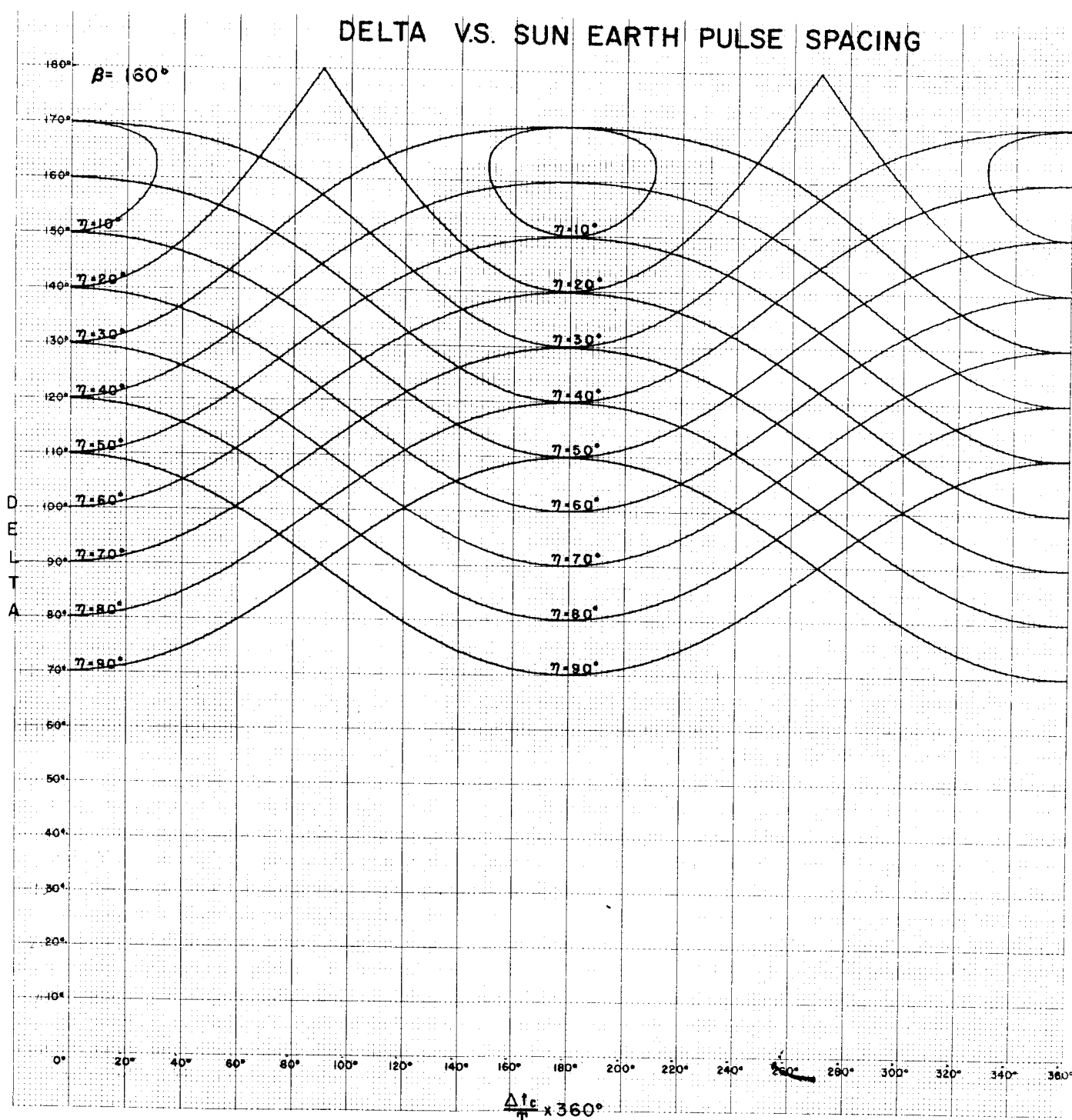


### DELTA V.S. SUN EARTH PULSE SPACING

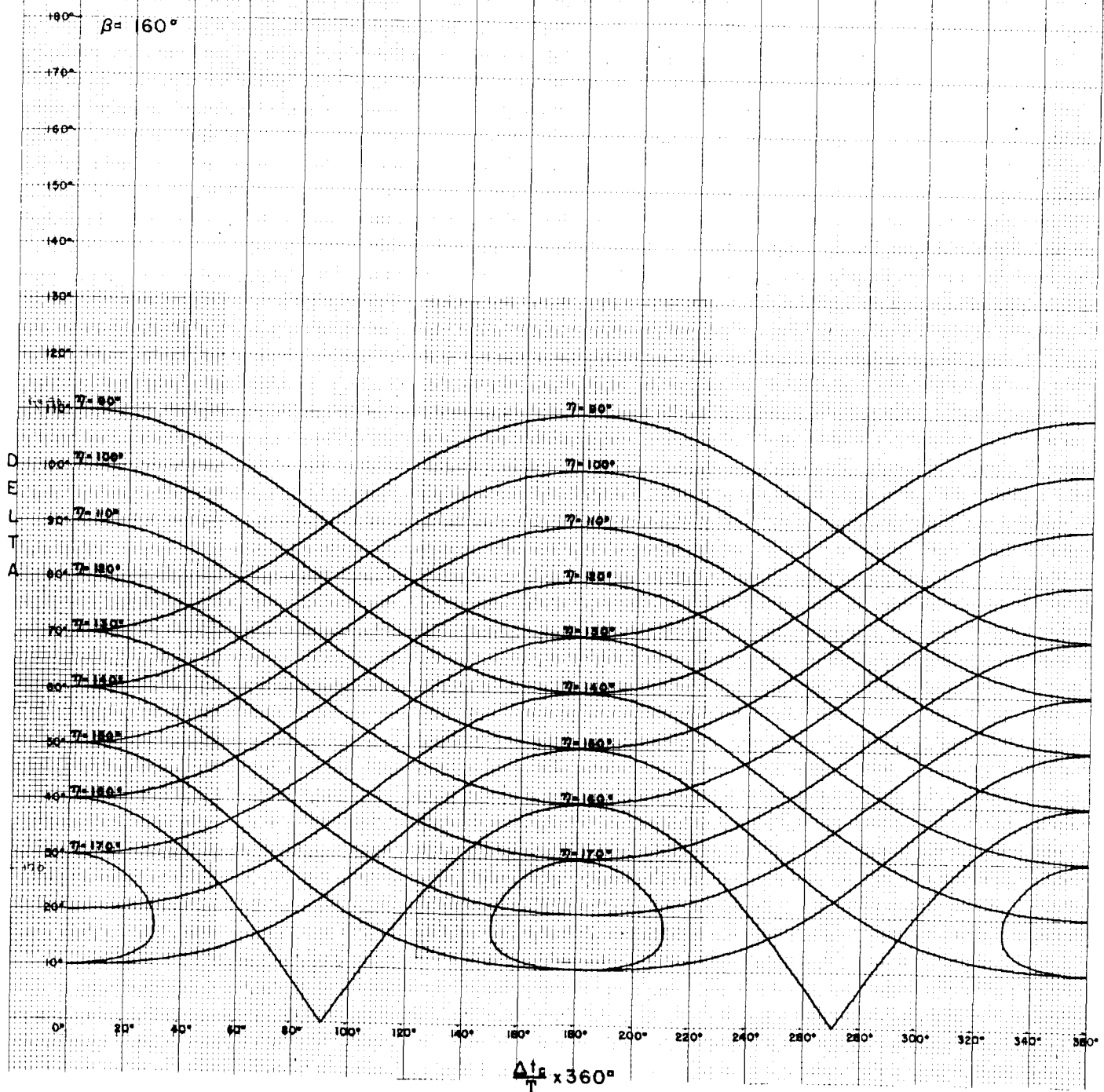


# DELTA V.S. SUN EARTH PULSE SPACING

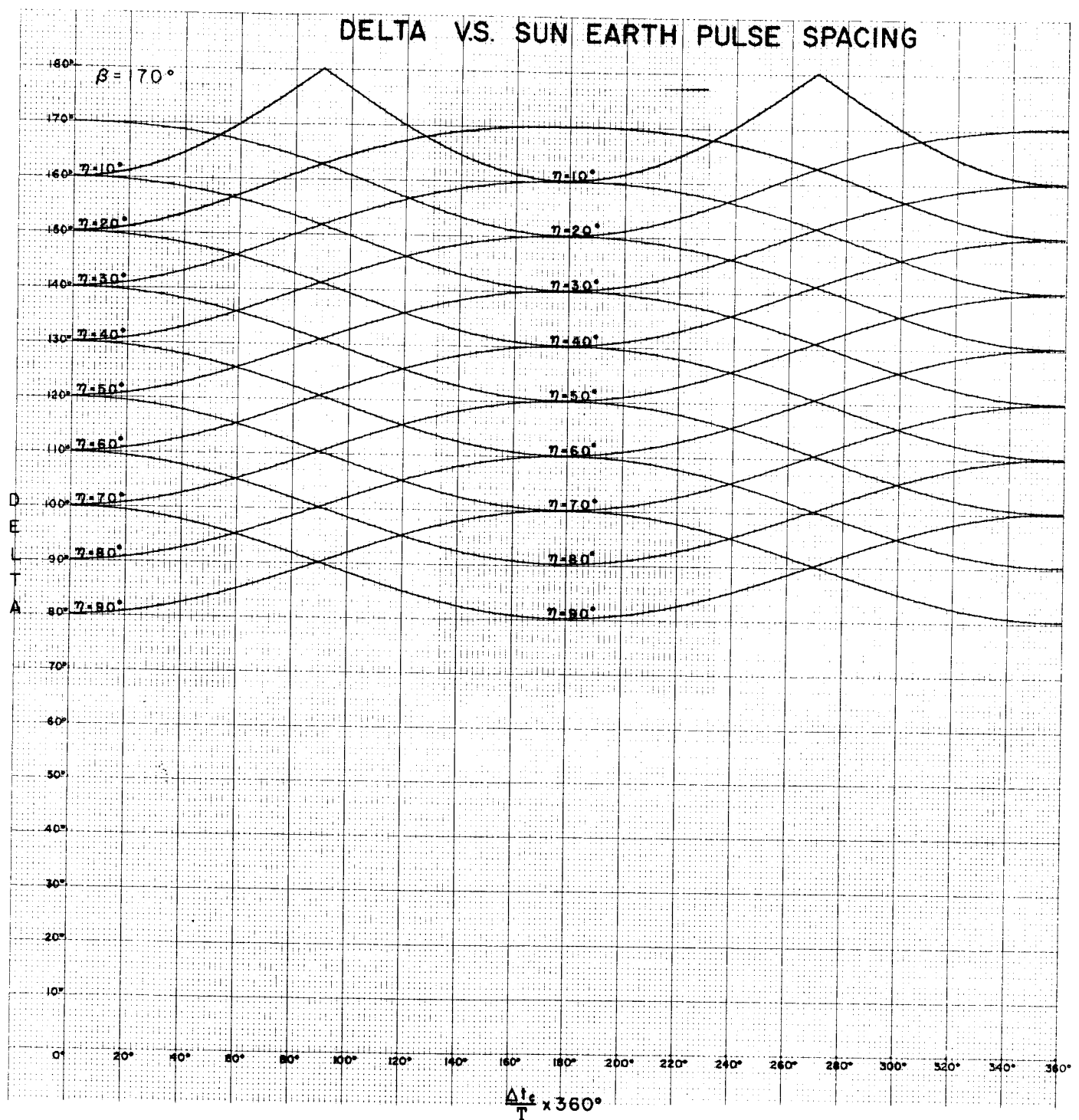




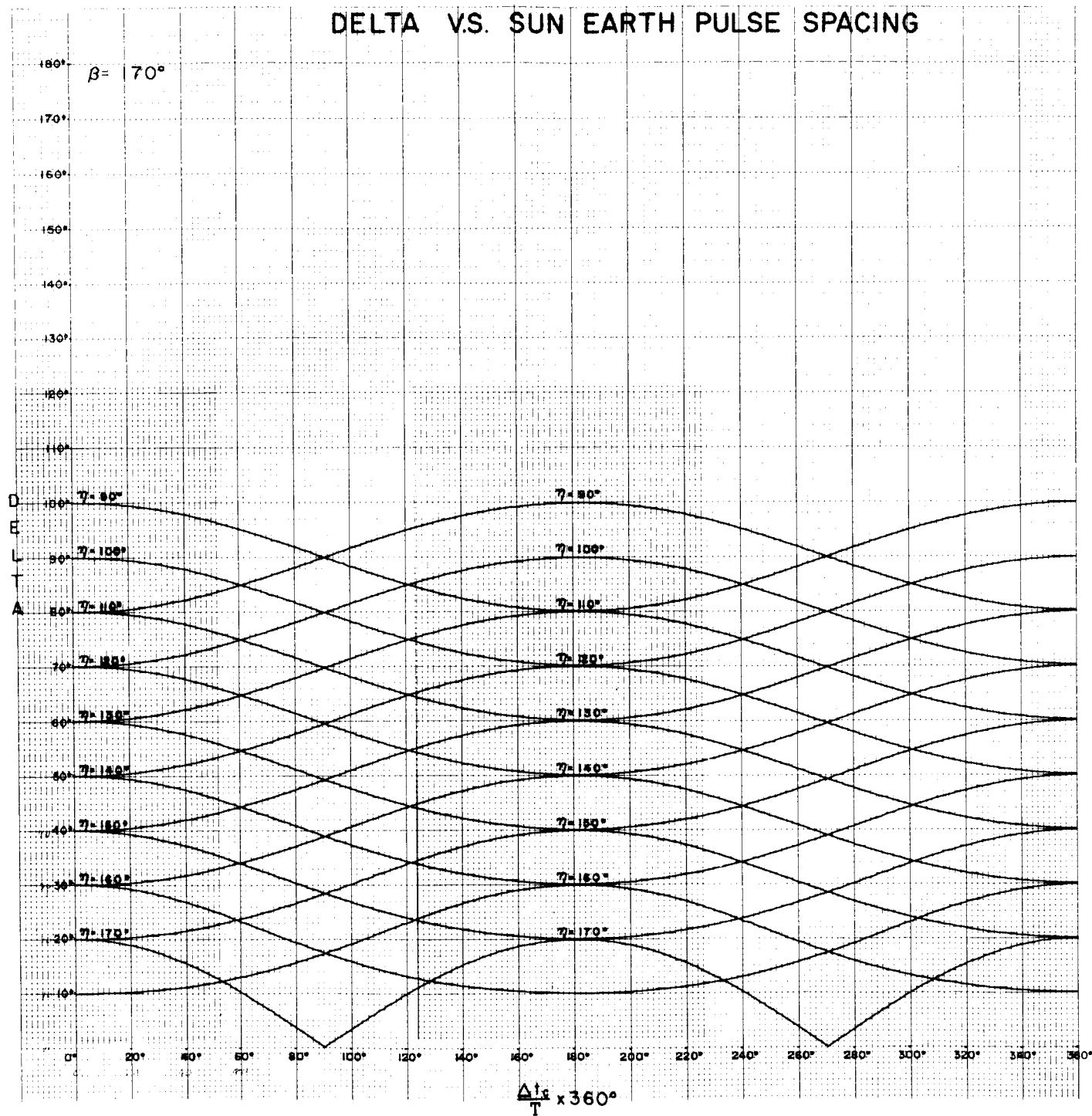
# DELTA V.S. SUN EARTH PULSE SPACING



# DELTA V.S. SUN EARTH PULSE SPACING



# DELTA V.S. SUN EARTH PULSE SPACING



## APPENDIX D

Tables of Error in Momentum  
Vector Position Caused by  $1^\circ$  Error in  
 $\delta$  for Various Values of  $\eta$  and  $\beta$ .





ETA= 30.0	BETA	DELTA	10	20	30	40	50	60	70	80	90	100	110	120	130	140	150	160	170	
2.0	0.	0.	1.0	0.	0.	0.	0.	0.	0.	0.	0.	0.	0.	0.	0.	0.	0.	0.	0.	
4.0	0.	0.	1.0	0.	0.	0.	0.	0.	0.	0.	0.	0.	0.	0.	0.	0.	0.	0.	0.	
6.0	0.	0.	1.0	0.	0.	0.	0.	0.	0.	0.	0.	0.	0.	0.	0.	0.	0.	0.	0.	
8.0	0.	0.	1.0	0.	0.	0.	0.	0.	0.	0.	0.	0.	0.	0.	0.	0.	0.	0.	0.	
10.0	0.	0.	3.8	1.0	0.	0.	0.	0.	0.	0.	0.	0.	0.	0.	0.	0.	0.	0.	0.	
12.0	0.	0.	1.4	1.0	1.9	0.	0.	0.	0.	0.	0.	0.	0.	0.	0.	0.	0.	0.	0.	
14.0	0.	0.	1.2	1.0	1.6	0.	0.	0.	0.	0.	0.	0.	0.	0.	0.	0.	0.	0.	0.	
16.0	0.	0.	1.1	1.0	1.4	0.	0.	0.	0.	0.	0.	0.	0.	0.	0.	0.	0.	0.	0.	
18.0	0.	0.	1.0	1.0	1.4	0.	0.	0.	0.	0.	0.	0.	0.	0.	0.	0.	0.	0.	0.	
20.0	19.6	1.0	1.1	1.3	7.8	0.	0.	0.	0.	0.	0.	0.	0.	0.	0.	0.	0.	0.	0.	
22.0	1.3	1.0	1.1	1.3	2.7	0.	0.	0.	0.	0.	0.	0.	0.	0.	0.	0.	0.	0.	0.	
24.0	1.1	1.0	1.1	1.3	2.1	0.	0.	0.	0.	0.	0.	0.	0.	0.	0.	0.	0.	0.	0.	
26.0	1.0	1.0	1.1	1.3	1.9	0.	0.	0.	0.	0.	0.	0.	0.	0.	0.	0.	0.	0.	0.	
28.0	1.0	1.0	1.1	1.3	1.8	0.	0.	0.	0.	0.	0.	0.	0.	0.	0.	0.	0.	0.	0.	
30.0	1.0	1.1	1.1	1.3	1.7	119.0	0.	0.	0.	0.	0.	0.	0.	0.	0.	0.	0.	0.	0.	
32.0	1.1	1.1	1.2	1.3	1.6	3.4	0.	0.	0.	0.	0.	0.	0.	0.	0.	0.	0.	0.	0.	
34.0	1.2	1.1	1.2	1.3	1.6	2.6	0.	0.	0.	0.	0.	0.	0.	0.	0.	0.	0.	0.	0.	
36.0	1.4	1.2	1.2	1.3	1.6	2.3	0.	0.	0.	0.	0.	0.	0.	0.	0.	0.	0.	0.	0.	
38.0	2.1	1.3	1.3	1.3	1.5	2.1	0.	0.	0.	0.	0.	0.	0.	0.	0.	0.	0.	0.	0.	
40.0	19.9	1.4	1.3	1.4	1.5	2.0	0.	0.	0.	0.	0.	0.	0.	0.	0.	0.	0.	0.	0.	
42.0	0.	1.5	1.4	1.4	1.5	1.9	3.9	0.	0.	0.	0.	0.	0.	0.	0.	0.	0.	0.	0.	
44.0	0.	1.7	1.4	1.4	1.5	1.8	3.0	0.	0.	0.	0.	0.	0.	0.	0.	0.	0.	0.	0.	
46.0	0.	2.1	1.5	1.5	1.5	1.8	2.6	0.	0.	0.	0.	0.	0.	0.	0.	0.	0.	0.	0.	
48.0	0.	3.2	1.6	1.5	1.6	1.8	2.4	0.	0.	0.	0.	0.	0.	0.	0.	0.	0.	0.	0.	
50.0	0.	39.9	1.7	1.5	1.6	1.7	2.2	0.	0.	0.	0.	0.	0.	0.	0.	0.	0.	0.	0.	
52.0	0.	0.	1.9	1.6	1.6	1.7	2.1	4.4	0.	0.	0.	0.	0.	0.	0.	0.	0.	0.	0.	
54.0	0.	0.	2.2	1.7	1.6	1.7	2.0	3.4	0.	0.	0.	0.	0.	0.	0.	0.	0.	0.	0.	
56.0	0.	0.	2.7	1.8	1.7	1.7	2.0	2.9	0.	0.	0.	0.	0.	0.	0.	0.	0.	0.	0.	
58.0	0.	0.	4.2	1.9	1.7	1.7	1.9	2.6	0.	0.	0.	0.	0.	0.	0.	0.	0.	0.	0.	
60.0	0.	0.	59.9	2.1	1.8	1.8	1.9	2.4	0.	0.	0.	0.	0.	0.	0.	0.	0.	0.	0.	
62.0	0.	0.	0.	2.3	1.8	1.8	1.9	2.3	4.6	0.	0.	0.	0.	0.	0.	0.	0.	0.	0.	
64.0	0.	0.	0.	2.6	1.9	1.8	1.9	2.2	3.6	0.	0.	0.	0.	0.	0.	0.	0.	0.	0.	
66.0	0.	0.	0.	3.2	2.0	1.8	1.9	2.1	3.0	0.	0.	0.	0.	0.	0.	0.	0.	0.	0.	
68.0	0.	0.	0.	4.9	2.1	1.9	1.9	2.1	2.7	0.	0.	0.	0.	0.	0.	0.	0.	0.	0.	
70.0	0.	0.	0.	79.9	2.3	1.9	1.9	2.0	2.5	0.	0.	0.	0.	0.	0.	0.	0.	0.	0.	
72.0	0.	0.	0.	0.	2.6	2.0	1.9	2.0	2.4	4.8	0.	0.	0.	0.	0.	0.	0.	0.	0.	
74.0	0.	0.	0.	0.	2.9	2.1	1.9	2.0	2.3	3.6	0.	0.	0.	0.	0.	0.	0.	0.	0.	
76.0	0.	0.	0.	0.	3.6	2.2	2.0	2.0	2.2	3.1	0.	0.	0.	0.	0.	0.	0.	0.	0.	
78.0	0.	0.	0.	0.	5.5	2.3	2.0	2.0	2.1	2.8	0.	0.	0.	0.	0.	0.	0.	0.	0.	
80.0	0.	0.	0.	0.	99.9	2.5	2.1	2.0	2.1	2.6	0.	0.	0.	0.	0.	0.	0.	0.	0.	
82.0	0.	0.	0.	0.	0.	2.8	2.1	2.0	2.1	2.4	4.8	0.	0.	0.	0.	0.	0.	0.	0.	
84.0	0.	0.	0.	0.	0.	3.2	2.2	2.0	2.0	2.3	3.6	0.	0.	0.	0.	0.	0.	0.	0.	
86.0	0.	0.	0.	0.	0.	3.9	2.3	2.0	2.0	2.2	3.1	0.	0.	0.	0.	0.	0.	0.	0.	
88.0	0.	0.	0.	0.	0.	5.9	2.4	2.1	2.0	2.1	2.7	0.	0.	0.	0.	0.	0.	0.	0.	
90.0	0.	0.	0.	0.	0.	119.8	2.6	2.1	2.0	2.1	2.5	0.	0.	0.	0.	0.	0.	0.	0.	
92.0	0.	0.	0.	0.	0.	0.	2.9	2.2	2.0	2.0	2.4	4.6	0.	0.	0.	0.	0.	0.	0.	
94.0	0.	0.	0.	0.	0.	0.	3.3	2.3	2.0	2.0	2.3	3.5	0.	0.	0.	0.	0.	0.	0.	
96.0	0.	0.	0.	0.	0.	0.	4.1	2.4	2.0	2.0	2.2	2.9	0.	0.	0.	0.	0.	0.	0.	
98.0	0.	0.	0.	0.	0.	0.	6.1	2.5	2.1	2.0	2.1	2.6	0.	0.	0.	0.	0.	0.	0.	
100.0	0.	0.	0.	0.	0.	0.	139.8	2.7	2.1	2.0	2.0	2.4	0.	0.	0.	0.	0.	0.	0.	
102.0	0.	0.	0.	0.	0.	0.	0.	2.9	2.2	2.0	2.0	2.3	4.3	0.	0.	0.	0.	0.	0.	
104.0	0.	0.	0.	0.	0.	0.	0.	3.3	2.2	2.0	1.9	2.1	3.2	0.	0.	0.	0.	0.	0.	
106.0	0.	0.	0.	0.	0.	0.	0.	4.1	2.3	2.0	1.9	2.0	2.7	0.	0.	0.	0.	0.	0.	
108.0	0.	0.	0.	0.	0.	0.	0.	6.1	2.5	2.0	1.9	2.0	2.4	0.	0.	0.	0.	0.	0.	
110.0	0.	0.	0.	0.	0.	0.	0.	159.6	2.6	2.0	1.9	1.9	2.2	0.	0.	0.	0.	0.	0.	
112.0	0.	0.	0.	0.	0.	0.	0.	0.	2.9	2.1	1.9	1.9	2.1	3.8	0.	0.	0.	0.	0.	
114.0	0.	0.	0.	0.	0.	0.	0.	0.	3.3	2.2	1.9	1.8	2.0	2.9	0.	0.	0.	0.	0.	
116.0	0.	0.	0.	0.	0.	0.	0.	0.	4.0	2.2	1.9	1.8	1.9	2.4	0.	0.	0.	0.	0.	
118.0	0.	0.	0.	0.	0.	0.	0.	0.	6.0	2.4	1.9	1.8	1.8	2.2	0.	0.	0.	0.	0.	
120.0	0.	0.	0.	0.	0.	0.	0.	0.	178.6	2.5	1.9	1.7	1.7	2.0	0.	0.	0.	0.	0.	
122.0	0.	0.	0.	0.	0.	0.	0.	0.	0.	2.7	2.0	1.7	1.7	1.8	3.2	0.	0.	0.	0.	
124.0	0.	0.	0.	0.	0.	0.	0.	0.	0.	3.1	2.0	1.7	1.6	1.7	2.4	0.	0.	0.	0.	
126.0	0.	0.	0.	0.	0.	0.	0.	0.	0.	3.7	2.1	1.7	1.6	1.6	2.1	0.	0.	0.	0.	
128.0	0.	0.	0.	0.	0.	0.	0.	0.	0.	5.6	2.2	1.7	1.6	1.6	1.8	0.	0.	0.	0.	
130.0	0.	0.	0.	0.	0.	0.	0.	0.	0.	159.8	2.3	1.8	1.6	1.5	1.7	0.	0.	0.	0.	
132.0	0.	0.	0.	0.	0.	0.	0.	0.	0.	0.	2.5	1.8	1.6	1.5	1.5	2.5	0.	0.	0.	
134.0	0.	0.	0.	0.	0.	0.	0.	0.	0.	0.	2.8	1.8	1.6	1.5	1.4	1.9	0.	0.	0.	
136.0	0.	0.	0.	0.	0.	0.	0.	0.	0.	0.	3.4	1.9	1.5	1.4	1.3	1.4	1.6	0.	0.	
138.0	0.	0.	0.	0.	0.	0.	0.	0.	0.	0.	5.0	1.9	1.5	1.4	1.3	1.3	1.3	0.	0.	
140.0	0.	0.	0.	0.	0.	0.	0.	0.	0.	0.	139.9	2.0	1.5	1.4	1.3	1.3	1.3	1.3	0.	0.
142.0	0.	0.	0.	0.	0.	0.	0.	0.	0.	0.	0.	2.2	1.5	1.3	1.2	1.2	1.3	1.7	0.	0.
144.0	0.	0.	0.	0.	0.	0.	0.	0.	0.	0.	0.	2.4	1.6	1.3	1.2	1.2	1.3	1.1	0.	0.
146.0	0.	0.	0.	0.	0.	0.	0.	0.	0.	0.	0.	2.9	1.6	1.3	1.2	1.1	1.1	1.0	0.	0.
148.0	0.	0.	0.	0.	0.	0.	0.	0.	0.	0.	0.	4.3	1.6	1.3	1.1	1.1	1.1	1.0	0.	0.
150.0	0.	0.	0.	0.	0.	0.	0.	0.	0.	0.	0.	120.0	1.7	1.3	1.1	1.1	1.0	1.0	1.0	0.
152.0	0.	0.	0.	0.	0.	0.	0.	0.	0.	0.	0.	0.	1.8	1.3	1.1	1.0	1.0	1.0	1.0	
154.0	0.	0.	0.	0.	0.	0.	0.	0.	0.	0.	0.	0.	2.0	1.3	1.1	1.0	1.0	1.1	1.1	
156.0	0.	0.	0.	0.	0.	0.	0.	0.	0.	0.	0.	0.	2.4	1.3	1.1	1.0	1.0	1.2	1.2	
158.0	0.	0.	0.	0.	0.	0.	0.	0.	0.	0.	0.	0.	3.4	1.3	1.1	1.0	1.0	1.6	1.6	
160.0	0.	0.	0.	0.	0.	0.	0.	0.	0.	0.	0.	0.	0.	100.0	1.3	1.0	1.0	1.0	20.0	0.
162.0	0.	0.																		



ETA\* 50.0

BE

ETA= 60.0		META															
DELTA	10	20	30	40	50	60	70	80	90	100	110	120	130	140	150	160	170
2.0	0.	0.	0.	0.	0.	1.0	0.	0.	0.	0.	0.	0.	0.	0.	0.	0.	0.
4.0	0.	0.	0.	0.	0.	1.0	0.	0.	0.	0.	0.	0.	0.	0.	0.	0.	0.
6.0	0.	0.	0.	0.	0.	1.0	0.	0.	0.	0.	0.	0.	0.	0.	0.	0.	0.
8.0	0.	0.	0.	0.	0.	1.0	0.	0.	0.	0.	0.	0.	0.	0.	0.	0.	0.
10.0	0.	0.	0.	0.	0.	4.3	1.0	0.	0.	0.	0.	0.	0.	0.	0.	0.	0.
12.0	0.	0.	0.	0.	0.	1.6	1.0	1.7	0.	0.	0.	0.	0.	0.	0.	0.	0.
14.0	0.	0.	0.	0.	0.	1.3	1.0	1.4	0.	0.	0.	0.	0.	0.	0.	0.	0.
16.0	0.	0.	0.	0.	0.	1.2	1.0	1.3	0.	0.	0.	0.	0.	0.	0.	0.	0.
18.0	0.	0.	0.	0.	0.	1.1	1.0	1.2	0.	0.	0.	0.	0.	0.	0.	0.	0.
20.0	0.	0.	0.	0.	0.	5.5	1.1	1.0	1.2	0.	0.	0.	0.	0.	0.	0.	0.
22.0	0.	0.	0.	0.	0.	1.9	1.1	1.0	1.2	2.3	0.	0.	0.	0.	0.	0.	0.
24.0	0.	0.	0.	0.	0.	1.5	1.0	1.0	1.1	1.8	0.	0.	0.	0.	0.	0.	0.
26.0	0.	0.	0.	0.	0.	1.3	1.0	1.0	1.1	1.6	0.	0.	0.	0.	0.	0.	0.
28.0	0.	0.	0.	0.	0.	1.2	1.0	1.0	1.1	1.5	0.	0.	0.	0.	0.	0.	0.
30.0	0.	0.	0.	0.	0.	5.8	1.1	1.0	1.0	1.1	1.4	0.	0.	0.	0.	0.	0.
32.0	0.	0.	0.	0.	0.	2.0	1.1	1.0	1.0	1.1	1.3	2.7	0.	0.	0.	0.	0.
34.0	0.	0.	0.	0.	0.	1.5	1.1	1.0	1.0	1.1	1.3	2.1	0.	0.	0.	0.	0.
36.0	0.	0.	0.	0.	0.	1.3	1.0	1.0	1.1	1.3	1.8	0.	0.	0.	0.	0.	0.
38.0	0.	0.	0.	0.	0.	1.2	1.0	1.0	1.1	1.2	1.7	0.	0.	0.	0.	0.	0.
40.0	0.	0.	0.	0.	0.	5.4	1.1	1.0	1.0	1.1	1.2	1.6	0.	0.	0.	0.	0.
42.0	0.	0.	0.	0.	0.	1.8	1.1	1.0	1.0	1.1	1.2	1.5	3.0	0.	0.	0.	0.
44.0	0.	0.	0.	0.	0.	1.4	1.1	1.0	1.0	1.1	1.2	1.4	2.3	0.	0.	0.	0.
46.0	0.	0.	0.	0.	0.	1.2	1.0	1.0	1.0	1.1	1.2	1.4	2.0	0.	0.	0.	0.
48.0	0.	0.	0.	0.	0.	1.1	1.0	1.0	1.0	1.1	1.2	1.3	1.8	0.	0.	0.	0.
50.0	0.	0.	0.	0.	0.	1.1	1.0	1.0	1.0	1.1	1.2	1.3	1.7	0.	0.	0.	0.
52.0	0.	0.	0.	0.	0.	1.5	1.0	1.0	1.0	1.1	1.2	1.3	1.6	3.2	0.	0.	0.
54.0	0.	0.	0.	0.	0.	1.2	1.0	1.0	1.0	1.1	1.2	1.3	1.5	2.5	0.	0.	0.
56.0	0.	0.	0.	0.	0.	1.0	1.0	1.0	1.1	1.1	1.2	1.3	1.5	2.1	0.	0.	0.
58.0	0.	0.	0.	0.	0.	1.0	1.0	1.0	1.1	1.1	1.2	1.4	1.9	0.	0.	0.	0.
60.0	0.	0.	0.	0.	0.	1.0	1.0	1.0	1.1	1.1	1.2	1.4	1.7	0.	0.	0.	0.
62.0	0.	0.	0.	0.	0.	1.0	1.0	1.0	1.0	1.1	1.1	1.2	1.3	1.6	3.3	0.	0.
64.0	0.	0.	0.	0.	0.	1.1	1.1	1.1	1.1	1.2	1.3	1.7	0.	0.	0.	0.	0.
66.0	0.	0.	0.	0.	0.	1.4	1.1	1.1	1.1	1.2	1.3	1.5	2.1	0.	0.	0.	0.
68.0	0.	0.	0.	0.	0.	2.0	1.1	1.1	1.1	1.2	1.3	1.4	1.9	0.	0.	0.	0.
70.0	0.	0.	0.	0.	0.	19.9	1.2	1.1	1.1	1.1	1.2	1.3	1.4	1.7	0.	0.	0.
72.0	0.	0.	0.	0.	0.	0.1	1.3	1.2	1.1	1.1	1.2	1.2	1.3	1.6	3.2	0.	0.
74.0	0.	0.	0.	0.	0.	1.5	1.2	1.1	1.1	1.1	1.2	1.2	1.3	1.5	2.4	0.	0.
76.0	0.	0.	0.	0.	0.	1.9	1.3	1.2	1.1	1.1	1.2	1.2	1.3	1.5	2.0	0.	0.
78.0	0.	0.	0.	0.	0.	2.8	1.3	1.2	1.1	1.1	1.2	1.2	1.3	1.4	1.8	0.	0.
80.0	0.	0.	0.	0.	0.	39.9	1.5	1.2	1.2	1.1	1.1	1.2	1.2	1.3	1.7	0.	0.
82.0	0.	0.	0.	0.	0.	0.1	1.6	1.3	1.2	1.2	1.1	1.2	1.2	1.3	1.6	3.0	0.
84.0	0.	0.	0.	0.	0.	0.1	1.8	1.3	1.2	1.2	1.1	1.2	1.2	1.3	1.5	2.3	0.
86.0	0.	0.	0.	0.	0.	0.2	2.3	1.4	1.3	1.2	1.2	1.2	1.2	1.3	1.4	1.9	0.
88.0	0.	0.	0.	0.	0.	0.3	3.4	1.5	1.3	1.2	1.2	1.2	1.2	1.2	1.4	1.7	0.
90.0	0.	0.	0.	0.	0.	0.5	59.9	1.6	1.3	1.2	1.2	1.2	1.2	1.2	1.2	1.3	1.6
92.0	0.	0.	0.	0.	0.	0.6	1.8	1.4	1.3	1.2	1.2	1.2	1.2	1.2	1.3	1.5	2.6
94.0	0.	0.	0.	0.	0.	0.7	2.1	1.4	1.3	1.2	1.2	1.2	1.2	1.2	1.4	2.0	0.
96.0	0.	0.	0.	0.	0.	0.8	2.5	1.5	1.3	1.2	1.2	1.2	1.2	1.2	1.3	1.7	0.
98.0	0.	0.	0.	0.	0.	0.9	3.8	1.6	1.3	1.2	1.2	1.2	1.2	1.1	1.2	1.3	1.5
100.0	0.	0.	0.	0.	0.	0.9	80.0	1.7	1.4	1.3	1.2	1.2	1.2	1.1	1.1	1.2	1.4
102.0	0.	0.	0.	0.	0.	0.9	1.9	1.4	1.3	1.2	1.2	1.2	1.1	1.1	1.1	1.2	1.7
104.0	0.	0.	0.	0.	0.	0.9	2.2	1.5	1.3	1.2	1.2	1.2	1.1	1.1	1.1	1.2	1.4
106.0	0.	0.	0.	0.	0.	0.9	2.7	1.6	1.3	1.2	1.2	1.1	1.1	1.1	1.1	1.2	1.6
108.0	0.	0.	0.	0.	0.	0.9	4.1	1.7	1.4	1.2	1.2	1.1	1.1	1.1	1.1	1.1	1.3
110.0	0.	0.	0.	0.	0.	0.9	100.0	1.8	1.4	1.3	1.2	1.1	1.1	1.1	1.1	1.1	1.2
112.0	0.	0.	0.	0.	0.	0.9	0.	2.0	1.5	1.3	1.2	1.1	1.1	1.1	1.1	1.1	1.6
114.0	0.	0.	0.	0.	0.	0.9	0.	2.3	1.5	1.3	1.2	1.1	1.1	1.1	1.1	1.1	1.2
116.0	0.	0.	0.	0.	0.	0.9	0.	2.8	1.6	1.3	1.2	1.1	1.1	1.1	1.1	1.0	1.1
118.0	0.	0.	0.	0.	0.	0.9	0.	4.2	1.7	1.4	1.2	1.1	1.1	1.1	1.0	1.0	1.0
120.0	0.	0.	0.	0.	0.	0.9	0.	120.0	1.8	1.4	1.2	1.1	1.1	1.1	1.0	1.0	1.0
122.0	0.	0.	0.	0.	0.	0.9	0.	0.	2.0	1.4	1.2	1.1	1.1	1.0	1.0	1.0	1.0
124.0	0.	0.	0.	0.	0.	0.9	0.	0.	2.3	1.5	1.3	1.2	1.1	1.0	1.0	1.0	1.1
126.0	0.	0.	0.	0.	0.	0.9	0.	0.	2.8	1.5	1.3	1.2	1.1	1.0	1.0	1.0	1.3
128.0	0.	0.	0.	0.	0.	0.9	0.	0.	4.1	1.6	1.3	1.2	1.1	1.0	1.0	1.0	1.8
130.0	0.	0.	0.	0.	0.	0.9	0.	0.	140.0	1.7	1.3	1.2	1.1	1.0	1.0	1.0	1.0
132.0	0.	0.	0.	0.	0.	0.9	0.	0.	0.	1.9	1.4	1.2	1.1	1.0	1.0	1.0	1.2
134.0	0.	0.	0.	0.	0.	0.9	0.	0.	0.	2.2	1.4	1.2	1.1	1.0	1.0	1.0	1.3
136.0	0.	0.	0.	0.	0.	0.9	0.	0.	0.	2.6	1.5	1.2	1.1	1.0	1.0	1.1	1.6
138.0	0.	0.	0.	0.	0.	0.9	0.	0.	0.	3.9	1.5	1.2	1.1	1.0	1.0	1.1	2.3
140.0	0.	0.	0.	0.	0.	0.9	0.	0.	0.	159.9	1.6	1.2	1.1	1.0	1.0	1.0	1.0
142.0	0.	0.	0.	0.	0.	0.9	0.	0.	0.	0.	2.0	1.3	1.1	1.0	1.0	1.0	0.
144.0	0.	0.	0.	0.	0.	0.9	0.	0.	0.	0.	0.	2.0	1.3	1.1	1.0	1.0	0.
146.0	0.	0.	0.	0.	0.	0.9	0.	0.	0.	0.	0.	2.4	1.3	1.1	1.0	1.0	0.
148.0	0.	0.	0.	0.	0.	0.9	0.	0.	0.	0.	0.	3.5	1.4	1.1	1.0	1.0	0.
150.0	0.	0.	0.	0.	0.	0.9	0.	0.	0.	0.	0.	0.	1.8	1.1	1.0	1.0	0.
152.0	0.	0.	0.	0.	0.	0.9	0.	0.	0.	0.	0.	0.	1.5	1.1	1.0	1.0	0.
154.0	0.	0.	0.	0.	0.	0.9	0.	0.	0.	0.	0.	0.	1.7	1.1	1.0	1.0	0.
156.0	0.	0.	0.	0.	0.	0.9	0.	0.	0.	0.	0.	0.	2.0	1.2	1.0	1.0	0.
158.0	0.	0.	0.	0.	0.	0.9	0.	0.	0.	0.	0.	0.	2.9	1.2	1.0	1.0	0.
160.0	0.	0.	0.	0.	0.	0.9	0.	0.	0.	0.	0.	0.	0.	1.2	1.0	1.0	0.
162.0	0.	0.	0.	0.	0.	0.9	0.	0.	0.	0.	0.	0.	0.	1.3	1.0	1.0	0.
164.0	0.	0.	0.	0.	0.	0.9	0.	0.	0.	0.	0.	0.	0.	1.4	1.0	1.0	0.
166.0	0.	0.	0.	0.	0.	0.9	0.	0.	0.	0.	0.	0.	0.	1.6	1.0	1.0	0.
168.0	0.	0.	0.	0.	0.	0.9	0.	0.	0.	0.	0.	0.	0.	2.1	1.0	1.0	0.
170.0	0.	0.															

ETA= 70.0  
BETA

DELTA	10	20	30	40	50	60	70	80	90	100	110	120	130	140	150	160	170	
2.0	0.	0.	0.	0.	0.	0.	1.0	0.	0.	0.	0.	0.	0.	0.	0.	0.	0.	
4.0	0.	0.	0.	0.	0.	0.	1.0	0.	0.	0.	0.	0.	0.	0.	0.	0.	0.	
6.0	0.	0.	0.	0.	0.	0.	1.0	0.	0.	0.	0.	0.	0.	0.	0.	0.	0.	
8.0	0.	0.	0.	0.	0.	0.	1.0	0.	0.	0.	0.	0.	0.	0.	0.	0.	0.	
10.0	0.	0.	0.	0.	0.	0.	4.4	1.0	0.	0.	0.	0.	0.	0.	0.	0.	0.	
12.0	0.	0.	0.	0.	0.	0.	1.6	1.0	1.7	0.	0.	0.	0.	0.	0.	0.	0.	
14.0	0.	0.	0.	0.	0.	0.	1.3	1.0	1.4	0.	0.	0.	0.	0.	0.	0.	0.	
16.0	0.	0.	0.	0.	0.	0.	1.2	1.0	1.3	0.	0.	0.	0.	0.	0.	0.	0.	
18.0	0.	0.	0.	0.	0.	0.	1.1	1.0	1.2	0.	0.	0.	0.	0.	0.	0.	0.	
20.0	0.	0.	0.	0.	0.	0.	5.7	1.1	1.0	1.2	0.	0.	0.	0.	0.	0.	0.	
22.0	0.	0.	0.	0.	0.	0.	2.0	1.1	1.0	1.1	2.2	0.	0.	0.	0.	0.	0.	
24.0	0.	0.	0.	0.	0.	0.	1.6	1.1	1.0	1.1	1.8	0.	0.	0.	0.	0.	0.	
26.0	0.	0.	0.	0.	0.	0.	1.4	1.0	1.0	1.1	1.6	0.	0.	0.	0.	0.	0.	
28.0	0.	0.	0.	0.	0.	0.	1.3	1.0	1.0	1.1	1.4	0.	0.	0.	0.	0.	0.	
30.0	0.	0.	0.	0.	0.	0.	6.3	1.2	1.0	1.0	1.1	1.4	0.	0.	0.	0.	0.	
32.0	0.	0.	0.	0.	0.	0.	2.1	1.1	1.0	1.0	1.1	1.3	2.6	0.	0.	0.	0.	
34.0	0.	0.	0.	0.	0.	0.	1.6	1.1	1.0	1.0	1.1	1.3	2.0	0.	0.	0.	0.	
36.0	0.	0.	0.	0.	0.	0.	1.4	1.1	1.0	1.0	1.1	1.2	1.8	0.	0.	0.	0.	
38.0	0.	0.	0.	0.	0.	0.	1.3	1.1	1.0	1.0	1.1	1.2	1.6	0.	0.	0.	0.	
40.0	0.	0.	0.	0.	0.	0.	6.3	1.2	1.0	1.0	1.1	1.2	1.5	0.	0.	0.	0.	
42.0	0.	0.	0.	0.	0.	0.	2.1	1.7	1.0	1.0	1.1	1.2	1.4	2.9	0.	0.	0.	
44.0	0.	0.	0.	0.	0.	0.	1.6	1.1	1.0	1.0	1.1	1.1	1.4	2.2	0.	0.	0.	
46.0	0.	0.	0.	0.	0.	0.	1.4	1.1	1.0	1.0	1.1	1.1	1.3	1.9	0.	0.	0.	
48.0	0.	0.	0.	0.	0.	0.	1.3	1.1	1.0	1.0	1.1	1.1	1.3	1.7	0.	0.	0.	
50.0	0.	0.	0.	0.	0.	0.	1.2	1.0	1.0	1.0	1.1	1.1	1.2	1.6	0.	0.	0.	
52.0	0.	0.	0.	0.	0.	0.	1.9	1.1	1.0	1.0	1.0	1.0	1.2	1.5	3.0	0.	0.	
54.0	0.	0.	0.	0.	0.	0.	1.5	1.1	1.0	1.0	1.0	1.1	1.2	1.4	2.3	0.	0.	
56.0	0.	0.	0.	0.	0.	0.	1.3	1.1	1.0	1.0	1.0	1.1	1.2	1.4	1.9	0.	0.	
58.0	0.	0.	0.	0.	0.	0.	1.2	1.0	1.0	1.0	1.0	1.1	1.2	1.3	1.7	0.	0.	
60.0	0.	0.	0.	0.	0.	0.	1.1	1.0	1.0	1.0	1.0	1.1	1.2	1.3	1.6	0.	0.	
62.0	0.	0.	0.	0.	0.	0.	1.5	1.0	1.0	1.0	1.0	1.1	1.1	1.2	1.5	2.9	0.	
64.0	0.	0.	0.	0.	0.	0.	1.2	1.0	1.0	1.0	1.0	1.1	1.1	1.2	1.4	2.2	0.	
66.0	0.	0.	0.	0.	0.	0.	1.1	1.0	1.0	1.0	1.0	1.1	1.1	1.2	1.4	1.9	0.	
68.0	0.	0.	0.	0.	0.	0.	1.0	1.0	1.0	1.0	1.1	1.1	1.1	1.2	1.3	1.7	0.	
70.0	0.	0.	0.	0.	0.	0.	1.0	1.0	1.0	1.1	1.1	1.1	1.2	1.3	1.6	0.	0.	
72.0	0.	0.	0.	0.	0.	0.	1.0	1.0	1.0	1.1	1.1	1.1	1.2	1.2	1.5	2.8	0.	
74.0	0.	0.	0.	0.	0.	0.	1.1	1.0	1.0	1.0	1.1	1.1	1.1	1.2	1.4	2.1	0.	
76.0	0.	0.	0.	0.	0.	0.	1.3	1.1	1.0	1.0	1.0	1.1	1.1	1.2	1.3	1.8	0.	
78.0	0.	0.	0.	0.	0.	0.	2.0	1.1	1.0	1.0	1.0	1.1	1.1	1.2	1.3	1.6	0.	
80.0	0.	0.	0.	0.	0.	0.	19.9	1.2	1.1	1.1	1.0	1.1	1.1	1.1	1.2	1.5	0.	
82.0	0.	0.	0.	0.	0.	0.	1.3	1.1	1.1	1.1	1.1	1.1	1.1	1.2	1.4	2.5	0.	
84.0	0.	0.	0.	0.	0.	0.	1.5	1.2	1.1	1.1	1.1	1.1	1.1	1.2	1.3	1.9	0.	
86.0	0.	0.	0.	0.	0.	0.	1.8	1.2	1.1	1.1	1.1	1.1	1.1	1.2	1.3	1.6	0.	
88.0	0.	0.	0.	0.	0.	0.	2.7	1.3	1.2	1.1	1.1	1.1	1.1	1.1	1.2	1.5	0.	
90.0	0.	0.	0.	0.	0.	0.	39.9	1.4	1.2	1.1	1.1	1.1	1.1	1.1	1.1	1.1	0.	
92.0	0.	0.	0.	0.	0.	0.	1.5	1.2	1.1	1.1	1.1	1.1	1.1	1.1	1.1	1.3	2.1	
94.0	0.	0.	0.	0.	0.	0.	1.8	1.3	1.2	1.1	1.1	1.1	1.1	1.1	1.1	1.1	1.6	
96.0	0.	0.	0.	0.	0.	0.	2.2	1.3	1.2	1.1	1.1	1.1	1.1	1.1	1.1	1.1	1.4	
98.0	0.	0.	0.	0.	0.	0.	3.3	1.4	1.2	1.1	1.1	1.1	1.1	1.1	1.1	1.1	1.3	
100.0	0.	0.	0.	0.	0.	0.	60.0	1.5	1.3	1.2	1.1	1.1	1.1	1.0	1.0	1.1	1.5	
102.0	0.	0.	0.	0.	0.	0.	1.7	1.3	1.2	1.1	1.1	1.1	1.0	1.0	1.0	1.1	1.2	
104.0	0.	0.	0.	0.	0.	0.	1.9	1.4	1.2	1.1	1.1	1.1	1.1	1.0	1.0	1.0	1.1	
106.0	0.	0.	0.	0.	0.	0.	2.4	1.4	1.2	1.1	1.1	1.1	1.1	1.0	1.0	1.0	1.1	
108.0	0.	0.	0.	0.	0.	0.	3.6	1.5	1.3	1.2	1.1	1.1	1.1	1.0	1.0	1.0	1.0	
110.0	0.	0.	0.	0.	0.	0.	80.0	1.6	1.3	1.2	1.1	1.1	1.1	1.1	1.1	1.1	1.0	
112.0	0.	0.	0.	0.	0.	0.	1.8	1.3	1.2	1.1	1.1	1.1	1.0	1.0	1.0	1.0	1.0	
114.0	0.	0.	0.	0.	0.	0.	2.1	1.4	1.2	1.1	1.1	1.1	1.0	1.0	1.0	1.0	1.1	
116.0	0.	0.	0.	0.	0.	0.	2.5	1.5	1.2	1.1	1.1	1.1	1.0	1.0	1.0	1.0	1.3	
118.0	0.	0.	0.	0.	0.	0.	3.8	1.5	1.3	1.1	1.1	1.1	1.0	1.0	1.0	1.0	1.1	
120.0	0.	0.	0.	0.	0.	0.	100.0	1.7	1.3	1.2	1.1	1.1	1.0	1.0	1.0	1.0	1.9	
122.0	0.	0.	0.	0.	0.	0.	1.8	1.3	1.2	1.1	1.1	1.1	1.0	1.0	1.0	1.0	1.2	
124.0	0.	0.	0.	0.	0.	0.	2.1	1.4	1.2	1.1	1.1	1.1	1.0	1.0	1.0	1.1	1.4	
126.0	0.	0.	0.	0.	0.	0.	2.5	1.4	1.2	1.1	1.1	1.1	1.0	1.0	1.0	1.1	1.6	
128.0	0.	0.	0.	0.	0.	0.	3.8	1.5	1.2	1.1	1.1	1.1	1.0	1.0	1.0	1.2	2.4	
130.0	0.	0.	0.	0.	0.	0.	120.0	1.6	1.3	1.1	1.1	1.1	1.0	1.0	1.0	1.1	40.0	
132.0	0.	0.	0.	0.	0.	0.	0.	1.8	1.3	1.1	1.1	1.1	1.0	1.0	1.0	1.1	0.	
134.0	0.	0.	0.	0.	0.	0.	2.0	1.3	1.1	1.1	1.0	1.0	1.0	1.0	1.0	1.0	0.	
136.0	0.	0.	0.	0.	0.	0.	2.4	1.4	1.2	1.1	1.0	1.0	1.0	1.0	1.0	1.1	0.	
138.0	0.	0.	0.	0.	0.	0.	3.7	1.6	1.2	1.1	1.0	1.0	1.0	1.0	1.0	1.2	0.	
140.0	0.	0.	0.	0.	0.	0.	140.0	1.5	1.2	1.1	1.0	1.0	1.1	1.1	1.3	60.0	0.	
142.0	0.	0.	0.	0.	0.	0.	0.	1.7	1.2	1.1	1.0	1.0	1.1	1.4	0.	0.	0.	
144.0	0.	0.	0.	0.	0.	0.	0.	1.9	1.2	1.1	1.0	1.0	1.1	1.5	0.	0.	0.	
146.0	0.	0.	0.	0.	0.	0.	0.	2.3	1.3	1.1	1.0	1.0	1.1	1.6	0.	0.	0.	
148.0	0.	0.	0.	0.	0.	0.	0.	0.	3.3	1.3	1.1	1.0	1.0	1.2	2.7	0.	0.	0.
150.0	0.	0.	0.	0.	0.	0.	0.	160.0	1.4	1.1	1.0	1.0	1.0	1.2	80.0	0.	0.	0.
152.0	0.	0.	0.	0.	0.	0.	0.	0.	1.5	1.1	1.0	1.0	1.3	0.	0.	0.	0.	
154.0	0.	0.	0.	0.	0.	0.	0.	0.	1.6	1.1	1.0	1.0	1.4	0.	0.	0.	0.	
156.0	0.	0.	0.	0.	0.	0.	0.	0.	1.9	1.1	1.0	1.1	1.7	0.	0.	0.	0.	
158.0	0.	0.	0.	0.	0.	0.	0.	0.	2.8	1.2	1.0	1.1	2.5	0.	0.	0.	0.	
160.0	0.	0.	0.	0.	0.	0.	0.	0.	179.3	1.2	1.0	1.0	1.1	100.0	0.	0.	0.	0.
162.0	0.	0.	0.	0.	0.	0.	0.	0.	0.	1.2	1.0	1.2	0.	0.	0.	0.	0.	
164.0	0.	0.	0.	0.	0.	0.	0.	0.	0.	1.3	1.0	1.3	0.	0.	0.	0.	0.	
166.0	0.	0.	0.	0.	0.	0.	0.	0.	0.	1.5	1.0	1.4	0.	0.	0.	0.	0.	
168.0	0.	0.	0.	0.	0.	0.	0.	0.	0.	2.1	1.0	2.0	0.	0.	0.	0.	0.	
170.0	0.	0.	0.	0.	0.	0.	0.	0.	0.	0.	1.0	0.	0.	0.	0.	0.	0.	
172.0</																		

ETA= 60.0	BETA	DELTA	10	20	30	40	50	60	70	80	90	100	110	120	130	140	150	160	170
2.0	0.	0.	0.	0.	0.	0.	0.	0.	1.0	0.	0.	0.	0.	0.	0.	0.	0.	0.	0.
4.0	0.	0.	0.	0.	0.	0.	0.	0.	1.0	0.	0.	0.	0.	0.	0.	0.	0.	0.	0.
6.0	0.	0.	0.	0.	0.	0.	0.	0.	1.0	0.	0.	0.	0.	0.	0.	0.	0.	0.	0.
8.0	0.	0.	0.	0.	0.	0.	0.	0.	1.0	0.	0.	0.	0.	0.	0.	0.	0.	0.	0.
10.0	0.	0.	0.	0.	0.	0.	0.	0.	1.0	0.	0.	0.	0.	0.	0.	0.	0.	0.	0.
12.0	0.	0.	0.	0.	0.	0.	0.	0.	1.6	1.0	1.7	0.	0.	0.	0.	0.	0.	0.	0.
14.0	0.	0.	0.	0.	0.	0.	0.	0.	1.3	1.0	1.4	0.	0.	0.	0.	0.	0.	0.	0.
16.0	0.	0.	0.	0.	0.	0.	0.	0.	1.2	1.0	1.3	0.	0.	0.	0.	0.	0.	0.	0.
18.0	0.	0.	0.	0.	0.	0.	0.	0.	1.2	1.0	1.2	0.	0.	0.	0.	0.	0.	0.	0.
20.0	0.	0.	0.	0.	0.	0.	0.	0.	5.9	1.1	1.0	1.2	0.	0.	0.	0.	0.	0.	0.
22.0	0.	0.	0.	0.	0.	0.	0.	0.	2.0	1.1	1.0	1.1	2.2	0.	0.	0.	0.	0.	0.
24.0	0.	0.	0.	0.	0.	0.	0.	0.	1.6	1.1	1.0	1.1	1.7	0.	0.	0.	0.	0.	0.
26.0	0.	0.	0.	0.	0.	0.	0.	0.	1.4	1.1	1.0	1.1	1.5	0.	0.	0.	0.	0.	0.
28.0	0.	0.	0.	0.	0.	0.	0.	0.	1.3	1.0	1.0	1.1	1.4	0.	0.	0.	0.	0.	0.
30.0	0.	0.	0.	0.	0.	0.	0.	0.	6.7	1.2	1.0	1.0	1.1	1.3	0.	0.	0.	0.	0.
32.0	0.	0.	0.	0.	0.	0.	0.	0.	2.3	1.2	1.0	1.0	1.1	1.3	2.5	0.	0.	0.	0.
34.0	0.	0.	0.	0.	0.	0.	0.	0.	1.8	1.1	1.0	1.1	1.2	1.9	0.	0.	0.	0.	0.
36.0	0.	0.	0.	0.	0.	0.	0.	0.	1.5	1.1	1.0	1.0	1.2	1.7	0.	0.	0.	0.	0.
38.0	0.	0.	0.	0.	0.	0.	0.	0.	1.4	1.1	1.0	1.0	1.2	1.5	0.	0.	0.	0.	0.
40.0	0.	0.	0.	0.	0.	0.	0.	0.	7.0	1.3	1.1	1.0	1.0	1.1	1.4	0.	0.	0.	0.
42.0	0.	0.	0.	0.	0.	0.	0.	0.	2.3	1.2	1.1	1.0	1.0	1.1	1.3	2.7	0.	0.	0.
44.0	0.	0.	0.	0.	0.	0.	0.	0.	1.8	1.2	1.0	1.0	1.1	1.3	2.1	0.	0.	0.	0.
46.0	0.	0.	0.	0.	0.	0.	0.	0.	1.5	1.1	1.0	1.0	1.1	1.3	1.8	0.	0.	0.	0.
48.0	0.	0.	0.	0.	0.	0.	0.	0.	1.4	1.1	1.0	1.0	1.0	1.2	1.6	0.	0.	0.	0.
50.0	0.	0.	0.	0.	0.	0.	0.	0.	1.3	1.1	1.0	1.0	1.0	1.2	1.5	0.	0.	0.	0.
52.0	0.	0.	0.	0.	0.	0.	0.	0.	2.2	1.2	1.1	1.0	1.0	1.1	1.2	1.4	2.7	0.	0.
54.0	0.	0.	0.	0.	0.	0.	0.	0.	1.7	1.2	1.1	1.0	1.0	1.1	1.3	2.1	0.	0.	0.
56.0	0.	0.	0.	0.	0.	0.	0.	0.	1.5	1.1	1.0	1.0	1.0	1.1	1.3	1.8	0.	0.	0.
58.0	0.	0.	0.	0.	0.	0.	0.	0.	1.3	1.1	1.0	1.0	1.0	1.1	1.2	1.6	0.	0.	0.
60.0	0.	0.	0.	0.	0.	0.	0.	0.	1.2	1.1	1.0	1.0	1.0	1.1	1.2	1.5	0.	0.	0.
62.0	0.	0.	0.	0.	0.	0.	0.	0.	2.0	1.2	1.1	1.0	1.0	1.0	1.1	1.2	1.4	2.6	0.
64.0	0.	0.	0.	0.	0.	0.	0.	0.	1.5	1.1	1.0	1.0	1.0	1.1	1.2	1.3	2.0	0.	0.
66.0	0.	0.	0.	0.	0.	0.	0.	0.	1.3	1.1	1.0	1.0	1.0	1.1	1.3	1.7	0.	0.	0.
68.0	0.	0.	0.	0.	0.	0.	0.	0.	1.2	1.1	1.0	1.0	1.0	1.1	1.2	1.5	0.	0.	0.
70.0	0.	0.	0.	0.	0.	0.	0.	0.	1.1	1.0	1.0	1.0	1.0	1.1	1.2	1.4	0.	0.	0.
72.0	0.	0.	0.	0.	0.	0.	0.	0.	1.5	1.1	1.0	1.0	1.0	1.1	1.2	1.3	2.4	0.	0.
74.0	0.	0.	0.	0.	0.	0.	0.	0.	1.2	1.0	1.0	1.0	1.0	1.1	1.2	1.3	1.8	0.	0.
76.0	0.	0.	0.	0.	0.	0.	0.	0.	1.1	1.0	1.0	1.0	1.0	1.1	1.2	1.6	0.	0.	0.
78.0	0.	0.	0.	0.	0.	0.	0.	0.	1.0	1.0	1.0	1.0	1.0	1.1	1.2	1.4	0.	0.	0.
80.0	0.	0.	0.	0.	0.	0.	0.	0.	1.0	1.0	1.0	1.0	1.0	1.1	1.2	1.3	0.	0.	0.
82.0	0.	0.	0.	0.	0.	0.	0.	0.	1.0	1.0	1.0	1.0	1.0	1.1	1.2	1.2	2.1	0.	0.
84.0	0.	0.	0.	0.	0.	0.	0.	0.	1.1	1.0	1.0	1.0	1.0	1.1	1.2	1.3	1.6	0.	0.
86.0	0.	0.	0.	0.	0.	0.	0.	0.	1.3	1.1	1.0	1.0	1.0	1.1	1.2	1.4	1.6	0.	0.
88.0	0.	0.	0.	0.	0.	0.	0.	0.	1.9	1.1	1.0	1.0	1.0	1.1	1.2	1.3	1.6	0.	0.
90.0	0.	0.	0.	0.	0.	0.	0.	0.	1.9	1.2	1.1	1.0	1.0	1.1	1.2	1.3	1.5	0.	0.
92.0	0.	0.	0.	0.	0.	0.	0.	0.	1.3	1.1	1.0	1.0	1.0	1.1	1.2	1.3	1.5	0.	0.
94.0	0.	0.	0.	0.	0.	0.	0.	0.	1.5	1.1	1.0	1.0	1.0	1.1	1.2	1.3	1.5	0.	0.
96.0	0.	0.	0.	0.	0.	0.	0.	0.	1.8	1.2	1.1	1.0	1.0	1.1	1.2	1.3	1.6	0.	0.
98.0	0.	0.	0.	0.	0.	0.	0.	0.	2.6	1.3	1.1	1.0	1.0	1.1	1.2	1.3	1.6	0.	0.
100.0	0.	0.	0.	0.	0.	0.	0.	0.	39.9	1.4	1.2	1.1	1.1	1.0	1.0	1.0	1.0	1.0	0.
102.0	0.	0.	0.	0.	0.	0.	0.	0.	0.	1.5	1.2	1.1	1.0	1.0	1.0	1.0	1.0	1.0	0.
104.0	0.	0.	0.	0.	0.	0.	0.	0.	0.	1.7	1.2	1.1	1.0	1.0	1.0	1.0	1.0	1.0	0.
106.0	0.	0.	0.	0.	0.	0.	0.	0.	0.	2.1	1.3	1.1	1.0	1.0	1.0	1.0	1.0	1.0	1.3
108.0	0.	0.	0.	0.	0.	0.	0.	0.	0.	3.1	1.4	1.2	1.1	1.1	1.0	1.0	1.0	1.0	1.9
110.0	0.	0.	0.	0.	0.	0.	0.	0.	60.0	1.5	1.2	1.1	1.1	1.0	1.0	1.0	1.0	1.0	19.9
112.0	0.	0.	0.	0.	0.	0.	0.	0.	0.	1.6	1.2	1.1	1.1	1.0	1.0	1.0	1.0	1.1	1.2
114.0	0.	0.	0.	0.	0.	0.	0.	0.	0.	1.9	1.3	1.1	1.1	1.0	1.0	1.0	1.0	1.1	1.6
116.0	0.	0.	0.	0.	0.	0.	0.	0.	0.	2.3	1.3	1.2	1.1	1.0	1.0	1.0	1.0	1.1	1.7
118.0	0.	0.	0.	0.	0.	0.	0.	0.	0.	3.4	1.4	1.2	1.1	1.0	1.0	1.0	1.0	1.1	2.5
120.0	0.	0.	0.	0.	0.	0.	0.	0.	80.0	1.5	1.2	1.1	1.1	1.0	1.0	1.0	1.0	1.1	40.0
122.0	0.	0.	0.	0.	0.	0.	0.	0.	0.	1.7	1.3	1.1	1.1	1.0	1.0	1.0	1.0	1.1	0.
124.0	0.	0.	0.	0.	0.	0.	0.	0.	0.	1.9	1.3	1.1	1.1	1.0	1.0	1.0	1.0	1.1	0.
126.0	0.	0.	0.	0.	0.	0.	0.	0.	0.	2.3	1.4	1.2	1.1	1.0	1.0	1.0	1.0	1.1	0.
128.0	0.	0.	0.	0.	0.	0.	0.	0.	0.	3.5	1.4	1.2	1.1	1.0	1.0	1.0	1.0	1.1	2.8
130.0	0.	0.	0.	0.	0.	0.	0.	0.	100.0	1.5	1.2	1.1	1.0	1.0	1.0	1.0	1.0	1.1	60.0
132.0	0.	0.	0.	0.	0.	0.	0.	0.	0.	1.7	1.2	1.1	1.1	1.0	1.0	1.0	1.0	1.1	0.
134.0	0.	0.	0.	0.	0.	0.	0.	0.	0.	1.9	1.3	1.1	1.1	1.0	1.0	1.0	1.0	1.2	0.
136.0	0.	0.	0.	0.	0.	0.	0.	0.	0.	2.3	1.3	1.1	1.1	1.0	1.0	1.0	1.1	1.2	0.
138.0	0.	0.	0.	0.	0.	0.	0.	0.	0.	3.4	1.4	1.2	1.1	1.0	1.0	1.0	1.1	1.3	3.0
140.0	0.	0.	0.	0.	0.	0.	0.	0.	0.	0.	0.	0.	0.	0.	0.	0.	0.	0.	0.
142.0	0.	0.	0.	0.	0.	0.	0.	0.	0.	0.	1.6	1.2	1.0	1.0	1.0	1.1	1.4	0.	0.
144.0	0.	0.	0.	0.	0.	0.	0.	0.	0.	1.8	1.2	1.0	1.0	1.0	1.1	1.6	0.	0.	0.
146.0	0.	0.	0.	0.	0.	0.	0.	0.	0.	2.2	1.2	1.1	1.0	1.0	1.2	1.9	0.	0.	0.
148.0	0.	0.	0.	0.	0.	0.	0.	0.	0.	3.2	1.3	1.1	1.0	1.0	1.2	2.9	0.	0.	0.
150.0	0.	0.	0.	0.	0.	0.	0.	0.	0.	0.	0.	0.	0.	0.	0.	0.	0.	0.	0.
152.0	0.	0.	0.	0.	0.	0.	0.	0.	0.	0.	1.4	1.1	1.0	1.0	1.4	0.	0.	0.	0.
154.0	0.	0.	0.	0.	0.	0.	0.	0.	0.	0.	1.6	1.1	1.0	1.1	1.5	0.	0.	0.	0.
156.0	0.	0.	0.	0.	0.	0.	0.	0.	0.	0.	1.9	1.1	1.0	1.1	1.8	0.	0.	0.	0.
158.0	0.	0.	0.	0.	0.	0.	0.	0.	0.	0.	2.7	1.1	1.0	1.1	2.6	0.	0.		

ETA= 90.0  
BETA

DELTA	10	20	30	40	50	60	70	80	90	100	110	120	130	140	150	160	170
2.0	0.	0.	0.	0.	0.	0.	0.	0.	1.0	0.	0.	0.	0.	0.	0.	0.	0.
4.0	0.	0.	0.	0.	0.	0.	0.	0.	1.0	0.	0.	0.	0.	0.	0.	0.	0.
6.0	0.	0.	0.	0.	0.	0.	0.	0.	1.0	0.	0.	0.	0.	0.	0.	0.	0.
8.0	0.	0.	0.	0.	0.	0.	0.	0.	1.0	0.	0.	0.	0.	0.	0.	0.	0.
10.0	0.	0.	0.	0.	0.	0.	0.	0.	4.5	1.0	0.	0.	0.	0.	0.	0.	0.
12.0	0.	0.	0.	0.	0.	0.	0.	0.	1.7	1.0	1.7	0.	0.	0.	0.	0.	0.
14.0	0.	0.	0.	0.	0.	0.	0.	0.	1.4	1.0	1.6	0.	0.	0.	0.	0.	0.
16.0	0.	0.	0.	0.	0.	0.	0.	0.	1.2	1.0	1.2	0.	0.	0.	0.	0.	0.
18.0	0.	0.	0.	0.	0.	0.	0.	0.	1.2	1.0	1.2	0.	0.	0.	0.	0.	0.
20.0	0.	0.	0.	0.	0.	0.	0.	0.	6.1	1.1	1.0	1.1	0.	0.	0.	0.	0.
22.0	0.	0.	0.	0.	0.	0.	0.	0.	2.1	1.1	1.0	1.1	2.1	0.	0.	0.	0.
24.0	0.	0.	0.	0.	0.	0.	0.	0.	1.7	1.1	1.1	1.1	1.7	0.	0.	0.	0.
26.0	0.	0.	0.	0.	0.	0.	0.	0.	1.5	1.1	1.0	1.1	1.5	0.	0.	0.	0.
28.0	0.	0.	0.	0.	0.	0.	0.	0.	1.3	1.1	1.0	1.1	1.3	0.	0.	0.	0.
30.0	0.	0.	0.	0.	0.	0.	0.	0.	7.1	1.3	1.0	1.0	1.0	117.5	0.	0.	0.
32.0	0.	0.	0.	0.	0.	0.	0.	0.	2.4	1.2	1.0	1.0	1.2	2.4	0.	0.	0.
34.0	0.	0.	0.	0.	0.	0.	0.	0.	1.8	1.2	1.0	1.0	1.0	1.8	0.	0.	0.
36.0	0.	0.	0.	0.	0.	0.	0.	0.	1.6	1.1	1.0	1.0	1.1	1.6	0.	0.	0.
38.0	0.	0.	0.	0.	0.	0.	0.	0.	1.5	1.1	1.0	1.0	1.1	1.5	0.	0.	0.
40.0	0.	0.	0.	0.	0.	0.	0.	0.	7.5	1.4	1.1	1.0	1.0	1.4	0.	0.	0.
42.0	0.	0.	0.	0.	0.	0.	0.	0.	2.5	1.3	1.1	1.0	1.1	1.3	2.5	0.	0.
44.0	0.	0.	0.	0.	0.	0.	0.	0.	1.9	1.2	1.1	1.0	1.1	1.7	1.9	0.	0.
46.0	0.	0.	0.	0.	0.	0.	0.	0.	1.7	1.2	1.1	1.0	1.1	1.2	1.7	0.	0.
48.0	0.	0.	0.	0.	0.	0.	0.	0.	1.5	1.2	1.1	1.0	1.1	1.2	1.5	0.	0.
50.0	0.	0.	0.	0.	0.	0.	0.	0.	1.4	1.1	1.0	1.0	1.0	1.1	1.4	0.	0.
52.0	0.	0.	0.	0.	0.	0.	0.	0.	2.5	1.3	1.1	1.0	1.0	1.1	2.5	0.	0.
54.0	0.	0.	0.	0.	0.	0.	0.	0.	1.9	1.2	1.1	1.0	1.0	1.2	1.9	0.	0.
56.0	0.	0.	0.	0.	0.	0.	0.	0.	1.6	1.2	1.1	1.0	1.0	1.2	1.6	0.	0.
58.0	0.	0.	0.	0.	0.	0.	0.	0.	1.5	1.2	1.1	1.0	1.0	1.2	1.5	0.	0.
60.0	0.	0.	0.	0.	0.	0.	0.	0.	1.4	1.1	1.1	1.0	1.0	1.1	1.4	0.	0.
62.0	0.	0.	0.	0.	0.	0.	0.	0.	2.3	1.3	1.1	1.0	1.0	1.1	2.3	0.	0.
64.0	0.	0.	0.	0.	0.	0.	0.	0.	1.8	1.2	1.1	1.0	1.0	1.2	1.8	0.	0.
66.0	0.	0.	0.	0.	0.	0.	0.	0.	1.5	1.2	1.1	1.0	1.0	1.1	1.5	0.	0.
68.0	0.	0.	0.	0.	0.	0.	0.	0.	1.4	1.1	1.1	1.0	1.0	1.1	1.4	0.	0.
70.0	0.	0.	0.	0.	0.	0.	0.	0.	1.3	1.1	1.0	1.0	1.0	1.1	1.3	0.	0.
72.0	0.	0.	0.	0.	0.	0.	0.	0.	2.0	1.2	1.1	1.0	1.0	1.2	2.0	0.	0.
74.0	0.	0.	0.	0.	0.	0.	0.	0.	1.5	1.1	1.1	1.0	1.0	1.1	1.5	0.	0.
76.0	0.	0.	0.	0.	0.	0.	0.	0.	1.3	1.1	1.0	1.0	1.0	1.1	1.3	0.	0.
78.0	0.	0.	0.	0.	0.	0.	0.	0.	1.2	1.1	1.0	1.0	1.0	1.0	1.2	0.	0.
80.0	0.	0.	0.	0.	0.	0.	0.	0.	1.1	1.0	1.0	1.0	1.0	1.0	1.1	0.	0.
82.0	0.	0.	0.	0.	0.	0.	0.	0.	1.5	1.1	1.0	1.0	1.0	1.0	1.5	0.	0.
84.0	0.	0.	0.	0.	0.	0.	0.	0.	1.2	1.0	1.0	1.0	1.0	1.0	1.2	0.	0.
86.0	0.	0.	0.	0.	0.	0.	0.	0.	1.1	1.0	1.0	1.0	1.0	1.0	1.1	0.	0.
88.0	0.	0.	0.	0.	0.	0.	0.	0.	1.0	1.0	1.0	1.0	1.0	1.0	1.0	0.	0.
90.0	0.	0.	0.	0.	0.	0.	0.	0.	1.0	1.0	1.0	1.0	1.0	1.0	1.0	0.	0.
92.0	0.	0.	0.	0.	0.	0.	0.	0.	1.0	1.0	1.0	1.0	1.0	1.0	1.0	0.	0.
94.0	0.	0.	0.	0.	0.	0.	0.	0.	1.0	1.0	1.0	1.0	1.0	1.0	1.0	0.	0.
96.0	0.	0.	0.	0.	0.	0.	0.	0.	1.3	1.1	1.0	1.0	1.0	1.0	1.3	0.	0.
98.0	0.	0.	0.	0.	0.	0.	0.	0.	1.9	1.1	1.0	1.0	1.0	1.0	1.9	0.	0.
100.0	0.	0.	0.	0.	0.	0.	0.	0.	19.9	1.2	1.1	1.0	1.0	1.1	1.2	19.9	0.
102.0	0.	0.	0.	0.	0.	0.	0.	0.	1.3	1.1	1.0	1.0	1.0	1.1	1.3	0.	0.
104.0	0.	0.	0.	0.	0.	0.	0.	0.	1.4	1.1	1.0	1.0	1.0	1.1	1.4	0.	0.
106.0	0.	0.	0.	0.	0.	0.	0.	0.	1.7	1.2	1.1	1.0	1.0	1.2	1.7	0.	0.
108.0	0.	0.	0.	0.	0.	0.	0.	0.	2.6	1.2	1.1	1.0	1.0	1.1	1.2	2.6	0.
110.0	0.	0.	0.	0.	0.	0.	0.	0.	40.0	1.3	1.1	1.0	1.0	1.1	1.3	39.9	0.
112.0	0.	0.	0.	0.	0.	0.	0.	0.	1.4	1.1	1.1	1.0	1.0	1.1	1.4	0.	0.
114.0	0.	0.	0.	0.	0.	0.	0.	0.	1.6	1.2	1.1	1.0	1.0	1.2	1.6	0.	0.
116.0	0.	0.	0.	0.	0.	0.	0.	0.	2.0	1.2	1.1	1.0	1.0	1.2	2.0	0.	0.
118.0	0.	0.	0.	0.	0.	0.	0.	0.	3.0	1.3	1.1	1.0	1.0	1.3	3.0	0.	0.
120.0	0.	0.	0.	0.	0.	0.	0.	0.	60.0	1.4	1.2	1.1	1.0	1.2	1.4	60.0	0.
122.0	0.	0.	0.	0.	0.	0.	0.	0.	1.5	1.2	1.1	1.0	1.0	1.2	1.5	0.	0.
124.0	0.	0.	0.	0.	0.	0.	0.	0.	1.7	1.2	1.1	1.0	1.0	1.2	1.7	0.	0.
126.0	0.	0.	0.	0.	0.	0.	0.	0.	2.1	1.3	1.1	1.0	1.0	1.3	2.1	0.	0.
128.0	0.	0.	0.	0.	0.	0.	0.	0.	3.2	1.3	1.1	1.0	1.0	1.3	3.2	0.	0.
130.0	0.	0.	0.	0.	0.	0.	0.	0.	80.0	1.4	1.1	1.1	1.0	1.1	1.4	80.0	0.
132.0	0.	0.	0.	0.	0.	0.	0.	0.	0.	1.6	1.2	1.1	1.0	1.1	1.6	0.	0.
134.0	0.	0.	0.	0.	0.	0.	0.	0.	1.8	1.2	1.1	1.0	1.1	1.2	1.8	0.	0.
136.0	0.	0.	0.	0.	0.	0.	0.	0.	2.1	1.3	1.1	1.0	1.1	1.3	2.1	0.	0.
138.0	0.	0.	0.	0.	0.	0.	0.	0.	3.2	1.3	1.1	1.0	1.1	1.3	3.2	0.	0.
140.0	0.	0.	0.	0.	0.	0.	0.	0.	100.0	1.4	1.1	1.0	1.0	1.1	1.4	100.0	0.
142.0	0.	0.	0.	0.	0.	0.	0.	0.	0.	1.5	1.1	1.0	1.0	1.5	0.	0.	0.
144.0	0.	0.	0.	0.	0.	0.	0.	0.	1.7	1.2	1.0	1.0	1.2	1.7	0.	0.	0.
146.0	0.	0.	0.	0.	0.	0.	0.	0.	2.0	1.2	1.0	1.0	1.2	2.0	0.	0.	0.
148.0	0.	0.	0.	0.	0.	0.	0.	0.	3.0	1.2	1.0	1.0	1.2	3.0	0.	0.	0.
150.0	0.	0.	0.	0.	0.	0.	0.	0.	120.0	1.3	1.1	1.0	1.1	1.3	120.0	0.	0.
152.0	0.	0.	0.	0.	0.	0.	0.	0.	0.	1.4	1.1	1.0	1.1	1.4	0.	0.	0.
154.0	0.	0.	0.	0.	0.	0.	0.	0.	0.	1.5	1.1	1.0	1.1	1.5	0.	0.	0.
156.0	0.	0.	0.	0.	0.	0.	0.	0.	0.	1.8	1.1	1.0	1.1	1.8	0.	0.	0.
158.0	0.	0.	0.	0.	0.	0.	0.	0.	0.	2.7	1.1	1.0	1.1	2.7	0.	0.	0.
160.0	0.	0.	0.	0.	0.	0.	0.	0.	140.0	1.2	1.0	1.2	1.0	1.2	140.0	0.	0.
162.0	0.	0.	0.	0.	0.	0.	0.	0.	0.	1.2	1.0	1.2	0.	0.	0.	0.	0.
164.0	0.	0.	0.	0.	0.	0.	0.	0.	0.	1.3	1.0	1.3	0.	0.	0.	0.	0.
166.0	0.	0.	0.	0.	0.	0.	0.	0.	0.	1.5	1.0	1.5	0.	0.	0.	0.	0.
168.0	0.	0.	0.	0.	0.	0.	0.	0.	0.	2.0	1.0	2.0	0.	0.	0.	0.	0.
170.0	0.	0.	0.	0.	0.	0.	0.	0.	160.0	1.0	1.0	1.0	0.	0.	0.	0.	0.
172.0	0.	0.	0.	0.	0.	0.	0.	0.	0.	1.0	0.	0.	0.	0.	0.	0.	0.
174.0	0.	0.	0.	0.	0.	0.	0.	0.	0.	1.0	0.	0.	0.	0.	0.	0.	0.
176.0	0.	0.	0.	0.	0.	0.	0.	0.	0.	1.0	0.	0.	0.	0.</td			

ETA=100.0		BETA															
DELTA	10	20	30	40	50	60	70	80	90	100	110	120	130	140	150	160	170
2.0	0.	0.	0.	0.	0.	0.	0.	0.	0.	1.0	0.	0.	0.	0.	0.	0.	0.
4.0	0.	0.	0.	0.	0.	0.	0.	0.	0.	1.0	0.	0.	0.	0.	0.	0.	0.
6.0	0.	0.	0.	0.	0.	0.	0.	0.	0.	1.0	0.	0.	0.	0.	0.	0.	0.
8.0	0.	0.	0.	0.	0.	0.	0.	0.	0.	1.0	0.	0.	0.	0.	0.	0.	0.
10.0	0.	0.	0.	0.	0.	0.	0.	0.	0.	4.6	1.0	0.	0.	0.	0.	0.	0.
12.0	0.	0.	0.	0.	0.	0.	0.	0.	1.7	1.0	1.6	0.	0.	0.	0.	0.	0.
14.0	0.	0.	0.	0.	0.	0.	0.	0.	1.4	1.0	1.3	0.	0.	0.	0.	0.	0.
16.0	0.	0.	0.	0.	0.	0.	0.	0.	1.3	1.0	1.2	0.	0.	0.	0.	0.	0.
18.0	0.	0.	0.	0.	0.	0.	0.	0.	1.2	1.0	1.2	0.	0.	0.	0.	0.	0.
20.0	0.	0.	0.	0.	0.	0.	0.	0.	6.3	1.2	1.0	1.1	119.6	0.	0.	0.	0.
22.0	0.	0.	0.	0.	0.	0.	0.	0.	2.2	1.1	1.0	1.1	2.0	0.	0.	0.	0.
24.0	0.	0.	0.	0.	0.	0.	0.	0.	1.7	1.1	1.0	1.1	1.6	0.	0.	0.	0.
26.0	0.	0.	0.	0.	0.	0.	0.	0.	1.5	1.1	1.0	1.1	1.4	0.	0.	0.	0.
28.0	0.	0.	0.	0.	0.	0.	0.	0.	1.4	1.1	1.0	1.0	1.3	0.	0.	0.	0.
30.0	0.	0.	0.	0.	0.	0.	0.	7.5	1.3	1.1	1.0	1.0	1.2	99.6	0.	0.	0.
32.0	0.	0.	0.	0.	0.	0.	0.	2.5	1.3	1.1	1.0	1.0	1.2	2.3	0.	0.	0.
34.0	0.	0.	0.	0.	0.	0.	0.	1.9	1.2	1.1	1.0	1.0	1.1	1.8	0.	0.	0.
36.0	0.	0.	0.	0.	0.	0.	0.	1.7	1.2	1.0	1.0	1.0	1.1	1.5	0.	0.	0.
38.0	0.	0.	0.	0.	0.	0.	0.	1.5	1.2	1.0	1.0	1.0	1.1	1.4	0.	0.	0.
40.0	0.	0.	0.	0.	0.	0.	0.	8.1	1.6	1.1	1.0	1.0	1.1	1.3	0.	0.	0.
42.0	0.	0.	0.	0.	0.	0.	0.	2.7	1.3	1.1	1.0	1.0	1.1	1.2	2.3	0.	0.
44.0	0.	0.	0.	0.	0.	0.	0.	2.1	1.3	1.1	1.0	1.0	1.0	1.2	1.8	0.	0.
46.0	0.	0.	0.	0.	0.	0.	0.	1.8	1.3	1.1	1.0	1.0	1.0	1.1	1.5	0.	0.
48.0	0.	0.	0.	0.	0.	0.	0.	1.6	1.2	1.1	1.0	1.0	1.0	1.1	1.4	0.	0.
50.0	0.	0.	0.	0.	0.	0.	0.	1.5	1.2	1.1	1.0	1.0	1.0	1.1	1.3	0.	0.
52.0	0.	0.	0.	0.	0.	0.	0.	2.7	1.6	1.2	1.1	1.0	1.0	1.1	1.2	2.2	0.
54.0	0.	0.	0.	0.	0.	0.	0.	2.1	1.3	1.1	1.0	1.0	1.0	1.1	1.2	1.7	0.
56.0	0.	0.	0.	0.	0.	0.	0.	1.8	1.3	1.1	1.0	1.0	1.0	1.1	1.5	0.	0.
58.0	0.	0.	0.	0.	0.	0.	0.	1.6	1.2	1.1	1.0	1.0	1.0	1.1	1.3	0.	0.
60.0	0.	0.	0.	0.	0.	0.	0.	1.5	1.2	1.1	1.0	1.0	1.0	1.1	1.2	0.	0.
62.0	0.	0.	0.	0.	0.	0.	0.	2.6	1.4	1.2	1.1	1.0	1.0	1.0	1.1	1.2	2.0
64.0	0.	0.	0.	0.	0.	0.	0.	2.0	1.3	1.2	1.1	1.0	1.0	1.0	1.1	1.5	0.
66.0	0.	0.	0.	0.	0.	0.	0.	1.7	1.3	1.1	1.1	1.0	1.0	1.0	1.1	1.3	0.
68.0	0.	0.	0.	0.	0.	0.	0.	1.5	1.2	1.1	1.1	1.0	1.0	1.0	1.1	1.2	0.
70.0	0.	0.	0.	0.	0.	0.	0.	1.4	1.2	1.1	1.1	1.0	1.0	1.0	1.0	1.1	0.
72.0	0.	0.	0.	0.	0.	0.	0.	2.4	1.3	1.2	1.1	1.1	1.0	1.0	1.0	1.1	1.5
74.0	0.	0.	0.	0.	0.	0.	0.	1.8	1.3	1.1	1.1	1.0	1.0	1.0	1.0	1.0	1.2
76.0	0.	0.	0.	0.	0.	0.	0.	1.6	1.2	1.1	1.1	1.0	1.0	1.0	1.0	1.0	1.1
78.0	0.	0.	0.	0.	0.	0.	0.	1.4	1.2	1.1	1.1	1.0	1.0	1.0	1.0	1.0	1.0
80.0	0.	0.	0.	0.	0.	0.	0.	1.3	1.1	1.1	1.0	1.0	1.0	1.0	1.0	1.0	1.0
82.0	0.	0.	0.	0.	0.	0.	0.	2.1	1.2	1.1	1.1	1.0	1.0	1.0	1.0	1.0	1.0
84.0	0.	0.	0.	0.	0.	0.	0.	1.6	1.2	1.1	1.1	1.0	1.0	1.0	1.0	1.0	1.1
86.0	0.	0.	0.	0.	0.	0.	0.	1.4	1.1	1.1	1.0	1.0	1.0	1.0	1.0	1.1	1.3
88.0	0.	0.	0.	0.	0.	0.	0.	1.2	1.1	1.0	1.0	1.0	1.0	1.0	1.0	1.1	1.9
90.0	0.	0.	0.	0.	0.	0.	0.	1.1	1.1	1.0	1.0	1.0	1.0	1.0	1.0	1.1	1.2
92.0	1.5	1.1	1.0	1.0	1.0	1.0	1.0	1.0	1.0	1.0	1.0	1.0	1.0	1.1	1.1	1.3	0.
94.0	1.2	1.0	1.0	1.0	1.0	1.0	1.0	1.0	1.0	1.0	1.0	1.0	1.0	1.1	1.1	1.5	0.
96.0	1.1	1.0	1.0	1.0	1.0	1.0	1.0	1.0	1.0	1.0	1.0	1.0	1.0	1.1	1.1	1.8	0.
98.0	1.0	1.0	1.0	1.0	1.0	1.0	1.0	1.0	1.0	1.0	1.0	1.0	1.0	1.1	1.1	2.6	0.
100.0	1.0	1.0	1.0	1.0	1.0	1.0	1.0	1.0	1.0	1.0	1.0	1.0	1.0	1.1	1.2	1.4	39.9
102.0	1.0	1.0	1.0	1.0	1.0	1.0	1.0	1.0	1.0	1.0	1.0	1.0	1.0	1.1	1.2	1.5	0.
104.0	1.1	1.0	1.0	1.0	1.0	1.0	1.0	1.0	1.0	1.0	1.0	1.0	1.0	1.1	1.2	1.7	0.
106.0	1.3	1.0	1.0	1.0	1.0	1.0	1.0	1.0	1.0	1.0	1.0	1.0	1.0	1.1	1.2	2.1	0.
108.0	1.9	1.1	1.0	1.0	1.0	1.0	1.0	1.0	1.0	1.0	1.0	1.0	1.0	1.2	1.4	3.1	0.
110.0	19.9	1.1	1.0	1.0	1.0	1.0	1.0	1.0	1.0	1.0	1.0	1.0	1.0	1.2	1.6	60.0	0.
112.0	0.	1.2	1.1	1.0	1.0	1.0	1.0	1.0	1.0	1.0	1.0	1.0	1.0	1.1	1.2	1.6	0.
114.0	0.	1.4	1.1	1.0	1.0	1.0	1.0	1.0	1.0	1.0	1.0	1.0	1.0	1.1	1.3	1.8	0.
116.0	0.	1.7	1.1	1.0	1.0	1.0	1.0	1.0	1.0	1.0	1.0	1.0	1.0	1.2	1.4	2.3	0.
118.0	0.	2.5	1.2	1.1	1.0	1.0	1.0	1.0	1.0	1.0	1.0	1.0	1.0	1.2	1.4	3.4	0.
120.0	0.	40.0	1.3	1.1	1.0	1.0	1.0	1.0	1.0	1.0	1.0	1.0	1.0	1.1	1.2	1.5	80.0
122.0	0.	0.	1.4	1.1	1.0	1.0	1.0	1.0	1.0	1.0	1.0	1.0	1.0	1.3	1.7	0.	0.
124.0	0.	0.	1.6	1.1	1.0	1.0	1.0	1.0	1.0	1.0	1.0	1.0	1.0	1.3	1.9	0.	0.
126.0	0.	0.	1.9	1.2	1.1	1.0	1.0	1.0	1.0	1.0	1.0	1.0	1.0	1.4	2.3	0.	0.
128.0	0.	0.	2.8	1.3	1.1	1.0	1.0	1.0	1.0	1.0	1.0	1.0	1.0	1.2	1.4	3.5	0.
130.0	0.	0.	60.0	1.3	1.1	1.0	1.0	1.0	1.0	1.0	1.0	1.0	1.0	1.2	1.5	100.0	0.
132.0	0.	0.	0.	1.5	1.1	1.0	1.0	1.0	1.0	1.0	1.0	1.0	1.0	1.2	1.7	0.	0.
134.0	0.	0.	0.	1.6	1.2	1.0	1.0	1.0	1.0	1.0	1.0	1.0	1.0	1.3	1.9	0.	0.
136.0	0.	0.	0.	2.0	1.2	1.1	1.0	1.0	1.0	1.0	1.0	1.0	1.0	1.3	2.3	0.	0.
138.0	0.	0.	0.	3.0	1.3	1.1	1.0	1.0	1.0	1.0	1.0	1.0	1.0	1.4	3.4	0.	0.
140.0	0.	0.	0.	80.0	1.3	1.1	1.0	1.0	1.0	1.0	1.0	1.0	1.0	1.5	120.0	0.	0.
142.0	0.	0.	0.	0.	1.4	1.1	1.0	1.0	1.0	1.0	1.0	1.0	1.0	1.4	0.	0.	0.
144.0	0.	0.	0.	0.	1.6	1.1	1.0	1.0	1.0	1.0	1.0	1.0	1.0	1.5	0.	0.	0.
146.0	0.	0.	0.	0.	1.9	1.2	1.0	1.0	1.0	1.0	1.0	1.0	1.0	1.6	0.	0.	0.
148.0	0.	0.	0.	0.	2.9	1.2	1.0	1.0	1.0	1.0	1.0	1.0	1.0	1.7	0.	0.	0.
150.0	0.	0.	0.	0.	100.0	1.3	1.0	1.0	1.0	1.0	1.0	1.0	1.0	1.3	140.0	0.	0.
152.0	0.	0.	0.	0.	0.	1.4	1.0	1.0	1.0	1.0	1.0	1.0	1.0	1.4	0.	0.	0.
154.0	0.	0.	0.	0.	0.	1.5	1.1	1.0	1.0	1.0	1.0	1.0	1.0	1.6	0.	0.	0.
156.0	0.	0.	0.	0.	0.	1.8	1.1	1.0	1.0	1.0	1.0	1.0	1.0	1.9	0.	0.	0.
158.0	0.	0.	0.	0.	0.	2.6	1.1	1.0	1.0	1.0	1.0	1.0	1.0	2.7	0.	0.	0.
160.0	0.	0.	0.	0.	0.	120.0	1.1	1.0	1.0	1.0	1.0	1.0	1.0	1.2	160.0	0.	0.
162.0	0.	0.	0.	0.	0.	0.	1.2	1.0	1.0	1.0	1.0	1.0	1.0	1.2	0.	0.	0.
164.0	0.	0.	0.	0.	0.	0.	1.3	1.0	1.0	1.0	1.0	1.0					

ETA=110.0

BETA

DELTA	10	20	30	40	50	60	70	80	90	100	110	120	130	140	150	160	170
2.0	0.	0.	0.	0.	0.	0.	0.	0.	0.	1.0	0.	0.	0.	0.	0.	0.	0.
4.0	0.	0.	0.	0.	0.	0.	0.	0.	0.	1.0	0.	0.	0.	0.	0.	0.	0.
6.0	0.	0.	0.	0.	0.	0.	0.	0.	0.	1.0	0.	0.	0.	0.	0.	0.	0.
8.0	0.	0.	0.	0.	0.	0.	0.	0.	0.	1.0	0.	0.	0.	0.	0.	0.	0.
10.0	0.	0.	0.	0.	0.	0.	0.	0.	0.	4.7	1.0	119.8	0.	0.	0.	0.	0.
12.0	0.	0.	0.	0.	0.	0.	0.	0.	0.	1.7	1.0	1.6	0.	0.	0.	0.	0.
14.0	0.	0.	0.	0.	0.	0.	0.	0.	0.	1.4	1.0	1.3	0.	0.	0.	0.	0.
16.0	0.	0.	0.	0.	0.	0.	0.	0.	0.	1.3	1.0	1.2	0.	0.	0.	0.	0.
18.0	0.	0.	0.	0.	0.	0.	0.	0.	0.	1.2	1.0	1.1	0.	0.	0.	0.	0.
20.0	0.	0.	0.	0.	0.	0.	0.	0.	0.	6.5	1.2	1.0	1.1	99.7	0.	0.	0.
22.0	0.	0.	0.	0.	0.	0.	0.	0.	0.	2.2	1.1	1.0	1.1	2.0	0.	0.	0.
24.0	0.	0.	0.	0.	0.	0.	0.	0.	0.	1.8	1.1	1.0	1.1	1.6	0.	0.	0.
26.0	0.	0.	0.	0.	0.	0.	0.	0.	0.	1.6	1.1	1.0	1.1	1.4	0.	0.	0.
28.0	0.	0.	0.	0.	0.	0.	0.	0.	0.	1.4	1.1	1.0	1.0	1.3	0.	0.	0.
30.0	0.	0.	0.	0.	0.	0.	0.	0.	0.	7.8	1.4	1.1	1.0	1.2	79.6	0.	0.
32.0	0.	0.	0.	0.	0.	0.	0.	0.	0.	2.6	1.3	1.1	1.0	1.1	2.1	0.	0.
34.0	0.	0.	0.	0.	0.	0.	0.	0.	0.	2.0	1.3	1.1	1.0	1.1	1.6	0.	0.
36.0	0.	0.	0.	0.	0.	0.	0.	0.	0.	1.8	1.2	1.1	1.0	1.1	1.4	0.	0.
38.0	0.	0.	0.	0.	0.	0.	0.	0.	0.	1.6	1.2	1.1	1.0	1.1	1.3	0.	0.
40.0	0.	0.	0.	0.	0.	0.	0.	0.	0.	8.6	1.5	1.2	1.1	1.0	1.0	1.2	0.
42.0	0.	0.	0.	0.	0.	0.	0.	0.	0.	2.9	1.4	1.2	1.1	1.0	1.2	2.1	0.
44.0	0.	0.	0.	0.	0.	0.	0.	0.	0.	2.2	1.4	1.1	1.1	1.0	1.1	1.6	0.
46.0	0.	0.	0.	0.	0.	0.	0.	0.	0.	1.9	1.3	1.1	1.1	1.0	1.1	1.4	0.
48.0	0.	0.	0.	0.	0.	0.	0.	0.	0.	1.7	1.3	1.1	1.1	1.0	1.1	1.3	0.
50.0	0.	0.	0.	0.	0.	0.	0.	0.	0.	1.6	1.2	1.1	1.1	1.0	1.1	1.2	0.
52.0	0.	0.	0.	0.	0.	0.	0.	0.	0.	3.0	1.5	1.2	1.1	1.0	1.0	1.1	1.9
54.0	0.	0.	0.	0.	0.	0.	0.	0.	0.	2.3	1.4	1.2	1.1	1.0	1.0	1.1	1.5
56.0	0.	0.	0.	0.	0.	0.	0.	0.	0.	1.9	1.4	1.2	1.1	1.0	1.0	1.1	1.3
58.0	0.	0.	0.	0.	0.	0.	0.	0.	0.	1.7	1.3	1.2	1.1	1.0	1.0	1.2	0.
60.0	0.	0.	0.	0.	0.	0.	0.	0.	0.	1.6	1.3	1.2	1.1	1.0	1.0	1.1	0.
62.0	0.	0.	0.	0.	0.	0.	0.	0.	0.	2.9	1.5	1.2	1.1	1.0	1.0	1.0	1.5
64.0	0.	0.	0.	0.	0.	0.	0.	0.	0.	2.2	1.4	1.2	1.1	1.0	1.0	1.0	1.2
66.0	0.	0.	0.	0.	0.	0.	0.	0.	0.	1.9	1.4	1.2	1.1	1.0	1.0	1.0	1.1
68.0	0.	0.	0.	0.	0.	0.	0.	0.	0.	1.7	1.3	1.2	1.1	1.0	1.0	1.0	1.0
70.0	0.	0.	0.	0.	0.	0.	0.	0.	0.	1.6	1.3	1.2	1.1	1.0	1.0	1.0	1.0
72.0	0.	0.	0.	0.	0.	0.	0.	0.	0.	2.8	1.5	1.2	1.1	1.0	1.0	1.0	1.0
74.0	0.	0.	0.	0.	0.	0.	0.	0.	0.	2.1	1.4	1.2	1.1	1.0	1.0	1.0	1.1
76.0	0.	0.	0.	0.	0.	0.	0.	0.	0.	1.8	1.3	1.2	1.1	1.0	1.0	1.1	1.3
78.0	0.	0.	0.	0.	0.	0.	0.	0.	0.	1.6	1.3	1.2	1.1	1.0	1.0	1.1	2.0
80.0	0.	0.	0.	0.	0.	0.	0.	0.	0.	1.5	1.2	1.1	1.1	1.0	1.1	1.1	1.9
82.0	0.	0.	0.	0.	0.	0.	0.	0.	0.	2.5	1.4	1.1	1.1	1.0	1.1	1.1	1.3
84.0	0.	0.	0.	0.	0.	0.	0.	0.	0.	1.9	1.2	1.1	1.1	1.0	1.1	1.2	0.
86.0	0.	0.	0.	0.	0.	0.	0.	0.	0.	1.6	1.3	1.2	1.1	1.0	1.1	1.2	1.8
88.0	0.	0.	0.	0.	0.	0.	0.	0.	0.	1.5	1.2	1.1	1.1	1.0	1.1	1.2	0.
90.0	0.	0.	0.	0.	0.	0.	0.	0.	0.	1.3	1.2	1.1	1.1	1.0	1.1	1.2	39.9
92.0	0.	0.	0.	0.	0.	0.	0.	0.	0.	2.1	1.3	1.1	1.1	1.0	1.1	1.1	0.
94.0	0.	0.	0.	0.	0.	0.	0.	0.	0.	1.6	1.2	1.1	1.1	1.0	1.1	1.1	0.
96.0	0.	0.	0.	0.	0.	0.	0.	0.	0.	1.4	1.1	1.1	1.1	1.0	1.1	1.1	0.
98.0	0.	0.	0.	0.	0.	0.	0.	0.	0.	1.3	1.1	1.1	1.1	1.0	1.1	1.2	0.
100.0	0.	0.	0.	0.	0.	0.	0.	0.	0.	1.2	1.0	1.0	1.1	1.0	1.1	1.2	0.
102.0	1.5	0.	0.	0.	0.	0.	0.	0.	0.	1.1	1.0	1.0	1.1	1.0	1.1	1.7	0.
104.0	1.2	0.	0.	0.	0.	0.	0.	0.	0.	1.0	1.0	1.0	1.1	1.0	1.1	1.4	0.
106.0	1.1	0.	0.	0.	0.	0.	0.	0.	0.	1.0	1.0	1.0	1.1	1.0	1.1	2.4	0.
108.0	1.0	0.	0.	0.	0.	0.	0.	0.	0.	1.0	1.0	1.0	1.1	1.0	1.1	3.6	0.
110.0	1.0	0.	0.	0.	0.	0.	0.	0.	0.	1.0	1.0	1.0	1.1	1.0	1.1	1.5	0.
112.0	1.0	0.	0.	0.	0.	0.	0.	0.	0.	1.0	1.0	1.0	1.1	1.0	1.1	1.6	0.
114.0	1.1	0.	0.	0.	0.	0.	0.	0.	0.	1.0	1.0	1.0	1.1	1.0	1.1	1.7	0.
116.0	1.3	0.	0.	0.	0.	0.	0.	0.	0.	1.0	1.0	1.0	1.1	1.0	1.1	2.5	0.
118.0	1.9	0.	0.	0.	0.	0.	0.	0.	0.	1.0	1.0	1.0	1.1	1.0	1.1	3.8	0.
120.0	19.9	0.	0.	0.	0.	0.	0.	0.	0.	1.0	1.0	1.0	1.1	1.0	1.1	40.0	0.
122.0	0.	0.	0.	0.	0.	0.	0.	0.	0.	1.0	1.0	1.0	1.1	1.0	1.1	0.	0.
124.0	0.	1.4	0.	0.	0.	0.	0.	0.	0.	1.0	1.0	1.0	1.1	1.0	1.1	2.1	0.
126.0	0.	1.6	0.	0.	0.	0.	0.	0.	0.	1.0	1.0	1.0	1.1	1.0	1.1	2.5	0.
128.0	0.	2.4	0.	0.	0.	0.	0.	0.	0.	1.0	1.0	1.0	1.1	1.0	1.1	3.8	0.
130.0	0.	40.0	0.	0.	0.	0.	0.	0.	0.	1.0	1.0	1.0	1.1	1.0	1.1	120.0	0.
132.0	0.	0.	1.3	0.	0.	0.	0.	0.	0.	1.0	1.0	1.0	1.1	1.0	1.1	0.	0.
134.0	0.	0.	1.5	0.	0.	0.	0.	0.	0.	1.0	1.0	1.0	1.1	1.0	1.1	2.0	0.
136.0	0.	0.	1.8	0.	0.	0.	0.	0.	0.	1.0	1.0	1.0	1.1	1.0	1.1	2.4	0.
138.0	0.	0.	2.7	0.	0.	0.	0.	0.	0.	1.0	1.0	1.0	1.1	1.0	1.1	3.7	0.
140.0	0.	0.	60.0	0.	0.	0.	0.	0.	0.	1.0	1.0	1.0	1.1	1.0	1.1	140.0	0.
142.0	0.	0.	0.	1.4	0.	0.	0.	0.	0.	1.0	1.0	1.0	1.1	1.0	1.1	0.	0.
144.0	0.	0.	0.	1.5	0.	0.	0.	0.	0.	1.0	1.0	1.0	1.1	1.0	1.1	0.	0.
146.0	0.	0.	0.	1.8	0.	0.	0.	0.	0.	1.0	1.0	1.0	1.1	1.0	1.1	0.	0.
148.0	0.	0.	0.	2.7	0.	0.	0.	0.	0.	1.0	1.0	1.0	1.1	1.0	1.1	0.	0.
150.0	0.	0.	0.	80.0	0.	0.	0.	0.	0.	1.0	1.0	1.0	1.1	1.0	1.1	160.0	0.
152.0	0.	0.	0.	0.	1.3	0.	0.	0.	0.	1.0	1.0	1.0	1.1	1.0	1.1	0.	0.
154.0	0.	0.	0.	0.	1.4	0.	0.	0.	0.	1.0	1.0	1.0	1.1	1.0	1.1	0.	0.
156.0	0.	0.	0.	0.	1.7	0.	0.	0.	0.	1.0	1.0	1.0	1.1	1.0	1.1	0.	0.
158.0	0.	0.	0.	0.	2.5	0.	0.	0.	0.	1.0	1.0	1.0	1.1	1.0	1.1	0.	0.
160.0	0.	0.	0.	0.	100.0	0.	0.	0.	0.	1.0	1.0	1.0	1.1	1.0	1.1	179.2	0.
162.0	0.	0.	0.	0.	0.	1.2	0.	0.	0.	1.0	1.0	1.0	1.1	1.0	1.1	0.	0.
164.0	0.	0.	0.	0.	0.	1.3	0.	0.	0.	1.0	1.0	1.0	1.1	1.0	1.1	0.	0.
166.0	0.	0.	0.	0.	0.	1.4	0.	0.	0.	1.0	1.0	1.0	1.1	1.0	1.1	0.	0.
168.0	0.	0.	0.	0.	0.	2.0	0.	0.	0.	1.0	1.0	1.0	1.1	1.0	1.1	0.	0.
170.0	0.	0.	0.	0.	0.	0.	0.	0.	0.	1.0	0.	0.	0.	0.	0.	0.	0.
172.0	0.	0.	0.	0.	0.	0.	0.	0.	0.	1.0	0.	0.	0.	0.	0.	0.	0.
174.0	0.	0.	0.	0.	0.	0.	0.	0.	0.	1.0	0.	0.	0.	0.	0.	0.	0.
176.0	0.	0.	0.	0.													

ETA=120.0	BETA	10	20	30	40	50	60	70	80	90	100	110	120	130	140	150	160	170		
2.0	0.	0.	0.	0.	0.	0.	0.	0.	0.	0.	0.	1.0	0.	0.	0.	0.	0.	0.		
4.0	0.	0.	0.	0.	0.	0.	0.	0.	0.	0.	0.	1.0	0.	0.	0.	0.	0.	0.		
6.0	0.	0.	0.	0.	0.	0.	0.	0.	0.	0.	0.	1.0	0.	0.	0.	0.	0.	0.		
8.0	0.	0.	0.	0.	0.	0.	0.	0.	0.	0.	0.	1.0	0.	0.	0.	0.	0.	0.		
10.0	0.	0.	0.	0.	0.	0.	0.	0.	0.	0.	0.	139.7	1.0	99.8	0.	0.	0.	0.		
12.0	0.	0.	0.	0.	0.	0.	0.	0.	0.	0.	0.	1.7	1.0	1.6	0.	0.	0.	0.		
14.0	0.	0.	0.	0.	0.	0.	0.	0.	0.	0.	0.	1.4	1.0	1.3	0.	0.	0.	0.		
16.0	0.	0.	0.	0.	0.	0.	0.	0.	0.	0.	0.	1.3	1.0	1.2	0.	0.	0.	0.		
18.0	0.	0.	0.	0.	0.	0.	0.	0.	0.	0.	0.	1.2	1.0	1.1	0.	0.	0.	0.		
20.0	0.	0.	0.	0.	0.	0.	0.	0.	0.	0.	0.	158.9	1.2	1.0	1.1	79.7	0.	0.	0.	
22.0	0.	0.	0.	0.	0.	0.	0.	0.	0.	0.	0.	2.3	1.2	1.0	1.1	1.9	0.	0.	0.	
24.0	0.	0.	0.	0.	0.	0.	0.	0.	0.	0.	0.	1.8	1.1	1.0	1.0	1.5	0.	0.	0.	
26.0	0.	0.	0.	0.	0.	0.	0.	0.	0.	0.	0.	1.6	1.1	1.0	1.0	1.3	0.	0.	0.	
28.0	0.	0.	0.	0.	0.	0.	0.	0.	0.	0.	0.	1.5	1.1	1.0	1.0	1.2	0.	0.	0.	
30.0	0.	0.	0.	0.	0.	0.	0.	0.	0.	0.	0.	8.2	1.4	1.1	1.0	1.0	1.1	59.7	0.	0.
32.0	0.	0.	0.	0.	0.	0.	0.	0.	0.	0.	0.	2.7	1.3	1.1	1.0	1.0	1.1	2.0	0.	0.
34.0	0.	0.	0.	0.	0.	0.	0.	0.	0.	0.	0.	2.1	1.3	1.1	1.0	1.0	1.1	1.5	0.	0.
36.0	0.	0.	0.	0.	0.	0.	0.	0.	0.	0.	0.	1.8	1.3	1.1	1.0	1.0	1.0	1.3	0.	0.
38.0	0.	0.	0.	0.	0.	0.	0.	0.	0.	0.	0.	1.7	1.2	1.1	1.0	1.0	1.0	1.2	0.	0.
40.0	0.	0.	0.	0.	0.	0.	0.	0.	0.	0.	0.	9.2	1.6	1.2	1.1	1.0	1.0	1.1	0.	0.
42.0	0.	0.	0.	0.	0.	0.	0.	0.	0.	0.	0.	3.0	1.5	1.2	1.1	1.0	1.0	1.1	1.8	0.
44.0	0.	0.	0.	0.	0.	0.	0.	0.	0.	0.	0.	2.3	1.4	1.2	1.1	1.0	1.0	1.1	1.4	0.
46.0	0.	0.	0.	0.	0.	0.	0.	0.	0.	0.	0.	2.0	1.4	1.2	1.1	1.0	1.0	1.0	1.2	0.
48.0	0.	0.	0.	0.	0.	0.	0.	0.	0.	0.	0.	1.8	1.3	1.2	1.1	1.0	1.0	1.0	1.1	0.
50.0	0.	0.	0.	0.	0.	0.	0.	0.	0.	0.	0.	1.7	1.3	1.2	1.1	1.0	1.0	1.0	1.1	0.
52.0	0.	0.	0.	0.	0.	0.	0.	0.	0.	0.	0.	3.2	1.6	1.3	1.2	1.1	1.0	1.0	1.0	1.5
54.0	0.	0.	0.	0.	0.	0.	0.	0.	0.	0.	0.	2.5	1.5	1.3	1.2	1.1	1.0	1.0	1.0	1.2
56.0	0.	0.	0.	0.	0.	0.	0.	0.	0.	0.	0.	2.1	1.5	1.2	1.1	1.1	1.0	1.0	1.0	1.0
58.0	0.	0.	0.	0.	0.	0.	0.	0.	0.	0.	0.	1.9	1.4	1.2	1.1	1.1	1.0	1.0	1.0	1.0
60.0	0.	0.	0.	0.	0.	0.	0.	0.	0.	0.	0.	1.7	1.4	1.2	1.1	1.1	1.0	1.0	1.0	1.0
62.0	0.	0.	0.	0.	0.	0.	0.	0.	0.	0.	0.	3.3	1.6	1.3	1.2	1.1	1.0	1.0	1.0	1.0
64.0	0.	0.	0.	0.	0.	0.	0.	0.	0.	0.	0.	2.5	1.5	1.3	1.2	1.1	1.1	1.0	1.1	1.1
66.0	0.	0.	0.	0.	0.	0.	0.	0.	0.	0.	0.	2.1	1.5	1.3	1.2	1.1	1.1	1.1	1.1	1.6
68.0	0.	0.	0.	0.	0.	0.	0.	0.	0.	0.	0.	1.9	1.4	1.3	1.2	1.1	1.1	1.1	1.1	2.0
70.0	0.	0.	0.	0.	0.	0.	0.	0.	0.	0.	0.	1.7	1.4	1.3	1.2	1.1	1.1	1.1	1.2	1.9
72.0	0.	0.	0.	0.	0.	0.	0.	0.	0.	0.	0.	3.2	1.6	1.4	1.2	1.1	1.1	1.1	1.2	1.3
74.0	0.	0.	0.	0.	0.	0.	0.	0.	0.	0.	0.	2.4	1.5	1.3	1.2	1.1	1.1	1.1	1.2	1.5
76.0	0.	0.	0.	0.	0.	0.	0.	0.	0.	0.	0.	2.0	1.5	1.3	1.2	1.1	1.1	1.1	1.2	1.9
78.0	0.	0.	0.	0.	0.	0.	0.	0.	0.	0.	0.	1.8	1.4	1.3	1.2	1.1	1.1	1.2	1.3	2.8
80.0	0.	0.	0.	0.	0.	0.	0.	0.	0.	0.	0.	1.7	1.4	1.3	1.2	1.1	1.1	1.2	1.5	39.9
82.0	0.	0.	0.	0.	0.	0.	0.	0.	0.	0.	0.	3.0	1.6	1.3	1.2	1.1	1.1	1.2	1.3	0.
84.0	0.	0.	0.	0.	0.	0.	0.	0.	0.	0.	0.	2.3	1.5	1.3	1.2	1.1	1.2	1.3	1.8	0.
86.0	0.	0.	0.	0.	0.	0.	0.	0.	0.	0.	0.	1.9	1.4	1.3	1.2	1.2	1.2	1.3	2.3	0.
88.0	0.	0.	0.	0.	0.	0.	0.	0.	0.	0.	0.	1.7	1.4	1.2	1.2	1.2	1.2	1.3	3.4	0.
90.0	0.	0.	0.	0.	0.	0.	0.	0.	0.	0.	0.	1.6	1.3	1.2	1.2	1.2	1.2	1.3	59.9	0.
92.0	0.	0.	0.	0.	0.	0.	0.	0.	0.	0.	0.	2.6	1.5	1.3	1.2	1.1	1.1	1.2	1.3	0.
94.0	0.	0.	0.	0.	0.	0.	0.	0.	0.	0.	0.	2.0	1.4	1.2	1.2	1.2	1.2	1.3	2.1	0.
96.0	0.	0.	0.	0.	0.	0.	0.	0.	0.	0.	0.	1.7	1.3	1.2	1.2	1.2	1.3	2.5	0.	0.
98.0	0.	0.	0.	0.	0.	0.	0.	0.	0.	0.	0.	1.5	1.3	1.2	1.2	1.2	1.3	3.8	0.	0.
100.0	0.	0.	0.	0.	0.	0.	0.	0.	0.	0.	0.	1.4	1.2	1.1	1.1	1.1	1.1	1.2	1.3	0.
102.0	0.	0.	0.	0.	0.	0.	0.	0.	0.	0.	0.	2.2	1.3	1.2	1.1	1.1	1.1	1.2	1.3	0.
104.0	0.	0.	0.	0.	0.	0.	0.	0.	0.	0.	0.	1.7	1.2	1.1	1.1	1.1	1.1	1.2	1.3	0.
106.0	0.	0.	0.	0.	0.	0.	0.	0.	0.	0.	0.	1.4	1.1	1.0	1.2	1.3	1.6	2.7	0.	0.
108.0	0.	0.	0.	0.	0.	0.	0.	0.	0.	0.	0.	1.3	1.1	1.0	1.2	1.4	1.7	4.1	0.	0.
110.0	0.	0.	0.	0.	0.	0.	0.	0.	0.	0.	0.	1.2	1.1	1.0	1.2	1.3	1.8	100.0	0.	0.
112.0	1.6	0.	0.	0.	0.	0.	0.	0.	0.	0.	0.	1.1	1.0	1.2	1.3	1.5	2.0	0.	0.	0.
114.0	1.2	0.	0.	0.	0.	0.	0.	0.	0.	0.	0.	1.1	1.0	1.2	1.3	1.5	2.3	0.	0.	0.
116.0	1.1	0.	0.	0.	0.	0.	0.	0.	0.	0.	0.	1.1	1.0	1.2	1.3	1.6	2.8	0.	0.	0.
118.0	1.0	0.	0.	0.	0.	0.	0.	0.	0.	0.	0.	1.0	1.1	1.2	1.3	1.7	4.2	0.	0.	0.
120.0	1.0	0.	0.	0.	0.	0.	0.	0.	0.	0.	0.	1.0	1.1	1.2	1.3	1.8	120.0	0.	0.	0.
122.0	1.0	0.	0.	0.	0.	0.	0.	0.	0.	0.	0.	1.0	1.1	1.2	1.3	2.0	0.	0.	0.	
124.0	1.1	0.	0.	0.	0.	0.	0.	0.	0.	0.	0.	1.0	1.1	1.2	1.3	1.5	2.3	0.	0.	0.
126.0	1.3	0.	0.	0.	0.	0.	0.	0.	0.	0.	0.	1.0	1.1	1.2	1.3	1.5	2.8	0.	0.	0.
128.0	1.8	0.	0.	0.	0.	0.	0.	0.	0.	0.	0.	1.0	1.1	1.2	1.3	1.6	4.1	0.	0.	0.
130.0	19.9	1.1	0.	0.	0.	0.	0.	0.	0.	0.	0.	1.0	1.1	1.2	1.3	1.7	140.0	0.	0.	0.
132.0	1.2	1.0	0.	0.	0.	0.	0.	0.	0.	0.	0.	1.0	1.1	1.2	1.4	1.9	0.	0.	0.	0.
134.0	0.	1.3	1.0	0.	0.	0.	0.	0.	0.	0.	0.	1.0	1.1	1.2	1.4	2.2	0.	0.	0.	0.
136.0	0.	1.6	1.1	1.0	0.	0.	0.	0.	0.	0.	0.	1.0	1.1	1.2	1.5	2.6	0.	0.	0.	0.
138.0	0.	2.3	1.1	1.0	0.	0.	0.	0.	0.	0.	0.	1.0	1.1	1.2	1.5	3.9	0.	0.	0.	0.
140.0	0.	40.0	1.2	1.0	0.	0.	0.	0.	0.	0.	0.	1.0	1.1	1.2	1.6	159.9	0.	0.	0.	0.
142.0	0.	1.3	1.0	0.	0.	0.	0.	0.	0.	0.	0.	1.1	1.3	2.0	0.	0.	0.	0.	0.	
144.0	0.	1.4	1.1	1.0	0.	0.	0.	0.	0.	0.	0.	1.1	1.3	2.0	0.	0.	0.	0.	0.	
146.0	0.	1.7	1.1	1.0	0.	0.	0.	0.	0.	0.	0.	1.1	1.3	2.4	0.	0.	0.	0.	0.	
148.0	0.	2.5	1.1	1.0	0.	0.	0.	0.	0.	0.	0.	1.1	1.4	3.5	0.	0.	0.	0.	0.	
150.0	0.	60.0	1.2	1.0	0.	0.	0.	0.	0.	0.	0.	1.1	1.4	178.7	0.	0.	0.	0.	0.	
152.0	0.	0.	1.3	1.0	0.	0.	0.	0.	0.	0.	0.	1.1	1.5	0.	0.	0.	0.	0.		
154.0	0.	0.	1.4	1.0	0.	0.	0.	0.	0.	0.	0.	1.1	1.7	0.	0.	0.	0.	0.		
156.0	0.	0.	1.6	1.0	0.	0.	0.	0.	0.	0.	0.	1.2	2.0	0.	0.	0.	0.	0.		
158.0	0.	0.	2.4	1.1	1.0	0.	0.	0.	0.	0.	0.	1.2	2.9	0.	0.	0.	0.	0.		
160.0	0.	0.	80.0	1.1	1.0	0.	0.	0.	0.	0.	0.	1.0	1.2	160.0	0.	0.	0.	0.	0.	
162.0	0.	0.	0.	1.1	1.0	0.	0.	0.	0.	0.	0.	1.3	0.	0.	0.	0.	0.	0.		
164.0	0.	0.	0.	1.2	1.0	0.	0.	0.	0.	0.	0.	1.4	0.	0.	0.	0.	0.	0.		
166.0	0.	0.	0.	1.4	1.0	0.	0.	0.												

ETA=130.0	BETA	10	20	30	40	50	60	70	80	90	100	110	120	130	140	150	160	170
2.0	0.	0.	0.	0.	0.	0.	0.	0.	0.	0.	0.	0.	1.0	0.	0.	0.	0.	0.
4.0	0.	0.	0.	0.	0.	0.	0.	0.	0.	0.	0.	0.	1.0	0.	0.	0.	0.	0.
6.0	0.	0.	0.	0.	0.	0.	0.	0.	0.	0.	0.	0.	1.0	0.	0.	0.	0.	0.
8.0	0.	0.	0.	0.	0.	0.	0.	0.	0.	0.	0.	0.	1.0	0.	0.	0.	0.	0.
10.0	0.	0.	0.	0.	0.	0.	0.	0.	0.	0.	0.	0.	119.8	1.0	79.8	0.	0.	0.
12.0	0.	0.	0.	0.	0.	0.	0.	0.	0.	0.	0.	0.	1.8	1.0	1.5	0.	0.	0.
14.0	0.	0.	0.	0.	0.	0.	0.	0.	0.	0.	0.	0.	1.5	1.0	1.3	0.	0.	0.
16.0	0.	0.	0.	0.	0.	0.	0.	0.	0.	0.	0.	0.	1.3	1.0	1.2	0.	0.	0.
18.0	0.	0.	0.	0.	0.	0.	0.	0.	0.	0.	0.	0.	1.3	1.0	1.1	0.	0.	0.
20.0	0.	0.	0.	0.	0.	0.	0.	0.	0.	0.	0.	0.	7.0	1.2	1.0	1.1	59.7	0.
22.0	0.	0.	0.	0.	0.	0.	0.	0.	0.	0.	0.	0.	2.4	1.2	1.0	1.0	1.8	0.
24.0	0.	0.	0.	0.	0.	0.	0.	0.	0.	0.	0.	0.	1.9	1.2	1.0	1.0	1.4	0.
26.0	0.	0.	0.	0.	0.	0.	0.	0.	0.	0.	0.	0.	1.7	1.2	1.0	1.0	1.2	0.
28.0	0.	0.	0.	0.	0.	0.	0.	0.	0.	0.	0.	0.	1.5	1.1	1.0	1.0	1.2	0.
30.0	0.	0.	0.	0.	0.	0.	0.	0.	0.	0.	0.	0.	8.7	1.5	1.1	1.0	1.0	39.6
32.0	0.	0.	0.	0.	0.	0.	0.	0.	0.	0.	0.	0.	2.9	1.4	1.1	1.0	1.1	1.7
34.0	0.	0.	0.	0.	0.	0.	0.	0.	0.	0.	0.	0.	2.3	1.4	1.1	1.0	1.0	1.6
36.0	0.	0.	0.	0.	0.	0.	0.	0.	0.	0.	0.	0.	2.0	1.3	1.1	1.0	1.0	1.6
38.0	0.	0.	0.	0.	0.	0.	0.	0.	0.	0.	0.	0.	1.8	1.3	1.1	1.0	1.0	1.6
40.0	0.	0.	0.	0.	0.	0.	0.	0.	0.	0.	0.	0.	9.9	1.7	1.3	1.1	1.0	1.6
42.0	0.	0.	0.	0.	0.	0.	0.	0.	0.	0.	0.	0.	3.3	1.6	1.3	1.1	1.0	1.4
44.0	0.	0.	0.	0.	0.	0.	0.	0.	0.	0.	0.	0.	2.5	1.5	1.3	1.1	1.0	1.4
46.0	0.	0.	0.	0.	0.	0.	0.	0.	0.	0.	0.	0.	2.2	1.5	1.2	1.1	1.0	1.0
48.0	0.	0.	0.	0.	0.	0.	0.	0.	0.	0.	0.	0.	1.9	1.4	1.2	1.1	1.0	1.0
50.0	0.	0.	0.	0.	0.	0.	0.	0.	0.	0.	0.	0.	1.8	1.4	1.2	1.1	1.0	1.0
52.0	0.	0.	0.	0.	0.	0.	0.	0.	0.	0.	0.	0.	3.5	1.7	1.4	1.2	1.1	1.1
54.0	0.	0.	0.	0.	0.	0.	0.	0.	0.	0.	0.	0.	2.7	1.6	1.4	1.2	1.1	1.2
56.0	0.	0.	0.	0.	0.	0.	0.	0.	0.	0.	0.	0.	2.3	1.6	1.3	1.2	1.1	1.4
58.0	0.	0.	0.	0.	0.	0.	0.	0.	0.	0.	0.	0.	2.1	1.5	1.3	1.2	1.1	1.2
60.0	0.	0.	0.	0.	0.	0.	0.	0.	0.	0.	0.	0.	1.9	1.5	1.3	1.2	1.1	1.3
62.0	0.	0.	0.	0.	0.	0.	0.	0.	0.	0.	0.	0.	3.6	1.8	1.5	1.3	1.2	1.4
64.0	0.	0.	0.	0.	0.	0.	0.	0.	0.	0.	0.	0.	2.8	1.7	1.4	1.3	1.2	1.6
66.0	0.	0.	0.	0.	0.	0.	0.	0.	0.	0.	0.	0.	2.3	1.6	1.4	1.3	1.2	1.6
68.0	0.	0.	0.	0.	0.	0.	0.	0.	0.	0.	0.	0.	2.1	1.6	1.4	1.3	1.2	1.4
70.0	0.	0.	0.	0.	0.	0.	0.	0.	0.	0.	0.	0.	1.9	1.5	1.4	1.3	1.2	1.3
72.0	0.	0.	0.	0.	0.	0.	0.	0.	0.	0.	0.	0.	3.6	1.8	1.5	1.4	1.3	1.7
74.0	0.	0.	0.	0.	0.	0.	0.	0.	0.	0.	0.	0.	2.7	1.7	1.5	1.3	1.3	1.9
76.0	0.	0.	0.	0.	0.	0.	0.	0.	0.	0.	0.	0.	2.3	1.6	1.4	1.3	1.3	2.4
78.0	0.	0.	0.	0.	0.	0.	0.	0.	0.	0.	0.	0.	2.1	1.6	1.4	1.3	1.4	3.6
80.0	0.	0.	0.	0.	0.	0.	0.	0.	0.	0.	0.	0.	1.9	1.5	1.3	1.3	1.4	59.9
82.0	0.	0.	0.	0.	0.	0.	0.	0.	0.	0.	0.	0.	3.5	1.8	1.5	1.3	1.4	0.
84.0	0.	0.	0.	0.	0.	0.	0.	0.	0.	0.	0.	0.	2.6	1.7	1.4	1.3	1.5	0.
86.0	0.	0.	0.	0.	0.	0.	0.	0.	0.	0.	0.	0.	2.7	1.6	1.4	1.3	1.6	0.
88.0	0.	0.	0.	0.	0.	0.	0.	0.	0.	0.	0.	0.	2.0	1.5	1.3	1.3	1.4	0.
90.0	0.	0.	0.	0.	0.	0.	0.	0.	0.	0.	0.	0.	1.8	1.5	1.3	1.3	1.4	0.
92.0	0.	0.	0.	0.	0.	0.	0.	0.	0.	0.	0.	0.	3.2	1.7	1.4	1.3	1.4	0.
94.0	0.	0.	0.	0.	0.	0.	0.	0.	0.	0.	0.	0.	2.4	1.6	1.3	1.3	1.4	0.
96.0	0.	0.	0.	0.	0.	0.	0.	0.	0.	0.	0.	0.	2.0	1.5	1.4	1.3	1.4	0.
98.0	0.	0.	0.	0.	0.	0.	0.	0.	0.	0.	0.	0.	1.8	1.4	1.3	1.3	1.4	0.
100.0	0.	0.	0.	0.	0.	0.	0.	0.	0.	0.	0.	0.	1.7	1.4	1.3	1.3	1.4	0.
102.0	0.	0.	0.	0.	0.	0.	0.	0.	0.	0.	0.	0.	2.8	1.5	1.3	1.3	1.4	0.
104.0	0.	0.	0.	0.	0.	0.	0.	0.	0.	0.	0.	0.	2.1	1.5	1.3	1.3	1.4	0.
106.0	0.	0.	0.	0.	0.	0.	0.	0.	0.	0.	0.	0.	1.8	1.4	1.3	1.3	1.4	0.
108.0	0.	0.	0.	0.	0.	0.	0.	0.	0.	0.	0.	0.	1.6	1.4	1.3	1.3	1.4	0.
110.0	0.	0.	0.	0.	0.	0.	0.	0.	0.	0.	0.	0.	1.5	1.3	1.2	1.2	1.3	0.
112.0	0.	0.	0.	0.	0.	0.	0.	0.	0.	0.	0.	0.	2.3	1.4	1.2	1.2	1.3	0.
114.0	0.	0.	0.	0.	0.	0.	0.	0.	0.	0.	0.	0.	1.7	1.3	1.2	1.2	1.3	0.
116.0	0.	0.	0.	0.	0.	0.	0.	0.	0.	0.	0.	0.	1.5	1.2	1.2	1.2	1.3	0.
118.0	0.	0.	0.	0.	0.	0.	0.	0.	0.	0.	0.	0.	1.3	1.2	1.1	1.1	1.2	0.
120.0	0.	0.	0.	0.	0.	0.	0.	0.	0.	0.	0.	0.	1.2	1.0	0.9	0.9	1.0	0.
122.0	1.6	1.1	1.1	1.1	1.1	1.1	1.1	1.2	1.2	1.2	1.2	1.2	1.0	2.0	1.5	1.4	1.5	0.
124.0	1.2	1.1	1.1	1.1	1.1	1.1	1.1	1.2	1.2	1.2	1.2	1.2	1.3	1.6	2.2	2.0	2.1	0.
126.0	1.1	1.1	1.1	1.1	1.1	1.1	1.1	1.2	1.2	1.2	1.2	1.2	1.4	1.7	3.0	2.8	2.9	0.
128.0	1.0	1.0	1.0	1.0	1.0	1.0	1.0	1.1	1.1	1.1	1.1	1.1	1.2	1.4	1.8	4.5	4.5	0.
130.0	1.0	1.0	1.0	1.0	1.0	1.0	1.0	1.1	1.1	1.1	1.1	1.1	1.2	1.4	1.9	159.9	0.	0.
132.0	1.0	1.0	1.0	1.0	1.0	1.0	1.0	1.1	1.1	1.1	1.1	1.1	1.2	1.4	2.0	0.	0.	0.
134.0	1.1	1.0	1.0	1.0	1.0	1.0	1.0	1.1	1.1	1.1	1.1	1.1	1.3	1.5	2.3	0.	0.	0.
136.0	1.3	1.0	1.0	1.0	1.0	1.0	1.0	1.1	1.1	1.1	1.1	1.1	1.3	1.5	2.8	0.	0.	0.
138.0	1.8	1.0	1.0	1.0	1.0	1.0	1.0	1.1	1.1	1.1	1.1	1.1	1.6	4.2	0.	0.	0.	0.
140.0	19.9	1.1	1.0	1.0	1.0	1.0	1.0	1.1	1.1	1.1	1.1	1.1	1.7	178.2	0.	0.	0.	0.
142.0	0.	1.2	1.0	1.0	1.0	1.0	1.0	1.1	1.1	1.1	1.1	1.1	1.9	0.	0.	0.	0.	0.
144.0	0.	1.3	1.0	1.0	1.0	1.0	1.0	1.1	1.1	1.1	1.1	1.1	2.1	0.	0.	0.	0.	0.
146.0	0.	1.5	1.0	1.0	1.0	1.0	1.0	1.1	1.1	1.1	1.1	1.1	2.5	0.	0.	0.	0.	0.
148.0	0.	2.2	1.1	1.0	1.0	1.0	1.0	1.1	1.1	1.1	1.1	1.1	3.7	0.	0.	0.	0.	0.
150.0	0.	40.0	1.1	1.0	1.0	1.0	1.0	1.1	1.1	1.1	1.1	1.1	159.9	0.	0.	0.	0.	0.
152.0	0.	1.2	1.0	1.0	1.0	1.0	1.0	1.2	1.2	1.2	1.2	1.2	0.	0.	0.	0.	0.	0.
154.0	0.	1.3	1.0	1.0	1.0	1.0	1.0	1.2	1.2	1.2	1.2	1.2	0.	0.	0.	0.	0.	0.
156.0	0.	1.5	1.0	1.0	1.0	1.0	1.0	1.2	1.2	1.2	1.2	1.2	0.	0.	0.	0.	0.	0.
158.0	0.	2.7	1.0	1.0	1.0	1.0	1.0	1.2	1.2	1.2	1.2	1.2	0.	0.	0.	0.	0.	0.
160.0	0.	60.0	1.1	1.0	1.0	1.0	1.0	1.2	1.2	1.2	1.2	1.2	0.	0.	0.	0.	0.	0.
162.0	0.	0.	1.1	1.0	1.0	1.0	1.0	1.3	0.	0.	0.	0.	0.	0.	0.	0.	0.	0.
164.0	0.	0.	1.2	1.0	1.0	1.0	1.0	1.4	0.	0.	0.	0.	0.	0.	0.	0.	0.	0.
166.0	0.	0.	1.4	1.0	1.0	1.0	1.0	1.6	0.	0.	0.	0.	0.	0.	0.	0.	0.	0.
168.0	0.	0.	1.9	1.0	1.0	1.0	1.0	2.2	0.	0.	0.	0.	0.	0.	0.	0.	0.	0.
170.0	0.	0.	0.	80.0	1.0	1.0	1.0	120.0	0.	0.	0.	0.	0.	0.	0.	0.	0.	0.
172.0	0.	0.	0.	0.	0.	1.0	0.	0.	0.	0.	0.	0.	0.	0.	0.	0.	0.	0.
174.0	0.	0.	0.	0.	0.	1.0	0.	0.	0.	0.	0.	0.	0.	0.	0.	0.	0.	0.
176.0	0.	0.	0.	0.	0.	1.0	0.	0.	0.	0								



ETA=150.0

BETA

DELTA	10	20	30	40	50	60	70	80	90	100	110	120	130	140	150	160	170
2.0	0.	0.	0.	0.	0.	0.	0.	0.	0.	0.	0.	0.	0.	0.	1.0	0.	0.
4.0	0.	0.	0.	0.	0.	0.	0.	0.	0.	0.	0.	0.	0.	0.	1.0	0.	0.
6.0	0.	0.	0.	0.	0.	0.	0.	0.	0.	0.	0.	0.	0.	0.	1.0	0.	0.
8.0	0.	0.	0.	0.	0.	0.	0.	0.	0.	0.	0.	0.	0.	0.	1.0	0.	0.
10.0	0.	0.	0.	0.	0.	0.	0.	0.	0.	0.	0.	0.	0.	0.	79.8	1.0	39.8
12.0	0.	0.	0.	0.	0.	0.	0.	0.	0.	0.	0.	0.	0.	0.	1.0	1.4	0.
14.0	0.	0.	0.	0.	0.	0.	0.	0.	0.	0.	0.	0.	0.	0.	1.0	1.2	0.
16.0	0.	0.	0.	0.	0.	0.	0.	0.	0.	0.	0.	0.	0.	0.	1.0	1.1	0.
18.0	0.	0.	0.	0.	0.	0.	0.	0.	0.	0.	0.	0.	0.	0.	1.0	1.0	0.
20.0	0.	0.	0.	0.	0.	0.	0.	0.	0.	0.	0.	0.	0.	0.	99.5	1.3	1.1
22.0	0.	0.	0.	0.	0.	0.	0.	0.	0.	0.	0.	0.	0.	0.	2.7	1.3	1.1
24.0	0.	0.	0.	0.	0.	0.	0.	0.	0.	0.	0.	0.	0.	0.	2.1	1.3	1.1
26.0	0.	0.	0.	0.	0.	0.	0.	0.	0.	0.	0.	0.	0.	0.	1.9	1.3	1.1
28.0	0.	0.	0.	0.	0.	0.	0.	0.	0.	0.	0.	0.	0.	0.	1.8	1.3	1.1
30.0	0.	0.	0.	0.	0.	0.	0.	0.	0.	0.	0.	0.	0.	0.	119.0	1.7	1.3
32.0	0.	0.	0.	0.	0.	0.	0.	0.	0.	0.	0.	0.	0.	0.	3.4	1.6	1.3
34.0	0.	0.	0.	0.	0.	0.	0.	0.	0.	0.	0.	0.	0.	0.	2.6	1.6	1.3
36.0	0.	0.	0.	0.	0.	0.	0.	0.	0.	0.	0.	0.	0.	0.	2.3	1.6	1.3
38.0	0.	0.	0.	0.	0.	0.	0.	0.	0.	0.	0.	0.	0.	0.	2.1	1.5	1.3
40.0	0.	0.	0.	0.	0.	0.	0.	0.	0.	0.	0.	0.	0.	0.	2.0	1.5	1.4
42.0	0.	0.	0.	0.	0.	0.	0.	0.	0.	0.	0.	0.	0.	0.	3.9	1.9	1.5
44.0	0.	0.	0.	0.	0.	0.	0.	0.	0.	0.	0.	0.	0.	0.	3.0	1.8	1.5
46.0	0.	0.	0.	0.	0.	0.	0.	0.	0.	0.	0.	0.	0.	0.	2.6	1.8	1.5
48.0	0.	0.	0.	0.	0.	0.	0.	0.	0.	0.	0.	0.	0.	0.	2.4	1.8	1.6
50.0	0.	0.	0.	0.	0.	0.	0.	0.	0.	0.	0.	0.	0.	0.	2.2	1.7	1.6
52.0	0.	0.	0.	0.	0.	0.	0.	0.	0.	0.	0.	0.	0.	0.	4.4	1.6	1.6
54.0	0.	0.	0.	0.	0.	0.	0.	0.	0.	0.	0.	0.	0.	0.	3.4	2.0	1.7
56.0	0.	0.	0.	0.	0.	0.	0.	0.	0.	0.	0.	0.	0.	0.	2.9	2.0	1.7
58.0	0.	0.	0.	0.	0.	0.	0.	0.	0.	0.	0.	0.	0.	0.	2.6	1.9	1.7
60.0	0.	0.	0.	0.	0.	0.	0.	0.	0.	0.	0.	0.	0.	0.	2.4	1.9	1.8
62.0	0.	0.	0.	0.	0.	0.	0.	0.	0.	0.	0.	0.	0.	0.	4.6	2.3	1.9
64.0	0.	0.	0.	0.	0.	0.	0.	0.	0.	0.	0.	0.	0.	0.	3.6	2.2	1.9
66.0	0.	0.	0.	0.	0.	0.	0.	0.	0.	0.	0.	0.	0.	0.	3.0	2.1	1.8
68.0	0.	0.	0.	0.	0.	0.	0.	0.	0.	0.	0.	0.	0.	0.	2.7	2.1	1.9
70.0	0.	0.	0.	0.	0.	0.	0.	0.	0.	0.	0.	0.	0.	0.	0.	2.5	2.0
72.0	0.	0.	0.	0.	0.	0.	0.	0.	0.	0.	0.	0.	0.	0.	4.8	2.4	2.0
74.0	0.	0.	0.	0.	0.	0.	0.	0.	0.	0.	0.	0.	0.	0.	3.6	2.3	2.0
76.0	0.	0.	0.	0.	0.	0.	0.	0.	0.	0.	0.	0.	0.	0.	3.1	2.2	2.0
78.0	0.	0.	0.	0.	0.	0.	0.	0.	0.	0.	0.	0.	0.	0.	2.8	2.1	2.0
80.0	0.	0.	0.	0.	0.	0.	0.	0.	0.	0.	0.	0.	0.	0.	2.6	2.1	2.0
82.0	0.	0.	0.	0.	0.	0.	0.	0.	0.	0.	0.	0.	0.	0.	2.4	2.1	2.0
84.0	0.	0.	0.	0.	0.	0.	0.	0.	0.	0.	0.	0.	0.	0.	3.6	2.3	2.0
86.0	0.	0.	0.	0.	0.	0.	0.	0.	0.	0.	0.	0.	0.	0.	3.1	2.2	2.0
88.0	0.	0.	0.	0.	0.	0.	0.	0.	0.	0.	0.	0.	0.	0.	2.7	2.1	2.0
90.0	0.	0.	0.	0.	0.	0.	0.	0.	0.	0.	0.	0.	0.	0.	2.5	2.1	2.0
92.0	0.	0.	0.	0.	0.	0.	0.	0.	0.	0.	0.	0.	0.	0.	119.8	0.	0.
94.0	0.	0.	0.	0.	0.	0.	0.	0.	0.	0.	0.	0.	0.	0.	4.6	2.4	2.0
96.0	0.	0.	0.	0.	0.	0.	0.	0.	0.	0.	0.	0.	0.	0.	3.5	2.3	2.0
98.0	0.	0.	0.	0.	0.	0.	0.	0.	0.	0.	0.	0.	0.	0.	2.9	2.2	2.0
100.0	0.	0.	0.	0.	0.	0.	0.	0.	0.	0.	0.	0.	0.	0.	2.6	2.1	2.0
102.0	0.	0.	0.	0.	0.	0.	0.	0.	0.	0.	0.	0.	0.	0.	4.3	2.3	2.0
104.0	0.	0.	0.	0.	0.	0.	0.	0.	0.	0.	0.	0.	0.	0.	3.2	2.1	2.0
106.0	0.	0.	0.	0.	0.	0.	0.	0.	0.	0.	0.	0.	0.	0.	2.7	2.0	1.9
108.0	0.	0.	0.	0.	0.	0.	0.	0.	0.	0.	0.	0.	0.	0.	2.4	2.0	1.9
110.0	0.	0.	0.	0.	0.	0.	0.	0.	0.	0.	0.	0.	0.	0.	2.2	1.9	1.9
112.0	0.	0.	0.	0.	0.	0.	0.	0.	0.	0.	0.	0.	0.	0.	3.8	2.1	1.9
114.0	0.	0.	0.	0.	0.	0.	0.	0.	0.	0.	0.	0.	0.	0.	2.9	2.0	1.8
116.0	0.	0.	0.	0.	0.	0.	0.	0.	0.	0.	0.	0.	0.	0.	2.4	1.9	1.8
118.0	0.	0.	0.	0.	0.	0.	0.	0.	0.	0.	0.	0.	0.	0.	2.2	1.8	1.8
120.0	0.	0.	0.	0.	0.	0.	0.	0.	0.	0.	0.	0.	0.	0.	2.0	1.7	1.7
122.0	0.	0.	0.	0.	0.	0.	0.	0.	0.	0.	0.	0.	0.	0.	3.2	1.7	1.6
124.0	0.	0.	0.	0.	0.	0.	0.	0.	0.	0.	0.	0.	0.	0.	2.4	1.7	1.6
126.0	0.	0.	0.	0.	0.	0.	0.	0.	0.	0.	0.	0.	0.	0.	2.1	2.1	1.6
128.0	0.	0.	0.	0.	0.	0.	0.	0.	0.	0.	0.	0.	0.	0.	1.8	2.2	2.0
130.0	0.	0.	0.	0.	0.	0.	0.	0.	0.	0.	0.	0.	0.	0.	1.7	2.2	2.0
132.0	0.	0.	0.	0.	0.	0.	0.	0.	0.	0.	0.	0.	0.	0.	1.5	2.5	0.
134.0	0.	0.	0.	0.	0.	0.	0.	0.	0.	0.	0.	0.	0.	0.	1.4	2.8	0.
136.0	0.	0.	0.	0.	0.	0.	0.	0.	0.	0.	0.	0.	0.	0.	1.5	3.4	0.
138.0	0.	0.	0.	0.	0.	0.	0.	0.	0.	0.	0.	0.	0.	0.	1.4	5.0	0.
140.0	0.	0.	0.	0.	0.	0.	0.	0.	0.	0.	0.	0.	0.	0.	1.3	1.4	1.5
142.0	1.7	1.2	1.2	1.3	1.5	2.0	2.2	0.	0.	0.	0.	0.	0.	0.	2.0	139.9	0.
144.0	1.3	1.2	1.2	1.3	1.6	2.4	0.	0.	0.	0.	0.	0.	0.	0.	1.7	1.5	0.
146.0	1.1	1.1	1.2	1.3	1.6	2.9	0.	0.	0.	0.	0.	0.	0.	0.	2.5	0.	0.
148.0	1.0	1.1	1.1	1.3	3.4	0.	0.	0.	0.	0.	0.	0.	0.	0.	0.	0.	0.
150.0	1.0	1.0	1.1	1.3	1.7	4.3	0.	0.	0.	0.	0.	0.	0.	0.	120.0	0.	0.
152.0	1.0	1.0	1.1	1.3	1.8	0.	0.	0.	0.	0.	0.	0.	0.	0.	0.	0.	0.
154.0	1.1	1.0	1.1	1.3	2.0	0.	0.	0.	0.	0.	0.	0.	0.	0.	0.	0.	0.
156.0	1.2	1.0	1.1	1.3	2.4	0.	0.	0.	0.	0.	0.	0.	0.	0.	0.	0.	0.
158.0	1.6	1.0	1.1	1.3	3.4	0.	0.	0.	0.	0.	0.	0.	0.	0.	0.	0.	0.
160.0	20.0	1.0	1.0	1.3	100.0	0.	0.	0.	0.	0.	0.	0.	0.	0.	0.	0.	0.
162.0	0.	1.0	1.0	1.4	0.	0.	0.	0.	0.	0.	0.	0.	0.	0.	0.	0.	0.
164.0	0.	1.1	1.0	1.5	0.	0.	0.	0.	0.	0.	0.	0.	0.	0.	0.	0.	0.
166.0	0.	1.2	1.0	1.7	0.	0.	0.	0.	0.	0.	0.	0.	0.	0.	0.	0.	0.
168.0	0.	1.7	1.0	2.3	0.	0.	0.	0.	0.	0.	0.	0.	0.	0.	0.	0.	0.
170.0	0.	40.0	1.0	80.0	0.	0.	0.	0.	0.	0.	0.	0.	0.	0.	0.	0.	0.
172.0	0.	0.	1.0	0.	0.	0.	0.	0.	0.	0.	0.	0.	0.	0.	0.	0.	0.
174.0	0.	0.	1.0	0.	0.	0.	0.	0.	0.	0.	0.	0.	0.	0.	0.	0.	0.
176.0	0.	0.	1.0	0.	0.	0.	0.	0.	0.	0.	0.	0.	0.	0.	0.	0.	0.
178.0	0.	0.	1.0	0.	0.	0.	0.	0.	0.	0.	0.	0.	0.	0.	0.	0.	0.



ETA=170.0	BETA																
DELTA	10	20	30	40	50	60	70	80	90	100	110	120	130	140	150	160	170
2.0	0.	0.	0.	0.	0.	0.	0.	0.	0.	0.	0.	0.	0.	0.	0.	0.	1.0
4.0	0.	0.	0.	0.	0.	0.	0.	0.	0.	0.	0.	0.	0.	0.	0.	0.	1.0
6.0	0.	0.	0.	0.	0.	0.	0.	0.	0.	0.	0.	0.	0.	0.	0.	0.	1.1
8.0	0.	0.	0.	0.	0.	0.	0.	0.	0.	0.	0.	0.	0.	0.	0.	0.	1.1
10.0	0.	0.	0.	0.	0.	0.	0.	0.	0.	0.	0.	0.	0.	0.	0.	39.4	1.2
12.0	0.	0.	0.	0.	0.	0.	0.	0.	0.	0.	0.	0.	0.	0.	0.	2.4	1.3
14.0	0.	0.	0.	0.	0.	0.	0.	0.	0.	0.	0.	0.	0.	0.	0.	2.1	1.4
16.0	0.	0.	0.	0.	0.	0.	0.	0.	0.	0.	0.	0.	0.	0.	0.	2.0	1.8
18.0	0.	0.	0.	0.	0.	0.	0.	0.	0.	0.	0.	0.	0.	0.	0.	2.0	2.6
20.0	0.	0.	0.	0.	0.	0.	0.	0.	0.	0.	0.	0.	0.	0.	0.	0.	19.7
22.0	0.	0.	0.	0.	0.	0.	0.	0.	0.	0.	0.	0.	0.	0.	0.	3.8	2.2
24.0	0.	0.	0.	0.	0.	0.	0.	0.	0.	0.	0.	0.	0.	0.	0.	3.2	2.5
26.0	0.	0.	0.	0.	0.	0.	0.	0.	0.	0.	0.	0.	0.	0.	0.	2.9	3.0
28.0	0.	0.	0.	0.	0.	0.	0.	0.	0.	0.	0.	0.	0.	0.	0.	2.9	4.5
30.0	0.	0.	0.	0.	0.	0.	0.	0.	0.	0.	0.	0.	0.	0.	78.1	2.9	39.6
32.0	0.	0.	0.	0.	0.	0.	0.	0.	0.	0.	0.	0.	0.	0.	5.1	3.1	0.
34.0	0.	0.	0.	0.	0.	0.	0.	0.	0.	0.	0.	0.	0.	0.	4.2	3.5	0.
36.0	0.	0.	0.	0.	0.	0.	0.	0.	0.	0.	0.	0.	0.	0.	3.8	4.2	0.
38.0	0.	0.	0.	0.	0.	0.	0.	0.	0.	0.	0.	0.	0.	0.	3.7	6.2	0.
40.0	0.	0.	0.	0.	0.	0.	0.	0.	0.	0.	0.	0.	0.	0.	3.7	59.5	0.
42.0	0.	0.	0.	0.	0.	0.	0.	0.	0.	0.	0.	0.	0.	0.	6.3	3.9	0.
44.0	0.	0.	0.	0.	0.	0.	0.	0.	0.	0.	0.	0.	0.	0.	5.1	4.3	0.
46.0	0.	0.	0.	0.	0.	0.	0.	0.	0.	0.	0.	0.	0.	0.	4.6	5.2	0.
48.0	0.	0.	0.	0.	0.	0.	0.	0.	0.	0.	0.	0.	0.	0.	4.4	7.7	0.
50.0	0.	0.	0.	0.	0.	0.	0.	0.	0.	0.	0.	0.	0.	0.	4.4	79.3	0.
52.0	0.	0.	0.	0.	0.	0.	0.	0.	0.	0.	0.	0.	0.	0.	7.2	4.6	0.
54.0	0.	0.	0.	0.	0.	0.	0.	0.	0.	0.	0.	0.	0.	0.	5.8	5.1	0.
56.0	0.	0.	0.	0.	0.	0.	0.	0.	0.	0.	0.	0.	0.	0.	5.2	6.1	0.
58.0	0.	0.	0.	0.	0.	0.	0.	0.	0.	0.	0.	0.	0.	0.	5.0	8.9	0.
60.0	0.	0.	0.	0.	0.	0.	0.	0.	0.	0.	0.	0.	0.	0.	5.0	99.2	0.
62.0	0.	0.	0.	0.	0.	0.	0.	0.	0.	0.	0.	0.	0.	0.	8.0	5.2	0.
64.0	0.	0.	0.	0.	0.	0.	0.	0.	0.	0.	0.	0.	0.	0.	6.4	5.7	0.
66.0	0.	0.	0.	0.	0.	0.	0.	0.	0.	0.	0.	0.	0.	0.	5.7	6.8	0.
68.0	0.	0.	0.	0.	0.	0.	0.	0.	0.	0.	0.	0.	0.	0.	5.5	9.9	0.
70.0	0.	0.	0.	0.	0.	0.	0.	0.	0.	0.	0.	0.	0.	0.	5.4	118.9	0.
72.0	0.	0.	0.	0.	0.	0.	0.	0.	0.	0.	0.	0.	0.	0.	8.5	5.6	0.
74.0	0.	0.	0.	0.	0.	0.	0.	0.	0.	0.	0.	0.	0.	0.	6.7	6.1	0.
76.0	0.	0.	0.	0.	0.	0.	0.	0.	0.	0.	0.	0.	0.	0.	6.0	7.3	0.
78.0	0.	0.	0.	0.	0.	0.	0.	0.	0.	0.	0.	0.	0.	0.	5.7	10.6	0.
80.0	0.	0.	0.	0.	0.	0.	0.	0.	0.	0.	0.	0.	0.	0.	5.7	138.4	0.
82.0	0.	0.	0.	0.	0.	0.	0.	0.	0.	0.	0.	0.	0.	0.	8.7	5.9	0.
84.0	0.	0.	0.	0.	0.	0.	0.	0.	0.	0.	0.	0.	0.	0.	6.9	6.4	0.
86.0	0.	0.	0.	0.	0.	0.	0.	0.	0.	0.	0.	0.	0.	0.	6.1	7.5	0.
88.0	0.	0.	0.	0.	0.	0.	0.	0.	0.	0.	0.	0.	0.	0.	5.8	11.0	0.
90.0	0.	0.	0.	0.	0.	0.	0.	0.	0.	0.	0.	0.	0.	0.	5.8	157.0	0.
92.0	0.	0.	0.	0.	0.	0.	0.	0.	0.	0.	0.	0.	0.	0.	8.7	5.9	0.
94.0	0.	0.	0.	0.	0.	0.	0.	0.	0.	0.	0.	0.	0.	0.	6.8	6.4	0.
96.0	0.	0.	0.	0.	0.	0.	0.	0.	0.	0.	0.	0.	0.	0.	6.1	7.8	0.
98.0	0.	0.	0.	0.	0.	0.	0.	0.	0.	0.	0.	0.	0.	0.	5.8	11.0	0.
100.0	0.	0.	0.	0.	0.	0.	0.	0.	0.	0.	0.	0.	0.	0.	5.7	168.9	0.
102.0	0.	0.	0.	0.	0.	0.	0.	0.	0.	0.	0.	0.	0.	0.	8.4	5.8	0.
104.0	0.	0.	0.	0.	0.	0.	0.	0.	0.	0.	0.	0.	0.	0.	6.6	6.3	0.
106.0	0.	0.	0.	0.	0.	0.	0.	0.	0.	0.	0.	0.	0.	0.	5.8	7.4	0.
108.0	0.	0.	0.	0.	0.	0.	0.	0.	0.	0.	0.	0.	0.	0.	5.5	10.7	0.
110.0	0.	0.	0.	0.	0.	0.	0.	0.	0.	0.	0.	0.	0.	0.	5.4	157.3	0.
112.0	0.	0.	0.	0.	0.	0.	0.	0.	0.	0.	0.	0.	0.	0.	7.8	5.5	0.
114.0	0.	0.	0.	0.	0.	0.	0.	0.	0.	0.	0.	0.	0.	0.	6.1	6.0	0.
116.0	0.	0.	0.	0.	0.	0.	0.	0.	0.	0.	0.	0.	0.	0.	5.4	7.0	0.
118.0	0.	0.	0.	0.	0.	0.	0.	0.	0.	0.	0.	0.	0.	0.	5.1	10.1	0.
120.0	0.	0.	0.	0.	0.	0.	0.	0.	0.	0.	0.	0.	0.	0.	5.0	138.7	0.
122.0	0.	0.	0.	0.	0.	0.	0.	0.	0.	0.	0.	0.	0.	0.	5.1	0.	0.
124.0	0.	0.	0.	0.	0.	0.	0.	0.	0.	0.	0.	0.	0.	0.	5.5	5.5	0.
126.0	0.	0.	0.	0.	0.	0.	0.	0.	0.	0.	0.	0.	0.	0.	4.8	6.3	0.
128.0	0.	0.	0.	0.	0.	0.	0.	0.	0.	0.	0.	0.	0.	0.	4.5	9.1	0.
130.0	0.	0.	0.	0.	0.	0.	0.	0.	0.	0.	0.	0.	0.	0.	4.4	119.2	0.
132.0	0.	0.	0.	0.	0.	0.	0.	0.	0.	0.	0.	0.	0.	0.	4.0	4.5	0.
134.0	0.	0.	0.	0.	0.	0.	0.	0.	0.	0.	0.	0.	0.	0.	4.7	4.8	0.
136.0	0.	0.	0.	0.	0.	0.	0.	0.	0.	0.	0.	0.	0.	0.	4.1	4.5	0.
138.0	0.	0.	0.	0.	0.	0.	0.	0.	0.	0.	0.	0.	0.	0.	3.8	7.9	0.
140.0	0.	0.	0.	0.	0.	0.	0.	0.	0.	0.	0.	0.	0.	0.	3.7	99.5	0.
142.0	0.	0.	0.	0.	0.	0.	0.	0.	0.	0.	0.	0.	0.	0.	4.8	3.7	0.
144.0	0.	0.	0.	0.	0.	0.	0.	0.	0.	0.	0.	0.	0.	0.	3.7	4.0	0.
146.0	0.	0.	0.	0.	0.	0.	0.	0.	0.	0.	0.	0.	0.	0.	3.3	4.5	0.
148.0	0.	0.	0.	0.	0.	0.	0.	0.	0.	0.	0.	0.	0.	0.	3.0	6.4	0.
150.0	0.	0.	0.	0.	0.	0.	0.	0.	0.	0.	0.	0.	0.	0.	2.9	79.7	0.
152.0	0.	0.	0.	0.	0.	0.	0.	0.	0.	0.	0.	0.	0.	0.	3.5	2.9	0.
154.0	0.	0.	0.	0.	0.	0.	0.	0.	0.	0.	0.	0.	0.	0.	2.7	3.0	0.
156.0	0.	0.	0.	0.	0.	0.	0.	0.	0.	0.	0.	0.	0.	0.	2.3	3.4	0.
158.0	0.	0.	0.	0.	0.	0.	0.	0.	0.	0.	0.	0.	0.	0.	2.1	4.8	0.
160.0	0.	0.	0.	0.	0.	0.	0.	0.	0.	0.	0.	0.	0.	0.	2.0	59.8	0.
162.0	2.1	2.0	0.	0.	0.	0.	0.	0.	0.	0.	0.	0.	0.	0.	0.	0.	0.
164.0	1.6	2.0	0.	0.	0.	0.	0.	0.	0.	0.	0.	0.	0.	0.	0.	0.	0.
166.0	1.3	2.2	0.	0.	0.	0.	0.	0.	0.	0.	0.	0.	0.	0.	0.	0.	0.
168.0	1.2	2.9	0.	0.	0.	0.	0.	0.	0.	0.	0.	0.	0.	0.	0.	0.	0.
170.0	1.1	39.9	0.	0.	0.	0.	0.	0.	0.	0.	0.	0.	0.	0.	0.	0.	0.
172.0	1.1	0.	0.	0.	0.	0.	0.	0.	0.	0.	0.	0.	0.	0.	0.	0.	0.
174.0	1.0	0.	0.	0.	0.	0.	0.	0.	0.	0.	0.	0.	0.	0.	0.	0.	0.
176.0	1.0	0.	0.	0.	0.	0.	0.	0.	0.	0.	0.	0.	0.	0.	0.	0.	0.
178.0	1.0	0.	0.	0.	0.	0.	0.	0.	0.	0.	0.	0.	0.	0.	0.	0.	0.

## APPENDIX E

### Removing Uncertainty in $t_0$ Caused by a Quantized Time Base in the Spacecraft

Assume that  $\theta = 0$ .

Assume that the time base is quantized in the spacecraft such that the time  $t_0$  at which the digitized fan crosses the sun is known to lie in the time interval between  $t_{0A}$  and  $t_{0B}$ . One revolution later the next time the fan crosses the sun the "see sun" time is  $t_1$  which lies in the interval between  $t_{1A}$  and  $t_{1B}$ . See Figure A.

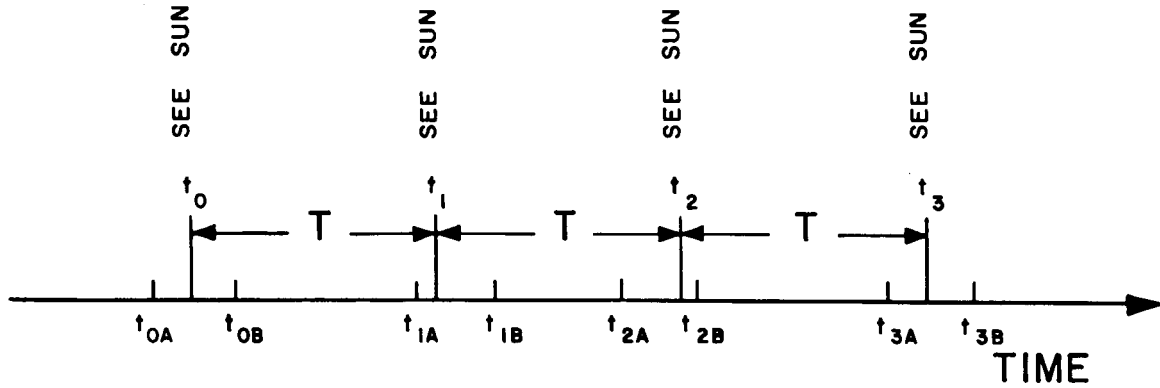


Figure A—Sun sightings defined within a quantized time base

Since  $\theta = 0$  the spin period  $T$  is constant and is stable over a long period of time. Thus  $T$  may be calculated very accurately over a large number of revolutions.

Now from Figure A we can see that

$$t_{\min} \leq t_0 \leq t_{\max}$$

where

$$t_{\min} \geq t_{0A} \quad \text{and} \quad t_{\max} \leq t_{0B}$$

We can also write

$$t_{\min} \geq (t_{1A} - T) \quad t_{\max} \leq (t_{1B} - T)$$

$$t_{\min} \geq (t_{2A} - 2T) \quad t_{\max} \leq (t_{2B} - 2T)$$

$$t_{\min} \geq (t_{3A} - 3T) \quad t_{\max} \leq (t_{3B} - 3T)$$

⋮

⋮

etc.

etc.

It should be possible to find a  $t_{\min}$  and a  $t_{\max}$  which will satisfy all the above inequalities. If the inequalities are satisfied over a sufficiently large number of revolutions, the value of  $t_{\min}$  should approach that of  $t_{\max}$ . Thus it is possible to define the value of  $t_0$  within any desired accuracy by merely solving the inequalities over a sufficiently large number of revolutions.

This method of solution is vulnerable to noise. It is therefore advisable to test to make sure that  $t_{\min} \leq t_{\max}$  holds at all times.

## APPENDIX F

Horizon sensors which operate in the visible spectrum may be used as long as the earth as seen from the satellite is fully illuminated. From Figure AA it can be seen that the spacecraft sees a fully illuminated earth as long as

$$\eta + (90^\circ - \rho) < 90^\circ$$

or

$$\eta < \rho$$

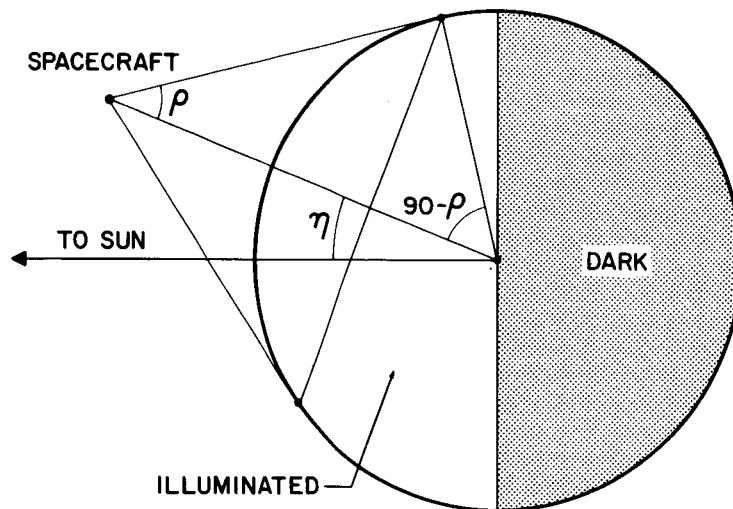


Figure AA—Relationships of spacecraft to sunlit earth